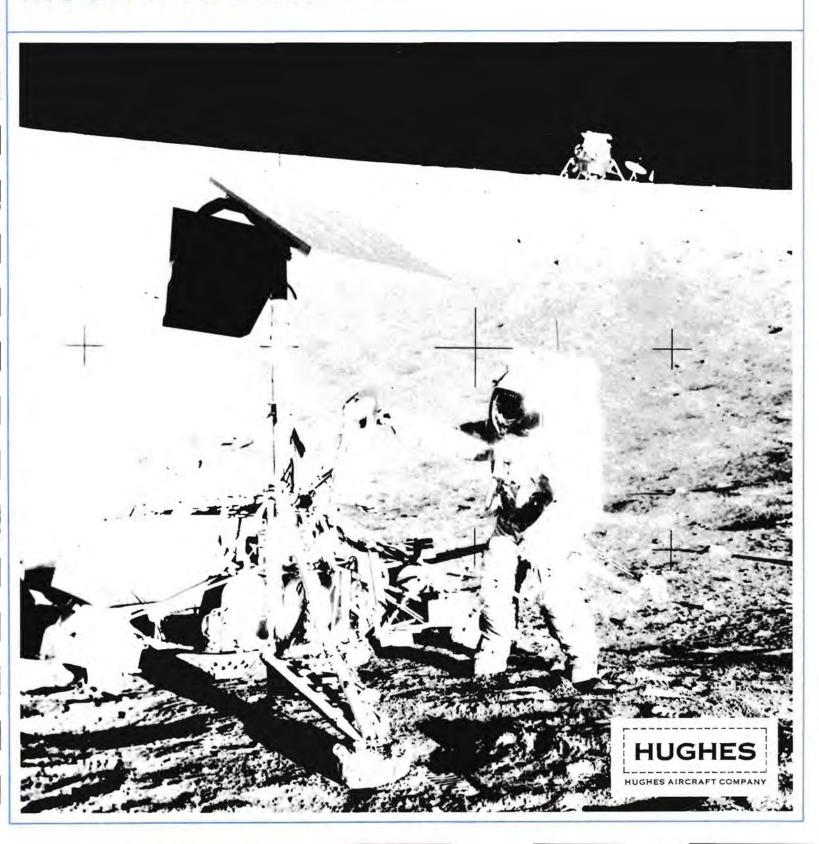
VOLUME I

TEST AND EVALUATION OF THE

SURVEYOR III TELEVISION CAMERA

RETURNED FROM THE

MOON BY APOLLO XII





Surveyor III Television Camera, Returned From The Moon By Apollo XII

TEST AND EVALUATION OF THE

SURVEYOR III TELEVISION CAMERA

RETURNED FROM THE

MOON
BY
APOLLO XII

SUBMITTED 31 DECEMBER 1970

VOLUME I

Contract 952792



ACKNOWLEDGMENTS

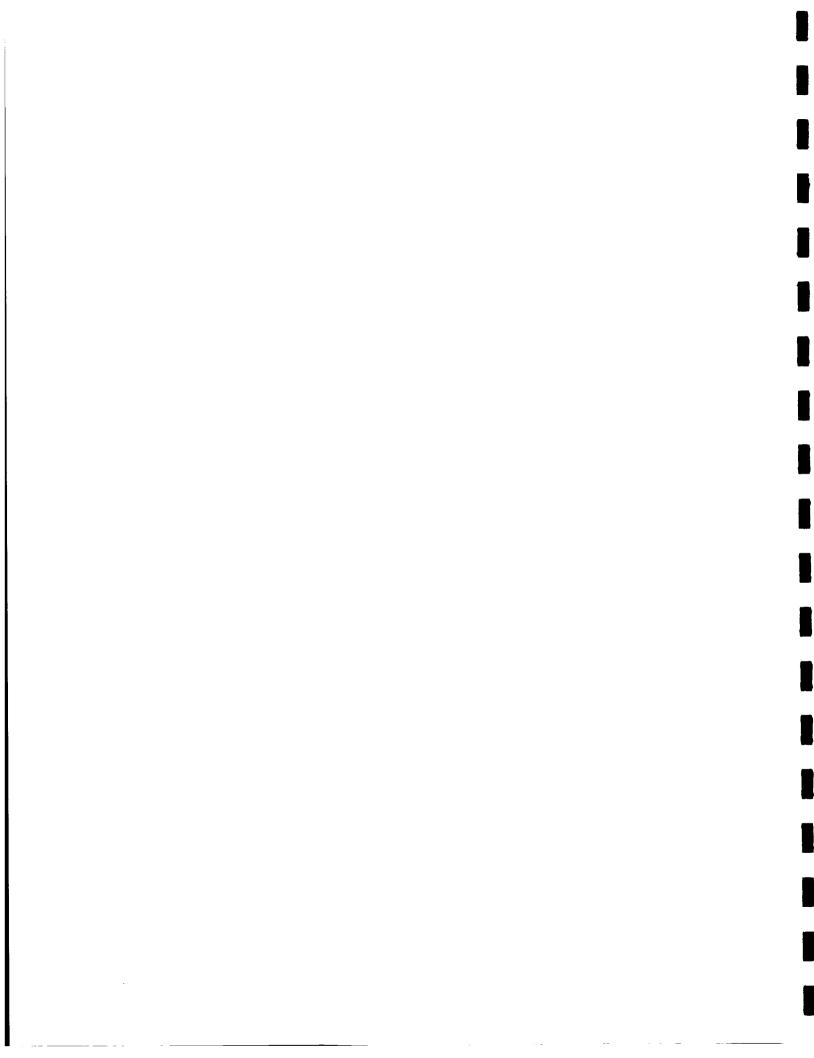
Test and evaluation of the many elements of the Surveyor III television camera involved several technical areas of the Hughes Aircraft Company and required the contributions of many Hughes personnel.

The following principal investigators merit special acknowledgement: P. M. Blair for his technical direction of materials tests and of the surface contamination studies, R. G. Riglin for circuit tests and evaluation, D. H. Buettner for optics and materials investigation, A. A. Abrams for technical coordination of electrical and electromechanical components tests, R. S. Buritz for his work on the vidicon, and K. G. Bingemann for test and evaluation of optical subassemblies.

This report was prepared by the Program Manager, E. I. Hawthorne, with technical inputs from the various investigators. Special acknowledgment is due W. F. Carroll, Jet Propulsion Laboratory technical coordinator, for his contributions in the course of the program and in the preparation of this final report.

The support of JPL is acknowledged in providing the technical direction and furnishing a spare Surveyor television camera from stores in addition to sundry Surveyor test equipment. Recognition should also be made of the support of B. Milwitzky of NASA Headquarters and J. Zarcaro of MSC, Houston, without whose personal interest this program could not have been carried out.

Special tribute is extended by the designers and builders of Surveyor III to the Apollo Program Office and to the Apollo XII astronauts who made the return of this valuable hardware from the surface of the moon possible.



ABSTRACT

Results are presented of engineering tests of the Surveyor III television camera, which resided on the moon for 2-1/2 years before being brought back to earth by the Apollo XII astronauts. Electric circuits, electrical, mechanical, and optical components and subsystems, the vidicon tube, and a variety of internal materials and surface coatings were examined to determine the effects of lunar exposure. Anomalies and failures uncovered were analyzed.

For the most part, the camera parts withstood the extreme environment exceedingly well except where degradation of obsolete parts or suspect components had been anticipated. No significant evidence of cold welding was observed, and the anomalies were largely attributable to causes other than lunar exposure. Very little evidence of micrometeoroid impact was noted. Discoloration of material surfaces — one of the major effects noted — was found to be due to lunar dust contamination and radiation damage.

The extensive test data contained in this report are supplemented by results of tests of other Surveyor parts retrieved by the Apollo XII astronauts, which are contained in a companion report.

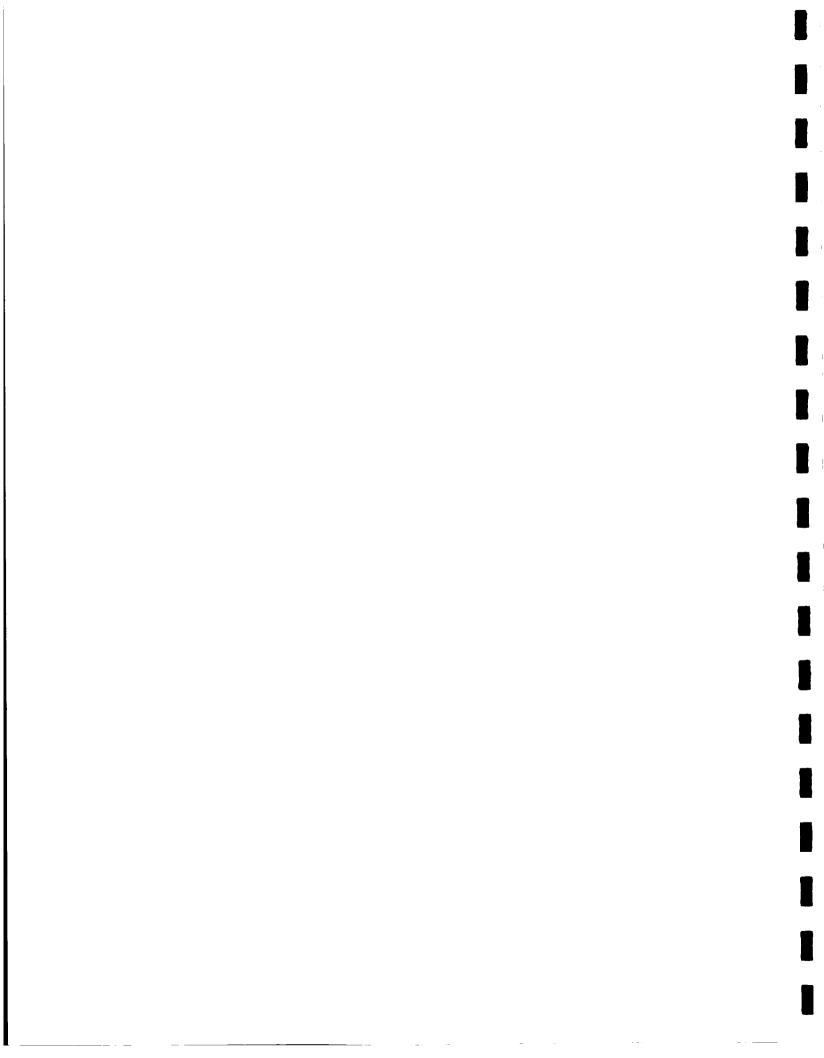
(

CONTENTS

		VOLUME I	Page
1.	SUMMA	RY	
	1.1 1.2	Introduction and Background Information Objectives and Scope of Test and Evaluation	1 - 1
	1.3	Program Assessment of Anomalies	1-3 1-9
		Observed Changes Attributable to Lunar Environment	1-13
	1.5	Environment	1-13 1-13
	1.6	Concluding Comments and Recommendations	1-13
2.		AM OBJECTIVES, SCOPE, AND BACKGROUND MATION	
	2.3	Program Objectives Background Information Description of TV Camera TV Camera Test History and Lunar Mission	2-1 2-4 2-7
		Operations TV Camera Retrieval and Return to Earth	2-15 2-22 2-23
3.	TV CAI	MERA TESTS IN ASSEMBLED CONFIGURATION	
	3.2 3.3	Test Plan MSC Operations Shipment to Hughes Survey Operations	3-1 3-2 3-23 3-23
4.		RIC CIRCUIT TESTS AND DISMANTLING OF SUBASSEMBLIES	
	4.1 4.2 4.3	Initial Dismantling Objectives and Scope of Electric Circuit Tests Selection of Chassis for Functional Performance	4-1 4-3
	4.4 4.5	Tests Test Equipment Checkout and Preliminary Tests	4-5 4-8 4-9 4-11

	4.7 4.8	Functional Performance Tests of Chassis A-6 Dismantling of Major Subassemblies and	4-15 4-19
		Completion of Chassis Tests	4-19
5.	OPTICA	L SUBASSEMBLY TESTS AND DISMANTLING	
		General Discussion	5 - 1 5 - 4
	5.2 5.3	Mirror Assembly and Filter Wheel Tests Dismantling of Mirror Assembly and Filter	
	E 1	Wheel Assembly Tests and Dismantling of Lens Assembly	5-6 5-9
		Tests of Shutter Assembly	5-13
6.	VIDICO	N TESTS	
	6.1	Vidicon Design Features, Tests, and Operations	6 - 1
	6.2	History Test Program Summary	6 - 5
		Vidicon Tests on Camera	6-7
		Vidicon Tests off Camera	6-19
	6.5	Opening of Vidicon and Diagnostic Tests	6-30
7.	ELECT	RICAL COMPONENTS TESTS	
	7.1	Scope and General Test Plan	7 - 1
		Resistor Tests	7 - 5 7 - 13
		Capacitor Tests Diode Tests	7-13 7-25
		Transistor Tests	7-35
8.		NICAL AND ELECTROMECHANICAL NENTS TESTS	
	8.1	Scope and General Test Plan	8-1
	8.2	Potentiometer Tests	8-4
		Stepper Motor Tests	8-7
		Magnetic Components	8 - 8 8 - 9
		Microdot Connector Tests Thermal Switch Tests	8-13
9.		AL COMPONENTS TESTS	
, -	_	Introduction	9-1
	•	Special Photographic and Optical Tests by	
		Science Investigators	9-2
		Tests of TV Azimuth Mirror Tests of Lens Barrel Subassembly	9-3 9-13
10.		RIALS TESTS	·
10.			10-1
		Objectives and Scope of Test Program Electric Circuit Materials	10-1
		Electrical Insulation Materials	10-16
		Organic Materials	10-29

10.6	Adhesive Materials Lubricants: Friction and Wear Evaluation Thermal Control Coatings and Materials	10-34 10-39 10-54
ll. SURFAC	E DISCOLORATION AND CONTAMINATION STUDIES	
11.2	Introduction Data Available From Prelaunch, Landing, and	11-1
11.3	Post-Recovery Examination Evolution of Test Plan Summary of Test Results Damage Model	11-3 11-7 11-10 11-25
12. FAILURI	E ANALYSIS	
12.2 12.3	Introduction General Assessment of Anomalies Suspected Cold Weld of Connector J2 Shell	12-1 12-5
12.4 12.5 12.6 12.7	to Shroud Analysis of Failed Filter Wheel Potentiometer Open Shutter Anomaly and Related Failures Discoloration and Curling of Teflon Skirt Cracked Glass Envelopes on Diodes and Resistors	12-7 12-10 12-14 12-29
12.8	and Related Component Failures Other Electrical Anomalies Other Mechanical and Electromechanical Analyses	12-31 12-38 12-47
REFERENCE	ES	R-1
	VOLUME II	
APPENDICE	S	
A B C	Program Management Description of Lunar Environment Description and Checkout of Electrical Test	A - 1 B - 1
D E F G H	Equipment Functional Description of Chassis A-4 Functional Description of Chassis A-5 Functional Description of Chassis A-6 Supplementary Data on Vidicon and Its Test Program Supplementary Data on Components Tests	C-1 D-1 E-1 F-1 G-1 H-1
J K	Supplementary Data on Materials Tests Supporting Data for Surface Effects Study Supplementary Data on Failure Analysis	I-1 J-1 K-1
REFERENCE	.o	R - 1



ILLUSTRATIONS

		Page
2 - 1	Survey Television Camera	2-8
2-2	Cutaway View of Survey Television Camera	2-9
2-3	Lower Electronic Portion of Survey Television Camera	
	With Mirror Unit Removed	2-10
2-4	Variable Focal Length Lens Assembly	2 - 12
2-5	Vidicon Tube	2 - 13
2-6	Electronic Conversion Unit	2 - 14
2-7	Electronic Circuits for Sweep, Control, and Amplification	2-14
3-1	Test Plan: Surveyor III TV Camera and Its Major	
	Subassemblies	3-4
3-2	Surveyor III TV Camera and Its Plastic Bag at LRL	3-8
3-3	Returned Surveyor III TV Camera	3-9
3-4	Area Under Support Collar Immediately Upon Its	,
	Removal in LRL	3-10
3-5	Mirror Elevation Drive Mechanism	3-11
3-6	Removal of External Lower Shroud Connector	3-14
3-7	Removal of External Shroud Connector Retainer Nut	3-14
3-8	Camera Mounting Collar - Left Section With Remnants	
	of Support Struts	3 - 15
3-9	Camera Support Collar - Right Section	3 - 15
3-10	External Connectors on Lower Shroud	3-16
3-11	Lower Shroud After Removal of External Connectors	3 - 17
3 - 12	Removal of Connector Cable Support Bracket and	
	Biological Assay	3-17
3-13	Biological Assays	3 - 18
3-14	Biological Assay — Removal of Piece of Foam From	
	TV Electronics	3-20
3-15	Exposed Lower Portion of TV Camera Upon Removal	J = 0
3 13	of Lower Shroud	3-21
3-16	Infrared Photograph of TV Camera	3-22
3 - 17	TV Camera Wrapped for Shipment to Hughes	3-24
3-18	TV Camera Placed in Carrying Case	3-24
3-19	Color Variations on Sunshade and Connector Bracket	3-26
3-20	Evidence of "Mud-Cracking" on Lower Shroud	3-27
3-21	Variations in "Mud-Cracking" on Lower Shroud Area	3-28
3-22	"Sandblasting" and Erosion on Elevation Drive Motor	J-20
J 2-2	Housing	3-29
		~ - /

3-23	Aluminized Teflon FEP and Nylon on Mirror Housing	
J J	Connector	3-30
3-24	Glass Fiber Cable Insulation	3-32
3-25	Teflon TFE on Mirror Assembly	3-34
3-26	Teflon TFE Skirt Seal	3 - 35
3-27	Color Variation and Banding on TV Mirror	3-36
4-1	Azimuth Drive Ring Gear Assembly	4-2
4-2	Bottom View of Upper Shroud of Camera	4-3
4-3	Typical Cordwood Module - TV Camera Electronics	4-6
4-4	Test Setup for Functional Checkout of Chassis A5	4-14
4 - 5	Test Setup for Functional Checkout of Chassis A6	4-18
4- 6	TV Camera After Removal of Mirror Assembly	
1- 0	and Shroud	4-22
4-7	Main Deck Structure of TV Camera	4-23
4-8	Front View of Lens Support Structure and Shutter	
1- 0	Assembly	4-26
4-9	Star Mode Chassis A10 After Disassembly	4-26
4- 10	Top View of Shutter Assembly	4-27
4-11	Bottom View of Lens Assembly	4-27
4-11	Chassis A5	4-28
4-12	Cordwood Module Sides of Various Chassis	4-30
4-13	Etched Braided Circuit Board Side of Chassis A6	4-33
4-15	Electronic Conversion Unit	4-34
4-15	Rear View of Vidicon Housing Assembly	4-35
4-10	Vidicon Boron Nitride Collar	4-36
4-17	Vidicon Deflection Coil	4-36
5-1	Mirror Assembly With Filter Wheel Subassembly	5-2
5-1	Lens and Shutter Assembly	5 - 3
5-3	Removal of Filter Wheel Potentiometer	5-4
5-3 5-4	Filter Wheel Subassembly	5-8
	Lens Frame With Focus Mechanism in Vacuum Chamber	5-12
5-5 6-1	Vidicon Tube of Surveyor III Camera	6-2
	Cross-Sectional View of Front Portion of Vidicon	6-3
6-2	Functional Diagram of Vidicon Transducing Process	6-4
6-3		6-6
6-4	Vidicon Test Program Flow Diagram	6-8
6-5	Front View of Vidicon Faceplate Diagrammatical Representation of Vidicon for	0 0
6-6		6-12
/ 7	Functional Tests	6-16
6-7	Beam Transmission Characteristics	0-10
6-8	Surveyor III Vidicon Transfer Characteristics:	6-17
/ 0	Cathode and Beam Currents	6-18
6-9	Vidicon Prior to Removal From Camera	0-10
6-10	Front View of Transparent Faceplate of Surveyor III	6-20
/ 11	Vidicon, Showing Cathode in Rear	0-20
6-11	Measurement of Nesa Conductivity on Surveyor III	6-22
/ 10	and Spare Vidicon	0=22
6-12	Appearance of Faceplate Photoconductor of a Spare	
	Vidicon After 118 Hours Exposure in Thermal	6-26
,	Simulation Test	0-20
6-13	Torn Piece of Grid 5 Mesh During Thermal	6-26
	Simulation Test	0-40

6-14	Block Diagram of Test Setup for Measurement of Vidicon Gas Content	6-26
6 - 15		0-20
	Results of Microscopic Examination of Pieces of Grid 5 Mesh	6-32
6-16	Optical Transmission Measurements of Nesa Coatings: Surveyor III Vidicon and Two Spare Vidicons	6-35
7 - 1		0-33
/ - 1	Resistance Versus Temperature of 1.5 Megohm	7-6
7 2	Carbon Composition Resistor	7-0
7-2	Impedance Versus Frequency of Three Carbon Composition Resistors	7-6
7-3	Metallographic Section of 1.5 Megohm Carbon	
13	Composition Resistors	7-8
7-4	Resistance Versus Temperature of Six Carbon	1-0
1-1	Film Resistors	7-9
7 - 5	Impedance Versus Frequency of Five Carbon Film	1 - 7
1-5	Resistors	7-10
7-6		7-10
7-0	Resistance Versus Temperature of Precision Wire-	7 - 12
7-7	Wound Resistor	1-12
1 - 1	Dissipation Factor Versus Susceptance of Solid	7 17
7-8	Tantalum Capacitors	7 - 17
1-0	Leakage Current Versus Temperature of Tantalum	7-18
7 0	Capacitors Capacitana Vanca Tampanatura of Dinned Miss	7-10
7-9	Capacitance Versus Temperature of Dipped Mica	7 22
7 - 10	Capacitors Capacitors Capacitors	7-22
7 - 10	Capacitance and Q Versus Temperature of Glass	7 24
7 11	Dielectric Capacitors	7-24
7-11	Insulation Resistance Versus Temperature of Dipped	7 24
7 - 12	Mica Capacitors	7-24
1-12	Insulation Resistance Versus Temperature of Glass	7 24
7 12	Dielectric Capacitors	7-24
7-13	Voltage Versus Temperature of Zener Diodes	7 - 32
7-14	SEM Photographs of Intermetallic Growth Bonds on	7 4/
7 10	Low Noise Transistor	7-46
7-15	SEM Photograph of Base Lead of Transistors	7-48
8-1	Apparent Cracks in Abrams Motor	8-6
8-2	Bent Connector Pin	8 - 12
8-3	TV Camera Connector Peeling of Gold Plating From	0 13
0 1	Base Metal of Contact	8-12
9-1	Experiment Setup for Specular Reflectance Measurements	9-7
9-2	of TV Mirror TV Mirror Pagions Managemed for Pagions	9-7 9-7
	TV Mirror Regions Measured for Reflectance	
9-3	Results of Specular Reflectance Measurements	9-8
9-4	Test Setup for Original Measurement of Flatness of	0 10
0 5	TV Mirror on Mirror Assembly	9-10
9 - 5	Illustration of Double-Pass Interference of Flatness	0 10
0 6	Measurement	9-10
9-6	Interference Patterns During Flatness Measurements	0 12
0.7	of TV Mirror	9-12
9-7 9-8	Lens Barrel Subassembly Results of Lens Transmission Measurements	9 - 13
7 - 0	RECORD OF LEADE I PANEMISSION WEASHPAMANTS	4-1/

10-1	Etched Circuit Board Sandwich Construction	10-4
10-2	Solder Flux on Cordwood Module of Chassis Al	10-6
10-3	Wrinkled Solder Joint on Mother Board of Chassis Al	10-7
10-4	Void in Solder Joint of Cordwood Module	10-8
10-4	Cross Sections of Solder Joints	10-9
10-6	Conductor Peel Strength Test Setup	10-11
10-0	Flaking of ML Coating From Surveyor III Internal	
10-7	Wire Harness	10-14
10.0	Infrared Spectra of Polyurethane Foam	10-18
10-8	Cracking of Conformal Coating on ECU of Surveyor III	
10-9		10-21
10 10	Camera Infrared Spectra of Samples of Conformal Coating	10-24
10-10		
10-11	Infrared Spectrogram of Filled Encapsulant of	10-26
10 12	Magnetic Reactor	10-30
10-12	SEM Photographs of Polyimide-Coated ML Wire	10-30
10-13	Modified Probe for Shore A Tester for Hardness of	10-36
10 14	Adhesives	10-30
10-14	Photomicrograph of Spur Gear From Mirror Elevation	10-41
	Drive (13X Magnification)	10-41
10-15	Photomicrograph of Ball Surface From TV Mirror	10-41
/	Support Bearing (250X Magnification)	10-41
10-16	Elevation Drive Outer Bearing (20X Magnification)	10-42
10-17	Film of Transferred Lubricant on Outer Bearing of	10-42
	Elevation Drive (50X Magnification)	10-42
10-18	Interference Rings on Outer Bearing of Elevation Drive	10-42
	(200X Magnification)	10-42
10-19	Galled Teeth Surfaces on Focal Length Potentiometer	10-44
	Spur Gear (17X Magnification)	10-44
10-20	DAP Carriage Lip of Focal Length Potentiometer	10-44
	(30X Magnification)	10-44
10-21	Pitting of Bearing Balls of Focal Length Potentiometer	10 45
	(200X Magnification)	10-45
10-22	Wear of Focal Length Potentiometer Slip Rings	10.4/
	(45X Magnification)	10-46
	Helical Winding of Focal Length Potentiometer	10-48
10-24		10.40
	Potentiometer Winding (65X Magnification)	10-49
10-25	Surface Wear of Wiper Contact of Surveyor III Focal	10.40
	Length Potentiometer (100X Magnification)	10-49
10-26	Surface Wear of Test Wiper Contact After Friction Test	10 51
	(40X Magnification)	10-51
10-27	Appearance of Surveyor III Focal Length Potentiometer	10 51
	Wire After Friction Test (40X Magnification)	10-51
11-1	Lower Shroud of Surveyor III Camera, Showing TRW	
	Measurement Positions	11-13
11-2	White Painted Tube Section Returned From Moon in	
	SESC in Quartz Vacuum Chamber	11-14
11-3	Separated Radiation and Dust Effects on Spectral	
	Reflectance	11-22
11-4	Effect of Radiation on Spectral Reflectance of White	
	Inorganic Painted Surfaces of Surveyor III Camera	11-29

12-1	J2 Connector Showing Area of Suspected Cold Weld	12-8
12-2	Segment of Shroud in Contact With Connector J2	
	(3X Magnification)	12-9
12-3	Surveyor III TV Potentiometer	12-11
12-4	Wiper Block and Shaft Assembly of Potentiometer	12-11
12-5	Cracked and Broken Off Guide Block of Filter Wheel	
	Potentiometer (30X Magnification)	12-12
12-6	Simplified Schematic of Shutter Coils and Drive Circuits	12-15
12-7	Logic Block Diagram Showing Relationship and Sequence	
	of Failures of Shutter Drive Transistor, Shutter Coil,	
	and Vidicon Photoconductor and Grid	12-17
12-8	Failed Shutter Solenoid Drive Transistor (Q5), Showing	
	Open Emitter Lead (10X Magnification)	12-20
12-9	Damaged Shutter Solenoid Coil	12-22
12-10	Possible Causes of Line Voltage Across Shutter Coil	
	Circuit	12-26
12-11	Cracked Diode Glass Envelope	12-32
12-12	Construction of Solid Tantalum Electrolytic Capacitor	12-42
12-13	Tantalum Capacitor Anode Slug, Showing Suspected	
	Areas of Breakdown	12-44
12-14	Deformed and Galled Teeth of Azimuth Drive Gear Train	12-49
12-15	Scratch Marks on Filter Wheel Gear Caused by Broken	
	Safety Wire	12-52
A - 1	Surveyor Parts Test Program Organization	A - 1
A - 2	Surveyor Parts Test Program Master Schedule	A- 5
A - 3	Sketch of Surveyor Parts Test Facility	A- 8
C-1	Test Fixture for Supporting Camera During Dismantling	C-3
D - l	Schematic of Chassis A4	D-3
D-2	Normal Mode Sweep Generating and Sync/Blanking	
	Function	D-5
D-3	Vertical Sweep Generator Waveforms — Normal Mode	D-6
D - 4	Vertical Blanking Timing Sequence — Normal Mode	D-7
D - 5	Horizontal Sweep Generator Waveforms - Normal Mode	D-8
D-6	Horizontal Sync/Blank Timing Sequence — Normal Mode	D-12
D - 7	Composite Sync/Blank Timing Sequence - Normal Mode	D-13
E-1	Schematic of Chassis A5	E-3
E-2	Normal Mode Logic Timing Sequence	E-8
E-3	Vidicon Thermal Control Timing Sequence - Normal Mode	E-16
F-1	Schematic of Chassis A6	F-2
F-2	Block Diagram of Shutter Control Circuits - 150 ms	
	and Time Exposure Modes	F-6
F-3	Block Diagram of Mirror Drive Circuits for Mirror	
	Stepping	F-7
F-4	150 ms Exposure Mode - Pulse Timing Sequence	F-8
F-5	Time Exposure Mode - Pulse Timing Sequence	F-11
G-1	Mounting of Grid 5 Mesh	G-2
G-2	Pressure Versus Heater Voltage Calibration of	
	Non-Flight Vidicon	G-6
G-3	Heater Voltage Versus Current Calibration of Flight	
	Vidicon	G-6

H-1	Example of Preliminary Test Plan Format – Solid	
	Tantalum Capacitor	H-4
H-2	Resistance Versus Temperature Measurements of Ten	,
	Carbon Composition Resistors	H-6
H-3	Resistance Versus Temperature Measurements of 510 Ohm	
	Carbon Composition Resistor	H-7
H-4	Resistance Versus Temperature Measurements of 10	
	Megohm Carbon Composition Resistor	H-7
H-5	Platinum Resistance Thermometer After Removal of Lead,	
	Showing Deformation of Coils	H-10
I – 1	Photomicrograph of Surveyor III ML-FEP Internal Harness	
	Wire (50X Magnification)	I - 9
I-2	Photomicrograph of Surveyor III Internal Harness Wire	
	Strands (1000X Magnification)	I - 9
I-3	Photomicrograph of TAT Camera Internal Harness Wife	
	Strands (1000X Magnification)	I-10
I - 4	Photomicrograph of Surveyor III Internal Coaxial Cable	
	(25X Magnification)	I-10
I - 5	Photomicrograph of Shield Conductors of Surveyor III	
	Coaxial Cable (1000X Magnification)	I-11
I - 6	Photomicrograph of Shield Conductors of TAT Camera	
	Coaxial Cable (1000X Magnification)	I-11
I-7	Infrared Transmission Spectra of Teflon TFE From	<u>-</u>
	Camera Mirror Assembly Collars	I-14
I-8	Infrared Transmission Spectrum of Surveyor III Camera	
	Mirror Hood	I - 15
I - 9	Ultraviolet Transmission Spectrum of Teflon TFE From	1 15
- /	Surveyor III Camera	I-17
I-10	DTA Thermograms	I-21
I-11	Schematic of Friction and Wear Test Assembly	I-24
I-12	Detailed Schematic of Location and Relative Motion of	1 - 1
	Wire Specimen and Wipers in Friction Test	I-25
J-1	Surveyor III on Crater Wall	J-2
J-2	Orientation of Surveyor III in Crater	J-4
J-3	Shadow Photograph of Surveyor III Model, Simulating	5 – 1
3 – 3	Position of Sun at 10 Degrees Before Sunset, Viewed	
	From Lunar Module Position	J-5
J - 4	Approach and Landing Configurations of Lunar Module	0-5
J - 1		J - 6
J-5	Relative to Surveyor III	3-0
J - J	View of Relative Locations on Lunar Surface of Surveyor III and Lunar Module	J -7
J-6		J-9
J-7	Illustration of Shadow Through Hole in Camera Clamp	J-10
J-8	Shadow Patterns on Elevation Drive Motor Housing	3-10
J - 0	Spectral Reflectance of White Inorganic Paint Before and	J-11
то	After Laboratory Ultraviolet Exposure	J = 11
J-9	Lower Shroud of Surveyor III Camera, Showing TRW	J-12
т 10	Measurement Positions Poffectings Versus Wavelength of Surveyor III Company	J = 14
J-10	Reflectance Versus Wavelength of Surveyor III Camera	
	Lower Shroud at Various TRW Locations Shown in	r 1c
	Figure J-9	J - 15

J-11	Quartz Chamber With Light-Tight Shield for Vacuum Tests of White Painted Tube	J-17
T 10		3 - 11
J-12	Sketch of White Painted Section of Tube Returned in	т 10
	SESC, Showing Measurement Positions	J-18
J-13	Spectral Reflectance Versus Wavelength of Four Samples	
	of White Painted Tube — High Vacuum Prior to Light	
	Exposure	J - 19
J-14	Spectral Reflectance Versus Wavelength of Four Samples	
	of White Painted Tube - Medium Vacuum Prior to Light	
	Exposure	J-20
J - 15	Spectral Reflectance Versus Wavelength of Four Samples	
0 10	of White Painted Tube - 1 AU Prior Prior to Light	
	Exposure	J-21
J-16	Spectral Reflectance Versus Wavelength of One Sample	·
J – 10	of White Painted Tube (Sample 778-70) After 6 Days at	
		J-22
T 17	1 AU Prior to Light Exposure	J - <i>L L</i>
J - 17	Spectral Reflectance Versus Wavelength of Different	
	Sample of White Painted Tube (Sample 800-70 in Figure	T 22
	J-12) After 48 Hours Exposure to Light at 1 AU	J-22
J-18	Spectral Reflectance Versus Wavelength of Four Samples	- 20
	of White Painted Tube After 48 Hours	J-23
J-19	Lower Shroud of Surveyor III Camera With Attached Cable	
	Bracket Upon Return From Moon	J-24
J-20	Cable Bracket Superimposed on Lower Shroud of Surveyor	
	III Television Camera: Shroud Exposed to Light for About	
	5 Months, Cable Bracket Unexposed	J-25
J-21	Location of Samples Cut From Cable Bracket	J-25
J-22	Spectral Reflectance Versus Wavelength of Sample of	
	Camera Cable Bracket (Sample 518 of Figure J-21):	
	Measurements Taken in May 1970 Prior to Light Exposure	J-26
J-23	Support Collar of Surveyor III Television Camera	J-28
J-24	Photograph of Surveyor III on the Moon, Showing TV	
·	Support Tubing	J-29
J-25	Reflectance of Bipod Bracket Tube	J-31
J-26	Experimental Configuration for Thermal-Vacuum	
0 =0	Exposure of Surveyor III Sample 909	J-39
J-27	Ratio of Reflectance of Painted Surfaces Covered With	0 0,
3 – 2 1	Lunar Dust to Reflectance of "Clean" Surfaces (White	
		J-43
TZ 1	Inorganic Paint)	J - 1 .
K-1	J2 Connector Thread Area, Showing Metal Blob (13X	K-2
77 2	Magnification)	K-2
K-2	SEM Photograph of Metal Blob of Figure K-1 (230X	77 2
	Magnification)	K-2
K-3	Transverse Cross Section of Metal Blob Shown in	2
	Figure K-2 (100X Magnification)	K-2
K - 4	Microprobe Scan of Area Adjacent to Metal Blob of	
	Figure K-2 (200X Magnification)	K-4
K - 5	Edge of Shroud in Contact With J2 Connector Shell	
	(22X Magnification)	K-6
K-6	SEM Photographs of Edge Surface of Hole in Shroud	K-7

K-7	Typical Cold Welded Area of 2014 Aluminum Specimen	
	After Separation (1400X Magnification)	K-7
K-8	Surfaces of Potentiometer Blocks Under Broken Off Guides	K-9
K-9	SEM Comparison of DAP Materials	K-11
K-10	Chip of Shutter Coil Drive Transistor Q5, Showing Melted	
11-10	Metallization Under Emitter Bond (44X Magnification)	K-12
K-11	"Punch Through" Region of Shutter Drive Transistor Q5	K-14
K-12	Solenoid Coil Showing Effects of Excessive Heat	K-15
K-12	Shorted Wires of Figure K-12 (50X Magnification)	K-16
K-13	Drive Circuit of Shutter Solenoid A2	K-17
K-15	Command and Power Control Circuit of ECU	K - 19
K-16	Internal View of Open Diode Showing Intermittent	
11 10	Contact (12X Magnification)	K-21
K-17	Die of High Leakage Diode, Showing Fracture of Chip	
1, 1,	(110X Magnification)	K-23

TABLES

		Page
1 - 1	Summary of Mission Performance of Surveyors	1-1
1-2	Program Tasks and Referenced Report Sections	l-5
1 - 3	Results of Investigation of Specific Anomalies	1-8
1-4	Observed Possible Effects of Lunar Environment	1-14
1-5	Significant Observations Relative to Absence of	
	Effects of Lunar Environment	1-16
2-1	Primary Program Objectives - Acquisition of	
	Engineering Design Data	2-2
2-2	Secondary Program Objectives - Support of	
	Scientific Investigation	2-3
3 - 1	Removal Torques of Lower Shroud Mounting Hardware	3-19
4-l	Results of Functional Performance Tests of Electrical	,
	Parameters of Chassis A-4	4-10
4-2	Power Sources and Terminations for Functional Tests	
	of Chassis A-4	4-11
4-3	Results of Functional Performance Tests of Electrical	
	Parameters of Chassis A-5	4-12
4-4	Results of Functional Performance Tests of Electrical	
	Parameters of Chassis A-6	4-16
4-5	Terminations for Functional Tests of Chassis A-6	4-19
4-6	Mounting Hardware Removal Torques	4-24
4-7	Mounting Hardware Installation Torques	4-24
5-1	Measured Torques During Removal of Components of	
	Iris and Focal Length Mechanism	5-12
5-2	Measured Torques During Removal of Components of	
	Focus Mechanism	5-13
5-3	Resistances of Shutter Assembly Coils	5-14
6-1	Results of Emission Measurements of Flight Vidicon	
	and Two Spare Vidicons	6-12
6-2	Results of Gas Ratio Measurements	6-14
6-3	Results of Gas Content Measurements on Samples	
	From Spare and Surveyor III Vidicons	6-28
6-4	Results of Microprobe Tests of Samples of Grid 5 Mesh	6-33
7-1	Types and Quantities of Electrical Components	7-2
7-2	Resistor Test Plan Summary	7-4
7-3	Resistance Versus Temperature Characteristics of	
	Platinum Resistance Thermometer	7-12

7-4	Capacitor Test Plan Summary	7 - 14
7-5	Summary of Leakage Tests on Seven Tantalum	
	Capacitors	7-16
7-6	Diagnostic Tests of Metallized Paper-Mylar	
	Capacitors	7-21
7-7	Results of Measurements of Capacitance of	- 22
	Glass and Mica Capacitors	7-22
7-8	Diode Test Plan Summary	7-26
7-9	Functional Tests of High Speed Switching	7. 30
	Diodes 1N3070	7-28
7-10	Functional Tests of Switching Diodes 1N3730	7 - 30
7-11	Functional Tests of Zener Voltage Reference	7 - 30
- 12	Diodes Figure 1 Tracks of Zonor Voltage Regulator	7-30
7-12	Functional Tests of Zener Voltage Regulator	7-32
7 12	Diodes 1N754A Functional Tests of High Voltage Diode Stack	, 3-
7-13	FA3075	7-34
7-14	Functional Tests of Silicon Controlled Rectifiers	
/ - 1 '±	2N1930	7 - 34
7-15	Transistor Test Plan Summary	7 - 35
7-16	Number of Transistors Tested on Chassis Versus	
, 10	Total on Camera	7 - 38
7-17	Functional Tests of General-Purpose Amplifier	
	Transistors NPN 2N718A	7-40
7-18	Functional Tests of General-Purpose Amplifier	
	Transistors PNP 2N722	7-40
7-19	Functional Tests of High Frequency Transistor	_ 40
	2N2192A	7-42
7-20	Functional Tests of High Voltage Transistors	7 42
	2N871	7-42
7-21	Comparison of VCE(sat) Measurements of High	7-44
	Voltage Transistor	7-44
7-22	Functional Tests of Power Transistor 2N1936 Functional Tests of Low Noise Transistors 2N2586	7-46
7-23	Mechanical Components Test Plan Summary	8-2
8-1	Summary of Potentiometer Tests	8-5
8-2 8-3	Measurements of Tests of Toroidal Inductors	8-10
8-4	Results of Temperature Cycling of Thermal Switches	8-14
9-1	TV Azimuth Mirror Tests	9-4
10-1	TV Camera Materials Selected for Test and	•
10-1	Evaluation	10-2
10-2	Circuit Board Materials	10-5
10-3	Solder Joint Pull Strength Test Results	10-10
10-4	Circuit Peel Strength Test Results	10-11
10-5	Hardness of Circuit Board Samples	10-13
10-6	Results of Visual Inspection of Conformal Coatings	10-20
10-7	Results of Electrical and Physical Measurements	
	of Conformal Coatings	10-22

10-8	Electrical	Measurements	of Potting	Compounds

- 10-9 Results of Hardness Measurements of Potting Compounds
- 10=10 Measurements of Tensile Strength and Elongation of Organic Materials
- 10-11 Surveyor III Camera Adhesives Tested
- 10-12 Measurements of Hardness of Adhesives
- 10-13 Measurement of Shear Strength of Adhesives
- 10-14 Surveyor III Camera Gears and Bearings
 Examined for Wear
- 10-15 Results of Friction Test of Worn Area of Surveyor III Focal Length Potentiometer Wire
- 10-16 Results of Friction Test of Unworn Area of Surveyor III Focal Length Potentiometer Wire
- 10-17 Relative Values of Friction Coefficients for Lubricated and Unlubricated Surfaces
- 11-1 Reflectance Measurements of Samples From Lower Shroud of Surveyor III Camera
- 11-2 Variation of Reflectance With Times as Result of Photo Bleaching
- 11-3 Effect of Thermal Bleaching (Vacuum Versus Air) on Spectral Reflectance of Irradiated Samples of Inorganic White Paint Used for Surveyors
- 11-4 Comparison of Several Techniques for Assessment of Fractional Area Covered by Lunar Dust
- 11-5 Possible Sources of Dust Contribution to Discoloration
- 12-1 List of Anomalies
- 12-2 Failure Analysis Summary Matrix
- 12-3 Summary of Components of Surveyor III Camera With Cracked Glass Envelopes
- 12-4 Electrical Component Anomalies Induced by Lunar Environment
- A-l Program Tasks
- A-2 Surveyor III TV Camera Test Log Books
- B-1 Solar Energy Distribution
- B-2 Ultraviolet Radiation Spectrum at 1 AU
- B-3 Some Twentieth Cycle Solar Proton Events
- B-4 Nineteenth Cycle Solar Proton Events
- G-1 Mass Spectrometer Measurements of Gas Samples From Spare and Surveyor III Vidicons
- H-1 Electrical Components in Surveyor III TV Camera
- H-2 Location of Components Selected for Tests on TV Chassis
- H-3 Potentiometer Noise Measurements Ambient and Vacuum Tests
- I-1 Measurements of Capacitance of Internal Harness
- I-2 Measurement of Conductor Resistance of Internal Harness

[-3	Measurements of Resistance of Contact to wife Junction of J2 Connectors	I-6
[-4	Results of Microhardness Tests of Internal	
L - 1	Wire and Cable	I-6
[-5	Measurement of Tensile Strength and Elongation	- 0
	of Internal Wires and Cable	1-8
I-6	Results of Measurement of Insulator Cut-	т 12
	through Ratings	I-12
I - 7	Measurement of Tensile Strength of Connector	I-13
	Solder Joints in Internal Cable Connector	1-15
I-8	Results of Elemental Analysis of Organic	I-18
	Materials	1-10
I-9	Electron Paramagnetic Resonance Measurements	I-20
	of Organic Materials	
J-1	Normal Emittance Measured on Lower Shroud	J-13
	Surface Percent of Spectral Reflectance Versus Wave	
J-2	Length of Samples From Surveyor III Camera	
	Connector Bracket After Exposure to White	
	Light Photo Bleaching	J-27
J - 3	Samples of Surveyor III Camera Shroud Cut in	
J – J	July 1970 for Science Studies	J - 33
J-4	Percent Reflectance of Samples From Surveyor	
J - 1	III Camera Shroud Cut for Science Studies in	
	July 1970	J-34
J-5	Percent Reflectance of Samples From Surveyor	
	III Camera Shroud Cut for Science Studies in	T 2/
	October 1970	J-36
J-6	Effect of Thermal Annealing in Air on Spectral	
	Reflectance of Samples Cut From Lower Shroud	J-37
	of Surveyor III Camera in October 1970	J = J1
J - 7	Effect of Thermal Annealing on Spectral	
	Reflectance of Surveyor III Camera and Labora-	J-38
	tory Samples of White Inorganic Painted Surfaces	5-30
K-1	Relative Contents of Copper, Manganese, and	K-4
_	Chromium in Connector and Shroud	
K-2	Results of Detent Breakaway Voltage and Current	K-15
T. 0	Measurements of Shutter Assembly Measured Electrical Characteristics of Open	<u></u>
K-3	Diode With Contact Restored by Lead Manipulation	K-21
V 1	Voltage Characteristics of High Leakage Diode	K-22

1. SUMMARY

1.1 INTRODUCTION AND BACKGROUND INFORMATION

This report presents the results of the tests conducted by the Hughes Aircraft Company during the period 7 January to 31 December 1970 on the Surveyor III television camera returned from the moon by the Apollo XII astronauts. This program was conducted under a contract with the Jet Propulsion Laboratory (JPL) of California Institute of Technology. A separate report (Reference 1) contains the results of tests conducted during the same period under a companion contract with NASA Manned Spaceflight Center (MSC), Houston, on the other parts of the Surveyor III spacecraft retrieved by Apollo XII, namely, the scoop of the soil mechanics/surface sampler (SM/SS), painted and unpainted sections of the aluminum support tubing of Surveyor, and sections of external cabling and of their teflon wrapping.

Surveyor III, one of seven Surveyors designed and built by Hughes, was the second of five spacecraft to land successfully on the surface of the moon. This soft landing took place 20 April 1967 in a small crater in the Ocean of Storms, subsequently named the "Surveyor Crater." All subsystems operated successfully throughout the first lunar day except for some minor anomalies. Three of these involved the television camera and have now been completely resolved, as discussed in the report. The television camera took more than 6000 photographs of the lunar terrain. Attempts to revive the spacecraft on the second lunar day were unsuccessful.* A brief summary of mission performance of the Surveyor is presented in Table 1-1.

As is well known, 2-1/2 years later, corresponding to 32 lunar day/night cycles, the lunar module of Apollo XII landed nearby. In accordance with that part of the mission plan, based on recommendations by Hughes (Reference 2), JPL, and others, the Apollo astronauts retrieved the Surveyor television camera and the other parts noted above after examining and taking a number of photographs of the spacecraft.

^{*}Survival of Surveyors throughout lunar nights was not a design requirement.

TABLE 1-1. SUMMARY OF MISSION PERFORMANCE OF SURVEYORS

Surveyor Spacecraft				Operation on Successive Lunar Days		
Design Class	Number	Major Payload	First Lunar Day Operation	Response to Commands	Photographs	Remarks
First- generation	I	Television camera	Nominal	2, 5, 6, and 8	2	Activation not attempted on third, fourth, and seventh day
	2	Television camera	(Unsuccessful)			Tumbled after mid- course maneuver
	ш	Television camera SM/SS	Nominal	None	None	Abnormal landing (several hops)
	4	Television camera SM/SS	(Unsuccessful)			Loss of communication during retro burning
Second- generation	v	Television camera Alpha scattering experiment	Nominal	2 and 4	2	Activation not attempted on third day
Improved design	VI	Television camera Alpha scattering experiment	Nominal	2	None	
	VII	Television camera SM/SS Alpha scattering experiment	Nominal	2	2	Activation not attempted after second day

The decision to retrieve the television camera and other hardware followed a comprehensive study of benefits to be accrued from and relative merits and difficulties of retrieving various parts of the Surveyor space-craft. In addition to listing the scientific benefits, the study (Reference 2) underlined the unique opportunity to obtain information on the effects of thermal cycling, radiation, and meteoroid exposure; the occurrence of cold welding; and the consequences of prolonged vacuum exposure of optics, materials, components, and subsystems for application to future programs.

The selection of the camera as a prime candidate was prompted by the fact that it was a readily retrievable package containing a great variety of candidate parts for such an investigation: electrical components and circuits, optical components and surfaces, mechanical and electromechanical units and components, a great variety of materials, and other items of value.

The frontispiece of this report shows the appearance of the retrieved camera, whose functional description is given in Section 2.3. The smudge visible on the mirror was made intentionally by one of the astronauts on the lunar surface in the course of photographing the camera. This was

done as a contingency measure in the event the retrieval of the camera was not possible; photographs of the mirror before and after this imprint would thus yield some data on the degree of contamination of the mirror surface. The camera was returned in a backpack in the lunar module and command module cabin environments. A severe jolt, probably experienced at the time of the landing of the Apollo command module in the Pacific Ocean, may have caused the dents on the camera hood, clearly visible in the frontispiece.

The camera was delivered to the Lunar Receiving Laboratory (LRL) in Houston and remained in quarantine until 7 January 1970. During the period from 7 to 16 January, a microscopic visual examination and extensive photography were conducted in the LRL, and tests were performed for the purpose of obtaining scientific data. These operations, described in Section 3.2, included a number of biological samples of protected external as well as internal regions of the camera. In order to perform these tests, the lower shroud of the camera was removed by Hughes personnel. Preparatory tests and trial runs were performed in Los Angeles on a spare television camera available from Surveyor stores prior to the release of the Surveyor III camera from quarantine.

The camera was shipped on a Hughes airplane on 16 January to the specially prepared Hughes facility in Culver City, California. The formal test and evaluation program was then initiated under the technical direction of JPL. The program entailed strict parts control and security measures and carefully planned and sequenced testing and dismantling procedures tailored to maximize the amount of information obtained for potential future applications. These operations were conducted in full cognizance of the uniqueness of the equipment and irreversibility of many of the steps. The management of the program is described in Appendix A.

1.2 OBJECTIVES AND SCOPE OF TEST AND EVALUATION PROGRAM

1.2.1 Objectives

The primary objectives of this study were to determine the various effects of the prolonged exposure to the lunar environment on the many component parts of the television camera. The test plan was structured to obtain maximum information on those conditions and changes which could be attributed to the effects of this exposure.

The study of the returned hardware offered a unique engineering opportunity. It was believed that the assessment of the conditions of the various camera components, materials, and subsystems would yield valuable engineering design data for future applications and could point out fruitful areas for research and development.

The returned hardware also presented a unique scientific opportunity. A parallel scientific investigation on the returned Surveyor parts, instituted under NASA-JPL coordination, was vigorously supported as a secondary objective of this program. In addition to active participation

in some of the tests, particular effort was made in the planning of the test operations to preserve a maximum amount of material and inherent conditions of value to the scientific investigations. Results of the science tests and evaluation program will be reported separately.

It was specifically understood at the inception of this program and throughout the study that testing and analysis of the television camera solely for the purpose of obtaining diagnostic data on the design integrity and the performance of the Surveyor III television subsystem was not a program objective.

Further discussion of the objectives of this program in terms of expected and accrued benefits is presented in Section 2.1.

1.2.2 Scope

The program tasks corresponded to the major categories of the above subsystems, components, and materials present in the camera. In accordance with the established ground rules discussed later in this report, no overall system tests were conducted. However, selected chassis were functionally tested before dismantling the camera in order to determine the integrity of circuits and to provide a basis of selection of samples of the various types of electrical components for subsequent investigation.

The tasks (listed in Table 1-2) thus constituted the scope of the program. The bulk of the program was conducted in three phases.*

Phase I concerned tests performed prior to major camera disassembly. These included the operations in the LRL and the subsequent initial survey operations at Hughes. Phase 2 operations encompassed tests at the subsystems level and the associated dismantling steps. Included in this phase were the functional tests of selected electronic chassis, optical subassemblies, and the vidicon. Phase 3 operations entailed detailed investigations of the selected camera components and materials after its complete disassembly.

An important feature of this test plan was the recognition and establishment of significant milestones, designated as decision points. Results of test operations prior to each of these milestones were carefully assessed and formed the basis for program decisions to either pursue the previously formulated test plans and procedures or to alter them appropriately. This was done to meet the objective of optimizing the amount of relevant information in recognition of the uniqueness of the hardware and of the irreversibility of the tests.

^{*}This is discussed in some detail in Section 3.1, <u>Test Plan</u>, and depicted diagramatically in Figure 3-1 there.

TABLE 1-2. PROGRAM TASKS AND REFERENCED REPORT SECTIONS

Test Phase	Task	Sections of Report
1	MSC Houston operations	Section 3
	Survey operations	Section 3
	Electric circuits tests	Section 4 and Appendices D, E, and F
_	Dismantling	Included in Sections 4 and 5
2	Optical subassembly and mechanism tests	Section 5
	Vidicon tests	Section 6 and Appendix G
	Electrical components tests	Section 7 and Appendix H
3	Mechanical and electromechanical components tests	Section 8 and Appendix H
3	Optical components tests	Section 9 and Appendix H
	Materials tests	Section 10 and Appendix I
	Surface contamination studies	Section 11 and Appendix J
All	Failure analysis	Section 12 and Appendix K
	Support of science investigations	As applicable

Selection of components was closely coupled to the results of the functional tests of the electronic chassis and to the results of other previous tests performed on the assembled or partially disassembled camera.

The test program outlined above entailed a detailed assessment of all or of appropriate representative samples of the following classes of units, components, and materials present in the television camera, whose examination for possible effects of lunar exposure was believed to be of importance to future space programs:

- Optical surfaces (mirror lenses and filters)
- Thermal control surfaces (paints and metals)
- Mechanical devices (gears, drives, bearings, motors, etc.)
- Electrical components (resistors, capacitors, diodes, transistors, and potentiometers)
- Circuit materials and interconnections (circuit boards, terminals, wires, cables, insulation, solder joints, and connectors)

- Magnetic components and transducers (inductors, thermal switches, temperature sensors, stepping switches, and solenoids)
- Vidicon tube and its elements (cathode and grid structure, photoconductor and its coatings, seals, deflection yoke, and content)
- Insulation materials (potting compounds, polyurethane foam, and conformal coatings)
- Organic materials (teflon TFE and FEP, nylon, and polyimide)
- Adhesives, lubricants, and seals (various types), including friction and wear studies

These tasks represented preplanned, "routine" tests. In parallel with these, a separate failure analysis task and special surface contamination studies were instituted.

The failure analysis task was conducted to resolve the previously reported mission anomalies, as well as the apparent anomalies or failures encountered in the course of testing. This special attention to failures was prompted by the desire to fully understand the contributory factors of lunar exposure although, as it later became evident, this degree of emphasis may not have been warranted. The anomalies uncovered, as discussed in Section 1.3, were primarily attributable to factors other than the effects of the lunar environment.

The surface discoloration and contamination study, initially considered integral to the materials task, was established later in the program as a special task — a special joint effort between this and the parallel NASA-MSC contract. Its purpose was to determine the nature and causes of the discoloration and contamination of the external surfaces. This study, which was coordinated with the pertinent science investigations by the JPL technical coordinator, also included an attempt to identify the relative contributions of the various possible causes: solar radiation, deposition of organic materials or other products of outgassing from other portions of the Surveyor spacecraft, impingement of lunar dust during the original Surveyor landing and during the Apollo lunar module descent, and even possible prelaunch contamination (e.g., during solar-thermal-vacuum testing).

A separate task was established for the activities in support of the science investigations: biological assay; special visual, microscopic and photographic examinations; optical measurements; removal of selected sections, samples, etc., for evaluation; preparation and transmittal of control samples and background information.

Of major significance to the successful performance of the tests and to the evaluation of results was the availability from Surveyor stores at JPL of spare Surveyor television cameras virtually identical to the retrieved Surveyor III camera, as well as the availability of other Surveyor parts: circuit boards, vidicons, etc. One of these spare cameras had previously undergone type approval tests (TAT). It was used extensively on this program for trial runs of critical dismantling and testing operations and for obtaining test comparison data. The other spare components were similarly used to maximum advantage.

Past Surveyor test procedures, appropriately revised, or specially prepared procedures were used in all test operations. These procedures were coordinated with the customer and were carefully reviewed prior to and during the conduct of each test.

The availability of the original Surveyor camera test position made it possible to conduct the circuit tests. Also, the availability of past Surveyor records obtained from Hughes Surveyor stores, including design data and, in many cases, previous test data, proved of value in evaluation of the results of tests at all levels: circuits, subsystems, components, and materials.

The test program of the retrieved television camera was fully coordinated with the parallel NASA-MSC sponsored program of tests of the other retrieved Surveyor III parts. The close coupling of test results obtained on similar parts, especially cabling, organic materials, and mechanical parts, proved to be of benefit to both programs. In particular, the surface discoloration and contamination study task was logically conducted as a joint effort.

Included in the companion report (Reference 1) are comments relative to certain other parts of Surveyor III which were not recovered—thermal compartment mirrors and solar panel. The comments were based on a preliminary engineering assessment of the photographs returned by the Apollo XII astronauts, coupled with the study of their comments when viewing the spacecraft on the moon. This assessment is by no means complete, and future studies may be useful.

1.2.3 Supplementary Notes on Report Organization

Results of work conducted on the tasks described above are presented in individual sections of this report, as shown in Table 1-2, with selected supplementary data in the appendixes indicated. Results of work done by the Bell and Howell Company under a Hughes subcontract, which consisted of an examination of the lens barrel subassembly, are included in the discussion of the optical components listed in Table 1-2. Some of the principal activities involved in the support of science investigations are included in Sections 3.2, 9.2, and 9.3.

TABLE 1-3. RESULTS OF INVESTIGATION OF SPECIFIC ANOMALIES

	Effect of Lunar Environment		Significance	
Anomaly	Primary Cause	Secondary or Contributory Cause	To Future Operations	To Surveyor III TV Camera
Surveyor III Mission Anomalies				
Inoperative filter wheel potentiometer	No	No	Negligible	Minor
Occasional difficulties with stepping in azimuth	No	No	None	Minor
Veiling glare	Yes		Could be appreciable	Moderate
Effects on Optical and Exterior Surfaces				
"Mud-cracking" of external painted surfaces	No	Yes	Minor	Minor
Dust on filter glass	Yes		Negligible	Minor
Discoloration and curling of teflon skirt	Yes		Minor	Minor
Discoloration of external painted and other surfaces*	Yes		Major	None
Open Shutter and Related Failures				
(Burnt out transistor, shorted solenoid, evaporated vidicon photoconductor, and torn grid)	No	Minor, if any	Negligible	Major
Defective Electronic Components				
Cracked glass cases	Yes		Minor	None
Defective diodes	No	Some	Negligible	Minor
Shorted tantalum capacitor	Yes		Minor	Major
Two burned out obsolete components	Yes		None	Major
Suspected Cold Weld of Connector Shell to Shroud	No	Yes	Negligible	None
Four Miscellaneous Minor Anomalies	No**	No***	None	None**

^{*}Included for completeness. As noted, this was not considered an anomaly and is treated in detail in Section 11. Also, see Sections 1.4 and 1.6.1.

^{**}With one relatively insignificant exception.

^{***}With one relatively minor exception.

In addition to the specific task references in Table 1-2, other sections of the report should also be noted. An expanded discussion of program objectives and scope, additional details on background data, a description of the television camera, and a discussion of its test history and mission performance are all presented in Section 2. The general test plan is outlined in Section 3.1. Program management is discussed in Appendix A. A brief discussion of the lunar environment is given in Appendix B. Test facilities and the checkout of test equipment are described in Section 4.4 and in Appendix C.

Each technical section of the report is essentially self-contained and includes discussion and evaluation of tests conducted and results obtained. While individual concluding comments are presented in each section as they arise, the overall program conclusions and recommendations are presented here in this section.

1.3 ASSESSMENT OF ANOMALIES

Results of failure analysis are presented first because of the concern which is generally associated with anomalies and because of the occurrence of several anomalies during the Surveyor III mission operations. It is shown below that, actually, the effect of the lunar environment on the specific anomalies uncovered in the course of the program was relatively minor. The significant observations and results were almost entirely in other areas of investigation — those concerned with systematic testing of the various parts of the camera. These revealed certain data on significant effects of the lunar exposure not in the nature of failures or produced significant findings on the absence of anticipated effects. These findings are summarized later in this section, following the treatment of the findings designated as failures or anomalies. The added virtue of discussing these specific anomalies first and thereby dispensing with significant effects caused by factors other than the lunar environment is that lunar exposure effects can then be assessed more systematically.

A failure analysis was conducted on 20 specific anomalies identified and so designated in the course of the program in coordination with JPL. The system employed for the treatment of these anomalies and a detailed discussion of test results are presented in Section 12, and only a summary assessment is presented here. Included are the three Surveyor mission anomalies discussed in Section 2.4, which were verified and resolved in the course of this study.

These 20 anomalies, listed in Tables 12-1 and 12-2 in Section 12, are grouped here in Table 1-3 into the six categories shown. Two considerations were stressed in the study of these anomalies: 1) the extent to which the lunar environment was a primary or a contributory cause and 2) the degree to which these anomalies have a potential bearing on future

applications. Table 1-3 presents in summary form the conclusions reached relative to these important considerations. Also included in Table 1-3 is the relative significance of these anomalies to the operability of the Surveyor III television camera.

The first two of the three mission anomalies in Table 1-3 were determined to have been caused entirely by prelaunch events. The guide of the filter wheel potentiometer was manufactured with defective material and was probably cracked before launch. The guide broke during mission operations and fell out of the potentiometer winding, partly as a result of a binding of the rotating guide block to the end seal (caused by somewhat less than perfect alignment during installation) and partly because the potentiometer had not been properly lubricated. The missing steps during camera positioning in azimuth were found to have been caused by several bent and worn teeth in two specific areas of the azimuth drive gear, corresponding precisely to the positions of the motor drive pinion and potentiometer gears in contact with the drive at the time of the occurrence of these anomalies on the moon. This problem was definitely attributable to occurrences in prelaunch tests.

The veiling glare was determined to have been caused by dust on the mirror, confirming the hypothesis at the time of the mission. No similar effects had been observed for other Surveyors; the contaminant was deposited as a result of the abnormal Surveyor III landing. The landing of the lunar module nearby clearly affected the contamination on one side of the camera and possibly on the mirror and filters as well. This contamination of the camera constituted one of the dominant effects observed. The small film deposit noted on the beamsplitter plates of the lens* might have contributed to the veiling glare had the camera been able to operate on the second lunar day.

In addition to the discoloration of the paint and the contamination of the mirror and of the filter glass, specific findings which were classed as anomalies included the observed extensive "mud-cracking" of the paint, and the discoloration and curling of a teflon skirt used as a seal between the upper rotating mirror assembly and the camera body. Mud-cracking, observed after prelaunch tests, was definitely aggravated by the lunar exposure and could be of significance to future applications because of the wide use of paints of this type for thermal control. The discoloration of teflon was due to an excessive application of bonding epoxy over exposed areas of the skirt. The curling, which may have been aggravated by the blast from the landing of the lunar module, was also found to be attributable to this epoxy, hardened by lunar exposure. The effects on external surfaces are discussed in more detail later in this section.

^{*}Probably caused by outgassing from nearby charred solenoid coil (discussed in Section 12.5).

While some of the remaining anomalies were of major significance to the integrity of the Surveyor camera, they were unimportant to future applications. Many of these were found to be entirely unrelated to the lunar environment. Those that were occurred as a result of the cryogenic thermal cycling through the lunar nights. They either occurred on components of obsolete design or on components whose design shortcomings were recognized and for which corrective measures are available for the future — particularly by means of better matching of thermal expansion coefficients. The occurrence of these component failures under cryogenic conditions had been anticipated.* In fact, it was surprising that so few of them had, indeed, failed, thereby confirming the appropriateness of prior cryogenic screening as a precautionary measure.

The most interesting of these anomalies was the complex, interrelated open shutter failure: burned out shutter drive transistor, shorted and charred shutter solenoid coil, evaporated vidicon photoconductor, and shattered vidicon grid 5 mesh. The considerable effort expended to unravel these anomalies and their interrelationships was originally motivated by the desire to obtain sufficient understanding so as not to overlook possible important factors of lunar exposure. In retrospect, since the contributions of lunar exposure proved of strictly secondary or relatively minor nature, this effort might have been less intensive.

The analysis presented in Section 12.5 led to the following explanation of this anomaly. Surveyor III was launched with a known suspect transistor with a somewhat degraded voltage breakdown characteristic, possibly stressed in test. This decision was vindicated by the spacecraft's successful performance on the first lunar day. The transistor, possibly further degraded by the effects of thermal cycling through the lunar nights, failed upon the application of voltage during the attempts to revive the spacecraft on the second lunar day. The cause of this occurrence may have entailed a failure of a solder joint elsewhere on the spacecraft and is explained in Section 12.5. The resulting current through one of the shutter solenoids permanently opened the shutter and subsequently damaged the coil. The vidicon photoconductor and grid 5 were subsequently damaged by solar radiation impinging through the open shutter in a manner verified by thermal simulation tests conducted in this program.

The cracked glass cases constituted a lunar-induced anomaly whose existence was anticipated. This cracking had been noted to occur in thermal-vacuum tests prior to launch and is attributed to mismatch in thermal expansion coefficients between the glass and the conformal coatings used. Remedial measures consisting of an improved process to prevent thick buildup of coated areas are available and were used in later Surveyors.

^{*}See footnote, page 1-1.

Improved conformal coating materials are also available. The two occurrences of faulty diodes partially triggered by the associated cracking of the glass cases were, in fact, traced to specific manufacturing deficiencies or weaknesses.

The failure of the tantalum capacitor as a result of the cryogenic exposure was not unexpected. It was surprising that only one of the 76 such units had failed. Surveyor III was launched with this knowledge of likely cryogenic failures, and design improvements were instituted on later spacecraft. Capacitors better capable of cryogenic survival are available for future designs. The information obtained here can be of significance in assessing the adequacy of such components. It also attests to the usefulness of preflight cryogenic screening. Similarly, the two other failed components, a metal film resistor and an alloy transistor, both of obsolete design, came as no surprise except, perhaps, to note that again only one of 33 such resistors and only one of 49 such transistors present on the camera had failed. These components were largely replaced in subsequent Surveyors and are not expected to be used for future space applications.

The analysis of the contact surfaces of the connector shell and camera shroud, where excessive binding was noted during the original removal of the connector, revealed that cold welding may have occurred. * It was determined that this was to a large extent due to a faulty installation: a loose fit of the connector permitted excessive rubbing to take place, thereby facilitating this occurrence. This anomaly, of no significance to the television camera, was investigated in some detail because of the general concern over cold welding for future applications. Assessment of the significance of this finding should be made with the realization that a simple precaution, such as elimination of the possibility of movement or rubbing, would have prevented this anomaly. No other properly installed connectors, screws, or similar fasteners on the returned camera showed any evidence of cold welding.

The other miscellaneous anomalies on Table 1-3 were of very minor significance. Their analysis and causes are discussed in Section 12.

^{*}This was the only specific evidence of possible cold welding uncovered in the entire test program except for some traces of possible cold welding on the surfaces of the potentiometer windings which had not been lubricated, as discussed in Section 10.6.3.

1.4 OBSERVED CHANGES ATTRIBUTABLE TO LUNAR ENVIRONMENT

A summary of the most significant findings, other than the specific twenty anomalies above, relative to the effect of the lunar environment on the subsystems, components, and materials of the television camera is presented in this subsection and the next. The observed changes attributable at least in part to the lunar exposure are described in this section; the following section discusses the absence of effects that might have been conjectured or anticipated. A list of such possible effects had previously been prepared (Reference 1).

The observed effects attributable to the lunar environment are summarized in Table 1-4. Detailed discussions of these, as well as of other less significant observations and changes which were determined not to have been caused by the lunar exposure, are presented in the individual sections of the report.

1.5 ABSENCE OF CONJECTURED EFFECTS OF LUNAR ENVIRONMENT

Those significant effects of the lunar environment which had been either anticipated or conjectured but for which no evidence was uncovered in the course of the program are presented in Table 1-5 in summary form. Supplementary discussion and supporting test data are contained in the individual sections of the report.

The observed instances of the absence of effects of lunar exposure may be used for the establishment of design limits. Caution should be exercised in the interpretation of these observations. Absence of these effects, reported in this section, is based on a limited number of samples and components and on one specific set of exposure conditions.

1.6 CONCLUDING COMMENTS AND RECOMMENDATIONS

A test program embracing so many diverse disciplines and detailed findings yields two categories of conclusions and recommendations: those of a general nature and those pertaining to specific design areas. In arriving at these conclusions and recommendations, the applicability to future designs, space programs, and research activities played a dominant role.

Conclusions and recommendations of a general nature, cutting across all the areas of investigation, are presented in Section 1.6.1. Specific conclusions are contained in Tables 1-4 and 1-5; these give rise to certain specific recommendations for design precautions and improvements presented in Section 1.6.2. Section 1.6.3 lists some examples of possible additional tests on the returned hardware. While it is believed that the engineering tests conducted on this program have explored all important areas of interest, further test effort might be productive for specific design applications.

TABLE 1-4. OBSERVED POSSIBLE EFFECTS OF LUNAR ENVIRONMENT

Components, and Materials	Observed Effects	Remarks
Vidicon		
Gas content	Hydrogen 70 percent versus 50 percent in spare unit. Helium 7 percent versus 1/2 percent in spare unit. Nitrogen 4-1/2 percent versus 43 percent in spare unit. Carbon dioxide 1/2 percent versus 3 percent in spare unit.	Difference could also be attributed to original manufacturing process.
Beam current	50 percent less than for spare unit (cathode current unchanged).	May be attributed to absence of focusing by grid 5. Reduction also expected after prolonged operation.
Wire-wound power resistors	1200 ohm resistor decreased by 2 percent. 200 ohm resistor decreased by 1 percent. No internal changes seen.	Value still within specifications. Could be caused by annealing.
Platinum resistance thermometer	Changed calibration (reduced resistance). Temperature coefficient decreased by 4 percent.	Could be caused by annealing. Could be caused by changes in electrical properties of bonding cement.
Tantalum capacitors	High leakage current on several units (one out of specification). High slope of leakage versus temperature (several units).	Possible correlation with low original forming voltage. All units still functionally adequate.
High speed switching diodes	One unit exhibited slightly higher leakage.	24 hour baking at 125°C restore original characteristics. Attributable to moisture penetration through cracked glass case.
Potenti- ometers	Somewhat higher noise and starting torques. Evidence of considerable wear. Some evidences of cold weld traces on wires.	Attributable to absence of lubricants. No information obtained on performance of lubricated potentiometers.
Thermal switch	Operating limits widened (0-10°C versus 0-6°C specification). No evidence of internal degradation.	Could be due to environment and the shearing forces in bimetalli disk. Might also have been launched in this condition.
Mirror	Several discoloration bands of varying thickness.	Presumed to be lunar dust. Shadowing by surrounding surfaces noticeable.
	Reduced specular reflectance:	Presumed caused by lunar dust
	Original value: 88 percent "Dirty" region: 10 to 15 percent (February 1970) 20 to 30 percent (April 1970)	Improvements attributable to partial loss of dust in handling.
	Clean region: 50 to 60 percent (April 1970)	
Lens barrel subassembly	Film on beamsplitter plate.	May be attributable to nearby burned shutter coil.
	Optical transmission degraded from 65 percent to 60 percent (primarily at shorter wavelengths).	Lens functionally acceptable.
	Some increase in focal length adjustment torque.	

Table 1-4 (continued)

Subsystems, Components, and Materials	Observation Effects	Remarks
Teflon/	Flaking off:	
polyimide wire coatings	1) Under exposed nylon tie wraps. 2) Near epoxy used to secure ties. 3) Near harness bends.	Two suspected contributory causes: 1) Abrasive action of tie cords. 2) Thermal cycling (improved materials available).
	Degraded physical properties of polyimide: Lower tensile strength and elongation.	
Wire and cable conductors	Lowered tensile strength, depending on exposure: 10 percent reduction of some internal wires. Over 50 percent reduction of external cables.*	Believed to be result of annealing.
Polyurethane foam	Absence of isocyanate	Attributable to chemical reaction at elevated temperatures. Negligible effect on performance. Outgassing may affect nearby parts.
Conformal coatings	Extensive axial cracking: (Particularly severe for coatings thicker than 0.1 inch). Glass-case diodes and resistors. Metal-case transistors and capacitors. Ceramic-case resistors. Gold-plated terminals.	Attributable to thermal cycling and differences in thermal coefficients. Chemical and physical tests eliminated other hypothesized mechanisms.
	Induced cracking of many component glass cases.	Bonds apparently still strong.
Teflon Cable wrap (TFE) Conductor insulation (TFE, FEP) Collar and seal (TFE)	Degraded physical properties. Reduced tensile strength. Lower elongation.	Extent of change apparently dependent on degree of exposure. Conclusive data on this relationship not available.
Adhesives Polyamide FM-1000	Darker color Cracking: Fiberglass-to-aluminum bonds. Adhesives to gold-plated circuits.	Difference in thermal coefficients believed to be the cause of cracking and decreased shearing strength.
	Change of physical properties: Increased hardness (exposed adhesives).	Lower shearing strength also attributed to hardening.
	Decreased shearing strength. Enbrittlement (FM-1000 only).	Enbrittlement of FM-1000 attributed to elevated temperatures of resultant outgassing of volatiles.
Gears	Galling Dearth of lubricants.	Microseal lubricant appears margina Application process caused cracking. Molybdenum disulfide lubricant rubbe off.
Bearings	Insufficient lubrication.	Lubricant apparently wore off or was wiped off.
External surfaces Paints Metals	Contamination by dust. Cracking and darkening of white organic paint. Cracking, color change, and change in optical properties of white inorganic paint.	Radiation damage proportional to solar exposure. Dust effect larger than expected.

^{*}Obtained in tests conducted on companion NASA/MSC contract (Reference 1).

TABLE 1-5. SIGNIFICANT OBSERVATIONS RELATIVE TO ABSENCE OF EFFECTS OF LUNAR ENVIRONMENT

Subsystems, Components, and Materials	Significant Observations and Test Results	Remarks
Camera and its	All torque values nominal (screws, nuts,	
various subsys- tems (dis- mantling oper- ations)	fasteners, etc.). No additional evidence of cold welding.*	
Electric circuits 3 chassis checked	All measured circuit functions nominal except for specific anomalies in Table 1-3.	
functionally 5 chassis checked passively	All passive checks nominal, except for specific components anomalies in Table 1-3.	
Vidicon	Retention of vacuum $(10^{-2} \text{ to } 10^{-3} \text{ Torr range})$.	Validated by three techniques: Pirani gauge Gas ratio Gas content
	No apparent structural changes.	
	Nominal heater and cathode emission.	
	Nominal electrical and functional parameters (those which could be measured in the absence of photoconductor and grid 5).	Functional measurements include Cutoff. Beam transmission. Beam transfer.
	Nesa coating apparently intact.	
	Indium seal intact.	
Optical sub- assemblies and mech-	Functional parameters nominal: Operating voltages. Torques and stepping rates.	Both ambient and vacuum tests conducted.
anisms	No apparent degradation of components: Motors, drives, gears, etc.	
Resistors Carbon	No evidence of changes of characteristics:	Selected units internally examine
composition Carbon film Precision	Resistance values. Noise. Temperature and frequency dependence.	
wirewound	No evidence of internal changes.	
Capacitors Metallized paper/mylar	No significant changes in parameters — slightly lower capacitance of paper/mylar units.	Selected units internally examine
Glass Mica	No degradation of mica insulation.	
Mica	No evidence of internal changes.	
Diodes	Functional parameters unchanged.	Selected units internally examine
High conduc- tance switch Zener (2 types) High voltage stacks Silicon control rectifiers	No evidence of internal changes.	

^{*}Except for connector shell anomaly (Table 1-3) and traces on potentiometer windings (Table 1-4).

Table 1-5 (continued)

		Г
Subsystems, Components,		
and Materials	Significant Observations and Test Results	Remarks
Transistors General-purpose (2 types) High frequency High voltage Power Low noise	Function parameters unchanged, except high noise figure of one transistor. No evidence of internal changes.	Selected units were internally examined. Intermetallic growth observed: Accounts for high noise figure. Attributable to Al-Al bonds (no longer used). Not unusual after prolonged storage.
Mechanical components Motors (2 types) Inductors (2 types) Connector	No change in functional parameters and internal structure of motors: Electrical parameters. Torques and stepping rates. Magnetic components nominal. No change in connector characteristics: Contact and insulation resistance. Separation forces.	One motor and inductors examined internally. Peeling of connector gold plating: Due to original contamination. Aggravated by lunar environment.
Optical components Mirror Lens barrel	No physical changes of mirror: No delamination. No significant change in flatness. Good lens resolution and image contrast. No significant changes of lens barrel subassembly.	Flatness not measured originally. Lens barrel not disassembled.
Wire and cable	Good appearance of harness: Teflon wrap tight and smooth. Internal cable and component leads generally unaffected: No changes in electrical characteristics No metallurgical effects (e.g., microhardness unchanged).	Discoloration of nylon ties due to epoxy.
Circuit boards	Nominal hardness and specific gravity of board materials. No appreciable changes of solder: No cracking and no corrosion. Strong joints and nominal peel strength. Nominal electrical properties. Nominal solderability. No apparent effects on terminals.	
Insulation Foam Potting com- pounds	Foam generally unchanged. No significant effects on potting compounds (filled and unfilled).	Voids observed in potting compounds. Characteristic of materials used. Voltage breakdown onset at 50 volts/mil.
Organics Teflon (FEP and TFE) Nylon ties Polyimide	No chemical changes of significance.	Tests conducted included: IR and UV. Elemental analysis. Viscosity. Electron paramagnetic resonance. Spin determination. Differential thermal analysis.
Adhesives	No significant change in electrical properties. Nominal peel strength.	,
Gears and bearings	No abnormal wear. No evidence of corrosion.	
Potenti - ometers	Nominal characteristics except: Excessive wear due to absence of lubricants. One defective potentiometer (see Table 1-2).	Completely satisfactory performance expected if properly lubricated.
Paints and metals White organic paint Black organic	No unexpected degradation by environment: No loss of adhesion of paints. Evidence of contamination by lunar dust. Evidence of some micrometeoroid impacts but	
paint Polished aluminum	no resultant damage	

It should also be recognized that the assessment of test results, conclusions, and recommendations presented here represent the judgment of only a small number of people. It is expected that for any particular future application the relative significance of some of the finds and recommendations would be viewed differently.

1.6.1 General Conclusions and Recommendations

It is considered in retrospect that return from the moon and subsequent test of the Surveyor III television camera were extremely worthwhile. However, similar return of another Surveyor television camera is not considered sufficiently useful to justify the effort. On the other hand, return of similar hardware from a different space environment is believed to be equally worthwhile and merits serious consideration.

Studies of the returned television camera and its parts are believed to have produced a wealth of useful information of direct applicability to future programs. Significant effects of lunar exposure have been noted. Of perhaps even greater significance is the observed absence of certain effects of the lunar environment that might have been expected or conjectured to occur.

It is believed that the test program has been reasonably comprehensive. Very few areas, if any, of potential value have been omitted from the investigation. Within the limited scope of the program, a fairly complete sequence of tests was conducted on all of the various parts, components, and materials of significance although these tests can by no means be termed exhaustive.

It is recommended that a careful review of the test data contained in this report be made in the course of designs of future spacecraft. It is expected that each particular application will find useful data of pertinence even though the emphasis may vary. Accordingly, depending on the particular areas of concern recognized, additional tests on some of the returned Surveyor III television camera hardware may be worthwhile (see Section 1.6.3 below). Wide dissemination of this report with appropriate recommendations to space system designers is therefore suggested.

Test results generally indicated that the camera hardware withstood the rigors of lunar exposure extremely well. Mechanical, electrical, and optical subsystems and components were generally unaffected, and no significant evidence of cold welding was noted. The variety of materials also withstood the hostile environment with few changes in their properties.

The most striking effects of the lunar environment observed appeared to be those associated with the discoloration of external surfaces. In addition, significant "mud-cracking" of the white organic paint was observed over many of the exposed surfaces. It was determined that the discoloration was primarily the result of radiation change and of contamination by lunar dust, with a relatively minor contribution from organic deposits. The degree of relative contributions of radiation and dust varied from all dust in some areas to all radiation in others, with the majority of exposed surface areas discolored by a combination of these two factors. Radiation-induced effects were proportional to the degree of solar exposure. Dust was generally much higher than expected. The resultant significant reduction of optical properties may be of major consequence to future applications. An assessment of results obtained on this program and further experiments and analysis, such as those indicated in Section 1.6.3, may be warranted.

Of noteworthy significance was the observed pronounced effect of the Apollo lunar module descent engine in blowing lunar dust onto the Surveyor television camera from the relatively large distance of more than 500 feet.

No evidence was noted of serious damage due to micrometeoroid impact or of physical changes due to radiation.

A number of specific failures and anomalies, including the three previously noted Surveyor III mission anomalies, were uncovered. Results of analysis revealed that the lunar environment played a relatively minor role as a primary cause of these anomalies except in those few instances where specific expected electronic component failures occurred. These failures, caused by cryogenic thermal cycling through the lunar night, were fewer than might have been expected. Survivability of these components through the lunar night (some were of obsolete design and were later replaced) was not generally expected prior to launch, * and the relatively small number of failures demonstrates the benefit of prelaunch cryogenic cycling and screening to which such components were subjected for the early Surveyors.

A relatively large number of the anomalies and changes observed were associated with two easily correctable design factors: mismatch of thermal coefficients of expansion between adjacent materials and improper or absent lubrication. Examples of the former are cracks in conformal coatings and associated cracks in component glass cases, degradation of adhesive contacts, cryogenically induced degradation, and failures inside the tantalum capacitor structures. Examples of the latter were found in potentiometers and bearings. These effects can be adequately simulated in the laboratory. Corrective action in these areas is indicated in future designs.

^{*}The Surveyor television camera performed extremely well throughout the first lunar day. The camera would have been rendered inoperable by these component failures.

The importance of adequate prelaunch quality control during manufacture, assembly, and installation was highlighted by some of the anomalies and failures uncovered.

Use of degraded components, or components or mechanisms stressed during prelaunch tests, poses a definite hazard to spacecraft survivability and should be avoided. Many examples in this area can be seen in reviewing the data presented in this report. Particular attention should be paid to ensuring in original inspection and during testing that all hardware is made of specified materials, is not damaged, is properly installed, and that all consequences of possible stress during known anomalous test occurrences be fully explored prior to launch.

It was fortunate and very helpful in assessing test results that control and comparison data were in many instances readily available. An important factor was also the availability of personnel originally involved in the design of the camera and familiar with its test history. The sources for this information included a similar, not-flown, Surveyor television camera; spare Surveyor parts available from stores, such as circuit chassis, vidicons, clear filter, etc.; Surveyor television camera test equipment; and past records, including design data and results of tests. Availability of such control and comparison data is considered vital for the proper assessment of any item of hardware that might be retrieved from space in the future, and adequate prior planning should be conducted to assure this availability.

1.6.2 Specific Recommendations for Future Designs

Specific design suggestions arising from the findings of the program are presented here in the context of the preceding general conclusions and recommendations. They should be viewed only as a set of examples; each individual application requires independent assessment.

Designs of space hardware should be carefully reviewed to ensure that adjacent surfaces are properly matched in terms of coefficients of thermal expansion. Notable examples include adhesives, coatings, and internal structure of electronic components.

Use of lubricants should be critically reviewed both in terms of selection of proper lubricants and from the standpoint of proper installation and verification procedures. For example, Microseal appears marginal for gears; for this application, large gear teeth should not be hard-anodized, etc. Steps should be taken to ensure that the lubricants have not worn in the course of prelaunch testing, such as on gears, bearings, potentiometers, and other critical surfaces in contact.

Manufacturing, inspection, and test records should be carefully reviewed for all components whose failure may be critical to the mission

in order to ensure that components with degraded characteristics are not employed. Particular attention should be given to possible degradation caused by stressing in prelaunch tests. Screening of components (particularly cryogenic screening) whose specifications are marginal or whose design poses some concern has proved valuable and should be employed to the maximum extent practicable.

Care should be exercised in the application of coatings, epoxy, and adhesives to ensure uniformity, use of acceptable processing, and avoidance of excessive amounts. For example, thickness of conformal coatings should be kept within acceptable limits, and epoxy bonding should be confined to the areas of contact.

Selection and use of adhesives should include, in addition to consideration of differential thermal expansion effects, precautions against unwarranted hardening (e.g., by use of resilient materials) and avoidance of bonds over plated surfaces (e.g., gold).

Susceptibility of conventional potting compounds to breakdown at voltage gradients in excess of 50 volts/mil should be recognized and improved materials and/or manufacturing processes developed for high voltage applications.

Where dust contamination is of concern, careful design attention should be given to the sealing and protection of critical mechanisms and of exposed optical and thermal control surfaces. This consideration should include the recognition that the integrity of seals and covers may be degraded by space environment effects, such as differential thermal expansion, hardening of adhesives, etc.

Adequate quality assurance should be provided in original manufacturing processes so that proper materials are utilized and marginal specifications are properly recognized.

Quality assurance in assembly and installation appears to need considerable strengthening. Apparently minor omissions, such as loose fittings or minor misalignments, could have a critical effect on the mission as a result of changes brought about by exposure to the space environment.

Future recovery of valuable hardware from space should carefully consider landing techniques and protection of critical surfaces in the light of specific information desired. For example, if a study of optical surfaces recovered is of importance, the returned parts should be carefully protected from environments (e.g., light exposure, air, etc.). If interaction with the landing terrain is of significance (e.g., lunar dust), the landing should be planned sufficiently far away from the parts to be recovered.

1.6.3 Possible Additional Tests of Parts of Returned Camera

It is recognized that additional science investigation is being and will be conducted on the returned camera hardware. Examples of such work include studies of cosmic ray tracks, solar wind implantation, and micrometeoroid impact.

Several examples of possible additional engineering tests that might be profitably conducted are presented here, without any specific recommendations, as examples of many such possible future activities. The advisability of conducting additional tests depends on the intended application. For any specific future design, an in-depth review of the results presented here will lead to the final selection of such follow-on tests, if any.

It may be of value to conduct certain additional optical tests after removal of the suspect film and/or lunar dust contamination. Included in this category would be optical transmission tests of the lens upon removal of the observed film or specular reflectance measurements of the mirror upon cleaning off of its presumed lunar dust coating.

Disassembly of the lens barrel may be appropriate in order to conduct additional tests of its elements. Included would be the determination of the reason for the observed increase in the focal length adjustment torque.

Additional tests may be useful in determining the possibility and nature of outgassing from the polyurethane foam. This investigation might also include an assessment of the resulting possible chemical reactions with or contamination of nearby materials in a particular space application.

Additional effort may be warranted to determine the cause of the observed degradation of the physical properties of certain organic materials, notably teflon TFE, whose causes remain somewhat uncertain. As indicated, both tensile strength and elongation exhibited a decrease, depending on the degree of exposure.

Certain changes in resistance value of resistors and platinum thermometers, as well as an apparent shift of the calibration of the thermal switch, remain unexplained and may be important to a potential application. Further studies of these observed effects may thus be warranted. For example, the cause of the apparent reduction of the resistance and of the temperature coefficient of the platinum thermometer may be further investigated to determine whether it was caused by an annealing process, whether it was attributable to the change in the electrical properties in the cement used as an adhesive, or whether other factors were involved. The bimetallic disk of the thermal switch might be further investigated as another example to determine whether shearing forces have been generated by lunar exposure which might account for the widening of its actuation limits.

More detailed tests might be considered for some of the capacitors and transistors whose parameters appear to have shifted slightly within specifications, yet whose values may be particularly critical in a special application. Such considerations should, of course, be tempered by the fact that, in most cases, acceptable designs can be achieved either by allowing for such small changes or by use of alternate, less susceptible, components.

Additional measurements and analysis relative to the surface discoloration and contamination studies, coupled with some of the yet incomplete science investigations (organic analysis, mirror reflectance measurements, etc.), may be warranted. This area of desired fruitful future investigation requires much further study. Examples of specific tests and analyses that may be warranted include:

- Measurements of reflectance of samples from the bottom of the television camera (unpainted) before and after removal of lunar dust for comparison of data with other areas of the camera and for partial validation of the analysis reported in Section 11
- Measurement and studies of samples from one area of the lower shroud which appears to be devoid of lunar dust
- Experimental and analytical comparison of sanded and unsanded areas of the camera support collar, including reflectance measurements, and the assessment of results of organic determination now in process as part of the science plan
- Investigation to determine the reason(s) for the apparent lesser degree of discoloration of surfaces touched up with organic white paint
- Additional tests following the assessment of the mirror reflectance data now in process as part of the science plan
- Such additional tests as may be warranted following completion of the organic determination and other science tests now in process

After further in-depth review of the test results presented in this report, many additional suggestions are expected to be generated for other tests of potential value.

2. PROGRAM OBJECTIVES, SCOPE, AND BACKGROUND INFORMATION

2.1 PROGRAM OBJECTIVES

This report presents the results of the Test and Evaluation Program of the Surveyor III Survey Television Camera, returned to earth by Apollo XII astronauts. The primary objectives of this study were to determine the effects of prolonged exposure of the TV camera and its many component parts to the lunar environment, which the camera endured over more than 2-1/2 earth-years (32 lunar day-night cycles). The secondary objective was to assist the scientific investigation conducted concurrently by NASA, JPL, and scientific personnel throughout the aerospace and university community, aimed at obtaining data on the lunar environment and its effect on materials and on thermal and optical surfaces of the camera and its parts. These objectives are summarized in Tables 2-1 and 2-2.

The Test and Evaluation Program was structured to pursue these objectives. The tests of the TV camera and its component parts — circuits, subassemblies, components, materials, and surfaces — were principally aimed at studying conditions and changes which can be attributed to the lunar environment. The purpose of these tests was to identify and quantitatively evaluate unexpected conditions, as well as to verify and analyze postulated changes. In the course of these studies, other effects and anomalies were also expected, such as those attributable to manufacturing defects, design deficiencies, excessive stressing during prelaunch testing, inherent reliability limitations of selected parts, etc. Analysis of these findings, if such a course of action were deemed advisable in some cases, would provide additional information on Surveyor spacecraft components and subsystems; but such findings would be considered to be by-products of the prime effort, rather than its objectives.

The objectives of this study can be further characterized and validated by the benefits expected to accrue from it to the general aerospace engineering community. The unusual opportunities afforded by the detailed laboratory examination of parts, components, and materials which experienced the 2-1/2 year exposure to the lunar environment are believed to be

TABLE 2-1. PRIMARY PROGRAM OBJECTIVES - ACQUISITION OF ENGINEERING DESIGN DATA

			Pro	Probable Environmental	nmental Cause		
Effect Sought	Source of Test Data	Radiation	Ultra- violet	Micro- meteorites	Temperature	Vacuum	Dust
Degradation of materials	Insulation, lubri- cants, adhesives, seals, potting, epoxy, foam, and conformal coating	×	×		×	×	×
Degradation of mechanisms	Drives, gears, bearings, and brushes				×	×	×
Degradation of electrical components	Vidicon, semiconductors, magnetics, other components, connectors, and solder joints	×			×	×	
Degradation of thermal control materials	Paints, mirror, teflon, film, and polished surfaces	×	×	×	×	×	×
Degradation of optical surfaces	Vidicon faceplate, TV mirror, lenses, and filters	×	×	×	×		×
Cold welding	Drives, gears, fasteners, and connectors				×	×	
Outgassing (from TV camera materials, solar panel, paint, radar antenna, etc.)	TV mirror, TV camera inside surfaces, cable wrap, and vidicon				×	×	

TABLE 2-2. SECONDARY PROGRAM OBJECTIVES — SUPPORT OF SCIENTIFIC INVESTIGATION

Desired Information	Potential Source of Data
Improved knowledge of lunar environment	
Micrometeorites	Camera mirror and camera surfaces
Particulate radiation	Camera surfaces and structural support tubes
Solar wind Solar flares Galactic particles	
Ultraviolet radiation	Camera mirror, camera surfaces, and teflon wrap
Lunar dust properties	Camera surfaces and various camera parts
Effects of environment	
On various materials	Selected camera materials and components
On surfaces	Selected thermal and optical surfaces
Biological data	
Survivability of trapped earth organisms	Selected external and internal surfaces
	Selected pieces of epoxy and foam

of great potential value to the design of many future space systems — not merely those intended for lunar surface applications. Results of this study could provide direct information on the suitability of various components and materials for space applications. Relative to other means, such as simulated ground tests or space flight experiments, certain flight qualification data may be obtained at a cost orders of magnitude smaller for comparable quality. The study would aid in the establishment of criteria for the design, selection, and test of space hardware.

Study of the returned hardware also represents a unique scientific opportunity. The returned hardware was exposed in a known orientation for a known period of time. Analysis of this hardware can significantly

augment our understanding of the lunar and space environment. Specific measurements that can be profitably conducted include: radio isotope production; tracks and damage by energetic particles; implantation of solar wind; effects of radiation and meteoroids on surfaces; lunar solar mechanics, albedo, and particle size; and survival of micro-organisms in space.

The study can also provide a better basis for identifying most critical areas of research and development needed for future space programs, both engineering and science oriented.

2.2 BACKGROUND INFORMATION

The Surveyor III spacecraft was the second of the series of unmanned Surveyors designed, built, and tested by Hughes Aircraft Company to be landed successfully on the surface of the moon. Surveyor III landed in a crater in the Ocean of Storms on 20 April 1967. With the successful landing of Apollo XI on the lunar surface in July 1969, considerable interest was generated on the possibility of landing subsequent Apollo spacecraft in the vicinity of one of the five Surveyors resting on the lunar surface. The decision to land Apollo XII in the proximity of the Surveyor III spacecraft was made in August 1969. While the primary motivation for selecting this landing site was to use the Surveyor spacecraft as a target for ascertaining the precision landing capability of the Apollo system, it became evident that an important secondary Apollo mission objective would be fulfilled if the astronauts could conduct an examination of the Surveyor III spacecraft on the lunar surface, and retrieve and return to earth some of its components.

Hughes had long been interested in the possibility of examining and recovering from the lunar surface parts of one or more of the Surveyor spacecraft. As early as January 1967, a recommendation had been submitted to NASA (Reference 3) suggesting an order of priorities for possible retrieval of Surveyor parts; topping the list of priorities was the television camera.

When the definite possibility of landing Apollo XII near Surveyor III arose, Hughes became immediately involved in early planning. Motivated by its strong technical capability in all facets of Surveyor design, and by an understandable emotional involvement and parental ties with the Surveyor spacecraft, Hughes personnel submitted a series of memoranda to NASA. These dealt with the proposed examination of Surveyor III by the astronauts, selection of candidate parts for retrieval, planning and logistics entailed in retrieval operations, and prelaunch tests and training of the astronauts (References 4 and 5). These memoranda also discussed

in some detail the rationale for the proposed recovery of various Surveyor parts, including, as the highest priority item, its survey TV camera: the consideration of scientific and engineering information obtainable; analysis of criteria for selection of parts to be recovered; discussion of possible recovery techniques; analysis of safety, logistics, and handling equipment; impact on Apollo mission, etc. As part of this supporting effort, several conferences were held at NASA Manned Spacecraft Center (MSC), Houston, and tests were conducted at Hughes to ascertain the validity of the proposed removal techniques.

When the final decision was made by NASA to include retrieval of selected Surveyor parts in the Apollo XII mission as a planned objective, Hughes submitted a proposal to NASA to generate a detailed plan for processing, testing, and evaluating the Surveyor III parts upon their return to earth (Reference 6). The Surveyor parts considered included the television camera, the soil mechanics/surface sampler (SM/SS) scoop, the thermal switch, a portion of the thermal blanket of a propellant tank, a small sheet of Kapton material from an electronic compartment, and selected sections of painted and polished support tubing. These parts had been selected on the basis of previous Hughes recommendations for possible recovery made as early as 1966. Other potentially desirable parts, such as a section of the solar panel, the tip of an omnidirectional antenna, and the Canopus star sensor, had been elminated from the final plan for operational, safety, and logistic reasons. Two weeks prior to the launch of Apollo XII, Hughes was awarded the contract for the conduct of such test planning and evaluation studies.

An intensive effort to generate the test and evaluation plan was conducted during the 2 week period prior to and concurrent with the Apollo XII mission. This effort resulted in the detailed test plan (Reference 2) submitted to NASA on the eve of the successful completion by Apollo 12 astronauts of the Surveyor III parts recovery operations.

The Hughes Test and Evaluation Plan, coupled with various other inputs to NASA by JPL, NASA, and interested university science and engineering investigators, resulted in an overall coordinated plan for the disposition and testing of the various retrieved Surveyor III parts. This plan included a separate contract to Hughes, technically directed by JPL, for testing and evaluation of the Surveyor television camera in accordance with the general plan outlined in Reference 2. This report presents the results of the study performed under that contract. A parallel contract was also awarded to Hughes under the technical direction of NASA-MSC for testing and evaluation of the other retrieved Surveyor parts: SM/SS scoop, section of cables and cable wraps, polished aluminum tube, and sections of painted structural support tubes. Results of studies under this contract are being reported in a separate volume (Reference 1). The

thermal switch was not recovered because of difficulty incurred by the astronauts in removing it. The piece of Kapton also was not recovered.

As part of this contract to test and evaluate the television camera, Hughes was also directed to conduct certain operations in support of the parallel science investigations by NASA, JPL, university, and other scientists.

From 20 November 1969 through 16 January 1970, during and shortly after the Apollo XII quarantine period, a number of planning and testing operations took place. NASA and JPL personnel were briefed by Hughes personnel on details of the proposed program. Subsequently, Hughes participated in the briefing at NASA Headquarters on 18 December 1969. An operations and management plan was generated by NASA Headquarters defining responsibilities for the various retrieved Surveyor parts. A formal debriefing of Apollo XII astronauts was conducted by Hughes, NASA, and JPL personnel in the Lunar Receiving Laboratory (LRL) at Houston on 8 December 1969.

A series of practice runs was conducted by Hughes personnel at the Jet Propulsion Laboratory on a non-flight Surveyor TV camera in preparation for work on the flight camera. Subsequently, initial operations were conducted on the flight camera at MSC in Houston, as described in Section 4.1. These operations entailed a visual examination, detailed photography, and the removal of the outer TV camera shroud by Hughes personnel. Subsequent science investigations at MSC, including the conduct of a biological assay with Hughes assistance, and several other science tests, are described in Reference 7.

Several important preparatory activities took place at Hughes during this time. A secure clean room facility was established for testing the retrieved Surveyor parts. A management plan was prepared, entailing special security measures and parts control. A search was initiated for the recovery of old Surveyor design and test data for comparison purposes. Original Surveyor camera electronic test equipment was obtained from JPL and installed in the new Surveyor test facility. A non-flight Surveyor TV camera was obtained from JPL for the checkout of this test equipment in preparation for testing of the retrieved camera.

The test program of the TV camera commenced with the arrival of the camera at Hughes on 16 January 1970, on a Hughes company aircraft, under the escort of Hughes, NASA, and JPL personnel.

2.3 DESCRIPTION OF TV CAMERA

The survey television camera installed aboard Surveyor III was part of its scientific payload. It was developed to record near and distant lunar scenes, as well as closeups of certain portions of the spacecraft, such as the landing leg, foot pad, and crushable aluminum blocks mounted beneath the vehicle. In operation, the photographic image of the viewed scene is placed onto the camera vidicon; the image is then read out electronically in a manner similar to that in a television camera, and, finally, the video signals are transmitted to earth for processing.

The survey camera is a self-contained unit requiring only external power, telemetry, command functions, and a video transmission link. A functional description of the TV camera has been published (see Reference 8). The camera, shown in Figure 2-1, consists of two main assemblies. The main body of the camera contains the power supply, vidicon, electronics, shutter, and zoom lens assembly. The top element is a rotatable mirror assembly, which contains the azimuth and elevation mirror drive mechanisms and the filter wheel assembly. The complete unit weighs 17.5 earth pounds. Figure 2-2 is a cutaway view of the camera, indicating major subassemblies. Figure 2-3 shows the lower electronic portion with the mirror unit removed for system test and evaluation.

The rotatable mirror assembly, also known as the hood assembly, can be rotated almost 360 degrees in azimuth and provides for an elevation range from -45 to +20 degrees from horizontal by varying the elevation angle of the movable beryllium mirror mounted in the camera hood. The mirror is a Kannigen processed beryllium blank, optically ground and coated. The camera is mounted nearly vertical. The beryllium mirror is driven in elevation by a stepper motor which tilts the mirror to various desired positions. The entire hood assembly is driven in azimuth by a second stepper motor. Both the elevation and the azimuth drives have individual potentiometer readout devices attached to them for telemetry of angular position data.

The filter wheel assembly, also installed in the hood, is composed of four optical filters to provide color photographs: clear, blue, red, and yellow/green. A separate stepper motor and potentiometer are used for providing the driving and telemetry readout functions, respectively. Figure 2-2 shows the location of these assemblies.

The hood assembly is made of aluminum with external surfaces coated with a white inorganic paint of high reflectance, and with its internal surface coated black to reflect stray light back into the vidicon. This passive thermal control design protects the filters, stepper motors, and potentiometers. The hood of the Surveyor III camera was the first to be modified to include an attached overhanging metal strip, several inches wide, to act as a visor in order to prevent stray reflectance of sunlight from hitting the beryllium mirror.

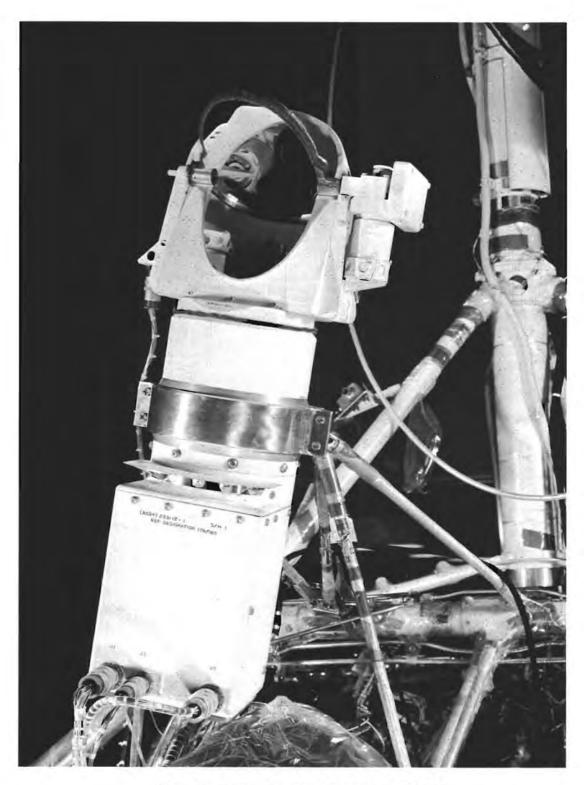


Figure 2-1. Survey Television Camera (Photo A07257)

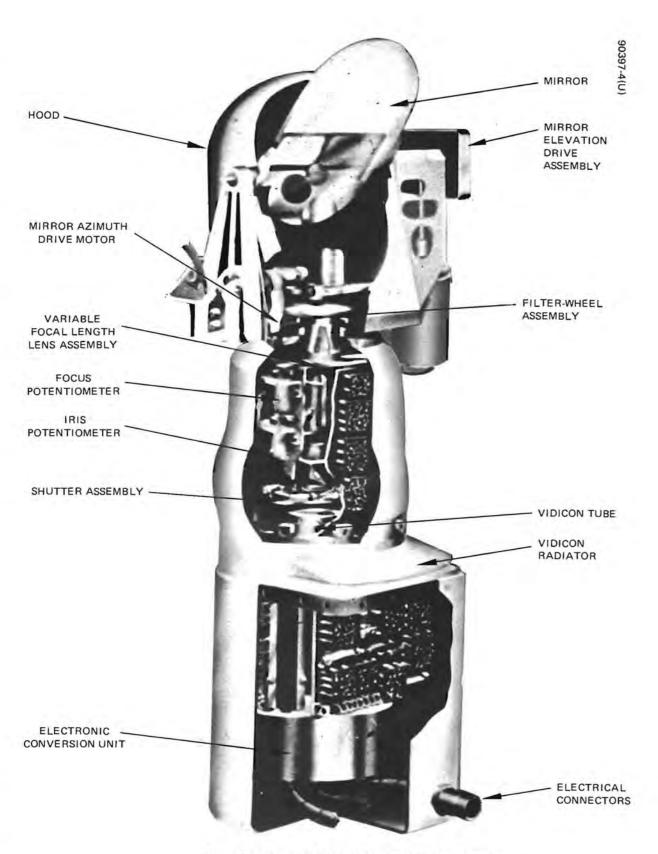


Figure 2-2. Cutaway View of Survey Television Camera

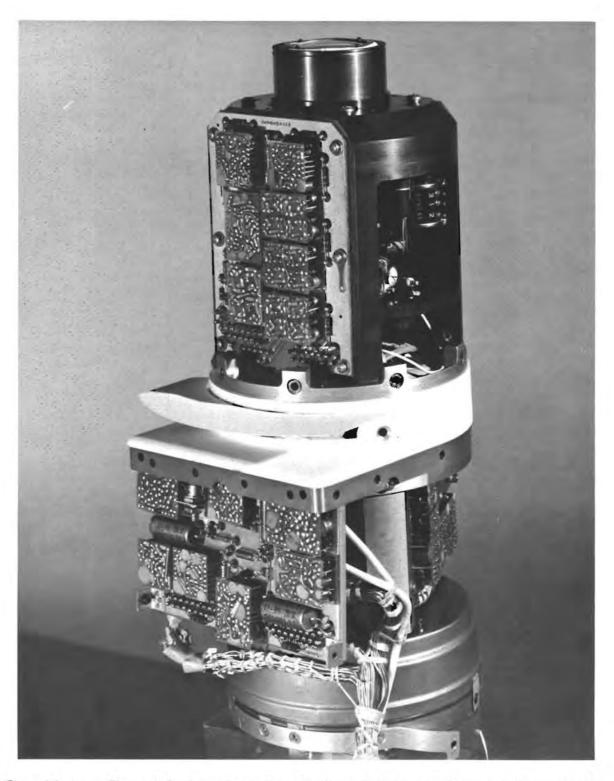


Figure 2-3. Lower Electronic Portion of Survey Television Camera With Mirror Unit Removed (Photo R96128)

The camera body is composed of several major assemblies, lenses, the vidicon tube, and electronics. The variable focal length lens assembly, shown in Figure 2-4, is located just below the filter wheel assembly. It has a variable focal length lens of 25 to 100 mm, and can also be focused from 4 feet to infinity. These lens functions are operated by commands from the earth and are motor driven. Attached to these drives are separate potentiometers for telemetry readout of position data to earth controllers.

The variable focal length lens assembly has a lens aperture range of f/4 to f/22. The lens aperture is adjusted automatically to the light level encountered, or it can be driven by command from earth in an override mode. The lens aperture adjustment also has a separate motor drive with an associated telemetry readout potentiometer.

Just below the lens assembly is the focal plane shutter. The shutter provides for a 150 ms exposure time of the vidicon faceplate. Variable duration time exposures can also be obtained by command. The shutter can also be commanded to remain open for a variable or for an indefinite length of time by command to obtain a variable duration time exposure. A beam splitter above the shutter feeds a percentage of incoming light energy to a photocell which controls the lens iris for automatic exposure control. This sensing device keeps the shutter from opening if the light level is too strong. The device can be overridden by a command from ground control.

The vidicon tube (Figure 2-5) is beneath the focal plane shutter and mounted vertically in the camera. The vidicon is described in some detail in Section 6. Thermal control for the vidicon is provided by a radiator extending from the camera body and thermally connected to the vidicon by means of a boron nitride collar.

Below the vidicon is the electronic conversion unit, as shown in Figure 2-6. This unit converts the 28 volt dc spacecraft bus voltage to camera operating voltages. This unit is enclosed in an RFI housing to prevent interference with vidicon operation. The electronic circuits for sweep, control, amplification, etc. are placed around the lens assembly and vidicon, as shown in Figure 2-7.

The Surveyor camera system provides for either 200 or 600 line photos. The latter requires the operation of the high-gain Surveyor directional antenna and the high power level of the transmitter. The 600 line mode provides a picture every 3.6 seconds, and the 200 line mode every 61.8 seconds.

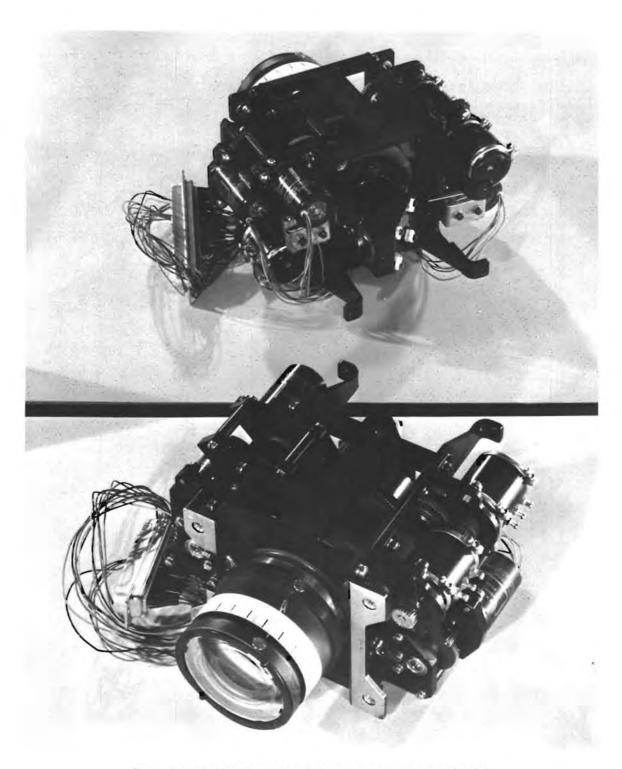


Figure 2-4. Variable Focal Length Lens Assembly (Photo R97597)

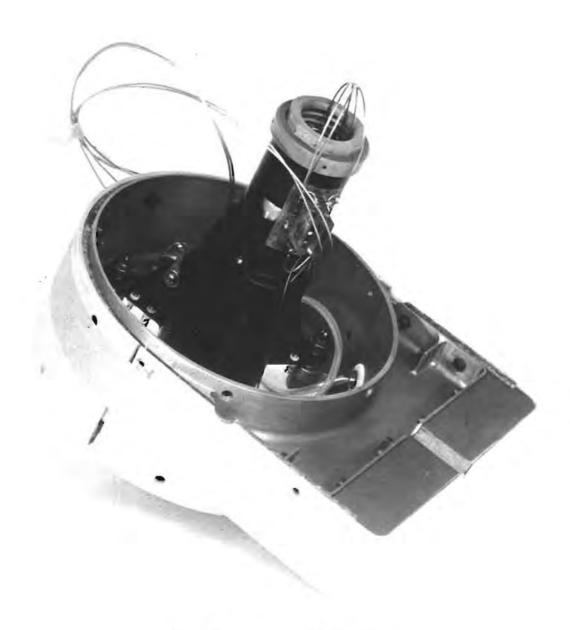


Figure 2-5. Vidicon Tube (Photo R98432)

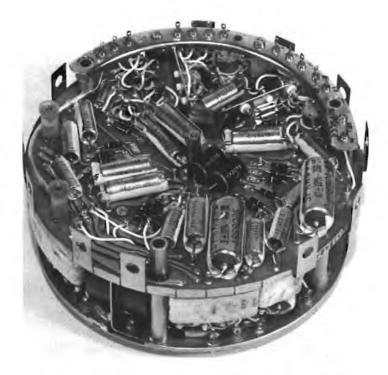


Figure 2-6. Electronic Conversion Unit (Photo R98455)

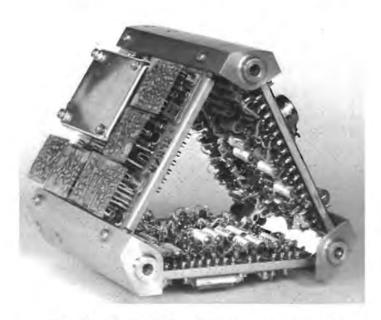


Figure 2-7. Electronic Circuits for Sweep, Control, and Amplification (Photo R98425)

The TV camera is encased in a 6061 aluminum alloy shroud, whose external surfaces are painted with a special Hughes-manufactured inorganic white paint for passive thermal control. The bottom plate of the camera, facing the lunar terrain, is unpainted polished aluminum. Power, control, command, and telemetry connections are channelled through four Microdot series 43 type connectors; three of these are on the lower front and one is at the side of the upper hood assembly. Incoming aluminized teflon-wrapped cables connect to the external two lower shroud connectors. A separate cable from the middle of the lower shroud to the hood assembly connector provides for the electrical connection between the camera body and the hood assembly. This so-called TV camera cable is flexible and rotates with the mirror assembly.

The performance characteristics of the survey camera are as follows:

Signal-to-noise	ratio	31 dB	minimum
-----------------	-------	-------	---------

Lens aperture
$$f/4$$
 to $f/22$ in $1/2$ stops

Azimuth	coverage	360	degrees
AZIIIIUUII	Coverage	300	degrees

Luminance range 100 footlamberts (f/4)

Additional design details and circuit schematics are provided in subsequent sections of this report, where results of individual tests of the various subassemblies are presented.

2.4 TV CAMERA TEST HISTORY AND LUNAR MISSION OPERATIONS

Performance of the TV camera during its entire history, ranging from original unit level testing through its operation on the lunar surface, was an important factor in planning and evaluating the tests conducted on its component parts. Knowledge of past performance could materially aid in the assessment of whether and to what extent the test results and anomalies observed are attributable to the effects of lunar exposure, or whether they can be explained and accounted for by other factors, such as inherent design and reliability features, prior condition of the camera, or stresses incurred in prelaunch tests. For this reason, a brief resume is presented here of the Surveyor III TV camera test history and its operation on the lunar surface prior to Surveyor III shutdown at the end of the first lunar day of its operation. This summary is obtained from a variety of records available at Hughes and from Surveyor mission reports (References 9 and 10).

2.4.1 Surveyor III TV Camera Test History

The camera was assembled as a unit in 1964. Its various sub-assemblies — chassis boards, vidicon tube, electronic conversion unit (ECU), lens assembly, and mirror assembly — were subjected to specified tests prior to camera assembly to verify their operational limits. These unit tests included the following:

- Cryogenic survival tests of the vidicon tube (immersion in liquid nitrogen, -325°F cryogenic soak)
- Thermal-vacuum and vibration tests of the lens and mirror assemblies
- Operational temperature tests of the ECU and chassis boards (ambient, -20° and +160°F)

Various upgrade and retrofit operations were conducted after the initial assembly of the camera until its launch on Surveyor III in 1967 to incorporate desired design improvements and to replace parts which failed in the course of unit and spacecraft system tests. Most important of these were the following:

- 1) The lubricant used in the lens assembly was replaced with an improved type.
- 2) The vidicon sensitivity was improved for low light level (star mode) operation.
- 3) A sun shade was added to the mirror assembly for the reduction of glare.
- 4) An access port was added for cleaning and inspection of the vidicon faceplate.
- 5) The TV cable from the lower chassis to the upper movable mirror assembly was redesigned for increased flexibility.

- 6) Electrical components in the vidicon circuit were replaced with selected parts to optimize the vidicon operating point.
- 7) A separate thermal regulator was added to the mirror assembly.

The camera underwent a series of tests as a complete unit assembly prior to its installation on the spacecraft. These unit tests were conducted during the period from 1965 through 1966.

A major replacement was made on the Surveyor III TV camera in August 1966. Because of problems encountered with the azimuth and elevation drives, which tended to hang up in stepping during environmental tests, the entire mirror assembly was replaced with another mirror assembly of the same design. Defective and suspect components — motor and potentiometer — were subsequently replaced on the mirror assembly removed from the Surveyor III TV camera. It should be noted that the TV camera subsequently underwent a major redesign to correct these marginal operational characteristics, and an improved model of the camera was installed on later Surveyor spacecraft, beginning with Surveyor V.

The camera with the new mirror assembly was subjected to a series of retests at the unit level in August 1966. In all, counting the unit tests with the original mirror assembly as well as the retests with the new mirror assembly, eight flight acceptance tests and six partial flight acceptance tests were conducted. A complete flight acceptance test included the following:

- Functional test under ambient conditions
- Vibration of 4 to 9 g at 125 to 2000 cps
- Postvibration functional test (ambient)
- Operational tests under thermal-vacuum conditions in a temperature range from -20° to +125°F at a pressure less than 10⁻⁵ Torr.
- Final ambient functional tests

In addition to the above tests, the TV camera was subjected to eight cryogenic soaks in order to isolate marginal components. Six of these cryogenic soaks were at -180° and two at -150°F. Some of the failures uncovered included defective tantalum capacitors and cracked components resulting from excessive conformal coating buildup on the

chassis boards. During the above unit test phases, approximately 45 failure reports were written. These can be summarized as follows:

Failure	Number of Reports
Azimuth and elevation stepping problems	12
Cryogenic failures (cracked resistors, diodes, and capacitors)	7
Mechanical/manufacturing discrepancies	3
System test anomalies (resolutions, horizontal response)	3
Erroneous test specifications	4
Faulty test equipment	2
Overstress of components in test - operational problems	12
Human errors	2
Total	45

The camera was further subjected to system level tests after it was installed on the Surveyor spacecraft. These included integrated system checkout tests, simulated mission sequence tests, electromagnetic interference tests, spacecraft vibration, solar-thermal-vacuum tests, and comprehensive prelaunch functional tests at Cape Kennedy.

Except for replacement of the mirror assembly in August 1966 (discussed above), no changes or replacement of parts were made on the Surveyor III camera in the course of the comprehensive testing in unit areas, and as part of the Surveyor III spacecraft; so the flight configuration was identical to that which had successfully passed the required tests. However, one significant event occurred early in 1967, which has a potential bearing on one of the Surveyor III camera failures uncovered and discussed in this report.

In March 1967, just before launch of the Surveyor III spacecraft, a problem was uncovered in the unit environmental area in the course of environmental testing of two other similar TV cameras: one supplied for Surveyor 4 and one a spare. Excessively high current was found in the shutter solenoid circuit of both of these cameras, leading to damage and,

on one camera, to burnout of components, i.e., drive transistor, series resistor, and shutter solenoid. The problem was traced to an improper termination of a coaxial cable in the test rack; the prime initial evidence of stressed components was the erratic operation of the camera shutter. The importance of this discovery to the Surveyor III camera lay in the fact that the same test rack had been used earlier in January 1967 to test this camera although apparently no damage had occurred.

Upon discovery of this problem, the Surveyor III camera was subjected to a special test to validate its integrity. This diagnostic test entailed operation of the shutter at both low and high voltages. No abnormal shutter operation was noted, and it was decided as a calculated risk that the camera was suitable for flight, notwithstanding the possibility of some stress. The confidence of its satisfactory performance appeared to be high. An alternative decision would entail a major delay since a retrofit of the camera would require a major retest. This decision was subsequently justified by the successful performance of the Surveyor III television system on the lunar surface. However, the potential stress to the shutter solenoid drive transistor should be recognized and is reflected in the failure analysis discussed in Section 12.

Prior to the launch of the Surveyor III spacecraft, a complete assessment was made of the acceptability of the TV camera as part of the consent-to-launch deliberations. The following potential failure modes were identified:

- 1) Operability of potentiometers at low temperatures
- 2) Performance of the variable focal length and iris under vacuum conditions
- 3) Low reliability of the tantalum capacitors at low temperatures
- 4) Marginal mirror drive mechanisms

Notwithstanding the existence of these potential failure modes, the camera was considered acceptable for launch. This decision was, in part, motivated by the previous successful performance of the Surveyor I camera and was completely vindicated by the subsequent successful performance of the Surveyor III TV camera during its mission.

2.4.2 Performance of the Camera on the Lunar Surface*

During transit from the earth to the moon, the camera was subjected to an estimated temperature excursion of -180° to +150°F and

^{*}Additional data are available in Reference 10.

vacuum environment of 10^{-5} to 10^{-11} Torr. It also experienced vibration and shock during the launch, midcourse, and lunar landing phases of the Surveyor spacecraft.

The landing of Surveyor III was not nominal. The vernier engines remained on through the first touchdown at a thrust level equal to about 90 percent of the spacecraft lunar weight. The spacecraft rebounded from the lunar surface and landed again a short distance away. This procedure was repeated twice until the vernier engines were shut down by ground command about 1 second before the third touchdown, when the spacecraft finally came to rest on the surface.

The failure of the engines to turn off through two touchdowns appeared to have caused contamination or pitting of the camera optical surfaces. For some camera angles, this resulted in glare in the pictures; this glare was caused by the scattering of sunlight from the degraded mirror surface. The camera was subjected to the landing shock three times. The landing sequence was presumed to have stirred up a considerable amount of lunar dust, which may have been deposited on parts of the TV camera. The amount of the deposit may have been aggravated by the fact that the sequential landing points were along the slope of the Surveyor crater. Details of the landing of Surveyor III and of the performance of the Surveyor TV camera on the lunar surface are presented in References 9 and 10.

All survey television camera functions were exercised on the lunar surface in April 1967 during the first lunar day of operation of the Surveyor III spacecraft. More than 6300 television pictures were obtained, meeting all of the objectives for scientific analysis. Certain abnormal operations, however, were encountered, attributable in part to the lunar environment.

Analysis of data retrieved provided some knowledge of the thermal environment to which the camera was subjected, which it is useful to summarize here. Just prior to landing on the lunar surface, camera electronic heaters were turned on to bring the camera up to its operating temperature in order to be ready to take pictures immediately after touchdown. This procedure raised the temperature from about -140°F (camera temperature in transit) to the minimum operating value of -20°F.

The expected lunar surface temperature at touchdown was about 0°F, rising sharply as the sun rose in this area. Peak lunar surface temperature rose to over 200°F within 6 earth days after touchdown, when camera operations were discontinued. The corresponding camera temperatures were 0°F at touchdown and 150°F peak during the lunar day.

Within this period, on April 24, 4 earth days after touchdown, a total eclipse of the sun by the earth occurred, dropping lunar surface temperatures from over 200°F to less than -100°, and then rising back again to over 200°F in a period of about 6 hours. The corresponding camera temperatures were approximately 150°, 0°, and 150°F. This provided an excellent opportunity to evaluate thermal aspects of the spacecraft and its television camera. In the course of the lunar operations, three major anomalies were noted, as described in the following paragraphs.

Veiling Glare

The failure of the vernier engines to shut down and the ensuing hopping maneuver of the spacecraft on the lunar surface appeared to have caused contamination or pitting of the camera mirror and optics.* Studies were performed to substantiate this conclusion. Detailed information is available in Reference 10, Part II, pp. 198 to 200. It was estimated that at least 30 percent of the upper half of the TV mirror had been affected. This caused severe veiling glare in some pictures at camera angles which had direct or reflected sunlight shining upon the upper portion of the mirror surface.

Elevation and Azimuth Drive Anomalies

The television camera experienced some difficulties in stepping the mirror both in elevation and in azimuth. The mirror azimuth drive failed to step 432 times out of a total of 10,045 commands. The fact that these occurrences were most severe when the camera was cold suggested that the azimuth stepping failures were probably due to one or more of the following factors: motor wear, binding of the azimuth bearing at one particular location (about +10 degrees) as a result of thermal stresses, and increased friction of the ring gear because of lunar dust. The elevation stepping failures — 67 times out of 3594 commands — indicated a motor/gear wearout trend. The camera had accumulated over 34,000 steps each in azimuth and elevation during prelaunch testing.

Filter Wheel Anomaly

Near the end of the lunar day, a failure occurred at the readout potentiometer of the filter wheel (containing the red, green, blue, and clear filters). Proper operation of the filter wheel was verified through television pictures; however, telemetry of this function was not operative.

^{*}For reliability reasons, the mirror was left open at launch. On subsequent spacecraft, the mirror was closed.

All other camera functions performed nominally. Recorded data were available on mission performance, such as sync levels, analog video, etc. At the end of the first lunar day, the camera was turned off prior to shutdown. Records are available relative to all commandable functions, such as positions of its azimuth and elevation drives, the filter wheel (from photographic data), iris, focus, and focal length.

Unsuccessful attempts were made on subsequent lunar days to revive the Surveyor spacecraft. In the course of these attempts, many signals were sent to the spacecraft. Records of these signals are available.

Prior to its recovery by Apollo XII astronauts, the camera resided on the lunar surface for approximately 2-1/2 years. During this period, the camera was exposed to the effects of the lunar environment, briefly described in Appendix B. It underwent 32 day-night lunar cycles, entailing temperature excursions of from -300°F during the extreme of a lunar night to +150°F at the height of the lunar day. Because of its location on the spacecraft, the camera experienced space radiation and bombardment from micrometeoroids. The TV camera was also subjected to possible contamination from the products of outgassing from other components of the Surveyor III spacecraft and to the effects of showers of dust from the lunar soil incurred both during the original multiple-bounce landing of Surveyor III and during the nearby landing of the Apollo XII lunar module. It is also possible that debris disturbed from the lunar surface by meteoroids during the 2-1/2 years of lunar exposure contributed to the presence of residual dust on the Surveyor spacecraft.

2.5 TV CAMERA RETRIEVAL AND RETURN TO EARTH

The Apollo XII astronauts retrieved the camera during the second extravehicular activity (EVA) in the early morning (PST) of 20 November 1969. Recovery of the TV camera was conducted essentially in accordance with a previously formulated plan and was monitored by ground controllers. While one of the astronauts held the camera, the other severed it from the spacecraft by cutting the five supporting struts and the cabling with a specially provided bolt cutter. The cables severed included two main cables leading to the outer two of the three front connectors on the lower shroud and the cable leading from the center connector of the lower shroud to the

upper mirror assembly connector. The TV camera, with the pieces of cabling and struts attached, was placed in a special bag provided and subsequently carried to the lunar module and returned to earth in the ambient environment. Vacuum-seal return of the camera was not feasible.

Prior to the removal of the TV camera from Surveyor III, a number of black and white photographs were taken by the astronauts. Included in these photographs were closeup pictures, emphasizing the appearance of the TV mirror which had been left at an angle of approximately 45 degrees. The astronauts had been instructed to swipe the TV mirror once with a finger, and to photograph the mirror to show its appearance before and after swiping, but only in the event that the TV camera could not be retrieved. This was planned in order to obtain some contingency data on the contamination or pitting of the camera surface. This operation was, in fact, conducted by the astronauts notwithstanding their retrieval of the camera; so the TV mirror bears striking evidence of the swiping, as seen in the frontispiece.

The TV camera was then transferred to the command module and remained in its recovery bag throughout its return flight to earth and its receipt in LRL, Houston. During the landing of the Apollo command module in the Pacific, a severe jolt occurred; the two dents noted in the TV camera hood, which can be seen in the frontispiece, are believed to have been incurred at that time. These dents were discovered upon removal of the camera from the carrying bag in LRL but do not appear in the photographs taken by the astronauts on the lunar surface.

The camera was delivered to quarantine at LRL in its carrying bag. Early in the quarantine period, one of the astronauts removed the camera from its carrying bag, presumably to separate it from the trapped lunar dirt and dust. After displaying the camera briefly through the window of the quarantine room, at which time several photographs of the camera were taken, the astronaut placed the TV camera in a new heat-sealed polyethylene bag. Loss of information may have resulted because of the possibility of photo-oxidation reaction. The camera was left in its new container for the remaining period of quarantine in LRL until it was examined and subjected to the MSC operations by Hughes and NASA personnel, as described in Section 3.2.

2.6 SCOPE OF THE TEST AND EVALUATION PROGRAM

The Test and Evaluation Program was designed to meet the objectives defined in Section 2.1. Several important ground rules were adopted to

ensure compliance with these objectives and with funding limitations, and a task structure was established to identify and define in detail the test and evaluation operations. The scope of this program was generally consistent with that previously postulated in the Surveyor Parts Test Plan (Reference 2).

2.6.1 Program Ground Rules

The following ground rules were established and followed in the conduct of the Test and Evaluation Program.

- 1) System level testing of the TV camera was excluded to ensure that all potential evidence on the effects of lunar exposure on camera parts and components was preserved since system level testing could lead to potential stress and degradation and since operability of the camera as a Surveyor spacecraft subsystem was not a program objective.
- 2) Strict guidelines were established early in the program, and officially pronounced by NASA letter (Reference 11), relative to the conduct of tests which would result in partial or total destruction of parts of the camera. Limited but careful preliminary analysis was to be conducted to determine the usefulness of destructive analytical techniques before committing to test any significant portions of TV camera parts and components, and at least 50 percent of similar parts, components, and materials of the TV camera were to be preserved for possible future follow-on investigations.
- The sequence of testing was to be in compliance with the above requirements. This entailed preliminary evaluation of test results as they were obtained, establishment of milestone decision points along the postulated test sequence plans, and close liaison with the customer in sequential execution of the steps of the testing process.
- The scope of the individual tests was planned to stress acquisition of data on the direct effect of lunar environment. Changes and failures that were attributable to the lunar environment were to be pursued on the highest priority basis, and a special effort was to be exerted to further assess the relative contributions of the components of this environment whenever it appeared likely that a combination of effects was instrumental in producing a change.

This important ground rule can be illustrated by the following examples: Observed deformation of azimuth drive ring gear teeth was not pursued in excessive detail, once it had been established that the cause was traceable to prelaunch history and not to the lunar environment. On the other hand, a more intensive investigation of surface contamination effects was undertaken because of the desire to identify the contributions of several components of the lunar environment: radiation, lunar dust, and deposition of products of outgassing.

- 5) Evaluation and failure analyses were to be motivated by the desire to generate useful design data for future programs, rather than merely by the need to explain all failures. As an example, it was decided not to conduct a failure analysis of the uncovered burned out metal film resistor and alloy transistor because these components are obsolete.
- 6) The selection and the extent of testing of circuits and electrical components were to be based on the categories of available components, their uniqueness and accessibility, the availability of preflight data, and the redundancy between similar components present in the chassis tested in circuit tests and those subjected to component level investigations.

2.6.2 Tasks

The Test and Evaluation Program was carried out in the form of 17 distinct tasks. Scope of the effort can best be described by the following quick summary of the objectives and content of these tasks.

Program Management

This task encompassed management, administration, security and facility coordination, documentation, inventory control, monthly reports, and oral presentations. Highlights of program management operations are described in Appendix A.

MSC Operations

This task was concerned with operations conducted at NASA-MSC before the shipment of the TV camera to Hughes. This task included preliminary survey, shroud removal, and assistance in biological assay and other scientific tests conducted at MSC, as well as all preparation and practice tests performed in Los Angeles. The MSC operations are described in Section 3.2.

Survey Operations

This task entailed the initial survey operations on the TV camera prior to its dismantling, as well as survey operations conducted throughout the rest of the program, primarily during the dismantling operations. Included in these survey operations were visual and microscopic examinations, extensive photography, and the analysis of contamination samples removed, if any. This task is discussed in detail in Section 3.3.

Camera Dismantling

This task included the dismantling operations of the TV camera to the levels necessary for a complete evaluation. The task was concerned with the removal of the various electrical chassis, optical subassemblies, and the vidicon. Detailed disassembly of the optical subassemblies formed part of the optical subassembly tests described below. The scope of the camera dismantling task included the procurement of all tools required, measurements during the dismantling operations (such as screw removal torque values), and maintenance of a comprehensive parts inventory system. Work conducted under this task is described in Sections 4.1 and 4.8.

Checkout of Electrical Test Equipment

This task involved the procurement of the test equipment required to evaluate the TV camera electrical circuits, and the installation, calibration, and checkout of this equipment, using spare non-flight television cameras. The bulk of this equipment was available from the Surveyor program. This task is discussed in Section 4.2 and Appendix C.

Electric Circuit Tests

This task comprised performance of selected functional tests on three of the eight electrical chassis of the TV camera. These carefully selected and planned tests were conducted before the dismantling of the TV camera as part of the overall plan to evaluate the electrical components. The tests were preceded by the checkout of similar chassis on a non-flight camera. They included a visual inspection, passive ohmmeter checks, and functional performance tests. They were conducted in accordance with existing Surveyor program procedures, using dummy terminations, circuit isolation, and gradually increasing applied voltages, as appropriate. Results of these tests were closely coordinated with the effort conducted under the electrical components tests. Results of this task are discussed in Sections 4.2 through 4.7. Description of the chassis tested is given in Appendices D, E, and F.

Optical Subassembly Tests

This task consisted of the functional testing of the mirror assembly, of the lens assembly, of the filter wheel subassembly, and of the shutter subassembly, both before and after their removal from the TV camera, as deemed appropriate. Included in this task were the required disassembly operations, as well as the establishment and validation of necessary test facilities. Electrical and mechanical functional performance tests were conducted, and a detailed assessment of optical and other parts of these subassemblies was carried out in close coordination with the effort under optical components tests. The conduct and results of this task are discussed in Section 5.

Vidicon Tests

This task pursued the examination, testing, and preliminary evaluation of the TV camera vidicon, both in the assembled and disassembled states. It was conducted in several phases. A detailed visual examination, followed by a measurement of gas pressure inside the vidicon, and certain functional tests were conducted prior to vidicon removal. These tests were subsequently repeated to a somewhat greater degree of depth and detail after removal of the vidicon. In the final phase, the vidicon was dismantled and certain component and material level tests were conducted. The task included extensive parallel or preparatory testing of similar non-flight vidicons and establishment and checkout of the required testing facilities. Work conducted under this task is described in Section 6 and Appendix G.

Electrical Components Tests

This task encompassed test of the four classes of electrical components of the TV camera: resistors, capacitors, diodes, and transistors. Representative samples of the various types of components in the camera were selected, visually and functionally checked on the camera, removed, and subjected to a carefully planned component level test program which was closely integrated with the previously conducted electric circuit tests. Component level testing included visual and microscopic examination, functional measurements, and destructive/diagnostic tests of sequentially smaller subsets of selected samples. Details of this test program are presented in Section 7 and Appendix H.

Mechanical and Electromechanical Components Tests

This task comprised tests of the six types of mechanical and electro-mechanical components present in the camera: potentiometers, two types of stepper motors, connectors, thermal switches, deflection yoke, and reactors. The tests included preliminary visual and passive tests, functional measurements, and detailed diagnostic/destructive tests of selected samples. In some cases, selected environmental tests were also conducted. Details of this test program are presented in Section 8 and Appendix H.

Optical Components Tests

This task included tests of the optical components of the TV camera after disassembly, and logically followed the work done during tests of optical subassemblies. Optical components tested were the camera primary mirror, filters, and the multiple-element lens barrel subassembly. Measurements of optical properties, as well as of potential changes in the mechanical properties and physical characteristics, were conducted. Results of this task are discussed in Section 9 and Appendix H.

Materials Tests

This task studied the various materials present in the TV camera from which useful data were thought to be obtainable. The task constituted one of the major efforts of the program.

Materials selected for study were grouped into the following categories: organic materials (teflon, nylon, and polyimide); epoxy adhesives; lubricants; seals; potting compounds and polyurethane foam; conformal coatings; epoxy fiberglass circuit boards; interconnections and solder joints; wires and cables; metals; paints (white organic, white inorganic, and black organic). Tests of these materials included, as applicable, mechanical, metallurgical, electrical, chemical, and optical property measurements, and other measurements such as wear, traces of possible cold welding, etc.

These tests were conducted on selected samples removed from the camera, following completion of the subsystem and component level tests previously described. These tests and the results obtained are described in Section 10 and Appendix I.

Surface Contamination Studies

A special task was established to study in more detail the nature and source of the contamination present on the exterior surfaces of the TV camera: discolored paint of the camera shroud, contaminated polished aluminum bottom plate, discolored external cable teflon wrap, and certain other optical surfaces. The task was closely coordinated with a similar task on the companion NASA contract involving surface contamination studies of the painted and polished tubing. The conjectured contributing factors to the discoloration and contamination of these surfaces included deposition and imbedding of lunar dust, chemical and physical changes induced in the paint by solar radiation, deposition of products of outgassing from surrounding components of the Surveyor spacecraft, and such possible prelaunch contaminants as oil deposition from thermal-vacuum ground testing. Various techniques were examined and utilized in the attempt to solve this problem, considered both important and difficult. The effort was closely integrated with certain parallel investigations, conducted under JPL technical coordination by other science investigators as part of the science plan. Results of this work are reported in Section 11.

Failure Analysis

A separate task was conducted to pursue in great detail those specific anomalies and failures uncovered in the course of the above investigations which were considered worthy of special effort. A separate failure analysis system was established for this purpose. Discrepant or failed parts, components, and materials were analyzed and tested to the extent required to identify the nature of the anomaly. In cases where the cause of the failure was definitely traceable to the effect of the lunar environment, the exact mechanism of the failure was investigated, using a variety of applicable diagnostic techniques. Results of this failure analysis program are described in Section 12 and Appendix J.

Support of Science Investigations

A separate task provided the required support and assistance to the parallel science investigation conducted under JPL coordination by many JPL, NASA, and university scientists. This task involved a variety of activities, such as cutting and preparation of samples, and physical and technical assistance in performing electrical, optical, and biological tests.

Evaluation and Reporting

While preliminary evaluation of test results was conducted as part of the effort of the individual tasks described above, the comprehensive overall evaluation was carried out as a separate task. Included in this task were the monthly reports, technical memoranda, and oral presentations, as well as the preparation and compilation of the final report.

Publication of the Final Report

A separate task was defined for the actual publication of this report, entailing final editing and efforts of the Publications Department.

The scope of the effort conducted under all of the technical tasks included, as applicable, planning of the tasks, preparation of appropriate detailed procedures, compilation of review of past records available from the Surveyor program for comparison purposes, and conduct of visual and photographic survey operations prior to initiation of testing. In addition, individual tasks entailed a preliminary evaluation of test data, as they were generated, to the degree required to determine the validity of the results obtained and to warrant the continuation of planned test operations. In the event that a definitive indication of an anomaly or of a failure was uncovered, the failed part was removed from the scope of the respective task, and the responsibility for further investigation transferred to the failure analysis task.

3. TV CAMERA TESTS IN ASSEMBLED CONFIGURATION

3.1 TEST PLAN

The major elements of the TV camera test program are shown in Figure 3-1, which describes grossly and sequentially the principal testing and dismantling operations. Further details of the TV camera tests are given in the following paragraphs and sections of this report.

The test program was conducted in three major phases, as indicated in Figure 3-1. The first phase entailed certain tests and operations conducted on the camera prior to any major disassembly. Work performed in this phase of the program is described in this section. The second phase, depicted in some detail in Figure 3-1, encompassed testing at a subsystem level and associated dismantling operations. Work conducted in this phase of the program is presented in Sections 4 and 5, and part of 6. The final phase consisted of the comprehensive test program at the components and materials level. This work, which constituted a major portion of the program, is discussed in detail in Sections 7 through 10, as well as the latter part of Section 6.

The sequence of operations shown in Figure 3-1 involved successive dismantling and testing steps. As already indicated, the sequence of these operations was contingent upon, and triggered by, major decisions along the way, coordinated with the customer. Figure 3-1 indicates these decision points.

Phase 2 operations, as depicted in Figure 3-1, constituted a simplified summary of the actual sequence of disassembly steps and tests conducted. Only major dismantling operations and subassembly level tests are indicated. Further details are presented in the respective sections of this report. Thus, for example, the box labeled "electric tests of selected chassis" pertains to the initial isolation and passive checkout of the ECU, followed by isolation and passive checkout of the three selected electronic chassis, and culminating in functional performance tests of these chassis. Similarly, other boxes, such as "lens assembly tests" and "mirror assembly tests," encompass sequences of tests of subassemblies and associated partial dismantling.

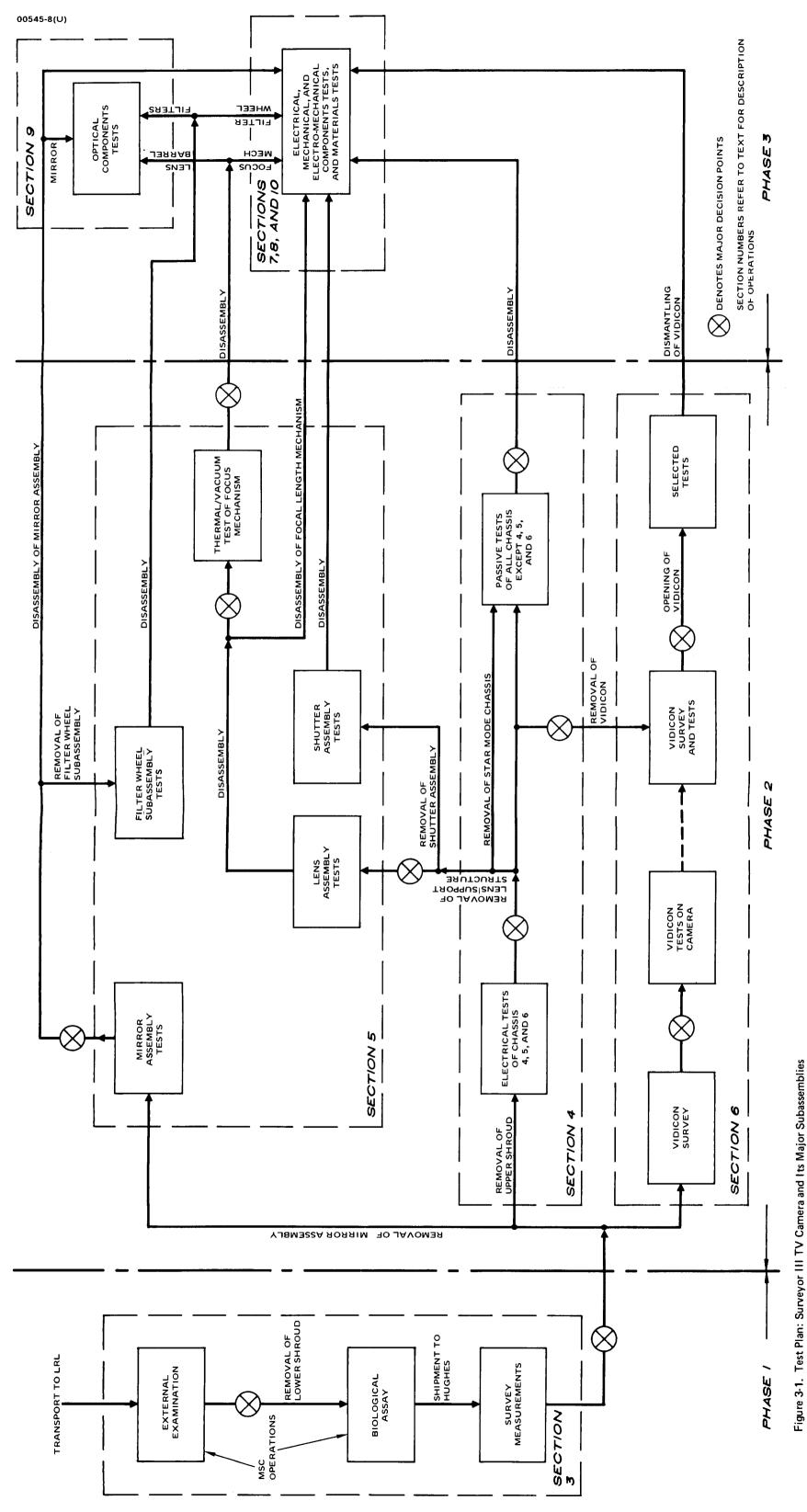
The simplified block diagram of the test plan in Figure 3-1 must be supplemented by noting a number of other aspects of the program. These are not explicitly indicated on the diagram for reasons of clarity and simplicity. Most important of these are use of test procedures and dismantling techniques carefully planned and approved in advance; checkout of test procedures and trial tests on spare non-flight TV cameras and subassemblies; concurrent preliminary evaluation of test results, using the past Surveyor data, wherever available and applicable; and certain auxiliary tests to assist in the understanding of uncovered anomalies and to help define subsequent operations on the retrieved camera. An example of the latter is the thermal simulation test conducted on non-flight vidicons, as discussed in Section 6.4.4. Advance planning and trial runs on spares were particularly important for all irreversible operations because of the unique nature of the camera parts and components.

Two major activities of the program are not indicated in Figure 3-1. One of these is the surface contamination study, conducted as a coordinated program with the companion NASA contract and science investigators, which is described in Section 11. Inclusion of a block labeled for this task on Figure 3-1 would be somewhat superfluous. Similarly, the failure analysis effort on such failures as were uncovered throughout the test operations and were deemed worthy of special investigation is not explicitly shown in Figure 3-1. This work could be described by drawing arrows from the many blocks of the figure into a separate box entitled "failure analysis". Results of the failure analysis test and studies are presented in Section 12.

Finally, it should be pointed out that the external survey operations, shown in Figure 3-1 as taking place during the initial phase, were, in fact, conducted to the required degree of depth and detail throughout all phases of the program. Similarly, support of the parallel efforts of the various science investigators was provided throughout the program although not explicitly indicated in the figure.

3.2 MSC OPERATIONS

The first phase of the test plan described above — tests of the TV camera assembly as a whole — included tests at NASA-MSC, Houston, and initial survey operations at Hughes prior to any major disassembly. The TV camera test plan intentionally did not include any electrical system tests; none were conducted. This section describes the MSC operations, which consisted of visual and photographic observations in the LRL, Houston, and certain science investigations in the LRL and other MSC laboratories.



3.2.1 Scope and Sequence of MSC Operations

The TV camera test program began with extensive advance preparations in Los Angeles. A trial run was performed at JPL in December 1969 on a non-flight television camera to evaluate the tools and the techniques used. This trial run entailed the removal of the lower shroud and conduct of the biological assay. Detailed procedures were prepared defining each individual step of the operations with the flight camera. Special tools and holding fixtures were provided.

Subsequently, MSC operations began at the LRL with the lifting of the quarantine on 7 January 1970. These operations took place between 7 and 15 January 1970. They can be grouped into the following major categories:

- Initial observations
- Initial dismantling removal of lower shroud
- Biological assay
- Various scientific measurements on TV camera
- Various science tests on items removed from camera

Color and IR photos of all operations and of all hardware were taken throughout.

The detailed time sequence in which all operations were conducted has been documented by NASA (References 7 and 12). These references also give the scope and results of some of the science investigations conducted. In summary, the sequence of these operations was as follows:

- Visual and photographic observation with camera in plastic bag
- 2) Overnight radiation counting (gamma ray spectrometry)
- 3) Removal of camera from bag, and visual examination and photographic documentation
- 4) Removal of camera mounting collar
- 5) Removal of loose debris from inside of mounting collar for semiquantitative emission spectroscopy and later evaluation
- 6) Installation of test support collar and mounting of camera on test tripod

- 7) Removal of external lower shroud connectors
- 8) Biological assay of connector wrap and lower connector areas
- 9) Removal of lower shroud*
- 10) Biological assay of selected areas inside TV camera
- 11) Visual and photographic observation of accessible inside portions of camera
- 12) Replacement of lower shroud (screws not reinserted)
- 13) IR photography and low power microscopic examination of camera
- 14) Collimated light photography of camera mirror**
- 15) Micrometeorite examination of camera
- 16) Preparation of camera for shipment

The following subsections present the significant results obtained in operations 1, 3, 4, 6, 7, 9, 11, and 12. Results obtained in the other operations listed are presumed to be described in separate reports by the respective science investigators.

During the LRL operations, strict cleanliness rules were observed. The camera was placed in a laminar flow bench, sterile clothing and equipment were used, and limited personnel access was enforced. Extensive photographs of all operations were taken, and the proceedings were recorded on video tape. Special protective handling measures were followed. All parts were identified, recorded, and placed in containers. This marked the beginning of the comprehensive inventory system instituted by Hughes for the program.

^{*}Scribe marks were made on all screws to record their orientation on the camera. All screws were cataloged and stored in plastic bags. It was later realized that contact with the bags destroyed some of the evidence of surface contamination.

^{**}Later repeated at Hughes with better equipment.

3.2.2 Initial Observations - Apperance of the TV Camera

Figure 3-2* shows the appearance of the camera prior to its removal from the bag. Additional photographs taken are available in Surveyor files (NASA photographs S-70-21127, S-70-21128, and S-70-21129). After careful inspection of the camera through the plastic bag, the camera underwent a gamma spectrometric analysis in the NASA Radiation Counting Laboratory. Results of this test are summarized in References 7 and 13.

Upon return of the camera to LRL, the plastic bag was removed in the laminar flow bench. The appearance of the camera immediately after removal of the bag is shown in the frontispiece and Figure 3-3*. The external surfaces of the camera were discolored and contaminated, presumably with lunar dust. The mirror was open with a view angle down and to the right. The filter wheel was in the "clear" position.

Following is a brief summary of the results of the detailed visual and photographic examination conducted at that time.

The camera mounting clamp, with remnants of the support struts, was still attached to the camera. A dent was noted on the lower shroud adjacent to one of the spacecraft support struts. This dent apparently occurred at the time the astronauts cut the struts on the lunar surface. Two dents in the mirror sunshade, which were probably incurred during the landing of the returned camera in the Pacific Ocean, as discussed in Section 2.5, were also noted.

The four external connectors were still mated to the camera. A section of the severed cable, approximately 7 inches long, was attached to one of the three bottom connectors, and a longer section of approximately 15 inches was attached to the upper mirror assembly connector. A separate section of the severed TV cable, approximately 8 inches long, was still attached by a cable clamp to the bottom side of the camera. These cable sections are clearly seen on Figure 3-3b.

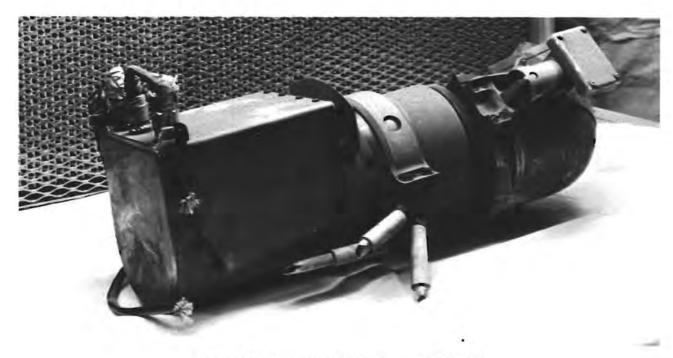
The exterior surface discoloration appeared grayish brown. This discoloration appeared to have been disturbed considerably by scuffing and handling during the retrieval and return operations.

There were some unusual light and dark patterns evidenced on some of the exterior surfaces. These patterns did not appear to correlate with solar illumination of coating degradation. There were sharply defined dark (shadow) areas under a wire on the mirror elevation drive mechanism and on the lower shroud under the spacecraft camera mount support struts. Figures 3-4 and 3-5* illustrate this effect.

^{*}The original photographs in the Surveyor Parts Test Program files are in color; black and white prints of these originals are presented here. This comment applies to many of the photographs throughout this report.



Figure 3-2. Surveyor III TV Camera and Its Plastic Bag at LRL (NASA Photo S-70-21126)



a) Side View Appearance (NASA Photo S-70-21153)



b) Front Appearance (NASA Photo S-70-21152)

Figure 3-3. Returned Surveyor III TV Camera

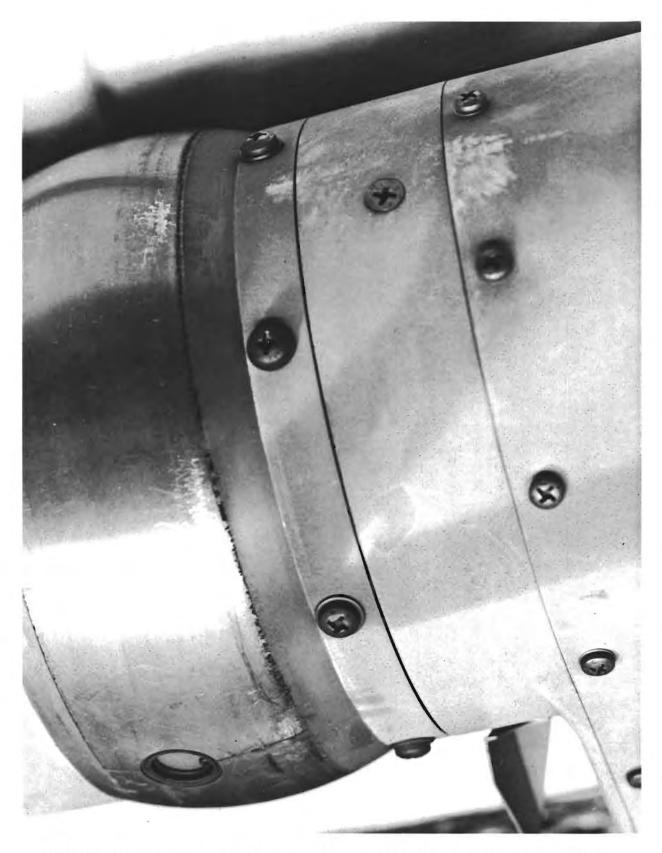


Figure 3-4. Area Under Support Collar Immediately Upon Its Removal in LRL (NASA Photo S-70-21138)

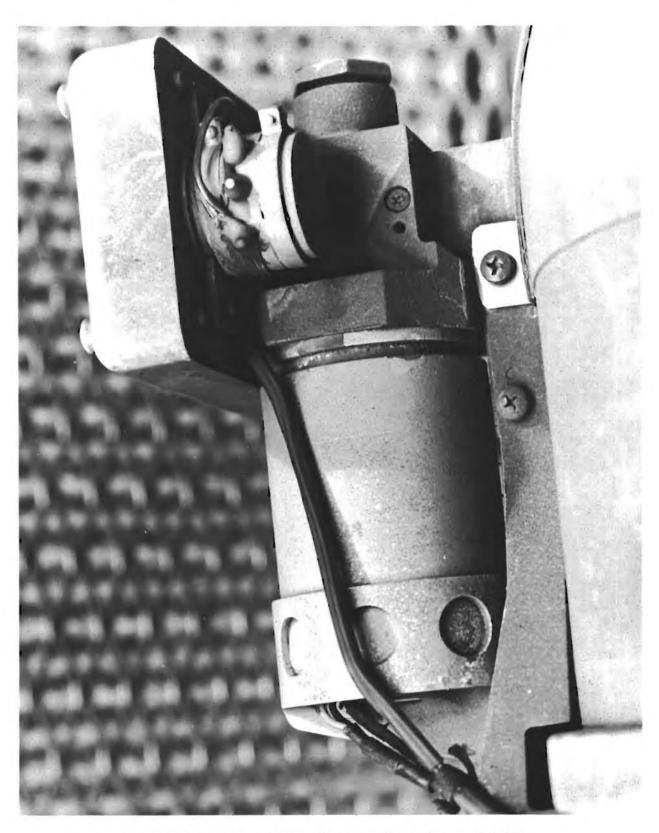


Figure 3-5. Mirror Elevation Drive Mechanism (NASA Photo S-70-21149)

Calibrated torque screwdrivers with a follow-up indicator gauge were used to remove the mounting hardware, and a tool gauge was utilized to measure the force required to unmate the external connectors. The tools and techniques employed in the removal of the connectors are illustrated in Figures 3-6 and 3-7. The values of all torques and forces were recorded.

The camera mounting collar, which was removed first, is shown in Figures 3-8 and 3-9*. The torques required to remove the four mounting screws which connect the two sections of this collar, thereby holding it tightly around the TV camera, ranged from 7.5 to 16 in-lb, compared with the original requirements of 14 to 16 in-lb. The first screw had the highest torque, as expected.

Dust and debris were noted under the support collar after its removal, and samples were collected for emission spectroscopy in NASA laboratories at Houston, and for later analysis. There was no evidence of any kind of adhesion in the interface of the collar-to-shroud, metal-to-metal contact.

The external connectors on the lower shroud, which were unmated next, are shown in Figure 3-10*. These connectors employ a snap-on lock mechanism, and the force required to unmate them, ranging from 10 to 21-1/2 pounds, compares to the original requirement of less than 25 pounds.

Figures 3-10 and 3-11* show the connector mounting hardware consisting of a lock washer and retainer nut, and the connector bracket for cable support, sandwiched between the connecting mounting hardware and the shroud. These connector retainer nuts were removed next. The recorded removal torques ranged from 24-1/2 to 37-1/2 in-1b compared with the original requirement of 48 to 64 in-1b. The connector bracket was then lifted off, as illustrated in Figure 3-12.

An initial biological assay was made during these operations. Biological samples were taken by NASA and JPL personnel by swabbing the areas under the mounting bracket, around the connectors, and the inner surfaces through the connector hole, as shown in Figures 3-12 and 3-13. In addition, samples were taken from inside the connector wrap.

^{*}Originals in color.



Figure 3-6. Removal of External Lower Shroud Connector (Photo 211-3999B)



Figure 3-7. Removal of External Shroud Connector Retainer Nut (Photo 211-4000B)

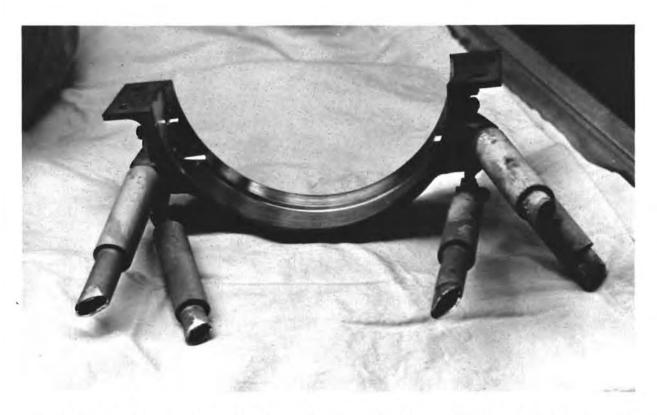


Figure 3-8. Camera Mounting Collar – Left Section With Remnants of Support Struts (NASA Photo S-70-21157)



Figure 3-9. Camera Support Collar — Right Section (NASA Photo S-70-21139)

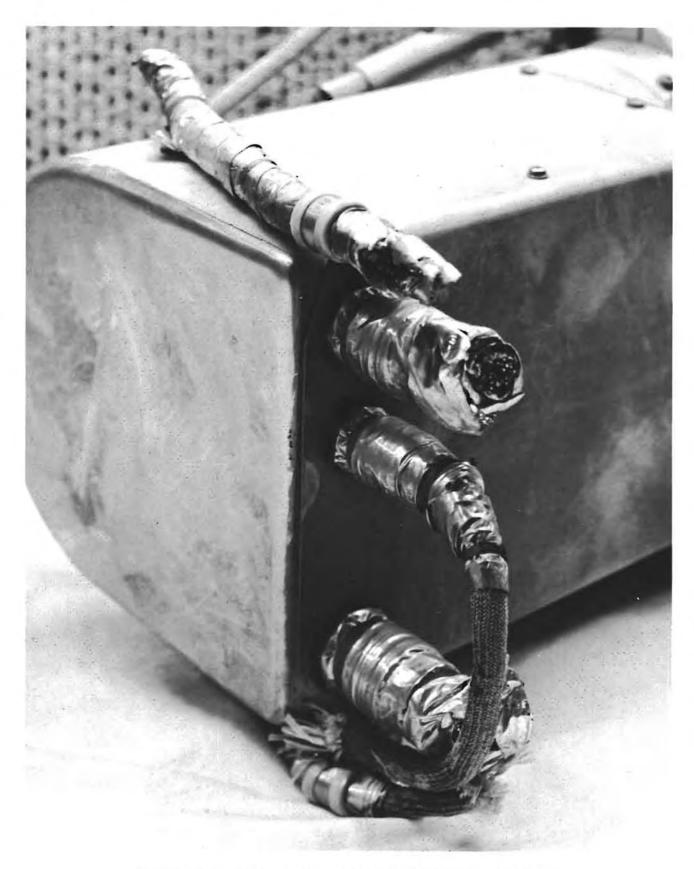


Figure 3-10. External Connectors on Lower Shroud (NASA Photo S-70-21146)

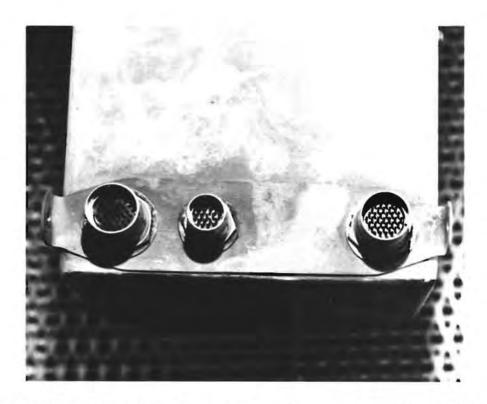


Figure 3-11. Lower Shroud After Removal of External Connectors (NASA Photo S-70-21142)

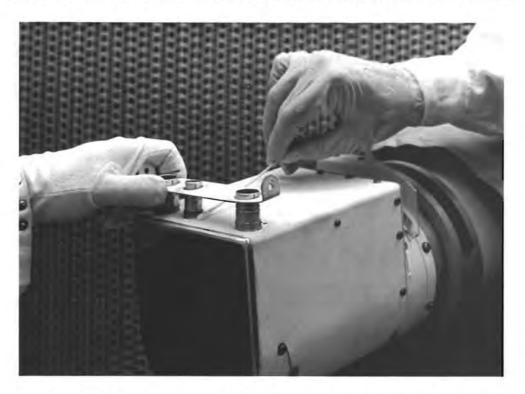
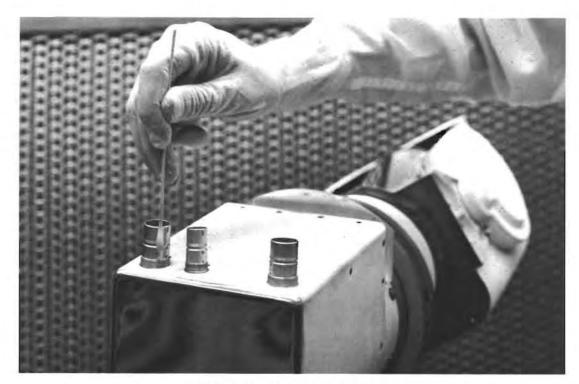
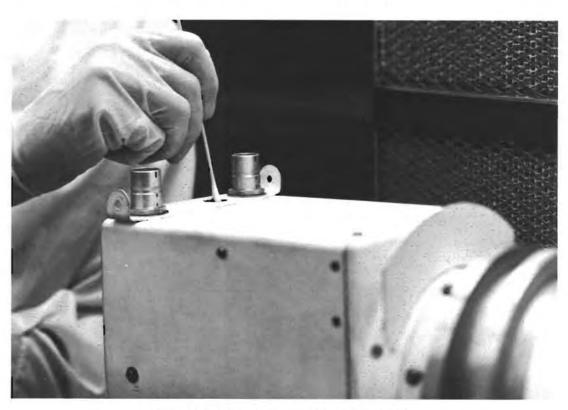


Figure 3-12. Removal of Connector Cable Support Bracket and Biological Assay (Photo 211-4001B)



a) Connector Surface (Photo 211-3998B)



b) Inside Surface of Shroud (Photo 211-3997B)

Figure 3-13. Biological Assay

TABLE 3-1. REMOVAL TORQUES OF LOWER MOUNTING HARDWARE

Screw Number	Measured Torque, in-lb	Screw	Measured Torque, in-lb
Υ	7.75	13	9.0
2	6.25	140	7.75
3 4 5	6.5	15	7.75
4	7.25	16	8.0
5	10.25	17	9.0
6	8. 25	18	8- 25
7	6.75	19	8.5
8	8.75	20	8.75
9	7.0	2.1	8.0
10	10.0	22	8.5
11	9.0	2.3	9.5
12	8.0	24%	4.0
Orig	inal Requirements		
NAS 4		3.5 to 6 in-1b	
NAS 6		7 to 9 in-15	

^{*}These two screws are NAS 4; all others are NAS 6.

The lower shroud is attached to the camera by 24 screws, of which 24 are NAS 6 and two are NAS 4. These screws were removed next. The recorded torque values are shown in Table 3-1.

In order to remove the lower shroud, the loosened connectors had to be pushed through the holes in the shroud. Difficulty was encountered with the right connector (J2). The external shell of this connector was firmly attached (binding or possible cold weld) to the inner rim of the hole in the shroud. Only after application of some force was this attachment severed. The surfaces in contact were carefully preserved for investigation for possible cold welding. No other difficulties were encountered in removal of the mounting hardware, and the lower shroud was successfully lifted off the camera.

Biological samples were then taken - 27 in all - of the interior of the camera. Swabs were made of the exposed electronic chassis and of the wiring harness without disturbing the wiring or the components. Also, small pieces of foam and epoxy were removed, as shown in Figure 3-14. Details of this operation are presented in Reference 7 and in the reports of the science investigators.

Numerous photographs were taken of the exposed electronics of the TV camera after the removal of the lower shroud. The general appearance of the exposed chassis is indicated in Figure 3-15*. Many additional photographs are available in the Surveyor files, in particular, NASA photographs S-70-21131, S-70-21132, and S-70-21133.

^{*}Original in color.

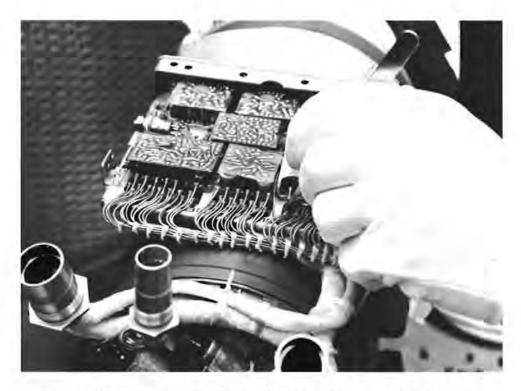


Figure 3-14. Biological Assay — Removal of Piece of Foam From TV Electronics (Photo 211-3998A)

The general conclusion upon completion of the shroud removal operations was that all connector and shroud mounting hardware torques were nominal and that no evidence of cold welding existed anywhere, with the possible exception of the attachment of the right connector external shell to the shroud, as noted above. The camera electronics appeared to be in excellent condition. The stainless safety wires appeared hard to cut. No evidence of any adhesion of interfaces was noted.

3.2.4 Summary of Tests After Shroud Removal

Visual examination and photographic documentation of the exposed interior of the camera were performed. No breakage or degradation of materials was noted. The lower shroud was replaced on the camera with six spare screws. These were not tightened but merely used to hold the shroud in place. The connector bracket was not reinstalled.

During the period 9 through 15 January 1970, a number of tests were conducted, as mentioned previously. The first of these was infrared (IR) photography of external surfaces. One of these IR photographs is shown (Figure 3-16). The next test was an attempt to conduct collimated light photography. Results were poor because of equipment limitations, and these tests were later repeated in the Hughes Surveyor facility. A

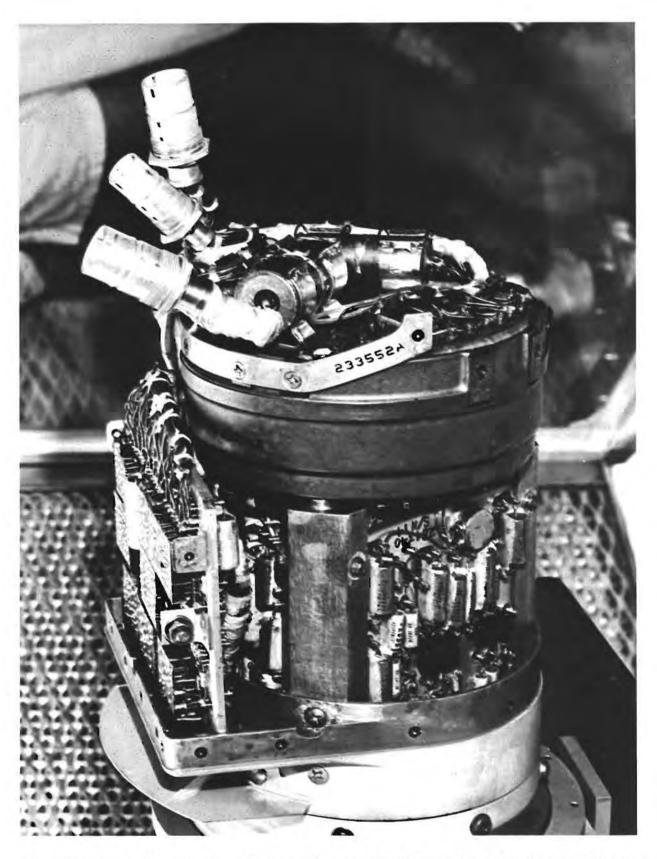


Figure 3-15. Exposed Lower Portion of TV Camera Upon Removal of Lower Shroud (NASA Photo S-70-21130)

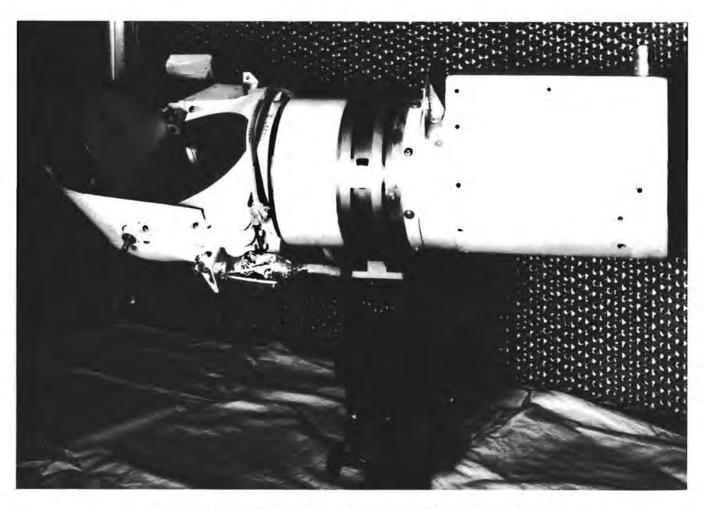


Figure 3-16. Infrared Photograph of TV Camera (NASA Photo S-70-21584)

low power microscope examination was then conducted to search for evidence of meteoroid impact. Results of these tests are presumed to be reported separately.

3.3 SHIPMENT TO HUGHES

Upon completion of the MSC operations, the TV camera was packaged and transported to the special Surveyor Parts Test Facility at Hughes.

The lower shroud was secured for shipment, as noted above. Protective covers were placed over the lower shroud front connectors, and the entire camera was wrapped with teflon FEP. Figure 3-17* shows the appearance of the camera just before shipment. The camera was placed in a special shipping container available from the Surveyor program, as shown in Figure 3-18*. The hardware removed from the camera was placed in a separate shipping container.

The camera and its associated hardware, together with other retrieved Surveyor III parts studied on the companion NASA contract, were shipped to Hughes on 16 January on a Hughes airplane, under a personal escort of NASA, JPL, and Hughes personnel, dispatched to Houston for this purpose. The aircraft landed at the Hughes airstrip in Culver City in heavy rain, but all parts were well protected. The parts were transported from the aircraft to the test facility in a Hughes car, a distance of several hundred feet. All hardware transported from Houston to Hughes was carefully documented. The arrival and transportation at Hughes, as well as removal of the TV camera from its carrying case inside the facility, were documented by photographs and movies. The camera was removed from the carrying case and placed on the test tripod in the laminar flow bench.

3.4 SURVEY OPERATIONS

The first phase of the Surveyor Test Program at Hughes, prior to any major dismantling, consisted of survey operations. This included visual, microscopic, and optical measurements of the external, readily accessible surfaces of the TV camera. As dismantling operations progressed, these survey operations were continued on the various surfaces. This section summarizes the findings of these operations.

The surfaces examined included painted surfaces — organic white, inorganic white, and organic black; polished aluminum; teflon TFE and aluminized teflon FEP; mirrors and filters; glass fiberboard; nylon tie cords; exposed wires; and conformal coatings. The microscopic examination

^{*}Originals in color.

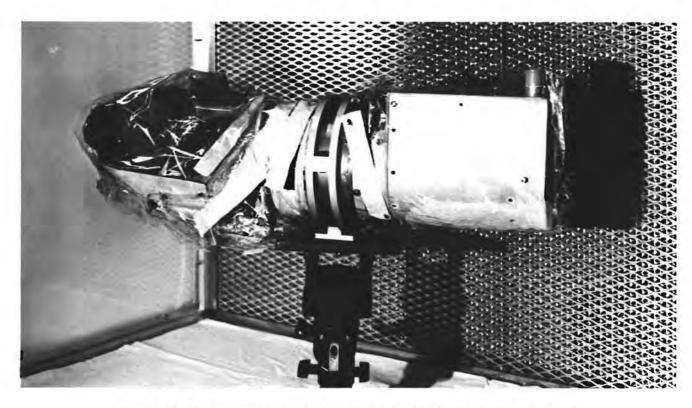


Figure 3-17. TV Camera Wrapped for Shipment to Hughes (NASA Photo S-70-22654)

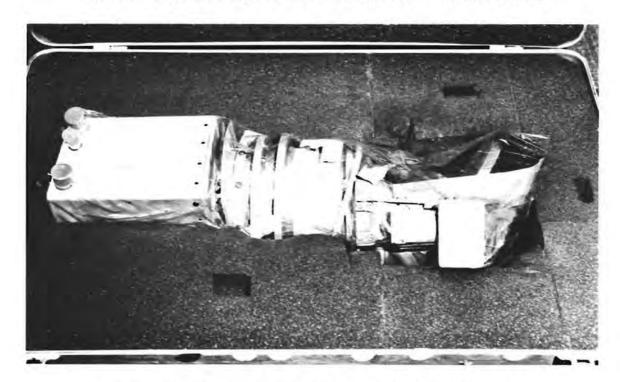


Figure 3-18. TV Camera Placed in Carrying Case (NASA Photo S-70-22667)

was conducted with a Zeiss microscope with a 200 mm objective at 6 to 40 X. Some of the areas examined as part of the external survey operations can be seen in the frontispiece to this report, as well as in Figure 3-3.

The survey operations constituted the first step in the effort to determine the apparent effects of the lunar environment and to relate these effects to other sources of degradation, such as the sun, the Apollo lunar module descent engine, and the Surveyor spacecraft itself (engines, landing, outgassing, etc.). This initial examination was to serve as a starting point for subsequent more detailed investigations prior to any dismantling or destruction which might result in some loss of original evidence.

3.4.1 Inorganic White Paint

Most of the exterior surfaces of the TV camera were coated with a white inorganic paint developed by Hughes for the Surveyor program. It is essentially an aluminum silicate (calcined china clay) pigment in a potassium silicate binder. The coating was applied to a thickness of 6 to 8 mils on a substrate that consisted for the most part of 6061-T4 aluminum alloy. All visual and microscopic examinations were performed on a laminar flow bench. At no time was the TV camera physically handled.

The most obvious change in appearance was the color. This change was noticed by the astronauts during retrieval operations when they described the surfaces as being a tan color. Actually, there was a range of colors noticed, including tan, gray, brown, and yellow. Some of these color variations are visible on the sunshade and on the connector bracket, which are shown after disassembly in Figure 3-19*. The circular areas on the bracket that appear white were shielded from direct lunar exposure by connector hardware. In general, where the paint surface was protected by brackets and screw heads, the color was still white **. Microscopic examination of these areas at 40X indicated little difference between the various colored areas. All areas had a fairly even distribution of dark particles that are presumably lunar material. There were some large areas that had a patchy appearance which was lighter in color than the surrounding areas. This is attributed to handling by the astronauts. Small areas that had been touched up prior to launch by sanding the damaged surface of the paint appeared to be much whiter.

All of the exterior white painted surfaces were affected to some extent by "mud-cracking" or "alligatoring." Figure 3-20 shows one side

^{*}Original in color.

^{**}These were the only remaining white areas.



Figure 3-19. Color Variations on Sunshade and Connector Bracket (Photo 70-5166)

of the lower shroud that was heavily affected. In those areas of the shroud that were protected, such as under the screw heads, mud-cracking did not take place. Other exposed areas seemed to be free of mud-cracking. Figure 3-21* shows an area on the lower shroud that was heavily mud-cracked, except for that area covered by the screw head. However, the adjacent area to the right in Figure 3-21* did not show evidence of mud-cracking.

Several areas had the appearance of shadows imprinted into the white paint. These shadows were characterized by a relatively dark gray area with distinct, very sharp boundaries. Under microscopic examination, these dark areas appeared to have a greater concentration of dust particles. It was noticed that, for each shadow, there was a corresponding object in the near vicinity. When viewed at the proper angle, the edges of this object would line up with the boundary line of the shadow. The viewing angle with respect to the TV camera, necessary to line up the object and the shadow, was the same for all shadow patterns, indicating that the source of the shadow effect had its origin at a single point. Figure 3-22 shows several areas around the mirror elevation drive motor that had been affected. The shadow on the motor case was originally lined up with the cable, which has been moved aside in this photograph.

^{*}This impact was previously reported by B. Cour-Palais at MSC.

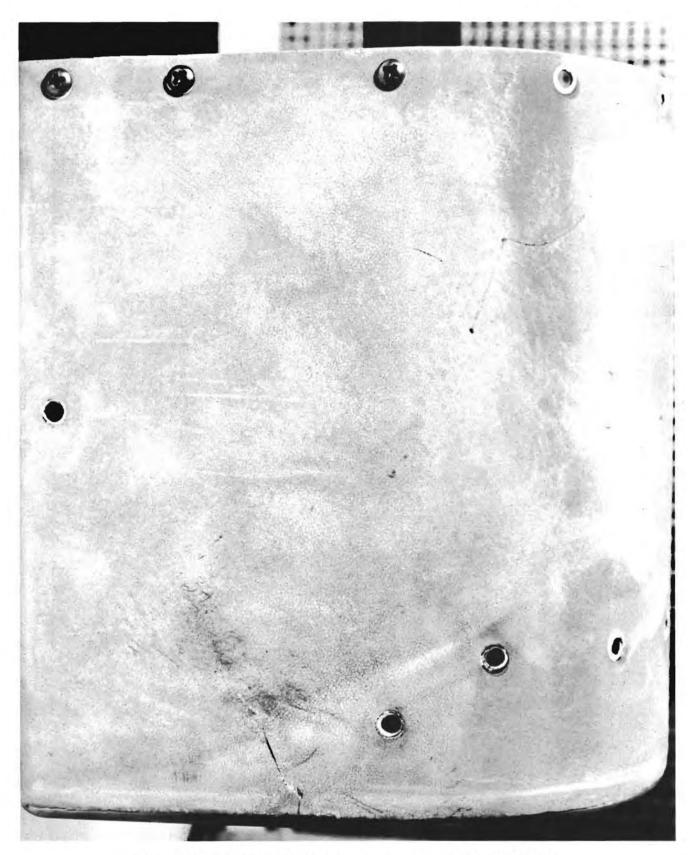


Figure 3-20. Evidence of "Mud Cracking" on Lower Shroud (Photo 4R14276)



Figure 3-21. Variations in "Mud Cracking" on Lower Shroud Area (Photo M917861)

Scrapes and chipping were noted in some areas, but these were probably the result of handling on the moon and during the transit back to earth and after recovery. One suspected micrometeroid impact area was detected visually and had a crater diameter of about 0.005 inch*. The fact that only one visible micrometeroid impact was detected was surprising. A uniform erosion of the paint from a larger amount of micrometeroid flux was expected.

3.4.2 Organic White and Black Paints

A white organic-based paint was applied over thin aluminum foil on the back of the mirror. It was a 3M velvet paint containing titanium dioxide pigment in an alkyd resin binder. The paint experienced no major color changes except for a slight loss of reflectance. The back of the mirror was shielded from the direct rays of the sun and from lunar material by the sun shade. It was also noticed that the paint was cracked in several areas. Some of the discoloration may have been the result of outgassing of the black organic paint in the mirror hood directly facing the back of the mirror.

A black organic-based paint was used inside the mirror assembly as an antireflectance coating. This was also a 3M velvet paint containing carbon pigment in an alkyd resin binder. A slight lightening in color of this paint was noted. This may be the result of coating of the surface by lunar material or caused by bleaching from the sun. No other effects were noted.

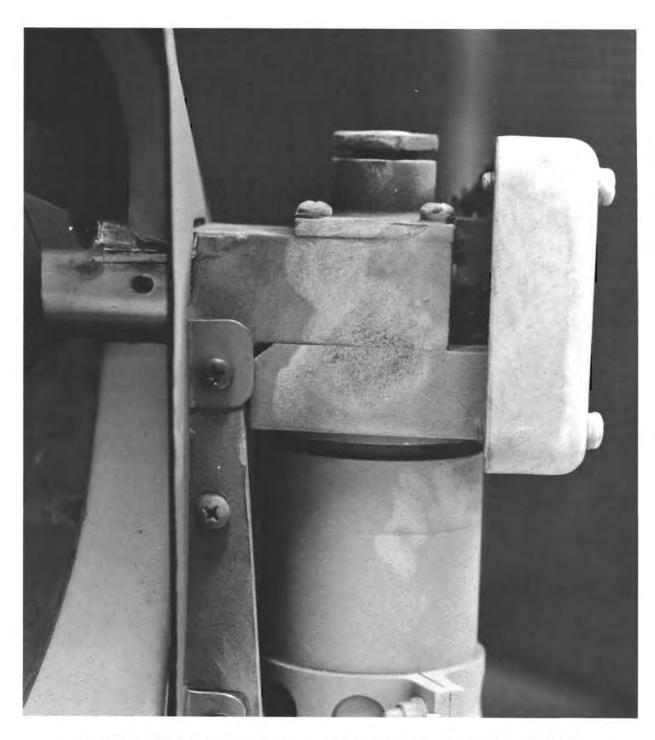


Figure 3-22. "Sandblasting" and Erosion on Elevation Drive Motor Housing (Photo 00545-31)

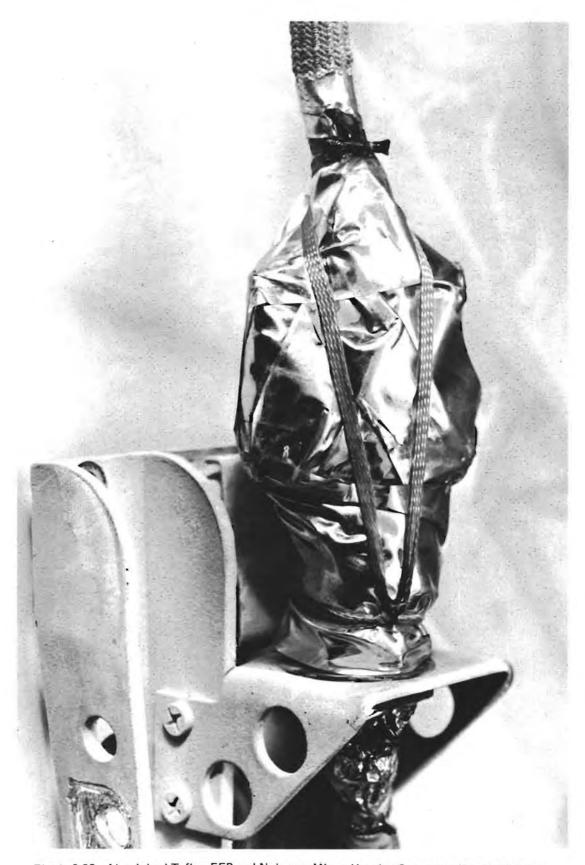


Figure 3-23. Aluminized Teflon FEP and Nylon on Mirror Housing Connector (Photo 70-5169)

3.4.3 Wires, Cables, and Electronics

The optical survey included examination of the exposed nylon tie cord used to secure the cable wrap, of the glass fiber braid insulation of the TV cable, of exposed wires within the mirror assembly, and of conformal coatings used on circuit boards.

The nylon cord seen in Figure 3-23* had the expected yellowish color, which, under microscopic examination, appeared to be only on the top surface of each individual strand. The color changes to a dark brown in the vicinity of the epoxy adhesive used to secure knots in the tie cord, indicating that some of the discoloration may be the result of the epoxy wicking along the cord and discoloring. The epoxy itself was dark brown. Physically, the nylon was in good condition; no adverse effects of the lunar exposure were noted.

The cable going from the mirror housing to the lower shroud was insulated with a glass fiber braid. The cable can be seen in the frontispiece and in detail in Figure 3-24*. This cable was heavily discolored in the area exposed directly to the external lunar environment, but was generally clean and white where protected by the teflon wrap. As with the nylon, the discoloration appeared to be only on the top surface of each strand when examined microscopically.

Within the mirror assembly, several insulated wires were in a position where they would be directly exposed to the sun. The insulation included multicolored teflon insulation, polyimide-coated teflon FEP insulation, and teflon TFE sleeving. In no case was there any evidence of lunar-induced effects, except for a slight dull appearance, probably due to a thin coating of lunar material.

The circuit boards were coated with an epoxy resin conformal coating. Numerous cracks were apparent in the coating, particularly where there appeared to be a heavy buildup of the coating. Some of these cracks appeared to extend into individual components, cracking the casings of the components. Further discussion of this effect is presented in Section 10.3.3. It should be noted that cracking of conformal coating was frequency observed after thermal-vacuum testing and generally did not cause any component failures.

^{*}Original in color.

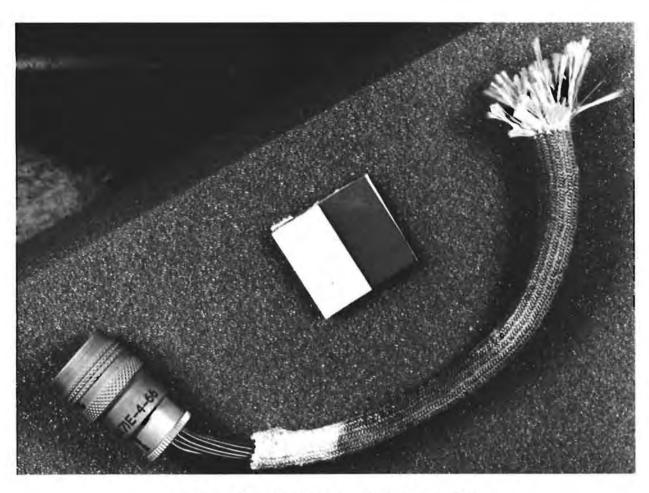


Figure 3-24. Glass Fiber Cable Insulation (Photo 70-5499)

3.4.4 Aluminized Teflon FEP and Teflon TFE

Aluminized teflon FEP, teflon side out, was used as a radiative temperature control coating on the mirror housing connector, as well as on cables (Figure 3-23). The surface exposed to the lunar environment exhibited color changes and was dust-coated. The aluminum coating on the inside was faulty. On areas of the teflon that were overwrapped, no visual color change was noted.

The horseshoe-shaped area on the mirror housing directly below the mirror, as seen in the frontispiece*, was intended as a seal when the mirror is in a closed position. It consisted of 2 mil thick teflon TFE bonded down with an epoxy adhesive. Figure 3-25* shows this area in detail. The teflon had turned a dark brown from its original white color and had turned up along the edges in some areas. No cracking was seen on the surface. The discoloration is believed to be attributable to the epoxy bonding. Absence of teflon in several places in Figure 3-25 was caused by removal of samples later in the program for special tests and science investigations.

Teflon TFE was also employed in the skirt, which is on the surface about which the mirror assembly rotates when stepped in azimuth. This area is visible in the frontispiece, and is shown in more detail in Figure 3-26*. Approximately one-half of the TFE teflon was bonded down. Discoloration was noted but not to the same extent as on the mirror housing. On the side of the camera facing the lunar module, the teflon was tucked under, allowing lunar material to enter. The teflon was also partially curled up along the edge. A more detailed investigation was instituted as part of the failure analysis task; additional data on this discolored and curled-up teflon TFE are presented in Section 12.

3.4.5 Polished Aluminum Mirrors and Filters

Two areas of the camera body were polished for purposes of radiative temperature control: the bottom of the lower shroud and the lower side of the vidicon radiator just above the lower shroud. Both of these areas faced the lunar surface and had a dull appearance caused by complete coating with lunar dust. No other effects of the lunar environment were observed. However, fingerprints made by the astronauts while on the lunar surface were noticed in both areas.

The azimuth mirror can be seen in the frontispiece. The mark at the top was made on the moon by one of the astronauts with his finger.

^{*}Originals in color.

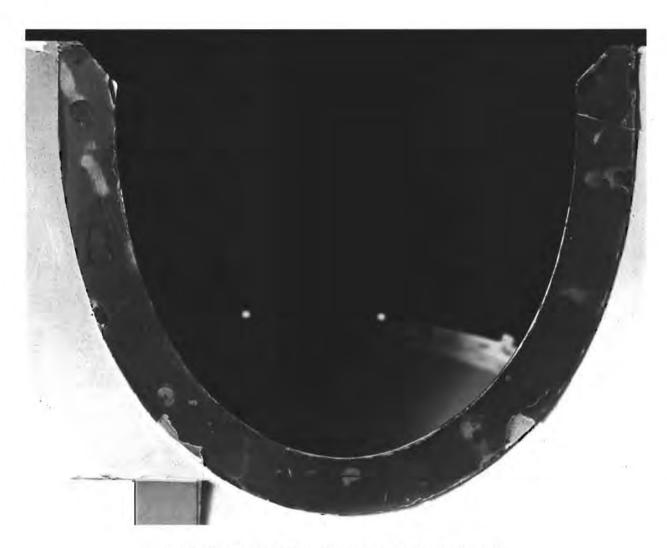


Figure 3-25. Teflon TFE on Mirror Assembly (Photo 70-5640)

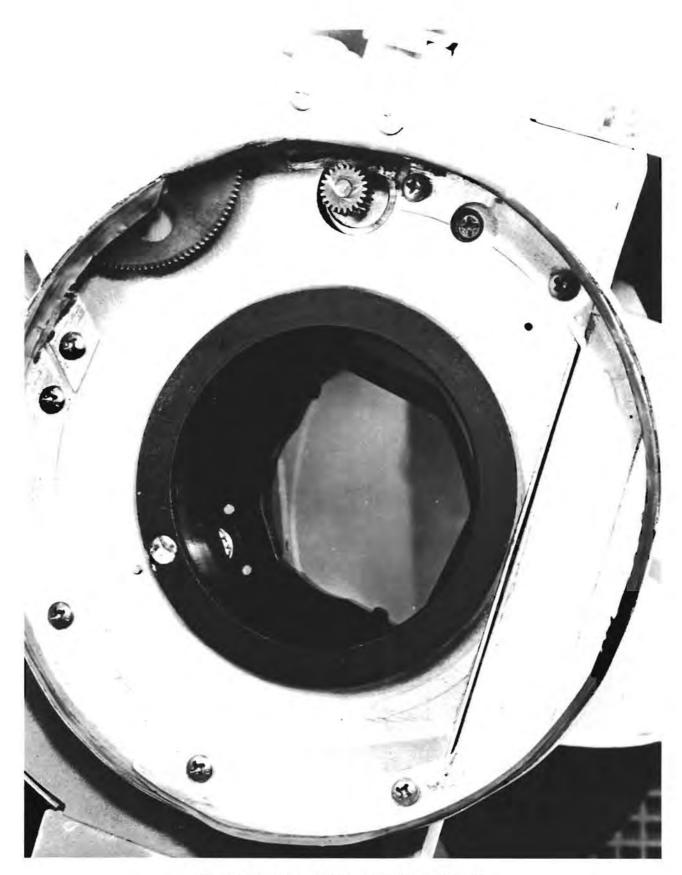
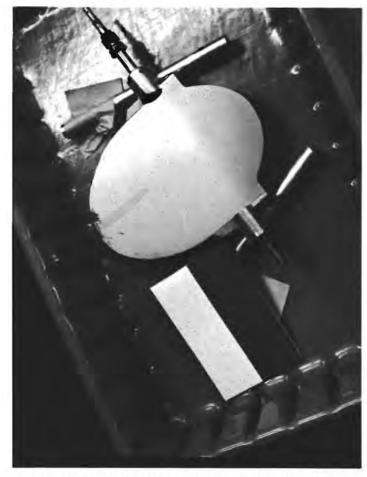
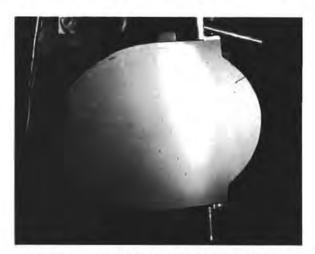


Figure 3-26. Teflon TFE Skirt Seal (Photo 70-4430)



a) One Set of Surface Lighting Conditions (Photo 70-4991)



b) Different Set of Surface Lighting Conditions (Photo 325-817BC)

Figure 3-27. Color Variation and Banding on TV Mirror

The mirror was heavily dust-coated and had a definite band pattern. The color differences and the band patterns were photographed; Figure 3-27 presents black and white replicas of the original color photographs which reveal these color differences and patterns in more detail. The two photographs shown were taken with different lightings; different optical effects are emphasized, clearly substantiating the importance of viewing angle and of lighting.

Further detail on the discoloration of the TV mirror is given in Section 9. Additional tests were conducted subsequently by science investigators and are presumed to be discussed separately.

Examination of the filters in the filter wheel assembly also revealed a coating of lunar dust. The filters were subsequently transmitted to JPL, as directed, for science tests. No further testing of the filters was conducted by Hughes.

4. ELECTRIC CIRCUIT TESTS AND DISMANTLING OF MAJOR SUBASSEMBLIES

4.1 INITIAL DISMANTLING

Phase 2 operations — tests at subsystem levels — commenced with the completion of initial survey operations and entailed progressive disassembly and tests of major units of the TV camera, as shown in Figure 3-1 (Section 3). The tests of electric chassis are presented in this section.

The first step consisted of certain preliminary dismantling operations. To gain access to the interior of the camera, it was necessary to remove the upper mirror assembly, as well as the ring gear and the upper shroud. Figure 2-3 (Section 2) shows the appearance of the TV camera after these initial dismantling operations. The decision to remove the mirror assembly was justified by the fact that functional testing of the entire TV camera was not planned. The mirror assembly is a separate unit which could be tested on a spare television camera. Also, the functioning of the mirror stepping electronics of the flight camera could be checked out with a spare mirror assembly unit, if required.

Following certain optical measurements of the mirror, discussed in Section 9, the mirror assembly and ring gear were removed. The mirror assembly azimuth gear train rotates on a ring gear installed in the camera before the mirror. In the mated condition, the mirror hub fits down over the lens support structure barrel below. The gear relationship between the mirror assembly gear train and the ring gear in the mated condition is maintained by means of a retainer ring which slides along a grooved slot cut into the lens support structure barrel. This retainer ring keeps the mirror hub from sliding out and off the lens support structure.

To remove the retainer ring, one end of it must be properly positioned directly in front. This is accomplished by stepping the mirror assembly in azimuth to the desired position. Fortunately, the returned camera was in the proper orientation so that no stepping was necessary. Therefore, the retainer ring was easily removed, and the mirror assembly was lifted from the camera by grasping it at each end of the housing, free of the ring gear. Both the retainer ring and the grooved slot of the lens support structure have lubricated surfaces.

The ring gear (Figure 4-1)*, comprising a main gear and an anti-backlash gear, was removed next. It is attached to the camera by eight mounting screws that mate to the lens support structure housing. Sandwiched between the ring gear and the lens support structure is the front flange of the upper shroud; thus, the ring gear must be lifted before the upper shroud can be removed.

^{*}Original in color.



Figure 4-1. Azimuth Drive Ring Gear Assembly (Photo 70-4434)

The mounting screws were removed with a torque screwdriver, with a follow-up indicator gauge to measure the removal torques. The torques required to remove these eight mounting screws were measured and ranged from 8 to 11.8 in-lb, compared with the original requirement of 10 to 12 in-lb; thus, the results were nominal, as previously demonstrated at LRL.

The lower shroud, which had been removed in the LRL and then reinstalled for shipment with 6 of the 24 mounting screws, was again removed.

Removal of the upper shroud was then carried out. After removal of the ring gear, this required the removal of eight screws attaching the upper shroud to the camera's main deck structure.

The torques required to remove these eight mounting screws, as measured with the torque screwdriver, ranged from 7 to 8 in-lb, compared with the original requirement of 10 to 12 in-lb; thus, the results were nominal. Figure 4-2 is a photograph of the upper shroud after removal, showing the flange under the ring gear and the holes for some of the mounting screws.



Figure 4-2. Bottom View of Upper Shroud of Camera (Photo 4R14061)

The removed mirror assembly of the Surveyor III camera was then installed as a unit on a spare camera and an overall optical transmission test was conducted to evaluate possible changes in video response. This test was run in the Hughes Surveyor Laboratory by science investigators with Hughes support. The test is described briefly in Section 9 and is presumed to be reported separately.

4. 2 OBJECTIVES AND SCOPE OF ELECTRIC CIRCUIT TESTS

As noted earlier, it was not planned to operate the TV camera as a whole, because of uncertainty of its operability, concern over destruction of evidence, and absence of the requirement to determine whether it was still operable. Therefore, as discussed in Section 2.6.1, no system test was conducted. However, it was decided to functionally check out selected electronic subsystems of the camera, that is, several chassis, which are self-contained except for input power and termination.

The objectives of the electrical tests of the selected chassis were to obtain a gross indication of the state of electronics, to verify packaging and assembly, to evaluate the performance of at least some of the circuits and compare functional parameters with previous data, and to establish a basis for selection of components for subsequent detailed testing.

The circuit test program was closely coordinated with the electrical components test plan. A detailed list was prepared of all the electrical components and their location on the various chassis. Components of special interest or those components which were only present in a few places were identified, and a priority list was generated in coordination with the customer. Using this list of components, annotated with component priorities and location on the chassis, the final selection of chassis to be tested was made on the basis of the following criteria:

- Presence of sufficiently large numbers of components of interest to warrant testing of the chassis
- Insurance that similar components were present elsewhere so that no critical components were unique to the chassis tested in case of an inadvertent stress
- 3) Ease of performing the electric chassis test, i.e., accessibility and ease of isolation, powering, and dummy terminations

The scope of the electric chassis tests can be defined by the sequence of steps carried out for each chassis selected for electric circuit functional and performance testing:

- Detailed test procedures were prepared in advance and coordinated with the customer.
- Preliminary tests were conducted on a spare TV camera closely following the agreed-upon procedure, and all results were recorded.
- A detailed visual and microscopic examination was conducted of the accessible components of the chassis to screen out obvious anomalies.
- 4) Passive ohmmeter checks were made on critical elements to the maximum extent feasible.
- 5) The chassis was isolated by clipping critical input and output leads without affecting its electronic integrity.
- 6) Appropriate dummy load terminations were applied.
- 7) External power was applied gradually to the input terminals while monitoring appropriate electrical outputs.

- 8) Upon ascertaining the validity of the test, a complete measurement of functional parameters was conducted in accordance with established Surveyor test procedures.
- 9) Results of functional performance tests were compared with available data and evaluated. Data used for comparison included: Surveyor flight acceptance test documents, previous test data for the chassis available at Hughes engineering and developmental test and design data, and results of tests conducted on the spare TV camera (item 2 above).
- 10) Those circuits which exhibited discrepancies or failures were subjected to a detailed failure analysis.
- In selected instances, failed components were replaced and chassis functional tests were conducted.
- 12) Based on results of evaluation of electric circuit test data, special instructions were generated for subsequent tests at the component level.
- 13) The electronic chassis was removed from the camera and further dismantled.
- 14) Selected components and materials were removed from the chassis for subsequent tests at the component and materials level.

The remaining chassis were not tested functionally. Their tests consisted of carrying out steps 1 through 4, and 12 through 14.

4.3 SELECTION OF CHASSIS FOR FUNCTIONAL PERFORMANCE TESTS

The TV camera contains eight chassis that are relatively independent functionally, both mechanically and in terms of electrical operation. These are listed below:

- Chassis A-1: Lens Control Timing Circuits Provides timing logic for filter, focal length, focus, and iris functions.
- Chassis A-2: Lens Control Control Drive Circuits Provides logic and power for driving lens and filter wheel drive motors.
- 3) Chassis A-3: 200 Line Sweep Circuit Generates sweep and timing signals required for vidicon operation and video readout.

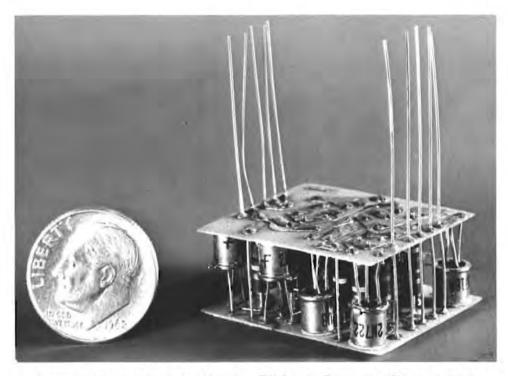


Figure 4-3. Typical Cordwood Module — TV Camera Electronics (Photo R87089)

- 4) Chassis A-4: 600 Line (Primary Mode) Sweep Circuit Generates sweep and timing signals required for vidicon operation and video readout.
- 5) Chassis A-5: Video Amplifier and Logic Circuits, Vidicon
 Thermal Control Generates and controls composite video
 output and provides thermal control of vidicon faceplate.
- 6) Chassis A-6: Shutter and Mirror Logic, Electronic and Vidicon Temperature Readout, and Lens Control Pulse Generators Provides shutter and mirror control and drive logic, and frame ID readout of electronics and vidicon faceplate temperature. It also generates timing pulses for lens control function.
- 7) Chassis A-10: Star Mode Chassis Provides output for blanking the vidicon for low light level time exposures.
- 8) <u>Electronic Conversion Unit</u> Provides required dc voltages for operating camera.

It is useful to summarize the construction of the chassis boards. The sandwich chassis comprises a core of 0.125 inch thick rigid polyurethane foam, a photochemically treated plate of 2024-T4 aluminum 0.015-inch thick, and an epoxy-glass circuit board 0.032 inch thick. The three members are bonded together with a modified epoxy-polyamide resin. This resin is also used as a high performance coating for etched circuit boards.

Large components, cordwood modules, and heat dissipating components are generally mounted on the metal plate side; small components are mounted on the etched circuit board side. Electrical connection to the plate side components is obtained by passing component leads through holes in the plate and foam core, and by soldering them to terminals which extend from the etched circuit board through holes in the foam core and plate. Components on the board side are secured by an epoxy-polyamide conformal coating. The coating also serves in its usual capacity to seal the circuitry against environmental stresses during storage and operation. The components on the plate side are also secured with the epoxy-polyamide resin to which has been added colloidal silica to increase its viscosity and allow application as a paste. This provides for sufficient adhesion to hold the component rigidly during any mechanical or structural stress.

A typical cordwood module is shown in Figure 4-3. The cordwood construction was utilized for units with severe volume limitations, where the module component density was greater than 30 parts/cubic inch. Below this density, an open-form board assembly is lighter.

The etched circuit boards are 0.011 inch thick and contain double-sided circuitry with plated-through holes. Circuitry is redundant wherever

possible. Board-to-board feedthroughs are accomplished with 0.025 inch diameter bus wire. Module leads are formed from discrete 0.015 inch diameter gold-plated Dumet wire. To eliminate problems caused by shock and vibration, an epoxy-polyamide resin conformal coating is applied to the module. This consists of a thin layer of resin over all parts within the module, a web of resin between adjacent components, and a resin fillet between the etched circuit board and component bodies, and leads in contact with the etched boards. Also, as part of the conformal coating process, a 0.010 inch epoxy-glass laminate insulator is bonded to the bottom of the module to provide positive insulation over the solder balls, as well as a flat mounting surface for the module.

In line with the criteria discussed in Section 4.2, Chassis A-4, A-5, and A-6 were selected for functional performance testing. All three chassis had a significant number of components, and all critical components on the prepared priority list were also available in one or more of the remaining chassis. Past data were available for comparison. Also, all three chassis were reasonably accessible, provided they were tested and removed in sequence. Chassis A-4 was selected in preference to Chassis A-3 because 600 lines was the primary mode of camera operation. Thus, this chassis could be used later for checking out vidicon performance parameters in the preferred mode should this test be desired and results could be directly compared with preflight data.

A summary of tests performed on these chassis and results obtained is presented in the following sections. A detailed description of the three chassis is given in Appendices D, E, and F, respectively.

4.4 TEST EQUIPMENT CHECKOUT AND PRELIMINARY TESTS

Prior to conduct of the functional chassis tests, preliminary and precautionary tests were conducted. These included passive tests of the flight camera, compilation and checkout of the electronic test equipment required, and functional performance tests of similar chassis from a spare camera, using the prepared test procedures.

In accordance with standard Surveyor TV camera procedures, the first step in examining the flight camera was to rotate the ECU so that the output terminals were exposed. Passive resistance checks of the ECU output terminals were conducted to determine whether any of the critical tantalum capacitors in the ECU has shorted in the lunar low temperature environment. Discovery at this point of the test program that significant failures had occurred would have mitigated against the performance of electrical functional tests because of possible catastrophic circuit failures upon application of power and resultant destruction of evidence.

Having ascertained that the ECU appeared to be in good condition, the ECU, vidicon tube, and chassis A-4, A-5, and A-6 were then isolated from each other and from the remaining camera electronics by cutting the appropriate interconnecting wires. This allowed each chassis to be properly terminated with dummy loads and separately powered from an external source.

The test equipment used in the performance of electrical chassis tests included standard commercial equipment, TV camera test position available from the Surveyor program, supporting Surveyor TV camera checkout equipment, and special tools. A more complete description of this equipment and of the calibration and checkout functions conducted is given in Appendix C. This equipment was compiled and successfully checked out at Hughes on a spare Surveyor TV camera before the arrival of the Surveyor III TV camera. This equipment was then used to conduct an operational performance check of the spare TV camera and the functional performance tests of the selected flight camera chassis.

4.5 FUNCTIONAL PERFORMANCE TESTS OF CHASSIS A-4

Chassis A-4 contained the sweep, blanking, and synchronization circuits required for the operation of the vidicon in the primary 600-line mode of operation. These circuits provide the following signals for camera operation:

- 1) Vertical and horizontal sweep signals for magnetic deflection of vidicon tube electron beam
- 2) Vertical and horizontal blanking pulses for blanking camera vidicon and test position TV monitor
- 3) Horizontal synchronization pulses for synchronizing horizontal sweep rate of monitor to that of camera
- 4) Vertical and horizontal retrace reference pulses for time reference in video logic and video summing circuits of chassis A-5

A detailed functional description of this chassis is presented in Appendix D. This section summarizes the tests conducted and the results obtained.

Table 4-1 gives results of the 18 parameters tested. These parameters comprised all of the specified Surveyor TV camera functional requirement tests for this chassis. Also shown in Table 4-1 for comparison purposes are the Surveyor program requirements for these parameters and the results of the last measurements made of these parameters prior to flight.

TABLE 4-1. RESULTS OF FUNCTIONAL PERFORMANCE TESTS OF ELECTRICAL PARAMETERS OF CHASSIS A-4

Parameter	Requirement	Post-Mission Measurement	Last Pre-Mission Measurement
Vertical sweep period, seconds	1.2 ±0.12	1.2003	1.203
Vertical blanking pulse width, ms	200 ±20	195.88	199.3
Vertical blanking pulse amplitude, volts	8.5 ±2	8.0	8.4
Horizontal sweep period, ms	1.67 ±83	1.643	1.653
Key clamp drive pulse amplitude, volts	-7 ±1.75	-6	-6.6
Horizontal vidicon blank- ing pulse width, ms	200 ±20	187	199
Horizontal vidicon blank- ing pulse amplitude, volts	15 ±3	13.7	15
Horizontal synch system blank pulse width, ms	266 ±26.6	264	258.5
Horizontal synch pulse width, ms	133 ±13.3	137	134.4
Horizontal system blank- ing pulse amplitude, volts	8 (minimum)	10	9.6
Horizontal sync pulse amplitude, volts	1.04 ±0.05	1.0	1.0
Vertical sweep ampli- tude, volts	1.3 to 2.3	1.6 peak- to-peak	1.3 to 2.3
Horizontal sweep ampli- tude, volts	1.3 to 2.3	2.2 peak- to-peak	1.3 to 2.3
Vidicon biasing voltages, volts			
Target Grid 5 Grid 2-4 Grid 3 Grid 1	12 300 220 39 -60	11.4 300 218 41 -63.5	12 297 224 +39 -60

These tests required proper powering and termination; these requirements are summarized in Table 4-2.

TABLE 4-2. POWER SOURCES AND TERMINATIONS FOR FUNCTIONAL TESTS OF CHASSIS A-4

Power Requirements		Terminations	
Source Voltages, volts	Pin Connections	Resistance, ohms	Pin Connections
+25 ±0.01	7 and 13	68 ±5%, 1/2 watt	3 to ground
-25 ±0.01	5 and 9	300 ±5%, 1/2 watt	6 to ground
+300 ±3	18		
-100 ±1	21		

Upon application of power to the A-4 chassis, a check of the various outputs revealed that only the vertical sweep circuit and the vidicon biasing network were operational. All other circuits were inoperable; this was traced to two failures identified at that point of the test program. The first failure was of an alloy transistor (Q14) in the vertical blanking circuit. The second failure was of an open metal film resistor (R36) in the horizontal sweep generator circuit.

It was decided to replace these failed components without disturbing other chassis elements. Fortunately, this could be readily accomplished. The two failed components were not subjected to failure analysis because they are no longer used in circuit applications. This is discussed in Section 12.

Chassis tests conducted after replacement of the two failed components produced the results shown in Table 4-1. All 18 parameters on chassis A-4 were well within specifications, and there was no indication of changes induced by the operation and residence of the TV camera on the lunar surface for 2-1/2 years.

4.6 FUNCTIONAL PERFORMANCE TESTS OF CHASSIS A-5

Chassis A-5 contained the video amplifier and summing circuits, video logic circuits, and vidicon thermal control circuits.

TABLE 4-3. RESULTS OF FUNCTIONAL PERFORMANCE TESTS OF ELECTRICAL PARAMETERS OF CHASSIS A-5

Parameter	Requirement	Post-Mission Measurement	Last Pre-Mission Measurement
Transmitter ON Amplitude, volts Pulse width, ms Rise time, microseconds	20.3 ±1.8 200 ±20 10 (maxi- mum)	19.5 196 2.2	20 195 2.3
Frame ID enable			
Amplitude, volts Pulse width, ms Rise time, microseconds	26 ±1.5 200 ±20 10 (maxi- mum)	25 196 1.6	26 195 1.4
Transmitter OFF			:
Amplitude, volts Pulse width, ms Rise time, microseconds	25 ±2 15 to 100 1.0	25.5 30 0.6	25 28 0.32
Video gate			
Amplitude, volts Pulse width, seconds	26.4 ±1.9 1.2 ±0.2	25.5 1.2	25. 5 1. 18
Horizontal sync level, volts	2.5 ±0.25	2.58	2. 65
Number of active TV lines	600 ±30	611	607
Vidicon thermal inhibit	First and third frame	First to third frame	First to third frame
Vidicon +29 volt heater current, ma			
ON OF F	85 to 130 10 to 30	96 15	100 20
Vidicon +29 volt heater switching point, ^O F	77 ±2	76	77

The purpose of the video amplifier and summing circuits was to amplify the output of the vidicon and to combine the horizontal sync/blanking and vertical blanking pulses in order to provide a composite video output signal. The video logic circuit supplied activation signals for the following functions: shutter operation, video gating, vidicon thermal control, and video or frame identification signals to the transmitter.

The vidicon thermal control circuits automatically provided power to the vidicon faceplate heater to maintain the faceplate within a specified temperature range. This function was performed upon receipt of the VIDICON TEMPERATURE CONTROL ON command. The temperature of the vidicon collar was sensed and power applied to the faceplate heater when the temperature dropped below the desired value. The vidicon thermal control circuits included the thermal control amplifier, vidicon thermal control switch, and control logic circuits. The logic circuits allowed the application of power to the faceplate heater only during the second erase frame. This prevented distortion of the video information during the picture readout and priming frames.

A detailed functional description of this chassis is presented in Appendix D. This section summarizes the tests conducted and the results obtained.

Table 4-3 shows the 17 parameters tested on chassis A-5 and results obtained. The specified Surveyor TV camera functional requirement tests for this chassis include three additional parameters, which were not tested, as discussed below.

Also shown in Table 4-3 for comparison purposes are the Surveyor program requirements for these parameters and the results of the last measurements made on these parameters prior to flight.

The conduct of these tests required proper powering and termination. External power was applied as follows:

+28 volts ±1 percent Terminals 27 and 29

+25 volts ±1 percent Terminal 3

-25 volts ±1 percent Terminal 15

Each composite video output was loaded with a 37,400 0.5 watt resistor in parallel with a 250 picofarad capacitor to the +29 return.

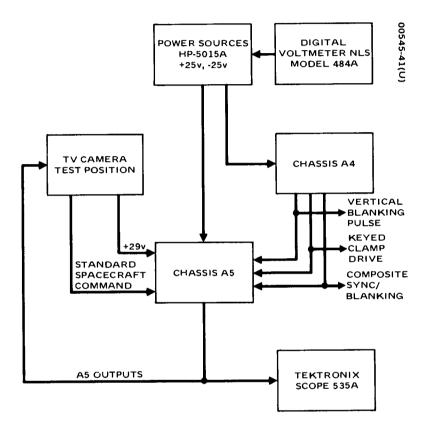


Figure 4-4. Test Setup for Functional Checkout of Chassis A 5

The three functions contained on chassis A-5 were tested in the following sequence:

- 1) Video logic
- 2) Vidicon thermal control
- 3) Video amplifier and summing circuits

To perform the chassis A-5 tests, it was necessary to use some of the outputs generated by the A-4 chassis, tested previously for this reason. The A-5 chassis tests also utilized the Surveyor TV camera test position (discussed in Appendix C), as well as standard commercial equipment. The test setup is shown in block diagram form in Figure 4-4.

Upon application of power to the chassis, the check of the chassis output revealed that no video was present in composite video outputs Al6 and Al7. This problem was evident by the absence of video noise normally present in the composite video output. The problem was traced to a shorted tantalum capacitor in the preamplifier circuit. One end of this capacitor was then severed, isolating the capacitor from the chassis. This allowed the continuation of the test, leading to the results shown in Table 4-3. Consequently, the following three parameters could not be checked:

- Video amplifier gain
- Video amplifier response
- Video amplifier noise level

The failed capacitor could not be replaced since it was a selected low-leakage component during original assembly and a suitable replacement was not available. Furthermore, replacement of this component might have stressed adjacent circuit board areas. The capacitor was subsequently subjected to a detailed failure analysis to determine the specific causes of failure. Results of this analysis are discussed in Section 12.

No other anomalies were uncovered in the course of the tests. As evident from Table 4-3, all parameters measured were well within specifications. There were no indications of any changes induced by the lunar environment.

4.7 FUNCTIONAL PERFORMANCE TESTS OF CHASSIS A-6

Chassis A-6 contained the shutter control circuits, mirror drive circuits, vidicon and electronic temperature readout circuits, and pulse generators for focal length, focus, and filter control.

TABLE 4-4. RESULTS OF FUNCTIONAL PERFORMANCE TESTS OF ELECTRICAL PARAMETERS OF CHASSIS A-6

Parameter	Requirement	Post-Mission Measurement	Last Pre-Mission Measurement
Focal length and filter pulse generator			
Pulse amplitude, volts Time interval, ms	+10 (minimum) 10 ±10%	22 9. 78	23 10.02
Focus pulse generator			
Pulse amplitude, volts	+10 (mini- mum)	16.5	23
Time interval, ms	62.5 ±10%	62.86	57.52
Shutter exposure pulse (pin 56)			
Time interval, ms	150 ±1%	149. 86	149. 95
Shutter reset (pins 21 and 57) Time interval, ms	200 ±20	196	195
Time exposure mode frame ID readout (J1-26), volts			
ON OFF	4. 36 to 5. 36 -0.93 to -0.13	4.979 -0.671	4.899 -0.620
Step mirror UP pulse, ms	125 ±20%	127	127. 12
Step mirror DOWN pulse, ms	125 ±20%	127	127. 18
Step mirror left Time interval, ms	125 ±20%	127	127. 11
Step mirror right Time interval, ms	125 ±20%	127	127. 19
Electronic temperature frame ID readout (J1-22), OF	70 - 96	83 (2.930 volts)	90 (3.155 volts)
Vidicon temperature frame ID readout (J1-18),* ^O F	70 - 96	8 (+0.660 volt)	85 (3.002 volts)
Two step mirror left Time interval, ms	250 ±20%	235	274.59
Two step mirror right Time interval, ms	250 ±20%	265	281. 9

^{*}Changed relative to preflight data

The shutter control electronic circuit provided the drive signals to the shutter solenoids, which actuated the two shutter blades. Circuits were provided for both the 150 ms mode and the time exposure mode.

The mirror drive circuits actuated the azimuth and elevation drive motors. Separate circuits were provided for the two modes of operation of the azimuth drive: single-step and two-step.

The microdiode temperature sensors were utilized to measure the temperature of the vidicon faceplate and of the ECU electronics. The temperature sensing and readout circuits on chassis A-6 processed the inputs from these two temperature sensors and delivered through a differential amplifier circuit appropriate voltage readouts corresponding to the sensed temperatures.

The optics control pulse generators provided appropriate signals for actuation and control of the filter wheel, focus, and focal length mechanisms.

A detailed functional description of this chassis is presented in Appendix F. This section summarizes the tests conducted and the results obtained.

Table 4-4 shows the 16 parameters tested on chassis A-6 and the results obtained. These parameters comprise all of the specified Surveyor TV camera functional requirements tests for this chassis. Also shown in Table 4-4 for comparison purposes are the Surveyor program requirements for these parameters, and the results of the last measurements made on these parameters prior to flight. These parameters were measured to the original Surveyor test specifications so that a comparable analysis could be performed with prelaunch data. Both the original chassis test data and the related TV camera unit test data were available for this analysis.

The conduct of these tests required the original Surveyor TV camera test position, certain commercial equipment, and certain outputs generated by the A-5 chassis, tested previously for this reason. A block diagram with the test setup utilized is shown in Figure 4-5.

The input power requirements were as follows:

+28 volts ±1 percent	Termination 22
-25 volts ±1 percent	Termination 39
+22 volts	Termination 32

Voltages were brought up slowly, employing current limiting. The high current mirror and shutter drive circuits were checked both at the nominal +22 line voltage and at a low voltage of +8 volts to verify the correct operation.

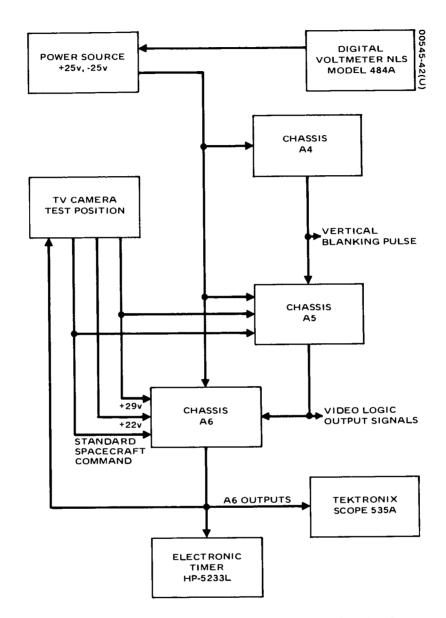


Figure 4-5. Test Setup for Functional Checkout of Chassis A6

All circuits were properly loaded and terminated for these tests. Table 4-5 summarizes the terminations employed.

Two anomalies were noted during the tests. A transistor in the shutter drive circuit was found open and burned out, along with one of the solenoids on the shutter assembly. This anomaly is discussed in more detail in Section 12. The second anomaly was an apparent change in the vidicon temperature readout circuit, as noted in Table 4-4. Further discussion of this anomaly is also presented in Section 12. This anomaly was thought to be attributable to changed characteristics of a transistor in the vidicon temperature differential amplifier circuit. Both the burned out silicon transistor and the suspected readout transistor are contained in the cordwood module, and it was not necessary to replace them to conduct the functional performance tests.

No other anomalies were uncovered during the tests, as evident from Table 4-4. All parameters measured were well within specifications except for the vidicon temperature readout. There were no indications of any changes induced by the lunar environment.

4.8 DISMANTLING OF MAJOR SUBASSEMBLIES AND COMPLETION OF CHASSIS TESTS

This section summarizes the dismantling operations which took place upon completion of the functional tests of chassis A-4, A-5, and A-6

TABLE 4-5. TERMINATIONS FOR FUNCTIONAL TESTS OF CHASSIS A-6

Mirror drive	25 ohms ±5 percent, 25 watts terminations 7 to 8
	25 ohms ±5 percent, 25 watts terminations 7 to 9
	25 ohms ±5 percent, 25 watts terminations 7 to 10
	25 ohms ±5 percent, 25 watts terminations 7 to 13
Shutter control	25 ohms ±5 percent, 10 watts terminations 18 to 32
	25 ohms ±5 percent, 10 watts terminations 21 to 32
	25 ohms ±5 percent, 10 watts terminations 55 to 32
	25 ohms ±5 percent, 10 watts terminations 57 to 32
Pulse generators	100 kilohms ±5 percent in parallel with 0.01 mf ±10 percent capacitor Terminations 24 to 35 Terminations 50 to 35

and the associated passive tests of the remaining chassis. The subassemblies removed included the lens support structure and its major subassemblies, all electronic chassis, vidicon subassembly, and the wiring harness. Each of these was, in turn, further disassembled into its major units, as discussed below. These disassembly operations are indicated in Figure 3-1 (Section 3).

As a result of these dismantling operations, the various optical sub-assemblies were available for test (described in Section 5), and the vidicon was delivered to the vidicon test laboratory for test (described in Section 6). The remaining chassis were delivered for materials and components tests. The only exception to the sequence of testing and dismantling described in this section is that certain vidicon tests were conducted prior to its removal. These tests are described in the beginning of Section 6.

4.8.1 Dismantling Sequence, Techniques, and Procedures

The following major subassemblies were removed in the sequence listed below. Each major subassembly was further disassembled into its subassemblies in the order indicated:

• Lens Support Structure

Shutter assembly Star mode chassis Lens assembly

Multichassis Assembly

Chassis A-3 Chassis A-4 Chassis A-5

- Chassis A-1
- Chassis A-2
- Chassis A-6
- ECU
- Wiring Harness
- Vidicon Assembly

Vidicon tube Boro nitride collar Deflection coil Vidicon housing Before each major disassembly, a complete visual and microscopic examination was conducted, extensive documentary photographs were taken, and planned circuit tests were conducted. The functional tests for chassis A-4, A-5, and A-6 have already been described. The remaining chassis were subjected to passive tests only, entailing selected ohmmeter tests across output terminals and of suspect components wherever advisable and feasible. Extreme care was taken to preclude any possible irreversible operations which would destroy evidence. Suspect electrical components (e.g., cracked glass envelopes) were noted and recorded for subsequent component level investigation.

During dismantling operations, each subassembly was supported by a special test fixture adapter until completion of the dismantling. All mounting hardware removal torques were measured and compared with installation torque specifications. Interconnecting wiring was cut rather than unsoldered to minimize damage, and each cut wire end was tagged and identified. Each removed part was packaged, tagged, and documented in a log book, and a complete inventory of all removed parts was maintained.

4.8.2 General Appraisal of Dismantling and Test Results

Figure 4-6 shows the appearance of the main TV camera structure after the removal of the mirror assembly and the shrouds, and prior to its disassembly. Another view of this assembly is also shown in Figure 2-3 (Section 2). The top of Figure 4-6 shows the lens support structure, the bottom portion the ECU. Figure 4-7 shows the camera main deck structure, which was the only remaining part after completion of the disassembly operations described in this section. The main deck structure is visible in the middle of Figure 4-6.

No problems were encountered during removal of the various camera assemblies. No evidence of cold welding was noted during removal of the mounting hardware. Table 4-6 indicates the observed torque values of the mounting hardware for the various subassemblies.

For comparison, Table 4-7 lists the range of original installation torques for the various screw sizes. Direct comparison, screw-by-screw and size-by-size, would not be fruitful and is not presented for several reasons. Removal torques were not expected to be identical with installation torques and depend on the sequence of the removal of screws. A difference does not necessarily imply an anomaly. It could be caused by shock, vibration, or other similar normal effects. The significant effects of the lunar environment which were looked for, on the other hand, would entail a major increase in the value of a removal torque. The important conclusion from comparing Tables 4-6 and 4-7 is that no effects such as galling or cold welding were noted.

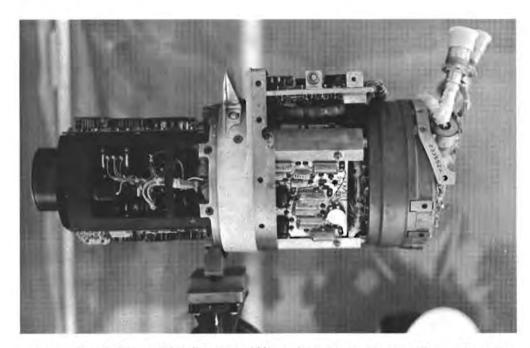


Figure 4-6. TV Camera After Removal of Mirror Assembly and Shroud (Photo 4R14058)

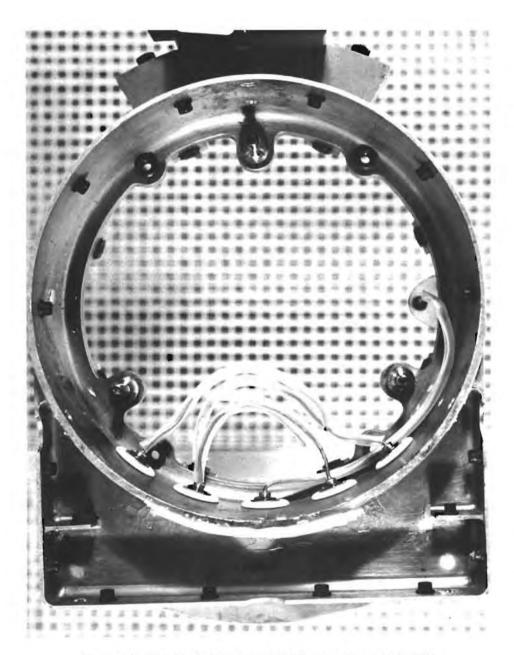


Figure 4-7. Main Deck Structure of TV Camera (Photo 4R15896)

TABLE 4-6. MOUNTING HARDWARE REMOVAL TORQUES

	Removal Torques, in-lb		
Major Subassemblies	Minimum	Maximum	
Lens support structure	17	23	
Shutter assembly	1.5	2.6	
Star mode chassis	3. 5	4.0	
Lens assembly	1.0	12.5	
Chassis A-1	4.0	5.0	
Chassis A-2	5.0	8.5	
Chassis A-6	6.0	6, 5	
Multichassis assembly	10.0	17. 5	
Chassis A-3	2. 0	2. 0	
Chassis A-4	2.0	2. 0	
Chassis A-5	2, 0	2.5	
ECU	30	40	
Vidicon housing	3.5	4.0	

TABLE 4-7. MOUNTING HARDWARE INSTALLATION TORQUES

Screw Sizes	Specified Torque Range, in-lb
2-26	3 to 4
4-40	7 to 9
6-32	10 to 12
8-32	12 to 14
10-24	25 to 30

Microscopic examination and passive tests of chassis A-1, A-2, A-3, A-10 (star mode), and ECU revealed no major anomalies except for a number of cracked resistor and diode envelopes and one open diode on chassis A-3. These are discussed in further detail in Sections 7 and 12.

4.8.3 Dismantling of Lens Support Structure

The lens support structure houses the lens assembly, the star mode chassis A-10, and the shutter assembly. The lens support structure also supports chassis A-1 and A-2.

The front of the lens support structure is shown in Figure 4-8. The lens assembly drives are seen on the top, and the shutter assembly on the bottom of this figure. The star mode chassis is hidden on the left side. Figure 4-9 shows the star mode chassis after disassembly. The top view of the shutter assembly looking down from the lens assembly after disassembly is shown in Figure 4-10.* Figure 4-11 is a bottom view of the lens assembly, as seen from the vidicon housing region below.

Dismantling of the lens support structure commenced with the removal of the mounting hardware attaching chassis A-1 and A-2. After cutting the appropriate interconnecting wires to the shutter, to the star mode chassis, and to the lens assembly, the four screws mounting the lens support structure to the camera main deck structure were removed. This allowed the lens support structure to be removed from the camera. The mounting hardware of the shutter assembly was then removed, separating it from the lens support structure. Finally, the star mode chassis was disconnected. Further dismantling of the lens assembly itself is described in Section 5.

4.8.4 Dismantling of Electronic Chassis

The next step of the dismantling operations entailed removal of the remaining seven electronic chassis: A-1, A-2, A-3, A-4, A-5, A-6, and ECU. The first step was to remove the multichassis assembly, which is the triangular structure containing chassis A-3, A-4, and A-5 shown in Figure 2-7. The three struts forming this triangular assembly were mounted to the main deck structure by six mounting screws. After these were removed and the triangular structure lifted off the camera, the three individual chassis were dismantled from the struts by removing the mounting screws two per chassis. After the visual and microscopic examination of the chassis and upon completion of the functional tests of chassis A-4, A-5, and A-6, appropriate interconnecting wires were cut and the three chassis were separated.

Figures 4-12a and b show the two sides of chassis A-5: the cordwood module side, which also shows the preamplifier, and the etched printed circuit board side, respectively.

The pattern visible through the open shutter is that of a plastic pad on which the assembly was placed for the photograph.

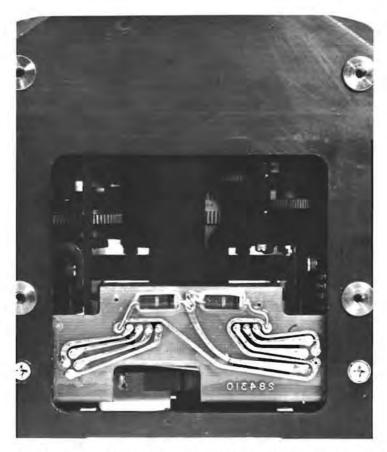


Figure 4-8. Front View of Lens Support Structure and Shutter Assembly (Photo 4R14816)



Figure 4-9. Star Mode Chassis A10 After Disassembly (Photo 4R15124)

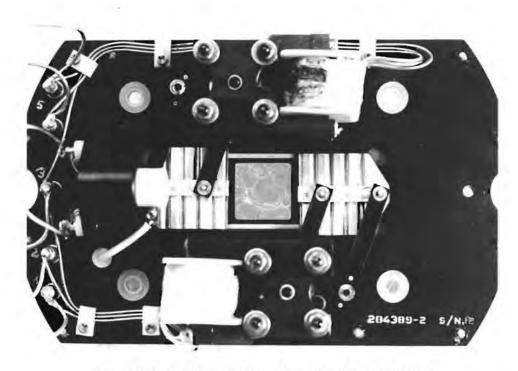


Figure 4-10. Top View of Shutter Assembly (Photo 4R15016)

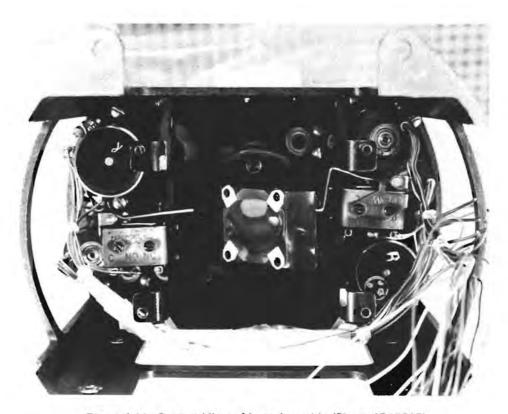
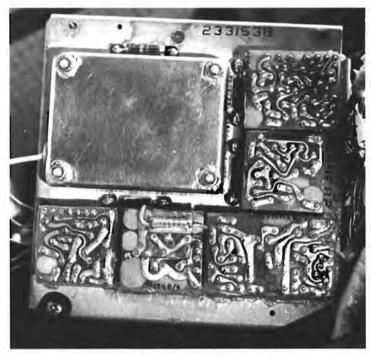
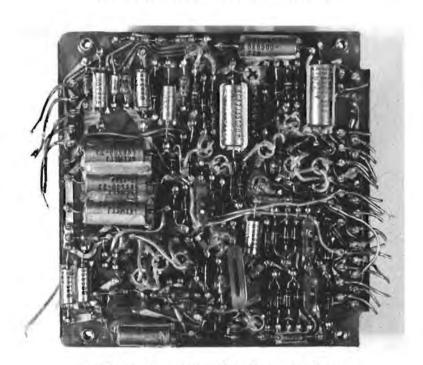


Figure 4-11. Bottom View of Lens Assembly (Photo 4R15017)



a) Cordwood Module Side (Photo 4R14650)



b) Etched Circuit Board Side (Photo 4R15697) Figure 4-12. Chassis A5

Figures 4-13a and b show the cordwood module sides of chassis A-3 and A-4 respectively.

Chassis A-1, A-2, and A-6 were then removed by unscrewing the mounting hardware and cutting the interconnecting wiring. Chassis A-1 and A-2 were attached to the lens support structure by six mounting screws each. Chassis A-6 was attached to the main deck structure by two mounting screws. Figures 4-13c and d show the cordwood module sides of chassis A-1 and A-2, respectively. Figures 4-13e and 4-14 show the cordwood modules side and the etched printed circuit board side of chassis A-6, respectively.

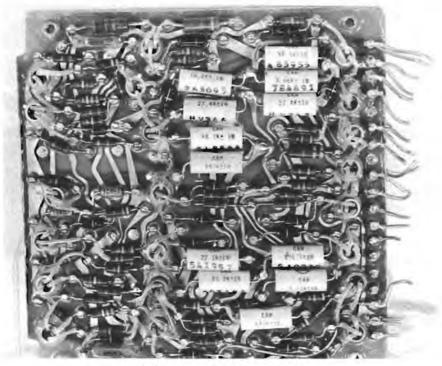
The ECU was mounted to the multichassis assembly support struts by three bolts. These had been removed prior to the removal of the ECU from the camera to allow for visual and passive tests. After completion of these tests, the interconnecting wires were cut and the ECU was removed. Subsequently, the ECU cover was removed from the ECU structure. Figures 4-15a and b show the bottom view of the ECU prior to and after removal of the ECU cover, respectively. Figure 14-15c is the side view of the ECU, showing its foam modules.

After cutting the appropriate interconnecting wires, the wiring harness was then removed. This was done by unscrewing the mounting hardware that attaches two nylon clamps that support the harness to the main deck structure. The teflon wrap and the spot ties around the harness were not disturbed, and handling was minimized so that these materials could be further analyzed, as discussed in Section 10.

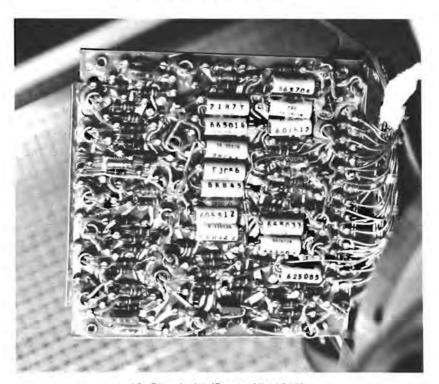
4.8.5 Dismantling of Vidicon Assembly

The final item to be removed and dismantled was the vidicon housing assembly. This assembly comprised the vidicon tube, vidicon deflection coil, and boron nitride thermal collar which contained sensing diodes for maintaining the vidicon faceplate temperature. These three parts were removed from the housing in sequence prior to the removal of the vidicon housing itself from the main deck structure.

The disassembly can best be understood by first reviewing the steps followed in the original assembly of the vidicon. During assembly of the housing, the deflection coil was first assembled and held in place by a retainer ring. The vidicon tube was then slid into the housing, with the boron nitride collar attached around its envelope, and positioned at the face-plate end. Wire braid leads protruding from the boron nitride collar were connected to the camera thermal radiator and were isolated from the main deck structure by teflon bushings. Inside the housing, the vidicon tube and collar were spring-loaded at each end and held in place by a tube socket, retainer rings, and phenolic cup. This allowed adjustment of the mechanical focus.

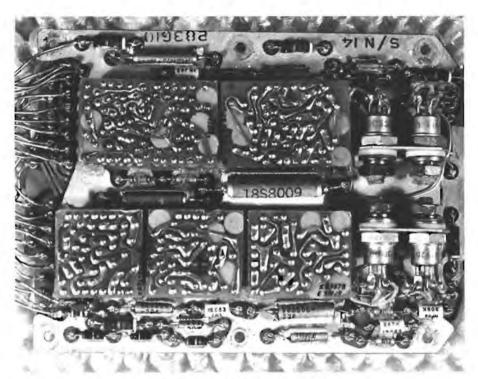


a) Chassis A3 (Photo 4R15117)

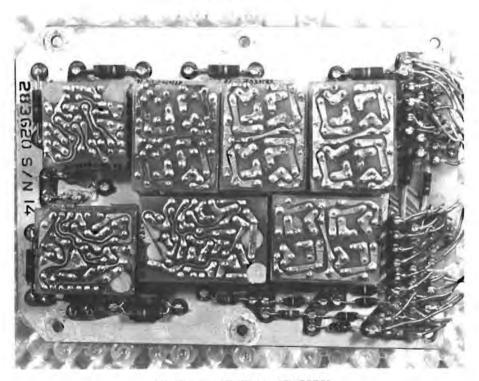


b) Chassis A4 (Photo 4R14649)

Figure 4-13. Cordwood Module Sides of Various Chassis

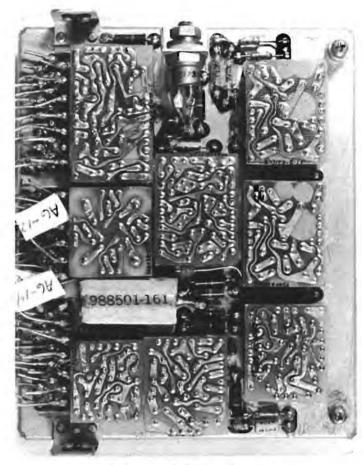


c) Chassis A1 (Photo 4R15374)



d) Chassis A2 (Photo 4R15373)

Figure 4-13 (continued). Cordwood Module Sides of Various Chassis



e) Chassis A6 (Photo 4R15699)

Figure 4-13 (continued). Cordwood Module Sides of Various Chassis

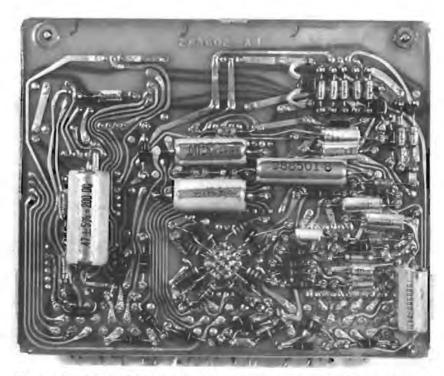
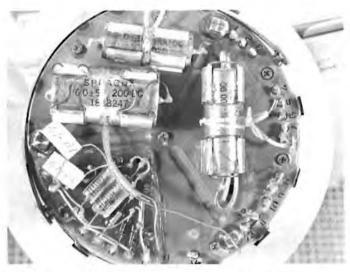


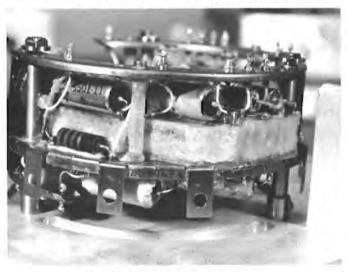
Figure 4-14. Etched Braided Circuit Board Side of Chassis A6 (Photo 4R15698)



a) Bottom View With Cover On (Photo 4R15121)



b) Bottom View After Cover Removal (Photo 4R15372)



c) Side View (Photo 4R15366)

Figure 4-15. Electronic Conversion Unit

The first step in the disassembly was to cut the thermal radiator straps and interconnecting wiring of the vidicon tube. Starting at the socket end, the retaining nut, socket, loading spring, and retainer ring were removed in that sequence. The phenolic cup, centering spring, loading spring, and target clip were then removed in that sequence from the faceplate end of the vidicon tube. This allowed the vidicon tube with the collar attached to be removed from the housing.

The collar was then removed from the vidicon as follows. The collar consisted of two halves held together by a wire ring which fitted into a slot around the collar. This wire ring was cut, rather than removed, to eliminate any possible pressure on the tube and to minimize any possible stress on the faceplate indium seal.

The deflection coil was then removed from the vidicon housing by removing its retainer ring and by cutting appropriate interconnecting wires. Finally, the vidicon housing itself was removed from the main deck structure. The housing was mounted to the main deck structure by three adjustable studs which allowed boresighting of the vidicon housing assembly. Removal of the housing entailed the removal of the remaining hardware which attached the housing to these adjustable studs.

A rear view of the vidicon housing assembly with the vidicon in place is shown in Figure 4-16; the vidicon pins can be seen on this figure. The boron nitride collar is shown in Figure 4-17, and the vidicon deflection coil after disassembly is shown in Figure 4-18.



Figure 4-16. Rear View of Vidicon Housing Assembly (Photo 4R15892)

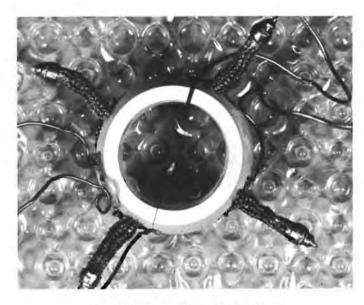


Figure 4-17, Vidicon Boron Nitride Collar (Photo 4R15891)

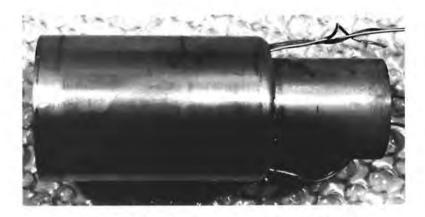


Figure 4-18. Vidicon Deflection Coil (Photo 4R15890)

5. OPTICAL SUBASSEMBLY TESTS AND DISMANTLING

5.1 GENERAL DISCUSSION

In this section are described the tests and disassembly operations conducted on the four optical assemblies of the TV camera: the TV mirror and its drives, filter wheel subassembly, variable focal length subassembly, and shutter subassembly. The objectives of these tests were to determine the operational and functional performance characteristics of these optical assemblies after long-term exposure to the lunar environment, primarily hard vacuum and thermal cycling from -270° to +250°F.

Following a thorough visual and microscopic examination, the assemblies were subjected to a series of electrical and mechanical diagnostic and functional tests. These were structured to take advantage of redundant components. In several instances, parallel tests were conducted to measure different functional parameters under different environmental conditions. During these tests, these optical assemblies were disassembled into their major components, which were later subjected to component level testing, described in succeeding sections of this report. Results of these tests were compared with information available from the Surveyor program — specifications, design data, and prelaunch tests. Special investigation was conducted whenever appropriate to explain anomalies uncovered and relate them to the effects of the lunar environment.

As indicated in Figure 3-1 (Section 3), the mirror assembly was removed early in the program, and its testing and dismantling proceeded in parallel with the work on the other electrical, mechanical, and optical subassemblies of the main TV structure. A sketch of the mirror assembly is shown in Figure 5-1. The mirror assembly contains the TV mirror and its azimuth and elevation drives. The drive mechanisms consist of gears and motors to provide the azimuth rotation of the mirror assembly and the elevation motion of the beryllium mirror. A potentiometer readout coupled to the gear train is provided on each axis for position data. The mirror assembly also houses the filter wheel assembly, consisting of a filter wheel, stepper motor, gear train, and a readout potentiometer coupled to the gear train. The filter wheel supports the four TV filters: clear, blue, green, and red.

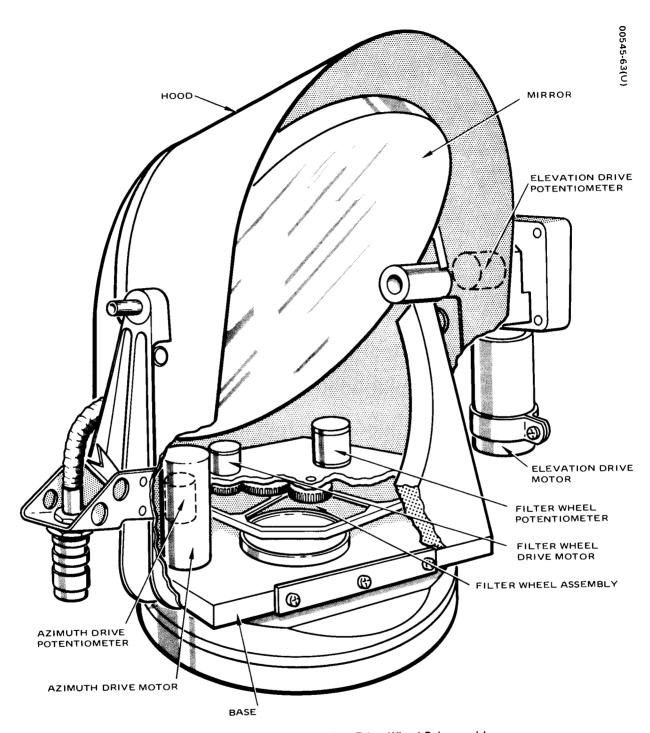


Figure 5-1. Mirror Assembly With Filter Wheel Subassembly

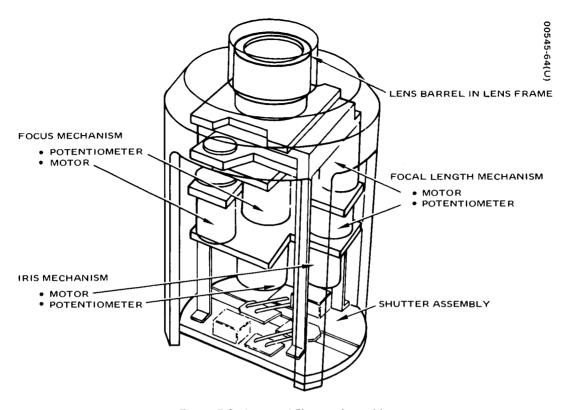


Figure 5-2. Lens and Shutter Assembly

Tests of the lens and shutter assembly commenced with their removal from the main TV structure, as described in Section 4.8. The lens and shutter assembly is shown in Figure 5-2. The lens assembly is also seen in Figures 4-6 and 4-8 (Section 4). Figures 4-8 and 4-10 depict the shutter assembly. The lens assembly consists of the lens barrel which contains the lens elements, and the mechanisms, drives, and components which provide for the following three functions: variable focus, variable focal length, and variable iris. Mechanization of these three lens functions is essentially identical. Each function comprises a stepper motor, a gear train, and a position potentiometer.

The sequence of visual inspection, electrical checkout, mechanical and electromechanical functional performance testing, and appropriate dismantling and disassembly of the various optical subassemblies throughout these tests to the dismantling level desired entailed careful observation of rules and procedures. Very detailed procedures, coordinated with the customer, were prepared prior to the conduct of any test or dismantling operation. These procedures were, to a large extent, based on the existing Surveyor Operational Instruction Sheets (OISs). Careful records were kept of all operations; and each part removed was identified, tagged, and inventoried. Each part removed from the assembly was subjected to a careful visual scrutiny, and suspect areas were examined microscopically and recorded photographically. Particular attention was given to the search for evidence of possible cold welding. The position of all rotating or moving

parts was determined and recorded prior to any disassembly. All operations were conducted by personnel thoroughly knowledgeable with the subassemblies by virtue of prior Surveyor test or design experience.

5.2 MIRROR ASSEMBLY AND FILTER WHEEL TESTS

The general sequence of tests and disassembly of the mirror assembly, including the filter wheel subassembly, was as follows:

- Assessment of general condition visual inspection and electrical checkout
- 2) Removal of filter wheel potentiometer
- 3) Functional checkout of filter wheel drive and removal of glass
- 4) Functional checkout of elevation drive
- 5) Dismantling of mirror assembly removal of drives, mirror, and filter wheel subassembly

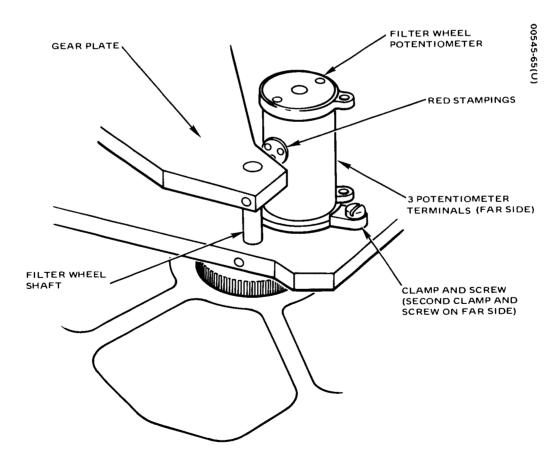


Figure 5-3, Removal of Filter Wheel Potentiometer

In parallel with these tests, a complete inspection was performed of the azimuth gear train, which, as discussed in Section 4.8, remained on the main TV structure upon removal of the mirror assembly. The azimuth drive therefore was not tested functionally at the subassembly level but only at the individual component level. Certain anomalies uncovered are discussed in Section 12 as part of failure analysis.

As the first step in the above sequence, the mirror assembly was visually inspected for its general appearance, particularly for damage and contamination of surfaces. The mirror was found to be contaminated, as already mentioned in Section 3.4.5; this is discussed further in Section 9. Dust was observed on the filters, presumably of lunar origin. A number of science tests were then conducted under JPL coordination with Hughes support, including scattering measurements of the TV mirror. The results of these are presumed to be reported by the science investigators.

Electrical checkout tests were then conducted, including continuity, resistance, and insulation resistance measurements. Access was provided through the TV connector at the side of the mirror assembly. This connector had intentionally been left intact for subsequent detailed examination at the component level. The integrity of this connector was carefully preserved during these tests since the other three connectors had previously been unfastened in order to remove the lower shroud (as discussed in Section 3.2). The individual wires were identified by a continuity check between the wire bundle protruding from the external cable and the wires inside the mirror assembly. Access to the individual wires inside the mirror assembly was obtained by puncturing through their insulation with a thin sharp sewing needle.

With all circuits properly identified, resistances were measured on all windings of the three motors and across the terminals of the three potentiometers of the elevation, azimuth, and filter wheel subassemblies. Insulation measurements included resistance between the windings and housings of all the drive motors and potentiometers, and between the housings of the azimuth and elevation drives. Results of the electrical checkout tests were nominal. Continuity checks revealed no opens, and resistances and insulation resistances were within specifications.

The next operation was to remove the filter wheel potentiometer which had exhibited anomalous behavior during the Surveyor III lunar mission operations. This was done to preserve the integrity of the potentiometer for the subsequent failure mode investigation, reported in Section 12.

The filter wheel potentiometer was removed by cutting the leads at the terminals and by removing the holding screws and clamps. Figure 5-3 is a sketch of the potentiometer in the mirror assembly prior to its removal. Poor accessibility to the screws made it impossible to measure screw removal torques. However, the gears appeared to be correctly positioned

on the shaft, and the set screw appeared to be properly contacting the flat surface of the shaft. The potentiometer was lifted straight up without turning the potentiometer gear.

A functional test of the filter wheel mechanism was then conducted. The purpose of this test was to determine the minimum voltage required to operate the mechanism for a partial (270 degree) revolution of the filter wheel at the nominal stepping rate of 100 ± 5 pulses/sec. Results of this test were nominal: the observed 8. 1 volts falls within the specified range of 7.5 to 9.5 volts.

The four filter glasses were removed from the filter wheel for a separate study of optical properties, surfaces, changes, etc. These studies were subsequently conducted by the science investigators under JPL coordination and are reported elsewhere. The filter wheel glasses were lifted out after the lock wires were cut and mounting screws and holding clips removed.

A broken safety wire was noted on a screw retaining one of the filter glasses. This anomaly is discussed further in Section 12.

The functional test of the mirror elevation drive was conducted next. The purpose of this test was to determine the minimum voltage required for stepping the drive upward from its extreme clockwise position to its extreme counterclockwise position and then back to its extreme clockwise position. The stepping was accomplished manually with pulse widths of 90 ms each, per specification. Results were nominal: Minimum required operating voltages in the upward direction were measured to be 8 volts compared with 7 to 9 volts specified; the measured minimum required voltage of 11.7 volts in the downward direction also was within the 10 to 12 volts expected range and well within the Surveyor specification of 14.5 volts minimum.

5.3 DISMANTLING OF MIRROR ASSEMBLY AND FILTER WHEEL ASSEMBLY

A sketch of the mirror assembly is shown in Figure 5-1. The mirror assembly consists of the base with several units mounted on it, two support arms, the beryllium mirror, the elevation drive subassembly on the outside of the mirror assembly mounted to the right support arm, and the hood and attached visor. The mirror assembly is visible in the frontispiece of this report and Figures 3-3 and 3-4 (Section 3).

A support bracket clamped to the end of the azimuth drive motor attaches to the right support arm to provide for additional stability. The support arms, in addition to the elevation drive mentioned above, also support the hood, visor, and mirror. The elevation drive subassembly, shown

in Figure 3-6, contains a motor, potentiometer, and gear drives. The mirror is mounted on its shaft in the bearings of the support arms. Two seals, attached to the mirror assembly, are provided to seal off the mirror in the closed position.

The first step in the dismantling sequence was to disassemble the visor by removing the mounting hardware attaching it to the support arms. This provided access to the elevation drive subassembly.

The removal torques of the 4-40 screws of the visor ranged from 5 to 6 in-lb. This compared well with the nominal installation range of 7 to 9 in-lb given in Table 4-7. In accordance with the discussion in Section 4.8.2 the range of values of removal torques recorded in all the dismantling operations below are presented for the record without comment since no major anomalies were uncovered.

The next step was to remove the beryllium TV mirror. This constituted a departure from the normal sequence of disassembly. It was done early in the dismantling sequence to preserve the integrity of the mirror surface. Removal of the mirror entailed removal of the screws attaching the hood to the support arms, removal of the two dust skirts (one from the mirror and one from the base), removal of the support bracket attaching the azimuth drive to the right support arm, removal of the mirror support arm screws, and loosening of the elevation drive shaft. The latter entailed removal of the elevation drive subassembly dust cover, and of the hardware holding the elevation drive unit to the mirror assembly. The elevation drive gears were thus disengaged from the mirror shaft gears.

Values of removal torques were recorded in all instances except on the inside of the hood where access was difficult. All recorded values were nominal, and no difficulty was experienced. The breakaway torques for the hood screws ranged from 2 to 4-1/2 in-lb on the outside and were estimated to be on the order of 2 in-lb on the inside. The azimuth motor bracket breakaway torque was 10.4 in-lb. The dust skirt torques ranged from 5 to 9 in-lb. The support arm screws torques ranged from 17 to 25 in-lb. The elevation drive dust cover torques ranged from 6 to 7 in-lb.

The elevation drive subassembly was then removed by taking off the torsion spring mounted to the main shaft and removing all mounting hardware. All torques were nominal: The torsion spring angle bracket screws measured 4-1/2 in-lb; the breakaway torque of the elevation motor bracket screw was 21 in-lb. This operation also required drilling out of a tapered pin from the gear train.

The two support arms and the hood were taken off next by removing the previously loosened mounting hardware, thereby providing access to the remaining units on the mirror assembly base. The azimuth motor, azimuth potentiometer, and filter wheel subassembly were accordingly removed as



a) Before Dismantling (Photo A07274)



b) After Dismantling, Showing Wheel Frame and Gears (Photo A10779)

Figure 5-4. Filter Wheel Subassembly

the last step in the dismantling sequence. All torques were again nominal. The azimuth drive motor and potentiometer mounting screws breakaway torques ranged from 3.7 to 6 in-lb. The filter wheel mechanism mounting screw breakaway torques were from 1-1/2 to 3 in-lb.

The elevation drive subassembly was not dismantled since the units contained in it for component level tests were similar to other units available from the dismantled mirror assembly. The elevation drive was thus left intact for possible subsequent tests at the subassembly level. It was also desired to retain the discolored surface of the elevation subassembly housing (shown in Figure 3-6) for subsequent investigations. The filter wheel subassembly, however, was further dismantled.

The filter wheel subassembly is shown on Figure 5-4a before its dismantling. The filter wheel gears are located between the two plates shown. The potentiometer and the motor are mounted on the extended base of the lower plate. The potentiometer had been removed earlier, as discussed in Section 5.2. The motor and its bearings were removed by unscrewing the mounting hardware, with breakaway torques found nominal and ranging from 1.5 to 3 in-lb.

The top plate was removed next, and all gears were scribed to identify their mating positions. Figure 5-4b shows the filter wheel subassembly at this stage of the dismantling. The filter wheel frame and shaft were removed next. This operation required some manual forcing to loosen the hardened paint which had been applied to the shaft during manufacture as an antireflection measure. Last to be removed were the filter wheel gears. One of the filter wheel gears revealed a symmetrical scratch pattern on its surface caused by a broken safety wire. Results of analysis of this anomaly are presented in Section 12, where a photograph of this scratched gear is presented.

All units removed from the mirror assembly, including motors, potentiometers, gears, etc., with the exception of the elevation drive, were subjected to further testing at the component level, as discussed in the succeeding sections of the report.

5.4 TESTS AND DISMANTLING OF LENS ASSEMBLY

The lens assembly is shown in Figure 4-8 (Section 4) in the lens support structure. Upon removal from the lens support structure, as discussed in Section 5.8, the lens assembly comprised the following subassemblies:

- 1) Lens frame containing lens barrel
- 2) Variable focal length mechanism containing motor, potentiometer, and associated gear train

- 3) Variable iris mechanism containing motor, potentiometer, and gear train.
- 4) Variable focus mechanism containing motor, potentiometer, and gear train

The sequence of testing and dismantling operations of the lens assembly was as follows:

- Assessment of general condition visual inspection and electrical checkout
- 2) Functional checkout of focal length mechanism
- 3) Removal of focal length mechanism components motor, potentiometer, and gear train
- 4) Dismantling of focal length gear train
- 5) Removal of iris mechanism components motor, potentiometer, and gear train
- 6) Functional test of focus mechanism still attached to lens barrel under vacuum conditions
- 7) Removal of focus mechanism components motor, potentiometer, and gear train

The three mechanisms, focus, iris, and focal length, are essentially identical in terms of their mechanical characteristics. To maximize the information obtainable relative to the condition of these mechanisms after lunar exposure, it was decided to test one of these (focal length) under ambient conditions and another (focus) under vacuum conditions.* Similarly, dismantling of the focal length gear train, while preserving the iris gear train intact, afforded the opportunity for subsequent possible investigation of the intact gear train after an evaluation of the results of study of the dismantled parts. Upon the completion of these tests, the various units—motors, potentiometers, and gears—were subjected to component level testing as discussed in Section 8. The lens barrel and the lens frame were subjected to special optical tests, as discussed in Section 9.

General assessment included visual observation, photography, and electrical checkout tests. Electrical tests included continuity checks and

^{*}This illustrates the dynamic nature of the test program. Decisions on testing were made in real time, based on previous results (see ground rules, Section 2.6.1).

measurements of resistances and insulation resistances. All results were nominal. Resistance of each of the four coils of all three motors was 45 ohms, per specification. Resistance of the three potentiometers in parallel was 1700 ohms, verifying the 5000 ohm rating of each. All insulation resistances measured in excess of 10^9 ohms for the potentiometers and 10^{12} ohms for the motors, in full compliance with the specification value of 5×10^6 ohms minimum.

The functional test of the focal length mechanism, conducted next, consisted of determining the minimum operating voltage required to run the motor in the continuous mode, both in forward and in reverse direction. This test was conducted with the aid of a special lens control position available from the Surveyor program. The voltage was increased at 1/2 volt steps, starting with about 6 volts, until a constant running time from stop to stop was obtained. The minimum required operating voltage was found to be 9.0 volts, corresponding to the time from stop to stop of 10 seconds; above 9 volts, no further reduction in time interval was obtained. This value of 9 volts falls within the specified range of 7.5 to 9.5 volts.

The motors, potentiometers, and gear trains associated with the focal length and iris mechanism functions were removed in sequence and the focal length gear train was further dismantled. Steps in this disassembly sequence and the recorded breakaway torques of mounting hardware are as shown in Table 5-1. All torque values were nominal.

Vacuum chamber tests on the variable focus mechanism, conducted next, entailed electrical checkout and measurement of minimum operating voltage. The chamber pressure was maintained in the range of 2×10^{-8} Torr to 4×10^{-8} Torr; the chamber temperature was $25 \,^{\circ}$ C. Figure 5-5 shows the lens frame and barrel, with the focus mechanism attached, in the vacuum chamber prior to the test. This figure shows the wiring and external connectors through which electrical access was provided.

Results of the vacuum test were nominal. Motor and potentiometer wiring resistances and insulation resistances were within specifications, similar to values obtained earlier in ambient tests. The minimum operating voltage of the focus mechanism measured to be 8.8 volts, also within the 7.5 to 9.5 volts specification range.

After completion of the vacuum test, the components of the focus mechanism were removed from the remaining lens frame and barrel assembly. The items removed and the torque values recorded are shown in Table 5-2. All results were nominal.

TABLE 5-1. MEASURED TORQUES DURING REMOVAL OF COMPONENTS OF IRIS AND FOCAL LENGTH MECHANISM

Removed Component	Recorded Range of Breakaway Torques of Mounting Hardware, in-lb
Lens support housing	10 to 12
Iris potentiometer	2 to 7.5
Focal length motor	2 to 2
Focal length gear train*	
Iris motor and gear train	4.5 to 5
Iris motor (from gear train)	1 to 2.7
Focal length potentiometer	4 to 4.8

*Dismantling of focal length gear train:

Focal length bearing retainers from mounting plate	2 to 2
Focal length drive gears from mounting plate	1.5 to 2



THERMOCOUPLE CONNECTED TO LENS FRAME, UNDER WASHER . AND SCREW HEAD

Figure 5-5. Lens Frame With Focus Mechanism in Vacuum Chamber

TABLE 5-2. MEASURED TORQUES DURING REMOVAL OF COMPONENTS OF FOCUS MECHANISM

Removed Component	Recorded Range of Breakaway Torques of Mounting Hardware, in-lb	
Focus drive motor	2 to 2	
Focus gear train	3.5 to 4	
Motor mount plate	0.9 to 1.3	
Focus potentiometer	3 to 4	

5.5 TESTS OF SHUTTER ASSEMBLY

The last optical subassembly tested was the shutter assembly. This assembly, removed as part of the dismantling operations described in Section 5.8, is shown in Figure 4-10 (Section 4).

The shutter assembly consists of two solenoids and two movable blades with associated linkage. Each solenoid consists of a stator with two windings and a rotor with a dry film lubricant over its surface. The shutter blades, attached to the rotors by the linkage, are actuated by the magnetic force between the rotor and the stator generated by the current through the solenoid coils. The shutter mechanism is activated by camera electronics to provide a time exposure or a 150 ms exposure for the TV pictures.

Shutter assembly tests included resistance measurements, and measurements of the minimum breakaway current required to actuate the blades. Inspection of the shutter assembly revealed that one of the coils had apparently burned out. This anomaly, which was subjected to a detailed failure analysis and shown to be in the nature of a secondary failure, is extensively treated in Section 12. Resistance measurements indicated that this coil had shorted rather than opened. The measured resistances of the four coils are indicated in Table 5-3. The short in winding 2 of coil B evidently resulted in a partial shorting of some of the turns of adjacent coil 1. Insulation resistance was found to be nominal, in excess of 5 x 10^{12} ohms.

TABLE 5-3. RESISTANCES OF SHUTTER ASSEMBLY COILS

		Resistance, ohms	
Coil	Winding	Measured	Nominal
А	1	33	33
A	2	33	33
В	1	24	33
В	2	0.2	33

Minimum breakaway current measurement could only be performed on coil A. Values measured were about 30 percent higher than nominal, ranging from 250 to 325 ma, compared to the specification range of 190 to 235 ma. This anomaly is also discussed in more detail in Section 12; it is believed to be attributable to the anticipated wear of the dry film lubricant on the rotor. Since coil B was inoperative, the shutter blade had to be manually returned after each closing operation of coil A during the minimum breakaway current tests.

6. VIDICON TESTS

6.1 VIDICON DESIGN FEATURES, TESTS, AND OPERATIONS HISTORY

The vidicon tube of the Surveyor III camera was manufactured by the General Electrodynamics Corporation of Garland, Texas. The vidicon, type 1335A-2, was manufactured in December 1963. The vidicon tube is shown in Figure 6-1. The vidicon mounted in its collar is shown in Figure 2-5 (Section 2). A more detailed description of the vidicon design features and operation is given in Appendix G.

The vidicon vacuum tube is a hybrid storage device designed to convert visual information — light energy from the object viewed — into an equivalent electrical signal in the image plane. The Surveyor vidicon utilizes electrostatic focusing and electromagnetic deflection. The tube employs an electron gun, collector, and photoconductive target; fine mesh screen (grid 5) is adjacent to the target. The target is coated on the back with a transparent conductive coating which acts as the backplate. Figure 6-2 is a cross-sectional view of the construction of the front part of the vidicon. Figure 6-3 shows schematically the elements of the target mesh area and illustrates the transducing process.

The principle of operation, whereby the vidicon signal is produced from the photoconductive surface, is briefly as follows: A low velocity scanning beam strikes one side of the surface; the other side receives illumination through a signal plate from which the video signal is taken. When the photoconductive surface is scanned in darkness, electrons deposited from the scanning beam reduce the potential to zero. The conductivity becomes so low under these conditions that very little current flows across the surface. If, on the other hand, the surface is illuminated, the conductivity increases and charge flows across the surface. The scanned surface becomes more and more positive in the interval between successive scans. The beam then deposits sufficient numbers of electrons to neutralize the accumulated charge, thereby generating the video signals. Further details are given in Appendix G. The electronic circuits necessary to provide the timing, power, and amplification, are discussed in Section 4 and Appendices D and E.

Extensive tests were conducted by Hughes on each Surveyor vidicon received from the manufacturer. Acceptance tests entailed, in addition to receiving inspection, a detailed visual inspection, electrical tests, reseau mapping, wedge measurements, spectral response, and low temperature survival tests at -196°C.

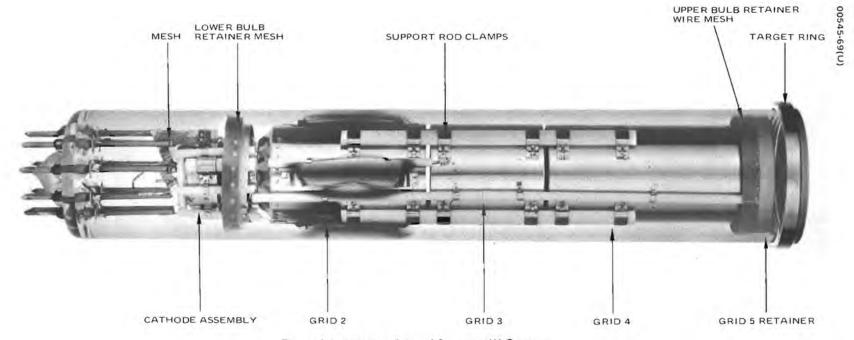


Figure 6-1. Vidicon Tube of Surveyor III Camera

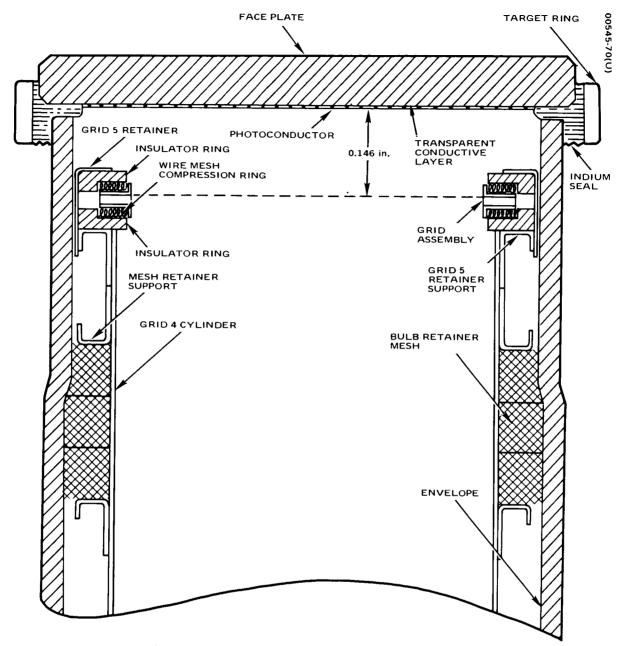


Figure 6-2. Cross-Sectional View of Front Portion of Vidicon

The vidicon design precludes its survivability at high temperatures. High temperatures would damage the photoconductor and melt the indium seal. The target mesh (grid 5) is mounted in a taut position, and the mismatch of thermal coefficients could adversely affect this critical alignment and could cause wrinkling of the grid. Similarly, distortion of internal elements could affect vidicon alignment, resulting in changes of beam focusing and cutoff characteristics. Accordingly, a thermal radiator was incorporated in the design to limit internal temperatures of the vidicon to about 125°F during the high temperature ambient environment of the lunar day. Furthermore, operation was limited during periods of maximum solar inputs. Shading by the Surveyor solar panel and planar array antenna was also utilized to limit the thermal exposure.

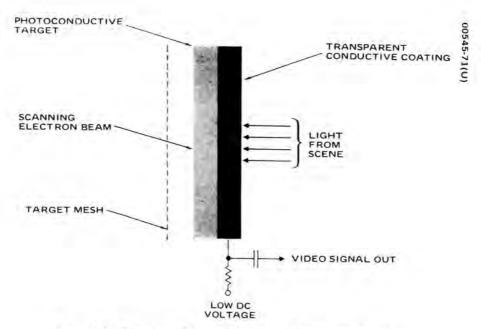


Figure 6-3. Functional Diagram of Vidicon Transducing Process

However, exposure to the high vacuum lunar environment was not detrimental to the vidicon. During the manufacturing process, the vidicon was evacuated and sealed off at a very low pressure. Integrity of the seals under vacuum conditions was validated in extensive qualification and acceptance tests.

Concern existed over the survivability of the photoconductor at the cryogenic temperatures during the lunar night since many of the vidicons exhibited peeling of the faceplate photoconductor. The percentage of unacceptable vidicons on the program was relatively high. Continued efforts throughout the Surveyor program to pinpoint the differences in process variables during manufacturing between survivable and nonsurvivable vidicons were not successful.

Although lunar night survival was not a Surveyor program requirement, operation of the Surveyor camera on successive lunar days was a desired program goal. Because of the potential use of vidicons in space applications, it was of particular concern to determine the condition of the returned Surveyor III vidicon. For future applications, it was also considered desirable to assess the performance of the indium seal after exposure to thermal cycling and to hard vacuum conditions.

The acceptance tests of the Surveyor III vidicon were conducted in 1964, and a comprehensive evaluation report, qualifying it for flight, was submitted. The vidicon successfully met all flight qualification requirements.

The performance of the Surveyor III vidicon on the lunar surface was nominal. The vidicon performance was apparently unaffected by the exposure of the Surveyor spacecraft to the environment, described in Appendix B, where the lunar surface temperatures approached 260°F at the height of the lunar noon. Since communication with the Surveyor III spacecraft was not

reestablished on succeeding lunar days, no information was available on vidicon survivability through the lunar nights. However, the vidicon did survive the total eclipse which took place 4 earth days after Surveyor III touchdown, as evidenced by the high quality of subsequent TV pictures. The eclipse lasted 6 hours, and the lunar surface temperature dropped below -100°F; the vidicon faceplate temperature is estimated to have gone down to about 0°F.

6.2 TEST PROGRAM SUMMARY

The plan for testing and evaluation of the vidicon, as for all other elements of this program, was designed to maximize the amount of information obtainable, while proceeding with extreme care to avoid destruction of evidence. Extensive use was made of a number of spare vidicons available in order to check out procedures and to obtain data for comparison with the flight vidicon. Results of each test step were evaluated and subsequent operations modified accordingly.

The test plan is summarized in Figure 6-4. This plan was formulated to determine the effects of the lunar environment on the critical structural parameters of the vidicon and on its materials. To this end, it was found desirable to conduct selected functional performance measurements in addition to the detailed examinations of the structure and materials.

The test plan consisted of three phases, distinguished from each other in Figure 6-4 by dashed lines. Phase I operations were conducted on the vidicon prior to its removal from the camera. Phase 2 operations were conducted after the removal of the vidicon but before its dismantling. Phase 3 operations consisted of the opening of the vidicon and diagnostic tests of its internal component parts and materials.

During the initial phase, a visual examination was conducted and an approximate measurement made of the vacuum in the vidicon, using the filament as a Pirani-type gauge. This measurement was considered to be a required precursor to subsequent tests. This was followed by selected functional tests, listed in Figure 6-4. Phase 2 operations entailed a more detailed visual and X-ray examination, and analysis of the gas content of the vidicon. The gas sample was removed without disturbing the basic integrity of the vidicon internal elements. A limited number of functional tests were also conducted. The final phase commenced with the opening of the vidicon, carefully rehearsed on spare units to prevent destruction of internal evidence by this operation. This was followed by tests of the several components of the vidicon assembly (noted in Figure 6-4) and by selected tests of certain materials.

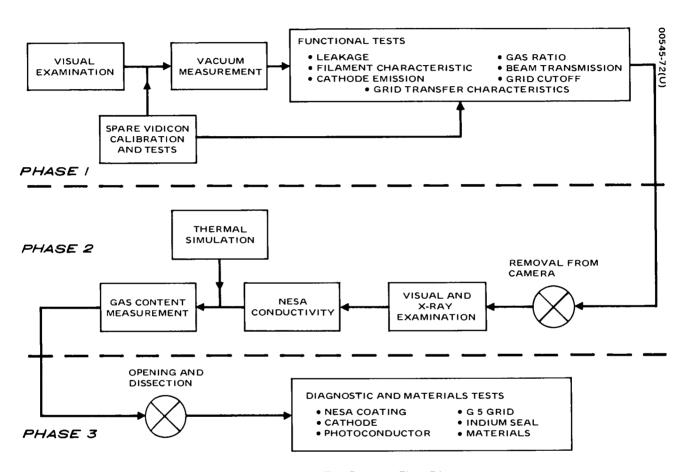


Figure 6-4. Vidicon Test Program Flow Diagram

It was noted in the initial visual examination that the vidicon photoconductor had totally disappeared and that its grid 5 was shattered. It was evident that this anomaly was not cryogenic in nature but, typically, the result of high temperature exposure. Parallel work on the other parts of the TV camera revealed that this was, indeed, a secondary failure brought about by the open camera shutter. It was reasonable to conclude that the shutter had opened early in the long dormant period of the Surveyor spacecraft on the moon, exposing the vidicon to a considerable solar energy input. A detailed discussion of the shutter anomaly and its causes (associated with the failure of the shutter circuit transistor, and with the damage of one of the shutter coils) is presented in Section 12. The missing photoconductor and the shattered grid 5 required a modification of the original test plan. On the other hand, finding that the vidicon had retained its vacuum permitted the conduct of the majority of the planned functional tests. The test program (Figure 6-4) reflects the work conducted to validate the hypothesized mode of photoconductor and grid 5 failure. An approximate thermal analysis was carried out, and thermal simulation tests were performed on spare vidicons to establish the modes of failure. Diagnostic examinations were conducted on the pieces of grid 5 removed from the vidicon.

The individual tests conducted in each phase of the vidicon test program and the results obtained are summarized in the following subsections, with supporting data in Appendix G.

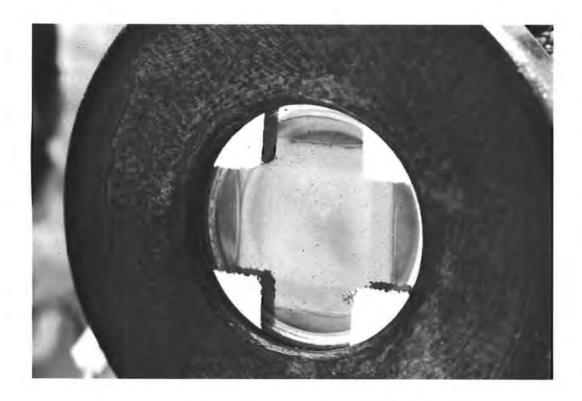
6.3 VIDICON TESTS ON CAMERA

6.3.1 Visual Examination

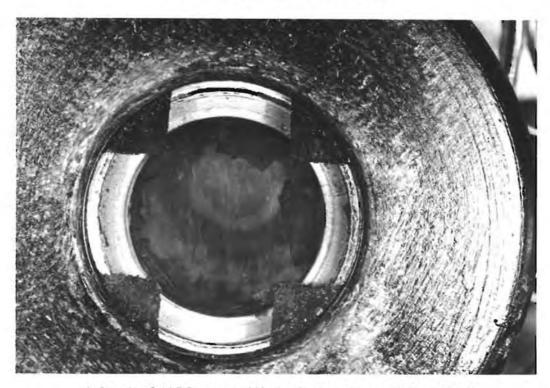
Phase I of the vidicon testing commenced, as illustrated in Figure 3-1 (Section 3), with visual inspection of the camera after removal of the mirror assembly but prior to any electrical tests. The camera disassembly test plan included provisions to prevent excessive illumination of the vidicon faceplate. It had been assumed that the shutter was closed. During the removal of the mirror assembly containing the shutter assembly, it was found that the shutter was open. No special provisions had been made in the design for protection of the vidicon faceplate under these conditions.

Visual examination of the vidicon then revealed that an image of the shutter opening was apparent on the faceplate, that the photoconductive coating had virtually disappeared, and that the grid 5 mesh behind it was shattered. The faceplate of the vidicon was virtually transparent. The appearance of the faceplate is shown in Figures 6-5a and b*, taken at different angles and with different lighting to reveal the different effects observed.

^{*}Originals in color.



a) Showing Discoloration (Photo 70-4865)



b) Showing Grid 5 Damage and Missing Photoconductor (Photo 70-4862)

Figure 6-5. Front View of Vidicon Faceplate

Access to the vidicon was limited at this time. After completion of electrical tests and removal of some of the chassis, a more thorough visual examination of the vidicon was conducted without disturbing the vidicon mounting arrangement and employing minimum lighting conditions. It was still not possible to examine the tube completely since a large portion of the envelope was covered by the deflection coil and the rear of the tube was covered by the tube socket. The collar surrounding the edge of the faceplate covered the target ring and the indium seal, so it was not possible to observe these. It was also not possible to see the getter. However, portions of the glass envelope and the tubulation at the rear of the tube could be examined for evidence of cracks; and the face of the tube with the remnants of the photoconductor could be easily seen.

The visual inspection included observation of the faceplate, photoconductor, corner reference marks, grid 5 mesh, and a portion of the glass envelope. The original color photograph of Figure 6-5a* shows the discoloration of the faceplate, the small piece of the photoconductor remaining, the damage to the dark reference marks, the reseau marks, and the two rectangular patterns, one of the raster and one of the shutter image. The grid damage is clearly seen on the original color photograph of Figure 6-5b.

A slightly discolored residue appeared to be present on the outside of the faceplate. Analysis of this residue, presented in Appendix G, did not indicate the presence of any organic materials. Two square patterns were visible on the faceplate. The inner square appeared to correspond to the normal raster pattern, while the outer square appeared to correspond to the image of the open shutter.

The corner dark reference marks appeared damaged at the edges. It is believed that this is attributable to handling and not to effects of the lunar environment. The reseau marks appeared to be intact. These small nichrome dots are evaporated on the rear face of the faceplate during manufacture, and are then covered by the Nesa coating.

The Nesa coating had a bluish-purple appearance, with a yellowish cast at the edges of the raster. The cause of this appearance was presumed to be interference reflections from traces of the photoconductor still adhering to the Nesa coating, and giving it a slight variation in thickness. The photoconductor disappeared except for a small piece at one corner of the dark reference mark of the faceplate.

The grid 5 mesh seemed to be severely damaged. A large piece had been torn from the mesh. The hole in the mesh extended on one side to the edges of the corner reference marks and on the opposite sides to the edge of the grid support ring. The damage observed was considerably more

^{*}Original in color.

extensive than, and different from, the damage noted during cryogenic testing of the vidicons. The worst damage that had been observed in previous tests was a wrinkling of the mesh, attributed to the difference between the thermal coefficient of expansion of the mesh and of the Kovar mounting ring.

The small portion of the glass envelope that could be seen, the tabulation in the area around the base which is normally strained by the sealing operation, and the indium seal at the faceplate all appeared to be undamaged.

6.3.2 Measurement of Internal Pressure

The degree of vacuum retained by the vidicon was determined next, using the Pirani gauge technique (Reference 14). This technique is capable of assessing the pressure inside a vacuum tube in the range of 10^{-2} to $\pm 10^2$ Torr, approximately.

Determination of the vidicon pressure, at least approximately, was considered to be a critical requirement prior to conduct of any tests. Concern existed that the vidicon was gassy for one of two reasons. A leak may have developed, such as a crack in the envelope or a leak in the indium seal, which would allow air to get inside upon return of the camera to earth. Internal outgassing over the 2-1/2 years of residence on the lunar surface may have increased the pressure to an unacceptable level even if all seals had remained intact. It was felt that if the pressure were found to be in excess of about 1 Torr, attempts to operate the vidicon at the rated filament current conditions would result in the destruction of the tungsten filament and, therefore, the vidicon.

The Pirani test was performed at relatively low current levels so as not to induce any of the abovementioned destructive effects. Details of this technique, and the test data obtained, are presented in Appendix G.3.

The basic principle of the Pirani gauge is that at any given power input to the tube filament an equilibrium temperature is reached which is uniquely determined by the pressure inside the tube. The higher the pressure, the better the thermal conduction of the heat from the filament and the lower the equilibrium temperature. At the same time, the resistance of the tungsten filament also uniquely varies with temperature. Thus, the unique relationship between the internal pressure and the filament resistance can be used to determine the pressure.

In performing this test, a spare vidicon was opened, placed in a vacuum chamber, and calibrated under controlled conditions: pressure was varied, and the relationship between the filament resistance and the pressure determined by plotting the required changes in the applied voltage at a constant filament current versus the pressure. The resistance of the flight vidicon filament was then measured at the same current level. The

pressure obtained from the calibration test of the spare vidicon at this value of resistance was then inferred to be that in the flight vidicon. It was tacitly assumed in this calculation that the two filaments and the two vidicons were essentially identical. This assumption determined the degree of accuracy obtainable. In practice, this is estimated to be about one order of magnitude.

Results of the Pirani gauge test are presented in Appendix G. 3. The measurements on the spare vidicon and on the flight vidicon were conducted at a filament current of 87 ma. This corresponded to about one-half of the rated operating value, which is in the range of 140 to 160 ma, to preclude damage in the event that the pressure was found to be over 1 Torr. Results of this test revealed that the internal pressure was less than 4×10^{-2} Torr.

As explained in Appendix G. 2, the pressure-resistance curve is asymptotically steep in this range, so a rather large reduction in apparent pressure results from a small change in resistance. The converse, however, is not true. Only a small increase in pressure corresponds to a significant decrease in resistance. The conclusion is that errors entailed in this measurement could imply pressure lower than the 4×10^{-2} Torr estimate but not much higher than about 10^{-1} Torr. Depending on the accuracy of the test and on the degree of similarity between the flight vidicon and the spare vidicon used for calibration, the flight vidicon pressure could be conceivably as low as 10^{-5} Torr.

The Pirani gauge demonstrated to a high degree of confidence that the vidicon had retained its pressure exceedingly well and that functional tests could be performed without any significant concern of damaging the filament.

6.3.3 Tests of Filament and Cathode Emission Characteristics

The initial electrical tests consisted of verifying the characteristics of the tungsten filament and ascertaining that the cathode emission was nominal, so that subsequent functional tests of the electrical parameters of the vidicon could be performed.

Measurements of the filament characteristics were made by applying a voltage to the heater filament in steps up to its full rated value. This test was conducted as a follow-on to the Pirani gauge test after it was ascertained that the vidicon was in good condition and could be safely operated. The filament voltage was varied until the filament current of 170 ma was reached; at this point, the voltage was 7.2 volts. At the rated current of 160 ma, the voltage was 6.4 volts, well within the specification of 6.3 volts in the current range of 140 to 160 ma.

Next in sequence was the emission test, entailing the measurement of the full cathode current at several values of voltages applied to grid 1 and to grids 2 through 5 connected together. This test was performed to ensure

TABLE 6-1. RESULTS OF EMISSION MEASUREMENTS OF FLIGHT VIDICON AND TWO SPARE VIDICONS

Vidicon	Grid İ Voltage, volts	Grid 2* Voltage, volts	Cathode Current, ma
Space S/N 109	0	300	4.0
Space S/N 123	0	300	4.3
Surveyor III vidicon	-23.5	185	0.7
Surveyor III vidicon	- 23. 5	300	2. 1
Surveyor III vidicon**	0	185	2. 2
Surveyor III vidicon	0	300	4.3

^{*}Grids 2, 3, 4, and 5 were connected together for this test.

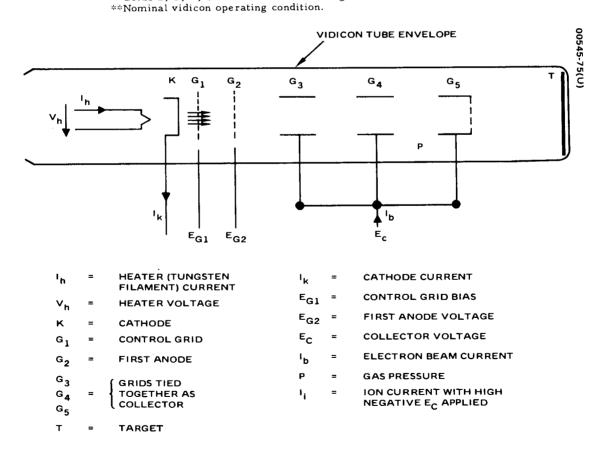


Figure 6-6. Diagrammatical Representation of Vidicon for Functional Tests

that the internal vacuum was adequate to permit the generation of an electron beam at the vidicon operating voltages. The Pirani test had merely ascertained that the vacuum was no worse than 10^{-1} Torr, so that the filament could be operated. Performance of the succeeding tests, such as the gas ratio test, however, required ascertainment that a much higher vacuum level existed.

Emission measurements were first made on two spare vidicons at the rated levels of zero voltage on grid 1 and 300 volts on grid 2. This was done to check out the experimental technique and the test setup and to provide useful data for comparison with the flight vidicon. The flight vidicon was then tested, starting with the lower values of grid voltages (lowest emission current) and progressively raising the voltages until the full current under rated conditions was reached.

Results are summarized in Table 6-1. It is evident that the flight vidicon emission currents were nominal. Cathode emission of 4.3 ma at the grid voltages of 0 and 300 compared favorably with the spare vidicons and the value of 2.2 ma at the normal operating voltages was within specifications.

6.3.4 Measurement of Functional Parameters

Having ascertained that the filament-cathode portion of the vidicon was nominal, the functional parameters that could be determined with the disabled grid 5 and evaporated photoconductor were measured next. These included the gas ratio and the beam transmission and grid transfer characteristics. The grid cutoff was also determined in the course of the measurement of beam transmission. The voltages applied externally for these tests and the measured parameters can be described with reference to Figure 6-6, which indicates schematically the vidicon electrodes and defines the terms. Grids 3, 4, and 5 were connected together for all of these tests to constitute the "collector."

The gas ratio is defined as the ratio of the ion current to the electron beam current at the nominal value of 140 ma for cathode current, i.e., with nominal voltages applied to grids 1 and 2. The beam current formed by electrons passing through a small aperture in the first anode is on the order of 0.001 of the cathode current under these conditions. The beam current and the ion current are measured separately, with the same voltages on grids 1 and 2 and with -300 and +100 volts applied to the collector, respectively. The vidicon is thus operated for this test as an ionization gauge.

The ion current is generated by an interaction of the beam electrons with the residual gases. It is, therefore, a reasonably accurate measure of the actual pressure inside the vidicon. In a typical triode vacuum tube, the gas ratio is linear in the pressure range from about 10^{-8} Torr to about 10^{-3} . The theory relating the pressure to the measurement of the gas ratio

is given in References 15 through 17 and summarized in Appendix G. 4. The gas ratio measurements served to estimate the vidicon pressure more accurately than previously determined from the Pirani test.

Gas ratio measurements were performed first on the two spare vidicons and then on the Surveyor III vidicon to verify the technique used and to obtain comparison data. Results are summarized in Table 6-2. The beam current in the flight vidicon was only about half of the nominal value. This is explainable by the fact that focusing action of grid 5 was absent. The gas ratio was found to be nearly in specification, and better than that of the spare vidicons. The gas ratio for all three vidicons is what would be expected after several years of normal shelf storage.

The flight vidicon pressure was calculated in Appendix G. 4 from the gas ratio measurements to be about 1.6 x 10^{-5} Torr. As explained in Appendix G. 3, this is compatible with the findings and limitations of the Pirani test. The steepness of the Pirani gauge curve in Figure G-2 (Appendix G) in this range could yield this value of pressure if the difference in the filament resistances between the spare vidicon used for calibration, and the

TABLE 6-2. RESULTS OF GAS RATIO MEASUREMENTS*

Vidicon	Ion Current, nanoamperes	Beam Current, microamperes	Gas Ratio
Spare S/N 109	7. 3	5.0	1.5 x 10 ⁻³
Spare S/N 123	16.5	6.6	2.5 x 10 ⁻³
Surveyor III camera	3. 7	3. 3	1.1 x 10 ⁻³
Specification valve			≤1 x 10 ⁻³

^{*}Calculated Surveyor III vidicon pressure = 1.6×10^{-5} Torr.

flight vidicon were only 5 percent. * It is recalled that pressure was determined by the Pirani method on the assumption that the two vidicon filaments were identical.

The vidicon internal pressure was later measured by still another technique during the measurement of its gas content. This is discussed in Section 6.4.5, where the final comparison of the three results of pressure measurements is given.

Measurements of beam transmission and grid transfer characteristics were then performed. These measurements were similar in that they both consisted of measuring the cathode and beam currents as functions of the control grid 1 voltage for various fixed values of the first anode (grid 2) voltage. Measurements of the beam transmission characteristics were conducted at low values of the cathode current corresponding to the normal operating range of the vidicon and included measurement of the grid cutoff, that is, the value of the control grid voltage at which the cathode current is down to 1 microampere. This characteristic is measured with precision, varying the controlling parameter — grid 1 voltage — incrementally. The grid transfer characteristics, on the other hand, were determined on an oscillograph and covered the full range of the cathode and beam currents.

Results of the measurement of the beam transmission characteristics are shown in Figure 6-7a for the Surveyor III vidicon. This test was performed at two values of grid 2 voltage: at the nominal operating value of 185 volts and at 300 volts. Figure 6-7b shows results obtained for comparison on a spare vidicon at the grid 2 voltage of 185 volts. The result for the flight vidicon can be interpreted as nominal. Its cathode current was somewhat higher than that of the spare vidicon although its beam current was less by about 40 percent. As discussed in Reference 18, however, this is representative of vidicons which have been operated for prolonged periods of time.

The grid cutoff was also obtained from the beam transmission measurements. At the nominal grid 2 voltage of 185 volts, the value of control grid cutoff, corresponding to the cathode current of 1 microampere, is seen on Figure 6-7a to be -80 volts. This is nominal.

Grid transfer characteristics of the flight vidicon are plotted in Figure 6-8. Figure 6-8a shows the control grid transfer characteristic at two values of voltage applied to the first anode, grid 2. Figure 6-8b shows the first anode transfer characteristics at two values of control grid bias. Results are nominal.

^{*}In Figure G-2, 4×10^{-2} Torr corresponds to the filament voltage of 1.96 volts and 2×10^{-5} Torr corresponds to an extrapolated filament voltage of about 2.08 volts.

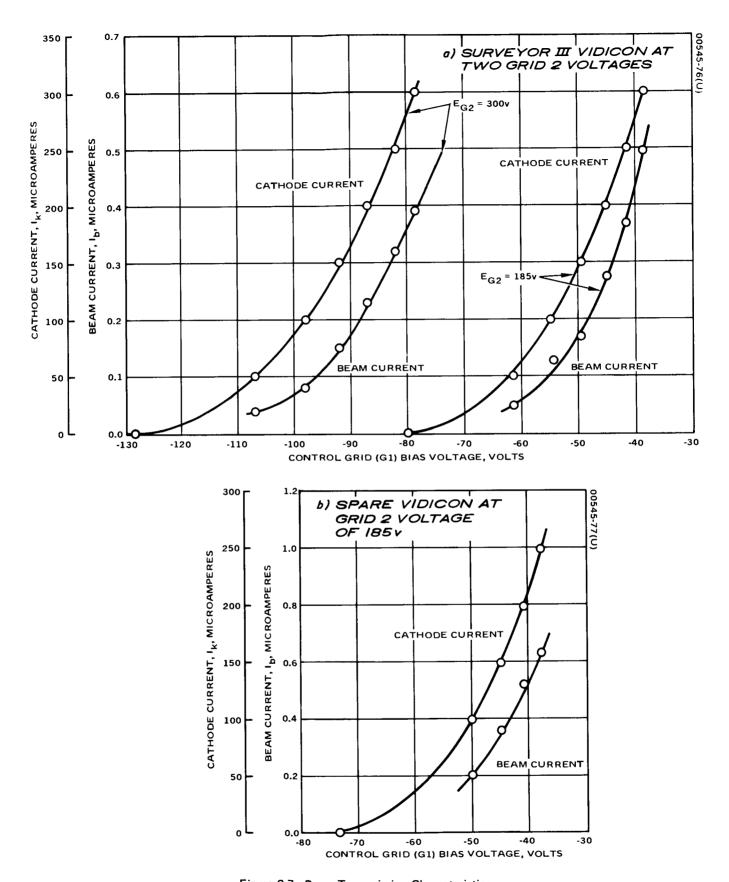


Figure 6-7. Beam Transmission Characteristics

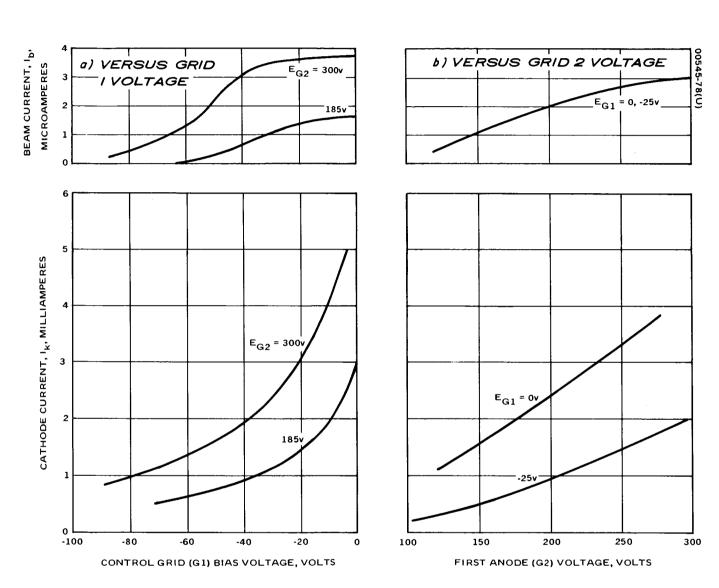
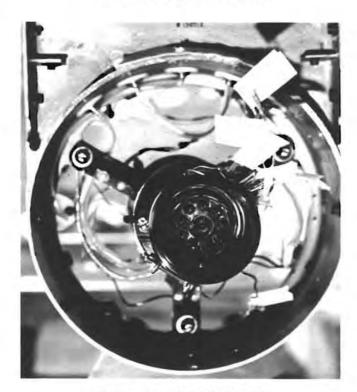


Figure 6-8. Surveyor III Vidicon Transfer Characteristics: Cathode and Beam Currents



a) Front View (Photo 70-4884)



b) Rear View (Photo 4R15892)

Figure 6-9. Vidicon Prior to Removal From Camera

Several changes intentionally introduced into the above measurements resulted in no perceptible changes of the electron beam current. These perturbations included floating, photoexcitation of the vidicon faceplate, and placing a transverse magnetic field near the floating target electrode.

Functional evaluation of the vidicon was limited to the above tests. The following tests, originally planned, could not be conducted because of the inoperability of the photoconductor:

- Video-to-dark ratio
- Sensitivity
- Image shading
- Erasure
- Gamma ratio
- Resolution
- Spectral response
- Test pattern

With the exception of the damaged grid 5 and evaporated photoconductor, the vidicon was found to be nominal to the extent tested.

6.4 VIDICON TESTS OFF CAMERA

6.4.1 Removal of Vidicon

The second phase of vidicon testing commenced with its removal from the camera. Photographs were taken to record the appearance and orientation of the vidicon on the camera. The front and the rear views of the vidicon just prior to its removal are shown in Figure 6-9. The front collar support can be seen in Figure 6-9a. Details of the removal operations were presented in Section 4.8.5. The vidicon is spring-loaded in its mounting with a force of about 7-1/2 pounds. No difficulty was encountered in the removal process.

6.4.2 Visual and X-ray Examination

A more complete visual examination of the removed vidicon was conducted than the original examination on the camera, discussed in Section 6.3.1. The vidicon was examined with a low powered microscope for evidence of physical damage and cracks, for grid spacings and getter appearance, and for the presence of particles of the shattered grid 5 mesh and of the photoconductor.

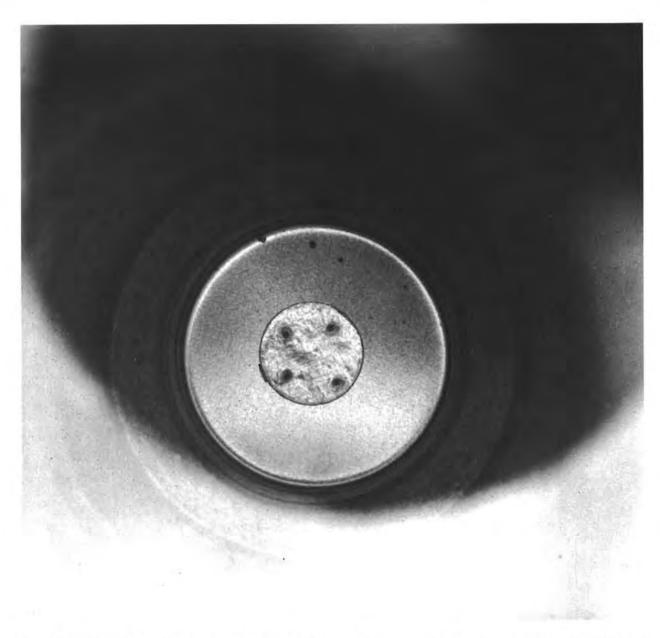


Figure 6-10. Front View of Transparent Faceplate of Surveyor III Vidicon, Showing Cathode in Rear (Photo 70-4863)

Absence of the photoconductor and tearing of the grid 5 mesh were confirmed. Figure 10*, taken at this time, shows the complete transparency of the faceplate. The cathode region in the rear can be seen clearly through the front of the vidicon. The presence of a small remaining piece of the photoconductor near the dark corner reference mark of the faceplate was confirmed. This piece was previously noted (Figure 6-5).

A number of pieces, presumed to have come from the grid 5 mesh, were noted. A large piece of grid 5 mesh, 1/8 by 1/8 inch, was seen wedged between the faceplate and the grid 5 ring assembly. Many small particles were also observed around this piece of the mesh. A larger piece, estimated to be about 3/16 by 1/4 by 1/2 inch, was found to be loose at the bottom of the tube. The size and shape of this piece appear to approximately the same as that of the hole in the grid 5 mesh. It was presumed that this was, indeed, the main torn section of the grid 5 mesh. In addition, there appeared to be a smaller piece, 1/8 by 1/8 inch, loose at the bottom of the tube.

The appearance of the surface of the getter was normal. This was expected from the earlier findings of a nominal gas ratio and fairly good vacuum in the vidicon.

Microscopic examination confirmed the normal appearance of the reseau marks, as previously shown in Figure 6-5. These dots are only 0.002 inch in diameter, and were difficult to see without the semiopaque background normally provided by the photoconductor.

Visual examination of the indium seal caused some concern that it may have melted. Subsequent tests, however, proved this hypothesis not to be valid (see Section 6.5.3).

Several fingerprints were found around the envelope behind the faceplate. These, however, are believed to have been made during the original installation and are not considered significant. Also, several scuff marks were noted on the glass envelope which were made by the boron nitride collar during the removal of the tightly fitting ring, as discussed in Section 4.8.5.

The vidicon was then X-rayed. It was of particular concern to investigate possible misalignments or anomalies in the area of the cathode structure. No irregularities were observed. The spacing between the grids appeared nominal, confirming the measurements of nominal beam transmission characteristics and grid cutoff.

^{*}Original in color.

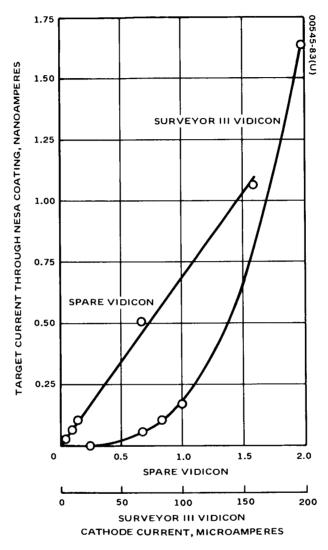


Figure 6-11. Measurement of Nesa Conductivity on Surveyor III and Spare Vidicon

6.4.3 Verification of Electrical Integrity of Nesa Coating

The only functional test conducted on the removed vidicon was the measurement of the electrical characteristics of the Nesa coating on the faceplate to determine whether it was still intact. In view of the nominal findings during the electrical tests on the vidicon, the planned functional tests were not repeated.

The measurement of the condition of the coating entailed operating the vidicon at low cathode currents, with a varying bias on the control grid l in the range of -150 to -80 volts, and with 300 volts applied to grids 2, 3, 4, and 5 connected together. This test was first conducted on a spare vidicon and then on the Surveyor III vidicon. Results for both vidicons are plotted in Figure 6-11. As seen in this figure, the current for the Nesa coating was considerably lower for the Surveyor III vidicon than for the spare. However, the presence of the conducting path confirmed that the Nesa coating did, indeed, appear intact. Discrepancies in the values recorded can easily be explained by the absence of the focusing effect normally produced by the grid 5 mesh.

It is not surprising that the Nesa coating had remained on the faceplate even though the photoconductor had disappeared presumably by the inadvertent, prolonged exposure to excessively high temperatures. It was noted in early tests of some of the vidicons, when peeling of the photoconductor occurred under cryogenic conditions, that no loss of the Nesa coating has ever occurred.

6.4.4 Analysis of Cause of Photoconductor Disappearance

During this phase, an intensive effort was conducted to identify the causes of the loss of the photoconductor and of tearing of the grid 5 mesh. It was postulated that this failure was the result of the solar heat input to the vidicon through the open shutter during lunar days rather than a consequence of the low temperature exposure during lunar nights. The extensive experience obtained in original cryogenic qualification tests of the vidicon indicated that partial peeling of the photoconductor may take place at the cryogenic temperatures; however, total disappearance of the photoconductor, such as found on the Surveyor III vidicon, had never been previously observed.

High likelihood existed, as evident from the discussion of the failed solenoid coil and its drive transistor in Section 12, that the opening of the shutter took place early in the 2-1/2 year period of residence of Surveyor III on the moon — probably during the second lunar day. The vidicon faceplate, therefore, had been exposed to direct solar rays during 30 to 31 lunar days.

The faceplate received the solar energy through the open shutter by reflection of sunlight from the TV mirror. It is estimated that this took place over the range of sun angles from about 7 to about 45 degrees above

horizon. This resulted in a total exposure of about 75 hours per lunar day or over 2000 hours for the total period of lunar residence. Thus, the vidicon experienced a considerable amount of solar thermal input.

The effect of this heat input, coupled with the extreme thermal cycling between successive lunar days, was postulated to have caused the photoconductor to evaporate and to deposit in part on the grid 5 mesh; subsequently, this caused the weakened grid 5 mesh to crack and tear. The effort conducted to verify this conjectured mechanism of failure included thermal analysis and thermal simulation tests on spare vidicons (as indicated in Figure 6-4). Additional tests were performed later, after opening the vidicon, on the severed grid 5 pieces (see Section 6.5.2).

Thermal calculations were made to estimate the temperature rise of the vidicon faceplate (Reference 19). Assuming, conservatively, that the reflection of the sun from the TV mirror was perfectly diffuse and assuming 150°F for the surroundings, the faceplate temperature was calculated to reach 207°F (96°C) during the solar day under conditions of equilibrium with these surroundings.

A simulation experiment was then conducted on spare vidicons to assess the effect of such a level of exposure to thermal inputs. No experimental data were available for comparison since operating conditions and design limits for the vidicon were substantially below the above estimated temperatures. Some data, however, available from independent sources indicated that the photoconductor would evaporate from the faceplate in vacuum if a constant temperature in the range of 115° to 125°C were maintained for 16 hours. The simulation experiment was concerned with the effect of the somewhat lower estimated temperature of about 100°C on the faceplate.*

The initial effort to simulate the thermal input to the vidicon faceplate in the air using a calibrated xenon source was unsuccessful. Cooling by atmospheric convection and conduction limited the faceplate temperature to 30°C even with a relatively high intensity radiant source.

Rather than resorting to the effort and cost of radiant heating in vacuum, an adequate test was performed using a small Stratham oven. The front part of the vidicon was placed in the door of the oven, with the rear portion of the tube left exposed to the room temperature. The oven temperature was maintained at 100°C. The vidicon photoconductor and grid 5 mesh were observed periodically in the course of this heating process, which extended for a total of 304 hours.

^{*}Care had to be exercised to monitor and limit temperatures. Indium seal melts at 156°C.

The results of the exposure of the spare vidicon to this temperature revealed a striking similarity with the apparent failure of the Surveyor III vidicon evident in Figure 6-10. Evidence of the evaporation of the photoconductor around the periphery of the faceplate was noted after 96 hours of exposure. Evaporation continued to be progressively greater as the length of exposure continued. After 118 hours, evidence of some photoconductor loss was seen over the entire surface of the faceplate, and a major portion of the outer edge area had evaporated completely. This can be seen on the original color photograph of the black and white Figure 6-12 — one of the many taken in this experiment.

After 140 hours, the circumferential area was completely clear and the central regions of the faceplate had a general lightening appearance. After 165 hours, the photoconductor had substantially evaporated, with only an outline of the raster remaining. The faceplate was now quite transparent. After 250 hours, the faceplate was clear and totally transparent. No further changes were noted when the test was concluded at the end of 280 hours. The appearance of the vidicon faceplate was virtually identical with that of the Surveyor III vidicon, as shown in Figure 6-10.

Evidence of condensation of the evaporated photoconductor on the inside of the glass envelope was noted after 118 hours of exposure. This condensation was concentrated in the vicinity of the gap between grid 3 and grid 4. Evidence of condensation of the photoconductor continued to be observed throughout the experiment.

After 165 hours of total heating, it was noted that the grid 5 mesh had torn and a large portion was missing in its center, again in striking resemblance to the appearance of the Surveyor III vidicon. After 250 hours of exposure, when the faceplate was totally transparent, a large piece of grid 5 mesh could clearly be seen on the bottom of the tube. Figure 6-13 shows the appearance and dimensions of this piece; it was later confirmed that this piece had, indeed, come from the central area of the grid 5 mesh. In addition, a number of small particles, which presumably came from the torn grid 5 mesh, were noted at the edge of the faceplate. Throughout the exposure and upon its completion, it was noted that grid 5 had become extremely fragile.

A special test was then conducted to determine the effect of exposure of the photoconductor in air. A faceplate with the photoconductor was removed from the spare vidicon and placed in the oven at 100°C. No evidence of evaporation or change in appearance of the photoconductor was noted after 150 hours of heating. This confirmed the expectation that the presence of the air would prevent the evaporation of the photoconductor by the formation of stable oxides.

Additional tests were conducted in the effort to obtain a better insight on the rate of evaporation as a function of exposure temperature.



Figure 6-12. Appearance of Faceplate Photoconductor of a Spare Vidicon After 118 Hours Exposure in Thermal Simulation Test (Photo 00545-84)

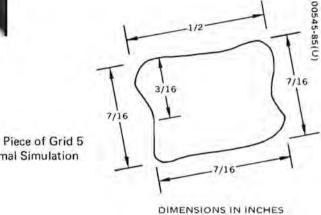


Figure 6-13. Torn Piece of Grid 5 Mesh During Thermal Simulation Test

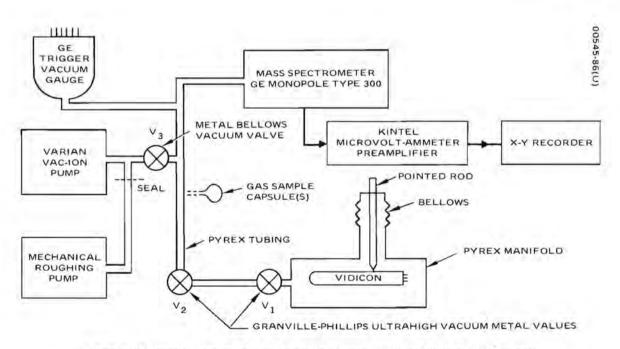


Figure 6-14. Block Diagram of Test Setup for Measurement of Vidicon Gas Content

Several spare vidicons were tested in the oven for various lengths of time at temperatures ranging from 90° to 130°C. As expected, the rate of evaporation was found to be much higher at the higher temperatures. For example, at 120°C, complete evaporation of the photoconductor was noted at the end of 15 hours of heating. Results at 90°C were similar to those at 100°, but the rate of evaporation appeared to be somewhat lower.

These tests verified the postulated mechanism of evaporation of the Surveyor III photoconductor by the solar radiation through the open shutter. The tests also confirmed to a degree the estimates made of the approximate temperature of the faceplate at which this evaporation took place on the moon. Wrinkling and tearing of the grid 5 mesh was also noted in these tests, confirming the hypothesis that this failure may have been related to the evaporation of the photoconductor. Close examination of the grid 5 mesh of the spare vidicon at the end of these tests revealed that its elements appear discolored and suggested that the evaporated photoconductor had deposited on them.

Subsequent analysis of the elements of the grid 5 mesh, conducted after the opening of the vidicon, is presented in Section 6.5.2.

6.4.5 Gas Content Measurement

The last test conducted before opening the Surveyor III vidicon was the measurement of the composition and partial pressures of the residual gases inside. This test was also performed on a spare vidicon to check out the procedure and obtain comparison data. Since both the spare vidicon and the Surveyor III vidicon had a comparable history — they were manufactured at about the same time and had not been operated for about 3 years—it was hoped that comparison of gas contents would shed some light on the effect of the lunar environment and thermal cycling.

Measurements of partial pressure and gas composition were made with a GE monopole 300 mass spectrometer on samples of the internal gas of the two vidicons. The test setup is shown in Figure 6-14. All equipment used, the test procedure, and results are discussed in Appendix G. 5.

The spare vidicon was placed in an evacuated pyrex manifold with the pressure inside the manifold and the connecting pyrex tubing maintained below about 10^{-8} Torr. The vacuum was obtained and maintained by a Varian vac-ion pump, and monitored by a GE trigger vacuum gauge. An opening was made mechanically in the vidicon under vacuum and samples of the gas permitted to flow to the mass spectrometer. The samples were controlled by two Granville-Phillips ultra-high vacuum metal valves.

The sampled contents of the spare vidicon were compared with the measurement of the background by the spectrometer just prior to the opening of the valves. This procedure was then repeated for the flight vidicon.

^{*}This confirmed the previously mentioned data from independent sources.

RESULTS OF GAS CONTENT MEASUREMENTS ON SAMPLES FROM SPARE AND SURVEYOR III VIDICONS TABE 6-3.

Percent Content	Surveyor III Vidicon	70.3	0.5	7.0	2.0	7. 0	4, 5	13.5	1.5	100
Percent	Spare Vidicon	47.9	9.0	0.4	1,3	L •0	33. 1	12.9	3.1	100
Relative Amplitude	Surveyor III Vidicon	15.5	0, 1	1,55	0.45	0.16	:	2, 95	0,33	22.04
Relative	Spare Vidicon	54.	0.65	0.5	1.5	8 •0	37.3	14.5	3.5	112.75
Gas Content	Presumed Element/ Compound	H ₂	ОН	He	CH_4	Ne	Z Z	A	COS	
Gas	Mass Number	2	٤	4	16	20	78	40	44	Total

Results of these tests are summarized in some detail in Appendix G. 5; the overall conclusions are presented in Table 6-3. These results are based on a study and interpretation of a number of measurements taken by the mass spectrometer. Only the relatively most abundant gases are listed in Table 6-3. The values given for relative amplitude were obtained by subtracting corresponding background readings from the data obtained from spectrometer measurements of the vidicon gas samples. The percent contents were calculated relative to the corresponding amplitude totals.

The relative amplitude values in Table 6-3 and the totals were related to the corresponding partial and total pressures, respectively; however, their accuracy was not assessed — total pressures were not known.

The identification of the elements and compounds in Table 6-3 corresponding to the mass numbers was made by inference. It should be recognized that specific molecular content cannot be identified conclusively in some cases. For example, a mass number of 28 could be attributed either to a molecule of nitrogen or to carbon monoxide, or both.

As seen from Table 6-3, the Surveyor III vidicon had proportionately much more hydrogen and helium than the spare vidicon. This was largely made up by the higher proportion of nitrogen in the spare vidicon. The percent carbon dioxide content of the spare vidicon was also somewhat higher. Since only one spare vidicon was sampled, it is not known to what degree these results are attributable to the processing differences during manufacture.

The final test conducted was to attempt to utilize this experimental setup to estimate the internal pressure of the Surveyor vidicon. With the mass spectrometer isolated from the system, the vacuum gage connected, and valves V1 and V2 closed (Figure 6-14), the pressure of the evacuated tubing volume, calculated to be 641 cc, was measured to be 6 x 10^{-5} Torr. Valves V1 and V2 were then opened and the remaining gas allowed to escape from the vidicon into the system. The vacuum gauge reading immediately increased to 2×10^{-4} Torr. Estimating the vidicon volumne to be 58 cc, the vidicon pressure was then calculated using Boyle's law to be 2×10^{-3} Torr.

The above calculation was then corrected for the fact that the vidicon had been previously sampled several times for the mass spectrometer measurements. This calculation led to the estimate of the original Surveyor vidicon pressure to be 4×10^{-3} Torr.

It is recognized that the above calculation was approximate. The pressure obtained by this method compared with the two values previously obtained, as summarized below:

Pirani method 4×10^{-2} Torr Gas ratio measurement 1.6×10^{-5} Torr Gas content measurement 4×10^{-3} Torr The range of uncertainty of the Pirani method, as mentioned earlier, extends from as low a value as perhaps 10^{-5} Torr to as high a value as perhaps 10^{-1} . The range of uncertainty of the results of the other two methods cannot be stated conclusively. It can be concluded, however, that the three results are not incompatible in the light of the accuracy obtainable. It can also be concluded with a high degree of assurance that the vidicon pressure was significantly less than 10^{-1} Torr. It is believed that the last of the three measurements, which yielded a value in the range between 10^{-2} and 10^{-3} Torr, probably reflects most closely the correct internal pressure of the Surveyor III vidicon.

In order to permit further analysis of the relatively high helium content of the Surveyor III vidicon, a number of samples of the gas were extracted under vacuum into vacuum-tight ampules, as indicated in Figure 6-14. This was performed by connecting the necks of the capsules to the pyrex tubing; after evacuation of the system and passing of the vidicon gas into the capsules, they were tipped off without disturbing the vacuum by a localized heating/glass melting technique. The samples removed were one 200 cc capsule and four 10 cc capsules.

The Surveyor III vidicon was then removed for the final diagnostic phase of the investigation. The vidicon had a 0.060 inch diameter hole in the envelope near the lower mesh retainer ring in the vicinity of the cathode, produced during opening in vacuum by the pointed rod in the above test (see Figure 6-14). The region of the faceplate was unaffected.

6.5 OPENING OF VIDICON AND DIAGNOSTIC TESTS

6.5.1 Opening of Vidicon

The final phase of the vidicon test program commenced with the opening of the Surveyor III vidicon, which was now at atmospheric pressure. The opening was therefore relatively easy to accomplish. A file mark was made around the tube envelope, starting with the 0.060 inch diameter hole, and the tube was gently broken in half by cracking the envelope. The vidicon was thus disassembled into two parts. The internal vidicon structure attached to the cathode was pulled apart from the second half, consisting of the length of the envelope attached to the faceplate. Subsequently, the tubing was cut circumferentially at the other end in the vicinity of the indium seal, leaving the small second section comprising the small piece of glass tubing with the faceplate and indium seal.

Diagnostic tests described in the following subsection were performed on the various portions of the open vidicon. In order to examine the indium seal, the faceplate section was cut into four 90 degree segments, using a glass cutting wheel. Cross sections of the indium seal were thereby obtained.

6.5.2 Visual Examination of Grid 5 and Diagnosis of Its Failure

Analysis and thermal simulation tests, discussed in Section 6.4.4, explained evaporation of the photoconductor and demonstrated a striking similarity between the failure of the grid 5 mesh of the spare vidicon at elevated temperatures and that of the Surveyor III vidicon. It was suggested that exposure to the solar energy through the open shutter, coupled with the deposition of the evaporated photoconductor on the grid, had precipitated the failure of the Surveyor III vidicon grid. Diagnostic tests, discussed in this section, were conducted on grid 5 mesh of the open vidicon to pinpoint the specific causes and mechanism of failure. Specifically, the examination was conducted to verify the hypothesis that the evaporated photoconductor deposited on the grid weakened it and caused it to break under the thermal cycling in the lunar environment.

Microscope and microprobe examinations were conducted on three samples of the grid 5 mesh, shown in Figure 6-15, to obtain comparison data:

- 1) Surveyor III vidicon
- 2) Spare vidicon, previously exposed to 100°C for 140 hours
- 3) Spare vidicon from storage

Results of the microscopic examinations are evident from the appearance of the three samples shown in Figure 6-15. The sizes are magnified, but the three samples are sketched so that the approximate relative dimensions are indicated. The grid elements of samples a and b are virtually identical in appearance. They both, however, differ considerably from the original vidicon grid wire of sample c in the following ways: the cross section of the copper portion of the elements of both damaged grids was much smaller, a thick layer of coating was present, and the thickest part of this coating was in both samples a and b on the side facing the vidicon faceplate. The thickness of the copper elements of samples a and b was of the order of 1 micron. The corresponding thickness of the original mesh elements, as indicated in Figure 6-15, was 2.5 microns.

To obtain further insight on the chemical composition and because of the small dimensions involved, a microprobe investigation was conducted. Microprobe measurements were made of the chemical composition of sections inside the three copper elements and inside the two coatings. The results obtained are summarized in Table 6-4. Other portions of the samples were tested, including the surface of the elements. Results generally confirmed the findings shown in the table.

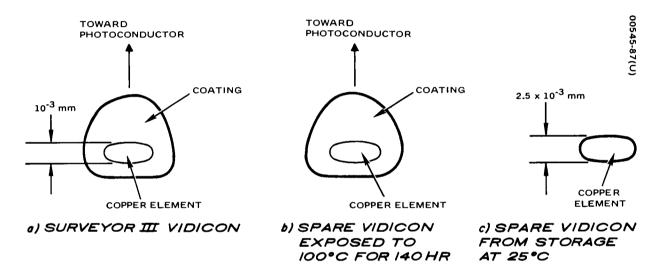


Figure 6-15. Results of Microscopic Examination of Pieces of Grid 5 Mesh

TABLE 6-4. RESULTS OF MICROPROBE TESTS OF SAMPLES OF GRID 5 MESH

	Composition in Percent							
	Sampl Survey Vidi	or III	Sample b Vidicon (F 100°C for	Heated to	Sample c — Spare Vidicon From Storage			
Element	Copper Element	Coating	Copper Element	Coating	Copper Element			
Copper	85	70	88	66	97			
Oxygen	12	13	5	5	2			
Silver	≈0	<1	≈0	<1	≈l			
Selenium		12		18				
Sulfur	3	5	7	10				

The following observations can be made from the data of Table 6-4:

- l) Elements of samples a and b contain more oxygen and sulfur than sample c. (Sample c has no sulfur.)
- 2) Coatings of samples a and b are similar in composition. Both coatings have sulfur and selenium in them. In addition, both coatings have a considerable amount of copper, presumably as a result of migration from the grid mesh.
- 3) The ratio of selenium to sulfur in both coatings is about 2:1 (somewhat higher in the Surveyor III vidicon).
- 4) Oxygen content is approximately the same in the coating as in the copper element of both samples. The oxygen content of the Surveyor III vidicon sample is higher.

The similarity between the Surveyor III vidicon and the vidicon exposed to high temperatures during the thermal simulation tests became even more striking now than after the earlier visual examination. Presence of sulfur and selenium in about the correct ratio virtually proved that the source of the coating was the photoconductor. The photoconductor composition is normally about 75 percent selenium and 25 percent sulfur but varies from batch to batch. Migration of copper into the coating accounted for the decrease in the size of the copper elements of the mesh. Some evidence of migration of some silver from the mesh into its coating, as noted in

Table 6-4, also confirmed this process, because of the usual presence of silver in copper.

The weakening of the mesh now became quite clear. Not only did the elements get smaller as a result of the loss of copper to the coating, but the migration of the sulfur into the mesh brought about additional weakening by the corrosive reaction normally forming copper sulfides. Furthermore, since the copper atoms are at a higher energy stage in the grain boundaries, the reaction of copper with sulfur would be expected to be somewhat more rapid in this region; this would exhibit itself as a further weakening of the remaining grain boundaries in the copper. The result of this surface weakening, internal corrosion, and reduced core cross section was a very fragile grid mesh, highly susceptible to failure during thermal cycling.

Even without thermal cycling, the fragile grid 5 mesh during the thermal simulation tests had shattered. It would certainly be expected to shatter on the lunar surface, particularly in view of the difference between the thermal expansion coefficients of the weakened grid elements and that of its acquired copper/selenium/sulfur coating. The fact that the grid ruptured into a number of pieces which curled toward the thicker coating side is the final proof of this mechanism of failure.

Thus, the mechanism of failure of the vidicon faceplate and grid 5 are believed to be completely understood. Both failures are the result of sunlight through the open shutter. Both are secondary in nature, and neither represents a potential degradation by the lunar environment of properly protected and operated vidicons. This failure, however, emphasizes the importance of inadvertent high radiant thermal inputs.

6.5.3 Tests of Indium Seal

The condition of the indium seal after its exposure to the lunar environment and to the thermal cycling was of interest because of its potential applications. It was already known that the internal pressure of the returned vidicon was in the nominal range, so that the seal evidently had not failed. However, it was of interest to determine the condition of the seal. It was particularly desirable to know whether any part of the seal had melted at any time during the lunar exposure.

Sections of the seal were available for examination from the sectioning operation described above in Section 6.5.1. These sections were examined microscopically, and results were compared with an examination of the three following additional samples:

- Indium seal on the spare vidicon, previously exposed to 100°C for 140 hours
- 2) Indium seal on a spare vidicon from storage
- 3) Indium seal on a spare vidicon, intentionally melted at 160°C and resolidified

Results of the microscopic examination indicated that the Surveyor III indium seal and samples 1 and 2 looked identical; only sample 3 appeared different. The indium seal sample 3, intentionally melted, showed a significant change in appearance. The indium had been severely deformed while making the seal between the glass enclosure and the faceplate. Melting of the seal apparently squeezed it out; subsequent cooling had pulled it back. Results of this process could be seen during the microscopic examination. On the other hand, the other samples, including the Surveyor III vidicon indium seal, retained the appearance of an unmelted sample.

It was concluded that no melting or other identifiable alterations of the indium seal had taken place during the lunar exposure.

6.5.4 Nesa Conductivity Measurements

The final diagnostic test entailed measurement of the transmission through the Nesa coating of the Surveyor vidicon as a function of wavelength. This measurement was performed using a Beckman DK 2 spectrometer, with an accuracy better than 2 percent. Results are shown in Figure 6-16. Also plotted on this figure are comparison data obtained on two other Nesa coatings, one of which was the coating of the spare vidicon which had undergone the thermal simulation exposure in the oven for 140 hours at 100°C. The photoconductor had evaporated during this test, as noted previously. The third sample was that taken from a spare vidicon from storage. To obtain comparative results, its photoconductor was removed prior to this test using carbon disulphide.

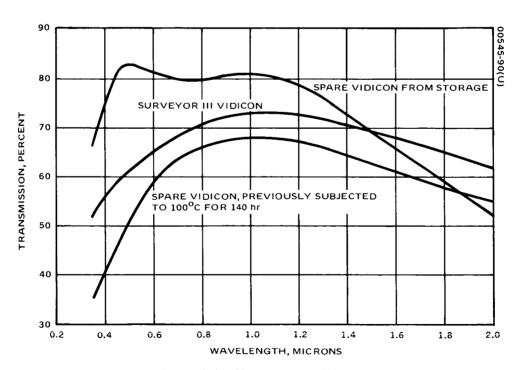


Figure 6-16. Optical Transmission Measurements of Nesa Coatings: Surveyor III Vidicon and Two Spare Vidicons

It is apparent from Figure 6-16 that the thermal exposure resulted in a significant degradation of the transmission of the coating of the spare vidicon over the entire spectrum relative to the vidicon from storage. Reduction in the order of 10 to 15 percent was noted in the infrared region and as much as 30 percent in the visible region. The Nesa coating of the Surveyor vidicon was also degraded relative to the vidicon from storage but not as much as the thermally exposed spare vidicon. The above observation should be qualified somewhat by recognition that the coatings may also have differed somewhat originally.

Results of this test suggest that exposure to thermal radiation tends to degrade the optical transmission characteristics of Nesa coatings and lends additional evidence to the postulated mechanism of the secondary failure of the Surveyor vidicon. It might be concluded from these results that the Surveyor vidicon had, perhaps, experienced a temperature and temperature-duration history somewhat less severe than the 100°C for 140 hours to which the spare vidicon was subjected although the fact that the Surveyor vidicon experienced its high temperatures somewhat more intermittently and over a period of several years may influence this conclusion.

6.5.5 Other Diagnostic Tests

The original test plan included, as an option, examination of certain elements of the dismantled vidicon in order to pinpoint the photoconductor and grid 5 failure. It was planned to examine possible deposits of the photoconductor on the various electrodes, as well as pieces of the shattered grid 5 mesh. The contemplated tests included visual, chemical, metallographic, and SEM measurements. It was decided not to conduct these tests for several reasons. Results of analysis described above gave fairly conclusive evidence as to the mechanism of the failures. Retrieval of the several grid pieces proved to be very difficult because of their extreme fragility. It was felt that no further light would be shed by pursuing this course of action.

Similarly, original plans to conduct a detailed examination of the cathode for evidence of contamination, discoloration, erosion, and ion damage were abandoned. Conduct of these tests would entail additional laborious dismantling of the vidicon structure, and it was felt that the amount of data obtainable would not justify the impact of this effort on program schedule and funding.

Likewise, detailed checks of the tube geometry — alignment and spacing of its elements, and microscopic examination of the getter — were not conducted. Results of functional tests verified that this portion of the vidicon appeared to be nominal. It was felt that the preliminary results obtained during the visual examination, which confirmed this, were adequate.

7. ELECTRICAL COMPONENTS TESTS

7.1 SCOPE AND GENERAL TEST PLAN

The electrical components of the TV camera — resistors, capacitors, diodes, and transistors — were tested with the primary objective of determining the effects of their long-term exposure to the lunar environment. Components tested were selected on the basis of their importance for future design applications. Analysis was directed toward determining electrical performance and detecting mechanical and structural changes. Mechanical discrepancies, changes in electrical characteristics relative to data available from earlier records, and component failures received special attention to identify specific causes.

Component testing was conducted in two distinct categories for two distinct reasons: routine examination of selected samples and specific analysis of failed components. This section of the report is concerned almost entirely with the former. The latter is treated separately in Section 12 as part of the failure analysis work on the program.

Table 7-1 shows the number of types and quantities of electrical components of the TV camera. Since it was impractical and not particularly useful to subject all of these to tests, a selection was made of a subset of these numbers. The types and quantities selected for testing are also shown in Table 7-1.

Selection of types of components to be tested was made on the basis of the relevance of the types to current technology and future applications. A complete list of all the components was made, and priorities were assigned in close coordination with the customer. An initial selection was made on the basis of these priorities on the rationale that it was more desirable within funding constraints to examine and analyze a smaller but useful set of components rather than to try to test more superficially all or samples of all types. The list of all types, and a brief discussion of the priorities, is presented in Appendix H.

TABLE 7-1. TYPES AND QUANTITIES OF ELECTRICAL COMPONENTS

	Total in Cam	era	Selected for Testing			
Components	Number of Types	Total Quantity	Number of Types	Total Quantity		
Resistors	11	781	5	116		
Capacitors	5	139	4	59		
Diodes	15	350	7	55		
Transistors	18	242	_6	<u>47</u>		
Total	49	1512	22	276		

A final selection of types to be tested was made by modifying the list to account for the fact that, in some cases, component types which nominally differed in part number designation were essentially similar from the standpoint of construction and fabrication technique. An adequate assessment of the effects of lunar exposure could be obtained for such a class of parts by examining only several, not necessarily all, of these types.

Selection of the quantities to be tested for each type was based on several criteria. One was the location of the components on the various chassis. As mentioned in Section 4.2, the Circuit Test Plan and the Component Test Plan were developed on a coordinated basis. Whenever possible, similar components were selected for comparison, both from the chassis which had undergone circuit tests and from the chassis which were left intact. Another basis for selection was the outcome of preliminary survey. All chassis were visually inspected with great care, and passive checks were conducted whenever possible prior to disassembly and component level tests. Those components which exhibited anomalous appearance or behavior were assigned high priority for subsequent testing. Still another criterion was the ease of removal. In some cases, removal could - or did in isolated cases - result in partial damage. In such cases, a similar, but more easily accessible and removable component was selected. Finally, the number of parts tested was constrained by customer direction that half of all the components and other critical parts be preserved for scientific and second-generation tests.

Tests of selected samples were conducted in three consecutive phases on successively smaller subsets. These phases were:

- Preliminary examination visual inspection and basic functional check
- Nondestructive tests detailed electrical performance tests, mechanical tests, and environmental tests as applicable
- Destructive tests dissection and diagnostic internal examination

During the first phase, each component was visually examined for changes such as discoloration, deformation, or cracking, and its basic electrical parameters were measured. This was accomplished by disconnecting essential leads, preferably without removing the component from the chassis. This examination was conducted on a large number of components—on the order of 1000. Electrical tests conducted during this phase were limited to those necessary to establish the basic condition of the component. Examples of such tests were ohmic resistance, capacitance, leakage current, dissipation factor, and breakdown voltage.

Selected samples of components examined during this initial phase were then subjected to detailed testing. Detailed procedures were prepared for these tests, starting with a preliminary format shown in Appendix H. A flexible approach was adopted to stress investigation of those performance parameters which would reveal most conclusively effects of lunar exposure. Actual conduct of tests was guided by results of initial examination. Parts that exhibited mechanical or electrical changes were processed differently from those which appeared to have been unaffected.

The final phase was conducted on a still smaller subset of samples tested above. Selected components were dissected and examined — those which were of particular interest because of specific findings as well as those routinely chosen as representative. A variety of techniques were employed, as applicable, including SEM, metallographic, and spectrographic analysis, to probe for specific changes, and to establish specific environmental factors instrumental in producing observed effects. This destructive diagnostic phase of testing was closely coordinated with the materials test program, reported in Section 10, and overlapped to some extent the corresponding effort related to the analysis of specific failed components, reported in Section 12.

The succeeding subsections summarize the tests and results obtained for each type of electrical component tested. Appendix H contains additional detailed information on the test plan followed and specific results obtained.

TABLE 7-2. RESISTOR TEST PLAN SUMMARY

	Tests Prior to F	Tests Prior to Removal From Chassis	Nondestr Remov	Nondestructive Tests of Removed Resistors	Number of
Type Description	Quantity Tested	Parameters Measured	Quantity Tested	Parameters Measured	Examined Internally
Carbon composition resistor, 1/4 watt, Allen-Bradley; similar to RCR07	53	Ohmic resistance	10	Resistance Noise Resistance versus temperature	2
Carbon film resistor, glass enclosed, 1/8 watt, Texas Instruments, Type CG 1/8; similar to RN55G	88 5	Ohmic resistance	7	Impedance versus frequency Resistance Noise Resistance versus temperature Impedance versus	2
Wire-wound power resistor, 2 watts, Sage Electronics;	2	Ohmic resistance	2	frequency Resistance Resistance versus temperature	٧
Platinum resistance thermometer, Rosemount Engineering, Type 118	2	Ohmic resistance	Г	Resistance at 4 temperatures: -196°, -85°, 0°, and 100°C	-
Precision wire-wound resistor, 1/8 watt; Daven Electronics; similar to RBR	1	Ohmic resistance	1	Resistance Resistance versus temperature	

7.2 RESISTOR TESTS

A summary of the tests of the 116 resistors indicated in Table 7-1 is presented here. The five types of resistors, quantities tested, and parameters measured are summarized in Table 7-2. The summary of findings, presented below, is supplemented by additional discussion in Appendix H.

Part removal required particular care in cutting away the epoxy coating and bonding materials with X-acto knives and, on occasion, employing an epoxy stripper. Considerable difficulty was experienced in removing glass packaged resistors which were bonded to circuit boards. Where the parts were bonded to metal surfaces, removal was much easier. A detailed visual examination was conducted immediately upon removal of the parts. Several of the parts were found to be cracked; with few exceptions, these cracks were primarily in the glass envelopes and are believed to be associated with the conformal coating.* Some of these cracks may have been incurred in the removal process. Except for components which were found to have failed, these cracks did not affect subsequent readings. A detailed discussion of the cracks and of the failed components is given in Section 12.

7.2.1 Carbon Composition Resistors

Fifty-three carbon composition resistors, ranging in resistance value from 51 ohms to 10 megohms, were checked on the chassis for their ohmic resistance. Of the 53 resistors, the 10 removed from the chassis ranged from 510 ohms to 10 megohms. Ohmic resistance values, measured on and off the chassis, as well as noise measurements of the 10 removed resistors, showed good correlation with past data and no deviation from specifications.

Resistance versus temperature measurements were conducted on the ten resistors. Excellent temperature retrace characteristics were obtained. Figure 7-1, plotted for a 1.5 megohm resistor in the middle of the range of resistors tested, illustrates the results. Additional curves are presented in Appendix H.

Results of impedance versus frequency measurements for three resistors are shown in Figure 7-2. All results were nominal, as illustrated by a control curve drawn for comparison for a new 20 kilohm resistor.

As noted previously, similar cracking was observed after prelaunch thermal vacuum tests.

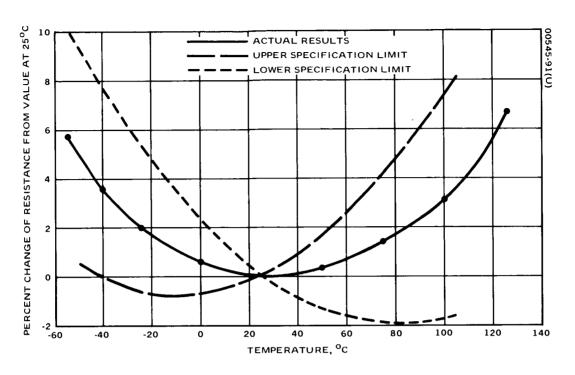


Figure 7-1. Resistance Versus Temperature of 1.5 Megohm Carbon Composition Resistor

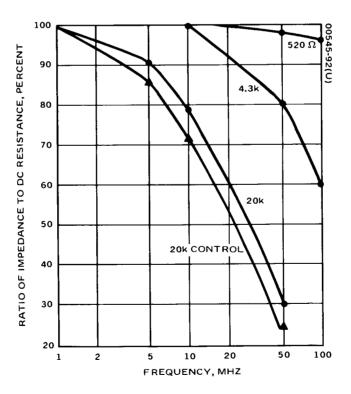


Figure 7-2. Impedance Versus Frequency of Three Carbon Composition Resistors

Internal examination was conducted on a 510 ohm and on a 1.5 megohm carbon composition resistor, respectively, as well as on new similar resistors for comparison. No evidence of voids, cavities, or unusual changes in grain structure were observed. As an example, Figure 7-3 shows photographs taken with 200X magnification of a section of the 1.5 megohm resistor from the Surveyor camera and from the control sample, respectively. No differences in appearance are noted. These results correlate with the absence of discrepancies in functional measurements.

7.2.2 Carbon Film Resistors

Fifty-eight glass-enclosed carbon film Texas Instruments resistors, similar in construction to metal film resistors, were checked on the chassis for their ohmic resistance. The value of their resistance ranged from 51 ohms to 93.8 kilohms. Seven of these resistors were rechecked after removal from the chassis. Changes in the resistances relative to original Surveyor data were well within design tolerances and the allowable long-term drift. The range was within ±0.13 and -0.44 percent, with the exception of one 51 ohm resistor which decreased by 1.4 percent. This latter value could be attributed to a degree to the accuracy of the test method used for measurements of smaller resistances.

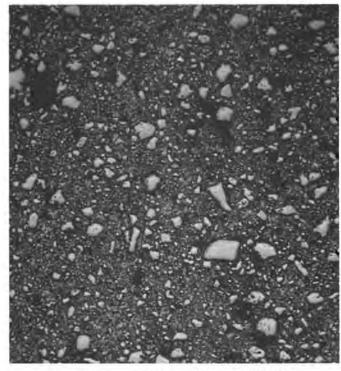
Noise measurements performed on the seven removed resistors correlated extremely well with original data. Results of resistance versus temperature, summarized in Figure 7-4, also indicate good correlation with expected characteristics. Low resistance temperatures follow the expected temperature coefficient curve of the 250 ppm plot, while the 93 kilohm components approach that of the 500 ppm.

Results of impedance versus frequency measurements, performed on the Hewlett-Packard 4815 vector impedance meter, are shown in Figure 7-5. A plot of a Mepco FH10 100 kilohm glass-enclosed metal film resistor is also presented for comparison. Results are considered nominal: apparently, there have been no abnormal changes in the carbon film structure and no changes in the core structure that would alter the distributed capacitance.

Two carbon film resistors were dissected and examined under a microscope at a magnification of 30X. As discussed further in Appendix H, no significant changes were noted.

7.2.3 Power Wire-Wound Resistors

The two Sage Electronics power resistors, wire-wound on alumina substrates, were checked for ohmic resistance on the chassis and then removed for resistance-temperature measurements and diagnostic testing.



a) New Sample (Control) (Photo 00545-93)



b) Surveyor III Camera Resistor (Photo 00545-94)

Figure 7-3. Metallographic Section of 1.5 Megohm Carbon Composition Resistors (200X Magnification)

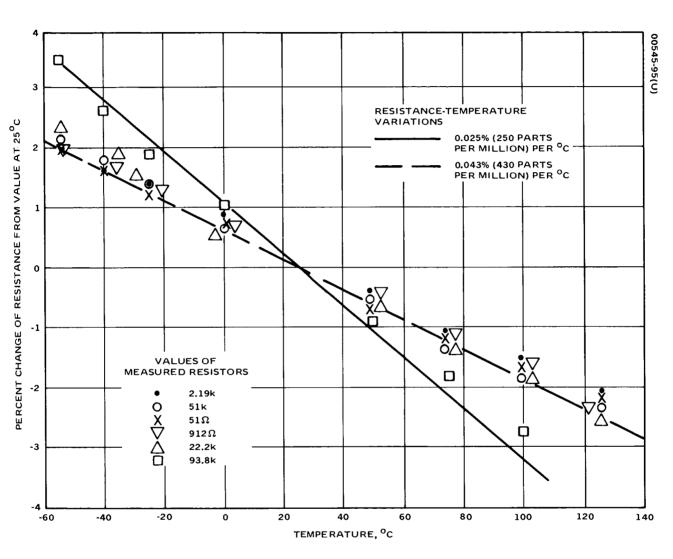


Figure 7-4. Resistance Versus Temperature of Six Carbon Film Resistors

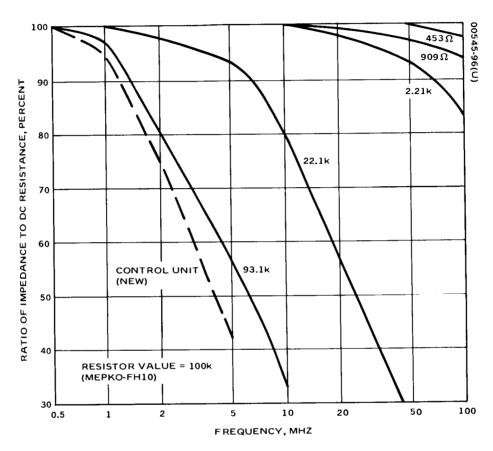


Figure 7-5. Impedance Versus Frequency of Five Carbon Film Resistors

The small number of samples available somewhat limits the conclusions that can be drawn from the tests. Ohmic resistance changed - 1.9 percent for the 1200 ohm components and -0.9 percent for the 20 ohm components. The resistance-temperature coefficient was measured to be under 4 ppm/°C, indicating that no abnormal stresses or strains were developed in the wires. While some of the changes in ohmic resistance may be attributed to instrumentation differences, calibration, and operator performance, and while at least part of the difference on the 20 ohm resistor can be attributed to errors associated with lead and contact resistances, the observed resistance changes are greater by at least a factor of 2 than would normally be expected for temperature cycling in the conventional specification range of -55° to +125°C. It can therefore be reasonably concluded that some additional change has been effected by prolonged exposure to the lunar environment.

To investigate the effects of the lunar exposure more thoroughly, the two resistors were examined more closely by stripping off the silicone coating and microscopically inspecting the wires for unusual stresses. The windings were found to be uniform, with some slack at each end. There was no evidence that strains had been induced in the wires in the original assembly. Resistance readings of the stripped units were essentially unchanged relative to previous readings, indicating that shunt resistance was not a factor.

Results obtained cannot be readily extrapolated to larger resistance values although, if the conjectured effect of the lunar environment is, indeed, valid, similar higher resistance components would be expected to change by a relatively larger amount because of the smaller wire diameters used in their construction.

7.2.4 Platinum Resistance Thermometer

The platinum resistance thermometer is a Rosemount Engineering Type 118 surface temperature sensor shaped like a postage stamp 0.5 inch square and 0.1 inch thick. The thermometer uses strain-free platinum wire for its resistance element. This component was not expected to be affected by the lunar environment since it was designed to measure temperatures as low as those of liquid nitrogen.

The two resistors were checked on the chassis and removed, but only one was further tested for its temperature characteristic and subsequently opened for analysis. Past calibration data were available for comparison for this selected resistor; calibration data could be obtained from the manufacturer for the other resistor. The significant measurement was the precise temperature calibration characteristic of this component conducted in the Hughes Certified Primary Standards Laboratory. Resistance was measured at four temperatures: reference ice point (0°C), liquid nitrogen, carbon dioxide freezing point, and steam. Results of these measurements and comparison with original calibration data are summarized in

TABLE 7-3. RESISTANCE VERSUS TEMPERATURE CHARACTERISTICS OF PLATINUM RESISTANCE THERMOMETER

Measure	d Values	Original Cal	ibration Data	Apparent Calibration C	Changes in Characteristics		
Temperature, °C	Resistance, ohms	Temperature, °C	Resistance, ohms	Equivalent Temperature for Measured Resistance, °C	Apparent Equivalent Error in Temperature, °C		
-195.70	97.286	- 196	96.2440	-195.48	+0.22		
-85.34	328.985	- 195 - 86 - 85	98.4037 327.8607 329.9193	-85.45	-0.11		
0.00	502.134	1.00	500.4542	-0.16	-0.16		
100.37	699.319	99 100.00	697.9151 699.8600	99.73	-0.64		
Original temperature coefficient 0.39287 Measured temperature coefficient 0.39124 Percent reduction 0.4							

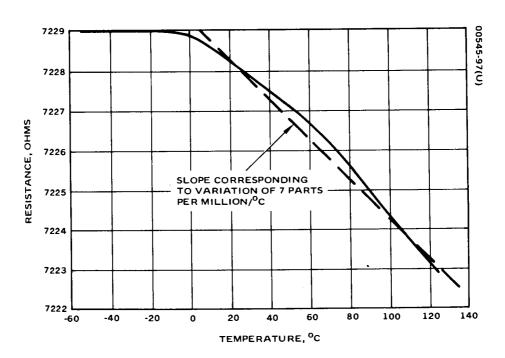


Figure 7-6. Resistance Versus Temperature of Precision Wire-Wound Resistor

Table 7-3. The observed changes in resistance values relative to the original calibration data are translated, by interpolation of the original data, into equivalent apparent temperature changes. Table 7-3 also includes the original value of the resistance-temperature coefficient, a, and its apparent change.

Results indicate that the calibration has changed although the resistance thermometer still meets the initial specifications. While this change is totally insignificant for Surveyor application, it was considered important to analyze it further because of the applicability of lunar environment effects on precision temperature measurement devices for future applications. Resistance apparently decreased at higher temperatures. The temperature coefficient calculated at the reference temperature of 0°C also decreased in value.

Internal examination revealed some deformation in the coils, but the results were not conclusive. The deformation was made in original manufacture. No definitive explanation could be found for the apparent change in resistance and temperature coefficient. Further details are given in Appendix H.

7.2.5 Precision Wire-Wound Resistors

One of the two precision wire-wound resistors of the TV camera was examined. The second resistor was buried in an encapsulated module and could not be removed. The resistor tested was a plastic-encapsulated Daven Electronics 1/8 watt resistor, wound on an epoxy bobbin, similar to the RBR type.

The resistance measurements on the chassis correlated perfectly with original data. Subsequent off-chassis measurements indicated a small change of -0.015 percent. Resistance versus temperature characteristics was measured, and the results plotted in Figure 7-6 shows that the variation is on the order of 7 ppm/°C at high temperatures and essentially zero at low temperatures. This result is well within specifications.

Both the resistance and temperature variation measurements show excellent correlation with original data. This indicates that no excessive stresses were applied to the wire during its exposure to the lunar environment. It was therefore decided not to subject this component to any further diagnostic testing.

7.3 CAPACITOR TESTS

A summary of tests of the 59 capacitors indicated in Table 7-1 is presented here. The four types of capacitors, quantities tested, and parameters measured are summarized in Table 7-4. An additional discussion of

TABLE 7-4. CAPACITOR TEST PLAN SUMMARY

Niversity of Care States	Examined Internally	2	7	-	2
Nondestructive Tests of Removed Capacitors	Parameters Measured	Capacitance, dissipation factor, ESR versus frequency, dielectric strength, scintillation, leakage current versus temperature	Capacitance, dissipation factor, ESR versus frequency, insulation resistance versus temperature, dielectric strength	Capacitance and dissipation factor, C and Df versus temperature, insulation resistance versus temperature, ESR versus frequency	Capacitance and O, C and Q versus temperature, insulation resistance versus temperature, ESR versus frequency
Nondestr	Quantity Tested	7	9	2	٣
Tests Prior to Removal From Chassis	Parameters Measured	Capacitance, dissipation factor, leakage current	Capacitance, dissipation factor	Capacitance, dissipation factor (approximate)	Capacitance, dissipation factor (approximate)
Tests Prior to F	Quantity Tested	38	13	2	9
	Type Description	Solid electrolyte tantalum capacitors, Sprague and Kemet; similar to CSR 13	Metallized paper/mylar capacitors, Sprague; similar to CH 09	Dipped mica capacitors, Electromotive Manufactur- ing; similar to CM 06	Glass dielectric capacitors, Corning Electronics CYFR; similar to CY 15

the diagnostic tests of the tantalum capacitors is given in Appendix H. This section does not include the discussion of one failed solid tantalum capacitor, treated in Section 12.

7.3.1 Solid Tantalum Capacitors

Thirty-eight solid electrolyte tantalum capacitors were measured on the chassis. These capacitors are hermetically sealed in cylindrical metal cases with glass end seals. The capacitors tested cover the range from 0.1 to 100 microfarads.

Chassis tests included room temperature measurements of the capacitance and the dissipation factor, and leakage current measurements at low voltage. The latter were conducted merely to observe radical changes without inducing scintillation effects or changes in the dielectric structure. Subsequently, more precise measurements of leakage current were performed on selected removed components, including examination of scintillation, as discussed below.

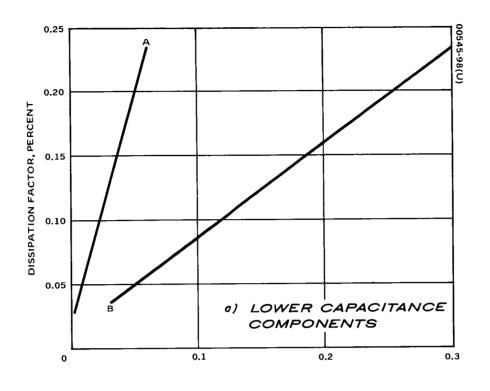
Results of measurements on the chassis were considered nominal. The values were well within specification limits. Dissipation factors were well grouped for parts with similar capacitance and voltage ratings. Capacitance values increased for 14 units, decreased for 17 units, and were unchanged for 4 units; past data were not available for 3 units. The change in capacitance ranged from -0.28 to a maximum of +4.1 percent. No major anomalies were noted in leakage current measurements, with the exception of the shorted tantalum capacitor, identified during chassis tests and discussed separately in Section 12.

The seven capacitors listed in Table 7-5 were removed from the chassis for more detailed functional examination. The parts selected covered the entire range of values and included components which had evidenced largest capacitance changes during chassis tests. Retest of capacitance and dissipation factors showed no changes with respect to measurements on the chassis.

Two functional tests were conducted to establish the general condition of the manganese dioxide-carbon-silver-solder structure of seven capacitors: dissipation factor (D_f) versus frequency and equivalent series resistance (ESR) versus frequency. The former is a low frequency test, while the latter is performed in the 0.1 to 1 MHz range. The dissipation factor is plotted as a function of the susceptance of the capacitor (ωC) in Figure 7-7. Also listed in this figure are the calculated values of the approximate equivalent series ohmic resistance, which is the slope of these lines. This equivalent resistance represents the ohmic equivalent for the structure in series with the dielectric in this frequency range. Results appear to be nominal.

SUMMARY OF LEAKAGE TESTS ON SEVEN TANTALUM CAPACITORS TABLE 7-5.

ic Tests	Torming	Voltage, volts				130	140		
Diagnostic Tests		Sample Inspected				×	×		
	ent Tests	Slope	Nominal	High	High	High	Nominal	Nominal	Nominal
	Leakage Current Tests	Leakage Current	Nominal	Nominal	High	Excessive	Nominal	Somewhat high	Somewhat high
	ngs	DC Voltage, volts	50	50	35	35	35	20	20
	Ratin	Microfarads	0.1	0.47	47	47	47	100	100
		Sample	Ą	В	υ	Q	ঘ	Ĺτί	Ů



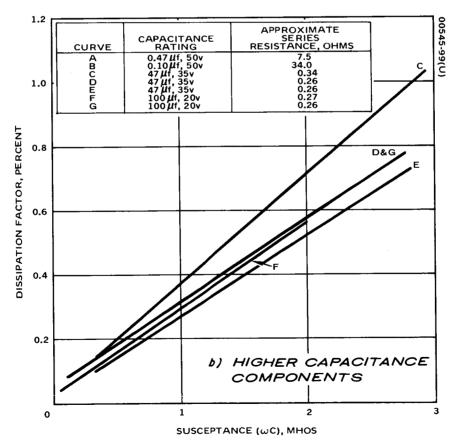


Figure 7-7. Dissipation Factor Versus Susceptance of Solid Tantalum Capacitors

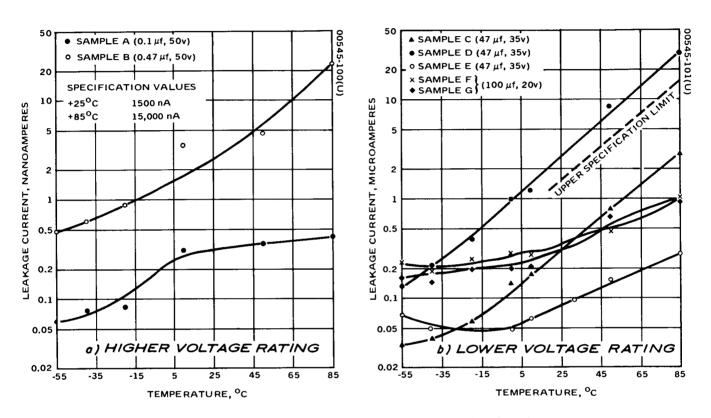


Figure 7-8. Leakage Current Versus Temperature of Tantalum Capacitors

Measurements of ESR versus frequency were performed on the seven capacitors on a 260A Q-meter. Results agreed reasonably well with published data and with the values obtained from the dissipation factor measurements. The ERS test lacks resolution and can be used only for an approximate evaluation of the component or for comparison purposes.

A voltage breakdown test was then conducted on the seven components. A 10,000 ohm resistor was placed in series with each capacitor, and voltage was increased in 10 percent increments up to the burnin voltage (130 percent of breakdown voltage). Each voltage was maintained for 1 minute, and an oscilloscope across the series resistor was used to observe the scintillation of the capacitor. Four of the seven units indicated some scintillation, while three showed none, but a healing was observed upon reduction of the voltage to below rated values. A rerun of the ESR versus frequency test was then conducted to determine whether the breakdown test had resulted in any changes in the dielectric or damage to the conductance paths. Results were nominal, indicating that no changes had taken place.

Leakage current measurements were then conducted on the seven capacitors at full rated voltage over the temperature range from -55° to +85°C. Results are plotted in Figure 7-8a for samples A and B, rated at 50 volts, and in Figure 7-8b for samples C through G, having the lower voltage ratings. The leakage current ordinates on Figures 7-8a and b differ by a factor of 1000.

Two major effects were noted, as summarized in Table 7-5: Two of the 47 microfarad capacitors exhibited high leakage. Sample D exceeded specifications by a factor of 2. The leakage current of sample C, while within specification by a factor of 10 was considerably higher than expected. Leakage currents for the two 100 microfarad capacitors, samples F and G, were also somewhat higher than expected. The second effect was the unexpectedly high slope of the leakage current versus temperature curves for the two 47 microfarad capacitors, samples C and D, which exhibited the high leakage current. One of the 50 volt capacitors, sample B, also appeared to have a high slope. The slopes of all other samples compared favorably with that of a typical tantalum capacitor.

In an attempt to explain apparent anomalies, further diagnostic tests were conducted on two capacitors, samples D and E. These two samples were from the 47 microfarad group which exhibited anomalous behavior; sample D had the excessive current and high slope, while sample E was normal in both respects. A more detailed discussion of the diagnostic tests and suspected effects of the lunar environment is given in Appendix H. The major difference between the parts noted was that the low leakage sample E also had been manufactured with a somewhat higher forming voltage: 140 volts versus 130 volts for sample D, as noted in Table 7-5. No evidence of scintillation of the surface of either anode was observed.

The conclusion that can be drawn from these tests is that the lunar environment had a definite effect on the dielectric of these capacitors. Low temperatures and temperature cycling degraded the dielectric by producing additional defect sites and crystalline regions in the amorphous tantalum pentoxide. This resulted in higher leakage, steeper increase of leakage with temperature, and lower breakdown voltage for some capacitors. Subsequent exposure to nominal voltages (on the moon or during the current test program) caused excessive scintillations; associated higher surge currents aggravated the affected regions of the dielectric, resulting in higher leakage currents. The total failure of one of the capacitors, analyzed separately in Section 12, and which exhibited a similar failure mechanism in a more pronounced fashion, further supports these conclusions.

It is suggested that manufacturing techniques of solid tantalum capacitors may have an impact on the extent to which these components are susceptible to the effects of the lunar environment. The fact that the capacitors which had a higher forming voltage employed in their manufacture were apparently less susceptible to degradation tends to support this although, admittedly, the number of samples available for drawing this conclusion was very limited here.

It is noteworthy that addition of a series-limiting resistor in circuit applications, whenever possible, would limit the surge currents during scintillation in dielectrics which might have been degraded by the lunar environment and would thus tend to minimize the enhancement and the effects of such degradations.

7.3.2 Metallized Paper-Mylar Capacitors

Thirteen metallized paper-mylar Sprague capacitors, ranging in value from 0.03 to 6 microfarads, were tested on the chassis for capacitance and dissipation factor. These capacitors are tubular units in metallic cases. Results indicated nominal dissipation factor and a decrease in capacitance ranging from -0.5 to -3.3 percent relative to prelaunch data.

Six of the capacitors were then removed for the functional tests indicated in Table 7-4. Externally, the components appeared undamaged. The end seals and soldered joints had no cracking or separation. Capacitance and dissipation factor measurements were repeated with the same results.

The insulation resistance was then measured at 10 percent of rated voltage at -55°, 25°, and 125°C with nominal results. ESR was measured on a 260A Q-meter at frequencies of 50, 100, 500, and 1000 kHz with nominal results. The capacitors were then subjected to a dielectric pulse voltage breakdown test similar to that described in Section 7.3.1 for the tantalum capacitors. Each step of this test consisted of the application of voltage for 1 minute and monitoring for dielectric breakdown with an

oscilloscope across a resistor inserted in series with capacitor. The test was started at 10 percent of rated voltage and increased in 10 percent increments until the burnin voltage level was reached, equal to 140 percent of the dc rating of the capacitor. Four of the six units exhibited dielectric breakdowns. The insulation test at 10 percent of rated voltage was then repeated. The results at 125°C were identical with those obtained earlier, while the 25°C insulation resistance showed general improvement.

The apparent decrease of capacitance and the evidence of the dielectric breakdowns observed above supported the decision to subject two of the six units to further diagnostic tests. As indicated in Table 7-6, one of these components had exhibited dielectric breakdowns, while the other did not. The units were disassembled by peeling off the cases. Internally, there was no evidence of damage or degradation. The sections were tightly wound with no indications of separation. The pigtails were still firmly attached. The sections were then unwound and the metallization examined. It was uniform with no irregularities, streaking, or splotching. There were no wrinkles in the dielectric that might be attributable to temperature cycling.

As indicated in Table 7-6, signs of eight dielectric failures were observed in the 6 microfarad units which had exhibited breakdowns in earlier testing, while no dielectric failures were observed in the other unit. The difference in construction, noted in Table 7-6, may readily account for this since a single layer dielectric was used for the lower voltage capacitor which had the traces of breakdowns.

It is concluded with reasonable assurance that the lunar environment did not significantly cause any degradation of the paper-mylar capacitors tested. Internal examination did not reveal any anomalies.

TABLE 7-6. DIAGNOSTIC TESTS OF METALLIZED PAPER-MYLAR CAPACITORS

Capacitor Rating	Construction	Results of Dielectric Strength Tests	Number of Dielectric Failures Found in Internal Inspection
6 microfarads, 200 volts	Single layer dielectric	Dielectric breakdown	8
1 microfarad, 400 volts	Dual layer dielectric	No breakdown	None

TABLE 7-7. RESULTS OF MEASUREMENTS OF CAPACITANCE OF GLASS AND MICA CAPACITORS

	Capac	itors		Capacitance, arads		
Type	Component Designation	Rating, picofarads	On-Chassis	Off-Chassis	Prelaunch Test Records, picofarads	
Mica	А	3300	3287	3287	3310	
	В	6800	6803	6803	Not available	
Glass	А	1000	1022	1023	1026.0	
	В	510	529	527	526.0	
	С	1000	953	951	954.7	
	D	1000	973		973.7	
	E	1000	954		955.3	
	F	510	526		524.4	

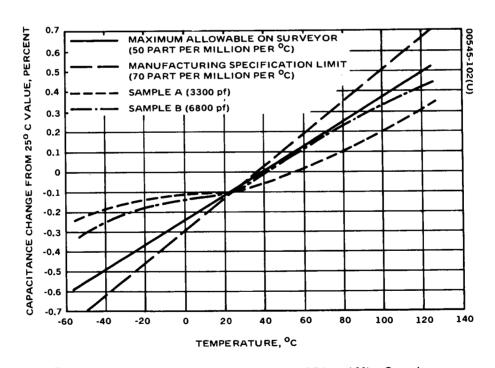


Figure 7-9. Capacitance Versus Temperature of Dipped Mica Capacitors

The dielectric breakdown tests indicated that some degradation takes place with time, as might be expected. The capacitors tend to develop clear areas, the size of which depend upon the applied voltage; it is reasonable to expect that, after prolonged exposure to a low voltage, additional breakdowns will occur upon the application of a higher voltage. The findings during dielectric strength measurements would probably be similar if the parts had been stored on earth for a like period of time.

The improvement in insulation resistance at room temperature after the breakdown tests, without a corresponding improvement at high temperatures, is probably merely indicative of a low magnitude surface leakage, which was improved by the dielectric clearing. This effect is proportionately less significant at higher temperatures.

The changes in capacitance, which is in the same direction for all components tested, cannot be readily attributed to the lunar environment in view of the fact that no separation of the windings was noted in the two open units. This change may be partly due to instrumentation differences. However, the magnitude of this change, which in some cases is as high as 3 percent, cannot be explained. While the specification is 5 percent, a change no greater than 1-1/2 to 2 percent would normally be expected on units which have been maintained on a shelf for this length of time.

7.3.3 Glass and Mica Capacitors

Two dipped-case mica capacitors and six glass dielectric capacitors were tested on the chassis for capacitance and dissipation factors although the latter parameter was only measured crudely because of access and instrumentation limitations. Subsequently, three of the six glass capacitors and both mica capacitors were removed for the off-chassis tests listed in Table 7-4.

The results of the capacitance tests, both on and off the chassis, are summarized in Table 7-7. All capacitors are rated at 5 percent. Results appeared to be reasonably nominal. The -0.7 percent change of mica capacitor A is not of particular significance. The differences between the original and latest measurements of the glass capacitors are undoubtedly due to the fact that these original tests were performed at 1 kHz, as stipulated in the receiving inspection, while the present measurements were made at 1 MHz.

The following measurements were then conducted:

- 1) Capacitance versus temperature for the mica capacitors, plotted in Figure 7-9
- 2) Capacitance and Q versus temperature for the glass capacitors (Figure 7-10)

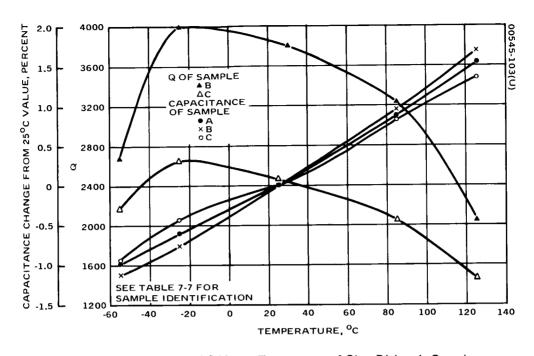


Figure 7-10. Capacitance and Q Versus Temperature of Glass Dielectric Capacitors

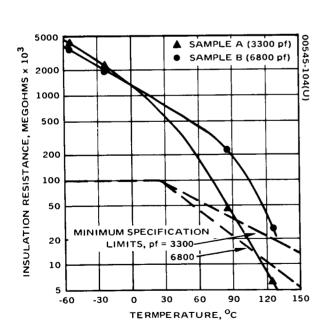


Figure 7-11. Insulation Resistance Versus Temperature of Dipped Mica Capacitors

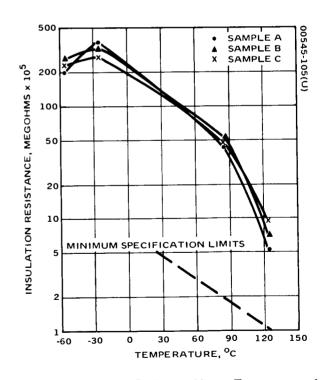


Figure 7-12. Insulation Resistance Versus Temperature of Glass Dielectric Capacitors

- 3) Insulation resistance at rated voltage versus temperature for mica capacitors (Figure 7-11)
- 4) Insulation resistance at rated voltage versus temperature for glass capacitors (Figure 7-12)

The dissipation factor of the mica capacitors was also measured and found nominal. ESR measurements were made for both the mica and the glass capacitors at 1, 5, 10, and 20 MHz, and no unusual conditions were noted. Results of these tests appear nominal, with the exception of the 3300 picofarad mica capacitor, which exhibited an excessively low insulation resistance at high temperatures; its dissipation factor at high temperatures was also outside specification limits.

Visual external examination of the mica capacitors disclosed no fracturing of the coating, which would be indicative of delamination or of fracturing of the mica sheets. Similarly, the glass capacitors appeared normal on visual examination.

The 3300 picofarad mica capacitor and two glass capacitors were then subjected to microsectioning and diagnostic examination. The mica capacitor showed no evidence of delamination, fracturing, voids, or other abnormalities that might have accounted for the observed low value of insulation resistance at high temperatures. The glass capacitors had voids within the dielectric, but these appeared not related in any way to lunar exposure. No dielectric fracturing of the glass was observed.

It is concluded that the lunar environment had virtually no effect on the glass and mica capacitors. The low value of the insulation resistance of the 3300 picofarad mica capacitor at high temperatures probably existed prior to launch since only room temperature measurements are performed during receiving inspection at Hughes and since only statistically selected samples are checked at high temperature by the manufacturer. Degradation of insulation resistance by the lunar environment, if any, would more likely occur on the higher capacitance mica component having a larger dielectric surface (sample B in Table 7-7). It is significant that this mica capacitor showed no degradation.

7.4 DIODE TESTS

A summary of tests of the 55 diodes, indicated in Table 7-1, is presented here. The seven types of diodes, quantities tested, and parameters measured are summarized in Table 7-8. Tests and analysis of two additional diodes which had failed are presented in Section 12.

TABLE 7-8. DIODE TEST PLAN SUMMARY

	Tests Prior to I	r to Removal From Chassis	Nondestructive	Nondestructive Tests of Removed Diodes	Number of Diodes
Type Description	Quantity Tested	Parameters Measured	Quantity Tested	Parameters Measured	Examined Internally
High speed switching diode, Fairchild; similar to 1N3070	25	IR, VF	E	I _R , V _F , C, B _V , t _r	-
High conductance switch, Raytheon; similar to 1N3730	13	IR, VF	2	IR, VF, C, Bv, trr, Vfr	
Voltage reference diode, 250 mw, Motorola; similar		$^{ m I}_{ m R},~^{ m V}_{ m Z}$	г	I _R , V _Z , Z _Z , V _Z versus T	
Voltage reference diode, 400 ms, Motorola; similar to 1N938B		^I R, ^V Z	-	I _R , V _Z , Z _Z , V _Z versus T	•
diodes Voltage regulator diode, 500 mw, Continental Devices and Pacific Semiconductor; similar to 1N754A	10	$^{ m I}_{ m R}$, $^{ m V}_{ m Z}$	2	¹ R, ^V Z ₁ , ^V Z ₂ , ^C	-
High voltage diode stack, selected Fairchild FA 3075 diodes	2	^I R, ^V F	2	IR, VF, C, Bv, tr	
Silicon controlled rectifier, Texas Instruments; similar	2	IR, VF, IF (off)	2	IR, VF, IGT, VGT, IH, IF(off), dV/dt	
IR VE C C C C C C C C C C C C C C C C C C	= reverse leakage current = forward voltage = zener impedance = junction capacitance = breakdown voltage = reverse recovery time (time to turn off)	$V_{\mathbf{fr}} = \mathbf{for}$ $T = \mathbf{ten}$ $Z_{\mathbf{Z}} = \mathbf{zer}$ $I_{\mathbf{F}}(\mathbf{off}) = \mathbf{for}$ $V_{\mathbf{H}} = \mathbf{min}$ $V_{\mathbf{H}} = \mathbf{min}$ $V_{\mathbf{H}} = \mathbf{min}$	= forward recovery voltage = temperature = zener impedance = forward leakage current with SCR off = minimum hold current (to keep SCR conducting)	$\begin{array}{c} I_{GT} \\ V_{GT} \\ \frac{dV}{dt} \end{array}$	= turnon (gate) current = turnon (gate) voltage = rate of change of forward voltage (measures ability of SCR not to turn on when its load voltage is varying)

Six types of diodes tested, that is, all except the SCR diodes, were contained in glass envelopes. As in the case of resistors, many cracks observed were believed to be associated with the thermal expansion mismatch between glass and the conformal coating. Except for the two failed diodes whose glass envelopes were also found cracked, in no instance were the diode parameters noticeably affected by the cracks in their envelopes. In all, 28 cracked envelopes were noted, including those of the two failed diodes. Some of these cracks were noted earlier in the inspection preceding circuit tests. Others were observed during the visual inspection of over 200 diodes prior to the initiation of tests of the selected 55 parts. Not all of the cracked envelope diodes were functionally tested as part of the program described below. Some were of the type not included in the test plan. Others could not be easily removed without destroying their properties. However, a substantial part of the 26 cracked envelopes is included in the 55 parts tested. For example, the original planned number of 20 high-speed 1N3070 switching diodes was intentionally increased to 25, as seen in Table 7-8, to include an additional 5 cracked envelope diodes.

Chassis tests were performed on all 55 parts, consisting primarily of forward voltage and reverse leakage current measurements to assess the basic integrity of these components. The quantities of diode switches (type 1N3730) and zener voltage regulators (1N754A) tested were lower than previously planned because of accessibility problems. A selected number of parts, as indicated in Table 7-8, were then removed from the chassis for detailed functional testing. Results of these tests were compared, whenever possible, with original inspection data. These original data were available, for the most part, just for the forward voltage and reverse leakage current values; only in selected instances were original data available for some of the other parameters. In all cases, a reasonably adequate assessment of lunar environment effects could be made by comparison with specification values. Any significant effects of the lunar environment would normally be expected to manifest a pronounced shift in the characteristics of these types of devices.

As indicated in Table 7-8, only 3 parts were opened for diagnostic testing, compared with the original plan, which contained some diagnostic tests of 12 parts. This reduction was made following the completion of the functional performance tests because it was found that virtually no significant changes in the characteristics of the parts tested were brought about by their exposure to the lunar environment.

Highlights of the data obtained are summarized in the following subsections. Details are recorded in the Program Log Books.

TABLE 7-9. FUNCTIONAL TESTS OF HIGH SPEED SWITCHING DIODES 1N3070

Par	ameter	Compa	rison Data		Test Results		
Sym-		•	Original Receiving	(Range o	Chassis** f Values)	Tests of	_
bol *	Unit	Spec Value	Inspection Data (Range of Values)	Parts Not Removed	Parts Later Removed	Removed Parts (Range of Values)	Test Conditions
v _F	Millivolts	1000 (max)	887 to 912	851 to 927	883 to 887	881 to 888	I _F = 100 ma
I _R	Nano- amperes	100 (max)	22 to 24	24 to 32	24 to 27***	21 to 25***	V _R = 175 volts
С	Pico- farads	5 (max)	Not measured	Not tested	Not tested	1.07 to 1.22	f = 1 MHz
B _V	Volts	200 (min)	Not measured	Not tested	Not tested	264 to 299	I _R = -100 micro- amperes
trr	Nano- seconds	50 (max)	Not measured	Not tested	Not tested	29 to 32	I _F = 30 ma R _L = 100 ohms I _R = -35 ma
				:			
							:

*See Table 7-8. for explanation of nomenclature.

**Total of 25 parts tested on chassis; 3 removed.

***Not including higher leakage diode, which was nominal after baking (see text).

7.4.1 High Speed Switching Diodes

The 25 components tested in this category were high speed, high conductance diodes, manufactured by Fairchild, similar to type 1N3070. These diodes were manufactured by a planar process and were packaged in a DO-7 glass envelope with conformal coating applied on the outside.

The tests conducted are summarized in Table 7-9, which also includes specification limits and data available from past records. The latter are available only for the specific components tested from receiving inspection measurements. Only forward voltage and reverse leakage current measurements were conducted at that time. The other parameters were only measured on statistical samples, so that the only basis available for component assessment are the specification values. Only ranges of values measured are given in Table 7-9; detailed values for each of the parts are available in program files. The column "Tests on Chassis" lists separetely the range of values recorded for components tested but not removed, and for components later removed for repetition of chassis tests (and additional functional tests). Thus, a direct comparison is available with the next column of the table, which gives results for the off-chassis functional tests. This format is repeated throughout this subsection and in Section 7.5, Transistor Tests.

As evident from Table 7-9, results of chassis tests for the 25 diodes tested were nominal, with the exception of 1 diode, as discussed below, which exhibited an excessive leakage current. The values recorded were well within specifications, and the forward voltage measurement showed a slight decrease from the original readings ranging from 1 to 3 percent.

The off-chassis tests of forward voltage and reverse leakage current were virtually identical with those obtained on the chassis. The other parameters tested, junction capacitance, breakdown voltage, and reverse recovery time, were all nominal and well within specifications.

As noted above, an exception to these measurements was recorded for a single diode. This diode was one of those found to have a cracked glass envelope. Its leakage current measured 90 nanoamperes on the chassis and 200 off the chassis. All other parameters were nominal. The diode was then baked for 24 hours at 125°C. Subsequently, the leakage current was remeasured and found to be 33 nanoamperes. It was concluded that this part had probably acquired some surface contamination through the crack, possibly after its return from the lunar surface; this contamination was removed by the baking process.

It should be noted that one other diode of this type not included in the above analysis had been found with a cracked glass envelope and to have failed (open). This failure is discussed in Section 12.

One of the parts was then subjected to diagnostic tests. The paint was removed and a microscopic examination conducted. These tests disclosed no anomalies.

TABLE 7-10. FUNCTIONAL TESTS OF SWITCHING DIODES 1N3730

Par	Parameter Comparison Data			Test Results			
Sym-		Spec	Original Receiving Inspection Data		Chassis** f Values) Parts Later	Tests of Removed Parts	Test
bol *	Unit	Value	(Range of Values)		Removed	(Range of Values)	Conditions
v _F	Milli- volts	650 to 900 (max) (depending on I _F)	730 to 740***	785 to 893***	824 to 893***	735 to 746***	IF = 100 ma or 750 ma
I _R	Nano- amperes	100 (max)	15 to 48	11 to 39	14 to 39	12 to 36	V _R = -60 volts
С	Pico- farads	12 (max)	7.2 to 7.3	Not tested	Not tested	6.95 to 7.0	V _R = -9 volts f = 1 MHz
ву	Volts	80 (min)	Not measured	Not tested	Not tested	112 to 125	IR = -100 micro- amperes
trr	Nano- seconds	75 (max)	Not measured	Not tested	Not tested	8 to 13	V _R = -5 volts R _L = 100 ohms I _F = 100 ma (recovery to 1 ma)
V _{fr}	Milli- volts	1200 (max)	Not measured	Not tested	Not tested	1000	I _F = 750 ma f = 1 MHz

^{*}See Table 7-8 for explanation of nomenclature.

**Total of 13 parts tested on chassis; 2 removed.

TABLE 7-11. FUNCTIONAL TESTS OF ZENER VOLTAGE REFERENCE DIODES

Test Conditions***
I _Z = 7.5 ma
V _R = -5 volts
$I_Z = 7.5 \text{ ma}$ $I_{ac} = 0.75 \text{ ma}$ (rms)
I _Z = 7.5 ma
V _R = -7.2 volts
I _Z = 7.5 ma I _{ac} = 0.75 ma (rms)

^{*}See Table 7-8 for explanation of nomenclature.

*** T = 25°C throughout

^{***} At $I_F = 750$ ma. *** At $I_F = 100$ ma.

^{**}Total of 2 parts tested on chassis; 2 removed (one of each type)

7.4.2 High Conductance Switching Diodes

The 14 components tested in this category were high conductance switching diodes, manufactured by Raytheon, similar to type 1N3730. These diodes employed a diffused junction and were packaged in a DO-7 glass envelope, with conformal coating applied on the outside.

The tests are summarized in Table 7-10. Original inspection data were available on the forward voltage and reverse leaking currents, as well as on the function capacitance. On-chassis tests are presented for only 13 of the 14 parts tested. One of the diodes was found to have an exceedingly high reverse leakage current of 6.6 microamperes; this part was subjected to a failure analysis, and results are discussed in Section 12.

As seen from Table 7-10, results of on-chassis tests were nominal. Two of the diodes which measured the lowest and highest leakage current were then removed for off-chassis tests. Results of the repetition of the chassis measurements, and of the measurements of the junction capacitance, breakdown voltage, reverse recovery time, and forward recovery voltage, were nominal. The small differences in values can be accounted for by differences in measurement techniques, test equipment, and ambient temperatures.

7.4.3 Zener Voltage Reference Diodes

The two types of Zener voltage reference diodes tested were a 250 mw 1N827 diode and a 400 mw 1N938B diode. Both diodes were manufactured by Motorola and packaged in a DO-7 glass envelope. The former uses an alloy process, while the latter has a diffused junction. Only one of each type was in the TV camera.

A summary of results of the on-chassis and off-chassis tests conducted on these two parts is presented in Table 7-11. All of these tests were conducted at the nominal ambient temperature of 25°C. Original inspection data were not available for the zener voltage of the 250 mw diode. Leakage current requirements are not included in the specification, and these measurements were not performed originally. In addition to zener voltage and leakage current measurements on and off-chassis, the zener impedance was measured after removal of the components. Results indicate excellent correlation with past data, wherever available, and with specifications. Leakage current was 26 and 2.5 microamperes for the 250 and 400 mw diodes, respectively, well within specifications.

Voltage versus temperature measurements were then conducted. Results are plotted in Figure 7-13. Both diodes indicated excellent compliance with specifications of 48 and 18 mv, respectively, over the test temperature range of from -60° to 100°C.

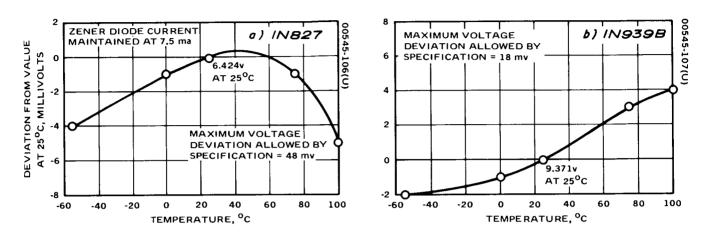


Figure 7-13. Voltage Versus Temperature of Zener Diodes

TABLE 7-12. FUNCTIONAL TESTS OF ZENER VOLTAGE DIODES 1N754A

Par	Parameter Compariso		arison Data		j		
Sym-			Original Receiving	(Range	Chassis** of Values)		_
bol *	Unit	Spec Value	Inspection Data (Range of Values)	Parts Not Removed	Parts Later Removed	Tests of Removed Parts	Test Conditions***
v _z	Volts	6.3 to 7.7	7.39 to 7.65	7.44 to 7.61	7.44 and 7.57	7.42 and 7.55	I _Z = 10 ma
v _z	Volts	6.2 (min)	7.29 and 7.42	Not tested	Not tested	7.29 and 7.42	IZ = 200 micro- amperes
ı _R	Nano- amperes	10 (max)	2.6 to 9.5	3. 2 to 6. 8	3. 2 and 6. 8	2.9 and 6.6	V _R = 4.2 volts
С	Pico- farads	300 (max)	Not measured	Not tested	Not tested	28.6 and 23.7	V _R = -4 volts f = 1 MHz
]						

*See Table 7-8 for explanation of nomenclature.

**Total of 10 parts tested on chassis; 2 removed.

*** T = 25°C throughout.

7.4.4 Zener Voltage Regulator Diodes

The ten diodes tested in this group were 500 mw voltage regulator zener diodes, similar to type 1N754A, manufactured by Continental Devices and Pacific Semiconductors. They employed a diffused junction and were packaged in a DO-7 glass envelope with conformal coating applied on the outside. A summary of the tests conducted is presented in Table 7-12. Tests of the ten diodes on the chassis were followed by a repetition of chassis tests and additional functional checks of two of these diodes subsequently removed from the chassis. Reverse leakage current and zener voltage at a current of 10 ma were measured on the chassis; the zener voltage was measured off the chassis both at 10 ma and 200 microamperes. The junction capacitance was also measured on the two removed parts. Past data were available for the leakage current and the zener voltages.

Excellent correlation with past data and with specifications was observed. The high correlation of the reference regulator current and zener voltage at 10 ma with original data is not directly evident in Table 7-12, which only summarizes the range of original data for all ten parts. For the two parts removed, the comparison was as follows:

•	Leakage	current
---	---------	---------

2.9 versus 2.6 nanoamperes originally and 6.6 versus 5.5 nanoamperes orginally

• Zener voltage at 10 ma

7.42 versus 7.39 volts originally and 7.55 versus 7.53 volts originally

The maximum difference of 0.03 volt is well within the normal accuracies of instrumentation and test conditions.

Zener voltage versus temperature characteristics were not measured for this diode because it is not of the temperature-compensating type, as were the two voltage reference diodes (Section 7.4.3). However, one of the two diodes removed was examined diagnostically. The paint was removed and a microscopic examination conducted. Some evidence was observed of gold splatter. This obviously occurred during the manufacturing process and is not attributable to effects of the lunar environment. Evidently, this had no effect on the functional characteristics of the part.

7.4.5 High Voltage Diode Stack

The two high voltage diode stacks present in the camera were each composed of six selected Fairchild FA 3075 diodes with diffused junctions, individually packed in DO-7 glass envelopes. The entire assembly of each diode stack was encapsulated.

TABLE 7-13. FUNCTIONAL TESTS OF HIGH VOLTAGE DIODE STACK FA 3075

Par	ameter	Compa	rison Data		Test Results		
Sym-			Original	Tests Or	n Chassis**		
bol *	Unit	Spec Value	Receiving Inspection Data	Parts Not Removed	Parts Later Removed	Tests of Removed Parts	Test Conditions
v _F	Volts	6 (max)	5.42 and 5.38	NA	5.21 and 5.16	5.20 and 5.17	I _F = 100 ma
I _R	Nano- amperes	1000 (max)	21 and 21	NA	22 and 19	15 and 13	V _R = -825 volts
С	Pico- farads	5 (max)	Not measured	NA	Not tested	0.81 and 0.83	V _R = 0 f = 1 MHz
В _V	Volts	1200 (min)	Not measured	NA	Not tested	1760 and 1780	I _R = -100 micro- amperes
trr	Nano- seconds	50 (max)	Not measured	NA	Not tested	45 and 45	I _R = -26 ma, R = 100 ohms i _f = 30 ma (recovery to 1 ma)

*See Table 7-8 for explanation of nomenclature.

TABLE 7-14. FUNCTIONAL TESTS OF SILICON CONTROLLED RECTIFIERS 2N1930

ameter	Comparison Data					
		Original	Tests O	n Chassis**		
Unit	Spec Value	Receiving Inspection Data	Parts Not Removed	Parts Later Removed	Tests of Removed Parts	Test Conditions
Milli- volts	1250 (max)	Not available	NA	856 and 863	990 and 360	I _F = 1 ampere
Nano- amperes	1000 (max)	Not available	NA	12 and 11	12 and 10	V _R = -50 volts
Nano- amperes	1000 (max)	Not measured	NA	18 and 13	17 and 11	V _{F(off)} = 50 volts
Milli- amperes	1 to 15	Not measured	NA	Not tested	5.0 and 5.1	V _{F(off)} = 50 volts R _L = 2000 ohns
Volts	0.35 to 2.0	Not measured	NA	Not tested	0.84 and 0.67	V _{F(off)} = 50 volts R _L = 2000 ohm
Milli- amperes	1 to 20	Not measured	NA	Not tested	11.1 and 12.5	Per Hughes specification
Volts per micro- second	200 (min)	Not measured	NA	Not tested	Greater than 10,000	Per Hughes specification
	Milli- volts Nano- amperes Nano- amperes Milli- amperes Volts Volts Volts ramperes Volts ramperes	Unit Spec Value Millivolts 1250 (max) Nano-amperes 1000 (max) Amperes 1000 (max) Milliamperes 1 to 15 Wolts 0.35 to 2.0 Milliamperes 1 to 20 Williamperes 200 (min) Per 1000	Unit Spec Value Receiving Inspection Data Millivolts Nano- amperes 1000 (max) Not available Nano- amperes 1000 (max) Not measured Milliamperes 1 to 15 Not measured Milliamperes 1 to 20 Not measured Milliamperes 200 (min) Not measured	Unit Spec Value Receiving Receiving Inspection Data Removed Millivolts Nano-amperes Nano-amperes 1000 (max) Not available NA Milliamperes 1 to 15 Not measured NA Milliamperes 1 to 20 Not measured NA Milliamperes 1 to 20 Not measured NA Milliamperes 200 (min) Not measured NA	Unit Spec Value Original Inspection Data Millivolts Nano-amperes Nano-amperes Milliamperes Volts O. 35 to 2.0 Not measured NA Not tested Milliamperes Volts O. 35 to 2.0 Not measured NA Not tested Milliamperes Volts O. 35 to 2.0 Not measured NA Not tested Milliamperes Volts O. 35 to 2.0 Not measured NA Not tested Milliamperes Volts O. 35 to 2.0 Not measured NA Not tested	Unit Spec Value Receiving Receiving Inspection Data Parts Not Removed Removed Parts Not Removed Parts Not Removed Parts Not Removed Parts Millivolts Nano- amperes Nano- aniperes 1000 (max) Not measured NA 18 and 13 17 and 11 12 and 10 15 Not measured NA Not tested S.0 and 5.1 Williamperes 1 to 15 Not measured NA Not tested 0.84 and 0.67 Milliamperes 1 to 20 Not measured NA Not tested 11.1 and 12.5 Wolts 200 (min) Not measured NA Not tested Greater than 10,000

*See Table 7-8 for explanation of nomenclature.

^{**}Total of 2 parts tested on chassis; 2 removed.

^{**}Total of & parts tested on chassis; 2 removed.

Both diode stacks were tested prior to and after their removal from the electronic conversion unit. Results are summarized in Table 7-13. Original receiving inspection data were available for the forward voltage and reverse leakage current, which were measured on and off the chassis. The other parameters: junction capacitance, breakdown voltage, and reverse recovery time, measured off-chassis, had not been previously measured during the original inspection. Results indicated excellent correlation with past data and compliance with specifications. The differences were minor and easily attributed to expected variations of instrumentation and test conditions.

Inspection of the two parts revealed no evidence of fracturing of the encapsulate nor any other effects of exposure to the lunar environment.

7.4.6 Silicon-Controlled Rectifier

Two of the four silicon-controlled rectifiers in the camera were tested, both on the chassis and after their removal. These parts were manufactured by Texas Instruments and are similar to type 2N1930. Results are summarized in Table 7-14. Past data on the forward voltage and leakage current could not be found in Surveyor files. Consequently, only a comparison with specification values could be made.

The forward voltage, reference leakage current, and forward leakage current under cutoff conditions were measured on the chassis. Upon removal from the chassis, the above parameters were measured and the following additional parameters checked under nominal test conditions (indicated in Table 7-14): turnon (gate) voltage, turnon (gate) current, minimum hold current, and rate of change of forward voltage under cutoff conditions. As seen from Table 7-14, results were nominal in all respects, indicating that no major effects were caused by the lunar environment. The apparent difference in forward voltage readings on and off the chassis is attributable to the test technique. Access was difficult during the initial tests on the chassis; and, undoubtedly, these measurements were subject to unavoidable inaccuracies, as were those associated with lead and contact resistances.

One of the units was subsequently opened, and internal examination was conducted. No anomalies were noted.

7.5 TRANSISTOR TESTS

A summary of tests of the 47 transistors, indicated in Table 7-1, is presented here. The six types of transistors, quantities tested, and parameters measured are summarized in Table 7-15. All are silicon transistors.

TABLE 7-15. TRANSISTOR TEST PLAN SUMMARY

			Prior to Removal om Chassis	Nondest	ructive Tests of Removed Transistors	Number of Transistors
Type Desc	cription	Quantity Tested	Parameters Measured	Quantity Tested	Parameters Measured	Examined Internally*
General-purpose	NPN; 2N718A	15	V _{CE(sat)} , V _{BE(sat)} , h _{FE}	2.	VCE(sat), VBE(sat), hFE, ICBO, IEBO, Cob, VCER(sus)	0
amplifiers	PNP; 2N722	11	V _{CE(sat)} , V _{BE(sat} , h _{FE}	3	VCE(sat), VBE(sat), hFE, ICBO, IEBO, Cob, VCEO(sus), (td + tr), (ts + tf)	1
High frequency tra NPN; 2N2192A	ansistor,	1	V _{CE(sat)} , V _{BE(sat)} , h _{FE}	1	VCE(sat), VBE(sat), hFE, ICBO, IEBO, Cob, VCEO(sus), tr, ts, BVCEO	0
High voltage ampl NPN; 2N871	ifier,	16	V _{CE(sat)} , V _{BE(sat)} , h _{FE}	3	V _{CE(sat)} , V _{BE(sat)} , h _{FE} , I _{CBO} , I _{EBO} , C _{ob} , V _{CEO(sus)}	1
Power transistor, NPN; 2N1936		1	V _{CE(sat)} , v _{BE(sat)} , h _{FE}	1	V _{CE(sat)} , V _{BE(sat)} , h _{FE} , I _{EBO} , BV _{CEO} , I _{CEV}	0
Low noise amplifi NPN; 2N2586	er,	3	V _{CE(sat)} , (DC and pulse), h _{FE}	3	V _{CE(sat)} , h _{FE} , I _{EBO} , I _{CEO} , C _{ob} , BV _{CEO} , N _f	1

Lege	~4	
Leve	пu	٠

h _{FE}	= dc gain	V _{CEO(sus)}	<pre>= collector to emitter sustaining voltage (base open)</pre>
V _{CE(sat)}	<pre>= collector-emitter saturation voltage</pre>	^t r	= rise time
V _{BE(sat)}	<pre> base-emitter saturation voltage</pre>	^t s	= storage time
I _{CBO}	= collector-base current	^t d	= delay time
CBO	(emitter open)	t _f	= fall time
I _{EBO}	= emitter-base current (collector open)	BV _{CEO}	= collector emitter breakdown voltage (base open)
ICEO	= collector-emitter current		= collector emitter current (base
	(base open)	^I CEV	voltage applied)
Cob	= collector to base output capacitance	$N_{\mathfrak{s}}$	= noise figure
V _{CER(sus}) = collector to emitter sustaining voltage (with base resistor)	Ī	•

^{*}See Section 7.5.6 for additional SEM data.

Analysis of another NPN silicon power transistor, similar to Fairchild 2N3891, for which a specified anomaly was suspected, is presented in Section 12. Another transistor, Sprague 2N859, which was found to have failed (open) but was not analyzed because of its obsolete alloy-type design, is also discussed in Section 12. The original test plan included PNP 2N2907A high frequency silicon transistors, but these were deleted when it was discovered that they were not incorporated in the TV camera. These transistors were used in later Surveyor cameras, replacing similar alloy-type transistors. This error in the Surveyor III camera records was found when the alloy construction was uncovered in X-ray tests.

Initial visual survey was conducted on the chassis of about 100 transistors of various types, including samples of the six types discussed below. Tests were then conducted on the chassis on the 47 transistors. These tests consisted primarily of measurements of the forward gain and of the collector and base saturation voltages in order to assess the basic integrity of the components. The quantities of transistors tested were, in most cases, lower than had been originally planned (as summarized in Table 7-16) because of accessibility problems. Selected samples were then removed from the chassis for the measurement of the various functional parameters, including repetition of the tests conducted on the chassis.

Tests on the chassis were difficult to perform accurately because of accessibility problems. Subsequent results conducted off the chassis should be considered as somewhat more reliable. Results of the functional tests were compared with specifications and with original inspection data, whenever possible. These original data were generally available for saturation voltages and forward gains. As noted in the succeeding tables, other parameters were also available for comparison in some cases. It should be recognized that the original receiving inspection tests were not designed to be precise but only to assess the basic compliance with specifications. Furthermore, significant differences existed between test equipment, test conditions, and operational techniques used here and at the receiving inspection. Some differences in the results could be expected to be attributable to these factors.

Significant effects of lunar exposure would be expected to manifest themselves by pronounced shifts in the measured transistor characteristics. Thus, unless marked deviations were noted, it could be reasonably concluded, as seen from the discussion below, that no major effects of exposure to the lunar environment occurred. For this reason, diagnostic tests were conducted on only three transistors, following completion of the functional tests. In addition, certain supplementary tests were concluded to dispel doubts regarding some of the largest deviations noted; and SEM photographs were taken of five representative transistors and of an SCR diode.

Highlights of the data obtained are summarized in the following sections. Details are recorded in the program log books.

TABLE 7-16. NUMBER OF TRANSISTORS TESTED ON CHASSIS VERSUS TOTAL ON CAMERA

Transist	ors	Total Quantity	Quantity Originally Planned	Quantity
Type	Description	in Camera	for Testing	Tested
General-purpose amplifier	2N718A	20	20	15
General-purpose amplifier	2N722	31	20	11
High frequency amplifier	2N2192A	5	5	1
High voltage amplifier	2N 87 1	36	20	16
Power transistor	ZN1936	1	1	1
Low noise amplifier	2N 2586	5	5	3

7.5.1 General-Purpose Amplifiers

The 26 transistors tested in this category were of two types:
1) NPN silicon transistors, manufactured by Fairchild and Pacific
Semiconductors, similar to type 2N718A, and 2) PNP silicon transistors,
manufactured by Fairchild and Hughes, similar to type 2N722. Both types
were constructed with a diffused junction using the planar process and
were packaged in TO-18 cans.

Tables 7-17 and 7-18 summarize tests of NPN and PNP transistors, respectively. For ease of reference, these tables are presented in the format used for diodes in the preceding section.

On-chassis tests of the 15 NPN transistors consisted of measurements of the forward gain and saturation voltages. Results were well within specifications and appeared nominal considering the above mentioned uncertainty of test conditions at the receiving inspections.

The two transistors selected to represent the highest and lowest readings of saturation voltages were then removed from the chassis for functional tests. In addition to repeating the chassis measurements, forward

gain was measured at two other operating points, as well as the four other parameters listed in Table 7-17. Results compared favorably with specifications, as well as with the original data available for one of the forward gain measurements. The collector base leakage current, however, measured much lower than at the receiving inspection: 0.2 versus about 5 nanoamperes originally (the specification is 10 nanoamperes). Uncertainty of original inspection techniques and test conditions could readily explain this difference.

In view of the differences noted in the saturation voltages and leakage currents relative to the available past data, a special test was conducted on the two transistors to determine whether subsurface contamination and resulting channelling had occurred.* The test consisted of subjecting the transistors to an 88 hour heating cycle at 150°C with a reverse bias applied and subsequent cooling with the bias voltage. No evidence of subsurface contamination or channelling was uncovered since remeasuring of the parameters showed essentially no change.

It should be noted that these apparent differences in saturation voltages and leakage current were observed in several of the other types of transistors tested, as discussed below. This test for subsurface contamination was conducted on a total of nine transistors, including samples from all six types tested.

On-chassis tests of the 11 PNP transistors, summarized in Table 7-18, consisted of measurements of forward gain and saturation voltages. Saturation voltage measurements compared favorably with the original data; original data for the forward gain were not available, but the values were well within specification.

Three of the transistors were then removed from the chassis. Repetition of chassis measurements disclosed no significant deviations. Additional functional tests consisted of measurements of leakage currents, collector to base capacitance, collector to emitter sustaining voltage (with the base open), and the two response times (delay time plus rise time and storage time plus fall time). Results were well within specifications although one capacitance was lower than the other two: 19 picofarads versus 31 and 34 picofarads (specification is 45 picofarads maximum). This is attributable to differences in the production lots. Original data were available only for the leakage currents. Measured values for the emitter-base current were in the range of 10 to 16 picoamperes, compared to the range of 1 to 700 nanoamperes recorded at receiving inspection (specification is

^{*}Note that this type of contamination would result in the increase of both V_{sat} and ICOB. Relative to receiving inspection data, V_{sat} was higher, and ICOB was lower. Thus, the original data was suspect, rather than appearance of subsurface contamination. The special test was conducted anyway to ascertain that no subsurface changes took place.

TABLE 7-17. FUNCTIONAL TESTS OF GENERAL-PURPOSE AMPLIFIER TRANSISTORS NPN 2N718A

Par	ameter	Comp	arison Data		Test Results		
Sym-		Original Receiving		(Range	Chassis** of Values)	Tests of	
bol *	Unit	Spec Value	Inspection Data (Range of Values)	Parts Not Removed	Parts Later Removed	Removed Parts (Range of Values)	Test Conditions
V _{CE}	Volts	1.5 (max)	0.78 to 1.01	0.41 to 1.25	1.25 and 0.59	1.05 and 0.61	I _B = 15 ma I _C = 150 ma
V BE (sat)	Volts	1.3 (max)	0.49 and 0.51	0.89 to 0.93	0.91 and 0.90	0.90 and 0.89	I _B = 15 ma I _C = 150 ma
h _{FE}	-	40 to 120	Not measured	43 to 90	65 and 71	71 and 75	VCE = 10 volts I _C = 150 ma
h _{FE}	-	20 (min)	Not measured	Not tested	Not tested	50 and 49	V _{CE} = 10 volts I _C = 500 ma
h _{FE}	-	20 (min)	44 and 38	Not tested	Not tested	43 and 37	V _{CE} = 10 volts I _C = 0.1 ma
I _{СВО}	Nano- amperes	10 (max)	4.5 and 4.8	Not tested	Not tested	0.24 and 0.21	V _{CB} = 60 volts I _E = 0
I _{EBO}	Nano- amperes	10 (max)	Not measured	Not tested	Not tested	0.022 and 0.039	V _{EB} = 5 volts I _C = 0
V _{CER}	Volts	50 (min)	Not measured	Not tested	Not tested	104 and 128	I _C = 0.1 ma RBE = 10 ohms I _B = 0
Cob	Pico- farads	25 (max)	Not measured	Not tested	Not tested	20.3 and 14.9	V _{CB} = 10 volts f = 1 MHz

*See Table 7-15 for explanation of nomenclature.

**Total of 15 parts tested on chassis; 2 removed.

TABLE 7-18. FUNCTIONAL TESTS OF GENERAL-PURPOSE AMPLIFIER TRANSISTORS PNP 2N722

		Test Results	ison Data	Comparison Data		Parameter	
Test	Tests of Removed Parts	Tests on Chassis** (Range of Values)		Original Receiving			Sym-
Conditions	(Range of Values)	Parts Later Removed	Parts Not Removed	Inspection Data (Range of Values)	Spec Value	bol S	bol *
I _B = 15 ma I _C = 150 ma	0.57 to 0.85	0.61 to 0.91	0.55 to 0.94	0.76 to 1.12	1.5 (max)	Volts	V _{CE}
I _B = 15 ma I _C = 150 ma	0.87 to 1.06	0.97 to 1.09	0.92 to 1.22	0.99 to 1.20	1.3 (max)	Volts	(sat) V _{BE}
V _{CE} = 10 volt I _C = 150 ma	44 to 52	43 to 50	42 to 54	Not available	30 to 90	-	(sat) FE
V _{CB} = -30 vol	0.7 to 34	Not tested	Not tested	1.2 to 40	1000 (max)	Nano- amperes	сво
V _{EB} = -2 volt I _C = 0	0.01 to 0.6	Not tested	Not tested	0.7 to 680	100,000 (max)	Nano- amperes	EBO
I _C = -100 ma I _B = 0	50 to 57	Not tested	Not tested	Not measured	35 (min)	Volts	V _{CEO}
V _{CB} = 10 volt f = 1 MHz	19 to 34	Not tested	Not tested	Not measured	45 (max)	Pico- farads	(sus) C _{ob}
pw = 10 micro seconds IC = 150 ma	70 to 90	Not tested	Not tested	Not measured	250 (max)	Nano- seconds	td +tr
I _B = 15 ma V _{BE} = 0.5 vo	220 to 260	Not tested	Not tested	Not measured	450 (max)	Nano- seconds	ts + tf

*See Table 7-15 for explanation of nomenclature.

**Total of 11 parts tested on chassis; 3 removed.

100 microamperes maximum). This difference is again attributable to the above mentioned difference in test conditions and techniques.

Two of these transistors were also subjected to the reverse bias heating and cooling test for evidence of possible subsurface contamination and channelling, mentioned above, particularly because of this difference in leakage current measurements. No changes in readings were noted after this test, and no evidence of channelling was uncovered.

One of the PNP transistors was subsequently subjected to diagnostic tests. The transistor was opened and examined microscopically. Internal examination disclosed no anomalies. An SEM photograph was then taken, as discussed in Section 7.5.6.

The general-purpose amplifier transistor appeared to have been unaffected by the lunar environment, and the few differences noted from original receiving inspection data were concluded to be attributable to differences in test conditions, instrumentation, and operational techniques.

7.5.2 High Frequency Transistor

The one high frequency silicon transistor tested was the Fairchild NPN transistor, similar to 2N2192A, produced epitaxially and packaged in a TO-5 can. It was intended originally to test all five of these transistors present in the camera, but only one was accessible and removable without damage.

The tests performed are summarized in Table 7-19. Saturation voltages and forward gain were measured on the chassis. After removal of the transistor, the following parameters were also measured: leakage current, output capacitance, breakdown voltage, collector sustaining voltage, and response times. The transistor appeared to be in an excellent condition. Results were within specification and correlated well with original inspection data, where available.

It was decided not to perform diagnostic tests on this transistor. However, it was included in the group tested for surface contamination and channelling (discussed in Section 7.5.1) and in the group of which SEM photographs were taken (discussed in Section 7.5.6).

7.5.3 High Voltage Transistors

The 16 high voltage amplifier transistors tested in this group were Fairchild silicon transistors, similar to 2N871. They were manufactured by the planar process and packaged in TO-18 cans.

TABLE 7-19. FUNCTIONAL TESTS OF HIGH FREQUENCY TRANSISTOR 2N2192A

Par	ameter	Compa	rison Data		Test Results]
			Original	Tests O	n Chassis**		
Sym- bol *	Unit	Spec Value	Receiving Inspection Data	Parts Not Removed	Parts Later Removed	Tests of Removed Parts	Test Conditions
V _{CE}	Volts	0.25 (max)	0.093	NA	0.09	0.08	I _B = 15 ma I _C = 150 ma
v _{BE}	Volts	1.3 (max)	0.82	NA	0.84	0.82	I _B = 15 ma I _C = 150 ma
h _{FE}	-	100 to 300	Not available	NA	160	161	V _{CE} = 10 volts I _C = 150 ma
СВО	Nano- amperes	10 (max)	0.1	NA	Not tested	0.057	V _{CB} = 3 volts I _E = 0
I _{EBO}	Nano- amperes	50 (max)	Not measured	NA	Not tested	0.011	V _{EB} = 3 volts I _C = 0
V _{CEO}	Volts	40 (min)	Not measured	NA	Not tested	45	I _C = 25 ma I _B = 0
BV CEO	Volts	60 (min)	116	NA	Not tested	110	I _C = 100 micro- amperes
Cob	Pico- farads	20 (max)	Not measured	NA	Not tested	7.1	V _{CB} = 10 volts f = 1 MHz
t _r	Nano- seconds	140 (max)	Not measured	NA	Not tested	10	pw = 10 micro- seconds
t _s	Nano- seconds	300 (max)	Not measured	NA	Not tested	20 }	$V_B = -13.5 \text{ volts}$
t _f	Nano- seconds	100 (max)	Not measured	NA	Not tested	20 J	V _{IN} = 15 volts
1			1				

*See Table 7-15 for explanation of nomenclature.

**Total of l parts tested on chassis; l removed.

TABLE 7-20. FUNCTIONAL TESTS OF HIGH VOLTAGE TRANSISTORS 2N871

Par	ameter	Comp	arison Data		Test Results		
Sym- bol *	Unit	Spec Value	Original Receiving Inspection Data (Range of Values)		Chassis** of Values) Parts Later Removed	Tests of Removed Parts (Range of Values)	Test Conditions
V _{CE}	Volts	5 (max)	0.14 to 1.60	0.64 to 1.56	1.29 to 2.4	1.01 to 1.98	IB = 15 ma IC = 150 ma
v _{BE}	Volts	1.3 (max)	0.70 to 0.89	0.90 to 0.92	0.90 to 0.90	0.89 to 0.90	I _B = 15 ma I _C = 150 ma
(sat) h _{FE}	_	100 to 300	118 to 216	114 to 163	114 to 143	113 to 142	V _{CE} = 10 volts I _C = 150 ma
I _{CBO}	Nano- amperes	10 (max)	0.40 to 4.8	Not tested	Not tested	0.16 to 0.39	$V_{CB} = 75 \text{ volts}$ $I_{E} = 0$
I _{EBO}	Nano- amperes	10 (max)	Not measured	Not tested	Not tested	0.017 to 0.033	V _{EB} = 5 volts I _C = 0
V _{CEO}	Volts	60 (min)	Not measured	Not tested	Not tested	86 to 108	$I_C = 30 \text{ ma}$ $I_B = 0$
Cob	Pico- farads	15 (max)	Not measured	Not tested	Not tested	10.6 to 11.8	V _{CB} = 10 volts f = 1 MHz
ĺ						:	
	l						

*See Table 7-15 for explanation of nomenclature.

**Total of 16 parts tested on chassis; 3 removed.

A summary of the tests conducted is presented in Table 7-20. Measurements of saturation voltages and forward gain, conducted on the chassis, were within specification and compared reasonably well with the original inspection data except that VCE(sat) values were higher.

Three transistors selected for removal and off-chassis tests include the one with the highest measured value of 2.4 volts for the collector-emitter saturation voltage. Repetition of on-chassis measurements resulted in somewhat lower values for VCE(sat), while the other parameters were unchanged. The values of VCE(sat) recorded off the chassis, on the chassis, and at the original inspection are presented for these transistors in Table 7-21. Results illustrate the difficulty in performing the measurements on the chassis. Errors are introduced because of difficulties in making connections and because of the long leads that must be used occasionally for access. While the values obtained off-chassis are all within specification, they are still higher than the values obtained at the receiving inspection.

Off-chassis measurements were then conducted of the other transistor parameters: leakage currents, collector-emitter sustaining voltage, and collector-base output capacitance.

Results were all within specification, and grouped well. The only original data available for comparison were for collector-base leakage current. Again, results indicated a reduction in leakage current for components whose saturation voltage had apparently increased.

As in the case of the general-purpose NPN amplifiers, discussed in Section 7.5.1, two of these transistors were subjected to the special test for subsurface contamination in order to ascertain that the apparent increase in the saturation voltage was not the result of channelling. Upon completion of this temperature cycling under bias conditions, the saturation voltage changed by less than 3 percent. The leakage currents increased slightly, but were still lower than the values recorded at the original receiving inspection.

To further ascertain that the lunar environment did not significantly affect these transistors, a diagnostic test was conducted of the transistor with the highest saturation voltage. The transistor was opened and examined internally. Some bubbles were observed in the oxide, but they were determined not to be significant. No other changes were found that could not be expected from a normal shelf storage for a comparable length of time. An SEM photograph was also taken of this transistor, as discussed in Section 7.5.6.

It was concluded that the exposure to lunar environment produced no significant effects on the high voltage transistor. Discrepancy in some of the data relative to that recorded at the receiving inspection reflects primarily the differences in test conditions and techniques. There was no

TABLE 7-21. COMPARISON OF VCE(sat) MEASUREMENTS OF HIGH VOLTAGE TRANSISTOR

Sample Designation	On-Chassis Measurement, volts	Off-Chassis Measurement, volts	Original Receiving Inspection Data, volts	Specification, volts
751	1.29	1.04	0.97	5.0
741	2.4	1.98	0.19	5.0
743	1.55	1.01	0.17	5.0

evidence of subsurface contamination. Variation in leakage current, which is well within specification requirements, is not considered significant because of the sensitivity of this parameter.

7.5.4 Power Transistor

The one power transistor of the camera was a Texas Instruments stud-mounted NPN Mesa transistor, rated at 100 watts, similar to 2N1936, and packaged in a TO-63 case.

The summary of tests conducted is presented in Table 7-22. Results were nominal for the on-chassis measurements of gain and saturation voltages. The collector-emitter saturation voltage compared favorably with the original data available.

The transistor was removed, and the above measurements were repeated. Forward gain was also measured at another operating point corresponding to that for which original inspection data were available. Correlation was found to be good. The other parameters measured — leakage current, and the collector-emitter current and breakdown voltage — were all well within specifications, with no past data available for comparison.

No apparent effects of the lunar environment were noted. It was decided not to conduct a destructive diagnostic test on this transistor, the only one available of its type. However, this transistor was included in the group of which SEM photographs were taken, as discussed in Section 7.5.6.

7.5.5 Low Noise Transistors

Three low noise transistors tested in this group were all Texas Instruments NPN silicon transistors, similar to 2N2586, produced by a planar process and packaged in TO-18 cans. All of the five transistors

on the camera had been originally slated for tests, but only three were accessible. These three were all tested on the chassis and then removed for the more detailed functional measurements.

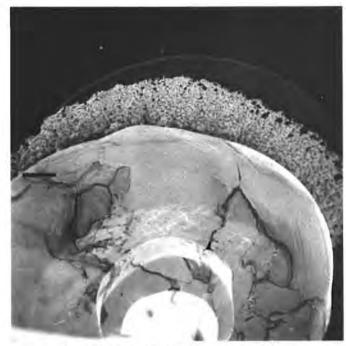
Results of tests are summarized in Table 7-23. On-chassis tests entailed measurement of the collector-emitter saturation voltage under both dc and pulse conditions, and the measurement of the forward gain. Saturation voltage was remeasured after removal from the chassis, and the dc gain was measured at a different operating point to obtain a direct comparison with the available receiving inspection data. In addition, the other parameters listed in Table 7-23 were measured off-chassis, i.e., leakage currents, breakdown voltage, output capacitance, and noise figure.

All parameters were within specifications except for the noise figure, which on one of the transistors was 1 dB above specification. No original inspection data were available for this parameter, which is only measured on statistical samples. The other parameters are well within specifications.

Comparison with the original data again cast some uncertaintly relative to the test conditions and techniques at the original inspection. Saturation voltage measurements were again somewhat higher, while leakage currents were substantially lower. This transistor was also included in the special subsurface contamination test, discussed in Section 7.5.1; and no evidence of channelling was noted. The other parameters for which original data were available, namely the forward gain, was measured to be higher now by about a factor of 2 for all three transistors. No explanation is available, other than suspicion of the accuracy of the original data.

Because of the apparent differences in results of present and original measurements and because of the out-of-specification value for the noise figure on one of the transistors, this transistor was subjected to detailed diagnostic tests. The transistor was opened and examined internally with a scanning electron microscope. A substantial intermetallic gold-aluminum growth was found around the ball bonds. The findings are presented in Figure 7-14. The top SEM photograph was taken at a magnification of 1190X. The bottom SEM photograph was obtained at a magnification of 2390X and shows this intermetallic growth in some detail. It is believed that this phenomenon accounts for the high noise figure. This intermetallic growth frequently develops under normal shelf storage conditions as long as the proper materials and the high temperature environments are present. It cannot be attributable to the low temperature lunar environment. It should be noted that future designs employ aluminum-to-aluminum bonds for this reason.

Internal examination revealed no other apparent anomalies, nor any effects of exposure to the lunar environment.



a) 1190X Magnification (Photo 00545-108)



b) 2390X Magnification (Photo 00545-109)

Figure 7-14. SEM Photographs of Intermetallic Growth Bonds on Low Noise Transistor

TABLE 7-22. FUNCTIONAL TESTS OF POWER TRANSISTOR 2N1936

Par	ameter	Comp	arison Data		Test Result	S-	
Sym-			Original	Tests C	n Chassiser		1
bol	Unit	Spec Value	Receiving Inspection Data	Parts Not Removed	Parts Later Removed	Tests of Removed Parts	Test Conditions
V _{CE} (sát)	Volts.	0.5 (max)	0. 18	NA	0. 24	0. 23	IB = 0.5 ampere IC = 5 amperes
V _{RE}	Volts	2 (0)8×)	Not available	NA	1.12	1.11	I _C = 10 ampere I _B = 1 ampere
h _{FE}		15 to 50	Not measured	NA	20. H	23	VCE = 10 valts
FE	3	18-to 75	32	NA	Not tested	34, 5	VCE = 10 volts IC = 1 ampere
Ona ¹	Milli- amperes	5 (max)	Not measured	NA	Not tested	Q. 24	VEH = 4 volts
CEY	Milli- amperes	10 (max)	Not measured	N.A	Not lested	0.26	V _{CB} = 120 volts V _{EB} = -1 volt
E V CEO	Volts	80 (min)	Not measured	NA	Not tested	1Ab	t _C = 200 ma 1 _B = 0 ampere

See Table 7-15 for explanation of nomenclature,

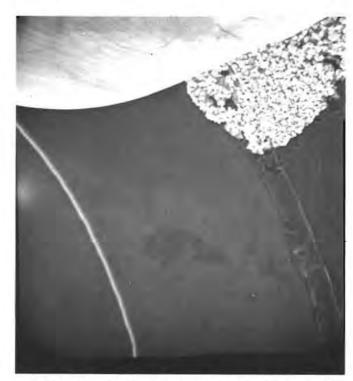
TABLE 7-23. FUNCTIONAL TESTS OF LOW NOISE TRANSISTORS 2N2586

Parameter		Comparison Data					
Sym-		Origina) Receiving			ts on Chassisee ange of Values)	Tests of	
bol	Unit	Spec Value	(Range of Values)		Paris Later Removed	(Range of Values)	Tesi Conditions
CE (sat)	Volts	I (max)	0. 18 to 0. 278	NA	0. 247 to 0. 410	Not measured	(g = 0.5 ma) 1 _C = 10 ma
GE (sār)	Volta	1 (max)	Not measured	NA	0. 22 to 0. 37	0. 20 to 0. 34	I _B = 0.5 ma I _C = 10 ma
FE	*	600 (max)	Not measured	NA	240 to 360	Not measured	VCE = 5 volts IC = 0:5 ma
FE	7	600 (max)	122 to 157	NA	Not measured	400	V _{CE} = 5 volts I _{CE} = 10 ma
EBO	Pico- aniperes	10,000 (max)	Not measured	NA	Not tested	4 10 9	V _{ER} = 5 volts I _C = 0 anipere
EO	Pico- amperes	2000 (max)	300 to 400	N.A.	Not tested	4 to 280	V _{CE} = 5 volts I _B = 0 anipero
CEO	Volts	45 (min)	71 to 110	NA	Not tested	71 to 104	1 _C = 10 ma
ob-	Pico- farada	8 (max)	Not measured	NA	Not tested	4.3 to 4/5	V _{CB} = 9 volts i = 1 Mijz
t	Decabels	2 (max)	Not measured	NA.	Not tested	0.5 to 3	Per Hoghen specification

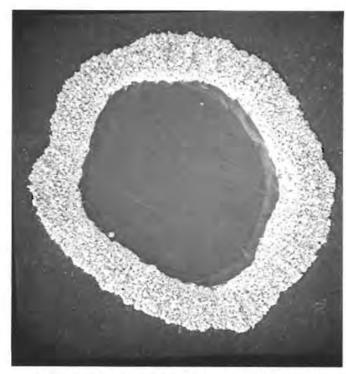
[&]quot;See Table 7-15 for explanation of nomenclature.

orTotal of | parts tested on chassis; | 1 removed.

or Total of 3 parts tested on chassis; 3 removed.



a) Base Lead of General-Purpose Amplifier PNP Transistor, Type 2N722 (1000X Magnification) (Photo 00545-110)



b) High Voltage NPN Transistor, Type 2N871 (500X Magnification) (Photo 00545-111)

Figure 7-15. SEM Photograph of Base Lead of Transistors

7.5.6 SEM Examination of Six Semiconductors

To obtain additional insight on possible structural changes induced by exposure to the lunar environment, six semiconductors were selected for detailed SEM examination. The parts selected for this diagnostic test provided a good representation of the components tested. They included the following: a general-purpose amplifier transistor, type 2N718A (NPN); a general-purpose amplifier transistor, type 2N722 (PNP); a high voltage transistor, type 2N871; a high frequency transistor, type 2192A; a power transistor, type 2N1936; and an SCR diode, type 2N1930.

Twenty photographs were taken in all. Although evidence of a number of manufacturing defects was found, illustrative of problems relating to fabrication techniques at the time of manufacture, no direct evidence of any degrading effect of the lunar environment was uncovered. The various observations made included presence of debris, circular growth of intermetallic formations, emitter metallization, gold-aluminum intermetallic growth, and formation of aluminum silicide and striations of the silicon.

Two examples of these SEM photographs are shown in Figure 7-15. Figure 7-15a is an SEM photograph taken at a magnification of 1000X of the base of the general-purpose PNP amplifier transistor. The intermetallic growth is seen here at the base lead, stopping at the oxide step. Figure 7-15b is an SEM photograph at a magnification of 500X of the emitter pad of the high frequency transistor. Substantial intermetallic growth can be seen, as well as striations of the silicon. These are believed to have been caused by the formation of aluminum silicide created during the thermal compression bonding. This material subsequently cracked, forming the striations.

8. MECHANICAL AND ELECTROMECHANICAL COMPONENTS TESTS

8.1 SCOPE AND GENERAL TEST PLAN

Results of component level tests of potentiometers, stepper motors, magnetic devices, electrical connectors, and thermal switches are presented in this section.* These components constitute all of the parts other than the electrical parts, discussed in Section 7, which were analyzed at the component level after their removal from the camera. They are grouped for convenience in this section.

The test program was designed to emphasize the objectives described in Section 7.1 for the electrical components. Extensive use, wherever applicable, was made of past design and test data available for these parts from the Surveyor program. Considered of particular significance were findings of the wear characteristics of wire-wound potentiometers as typical of the behavior of metal-to-metal contact surfaces, characteristics of moving parts and materials in the stepper motors, and condition of electrical connectors. The above design features are directly applicable to a large class of space hardware applications. Analysis of the thermal switch could also be singled out as valuable for potential future space applications involving thermal sensing and control.

As in the case of electrical components, this section describes testing conducted on parts other than those for which specific failures were discovered earlier in the test program. The failed components, or those for which significant anomalies were identified at the subassembly or circuit level, are treated separately in Section 12 as part of the failure analysis work on the program.

Table 8-1 lists the parts tested, indicates the numbers of each type and the quantities examined relative to the numbers present in the camera, and the parameters measured during functional tests. Whereas electrical component testing entailed selection of representative samples, testing of components described here was conducted on virtually all available parts

^{*}Mechanical subsystem tests were discussed in Section 5.

TABLE 8-1. MECHANICAL COMPONENTS TEST PLAN SUMMARY

	Description	_		Functional Tests	Number Disassembled
Class	Туре	Number in Camera	Number Tested	Parameters Measured	and Diagnosed
Precision wire-wound	Single turn (Spectrol)	1	1	End-to-end resistance Wiper continuity	0
potentiometers	Three turn (Duncan)*	5	3	Visual examination and X-ray Starting torque Linearity and noise Noise and torque vacuum	2
Stepper motors	Abrams, size 15, high torque; DMA	2	1	Visual examination and X-ray End and radial play, and detent	1
	Kearfott, size 08, low torque; CM40191010 Stepping rate Angular rotation per step Insulation resistance Dielectric strength		1		
Magnetic components	Torroidal inductors manufactured by Hughes	4**	3	Visual examination and X-ray Do resistance	1
	Vidicon deflection yoke Cleveland Electric MVY432	1	1	Rated inductance and Q Inductance versus magnetiza- tion current	1
Electrical connectors	Microdot 43-series, size A, 19 pins	2	1	Visual examination Contact resistance	1
	Microdot 43-series, size B, 39 pins	2	0	Contact separation force Insulation resistance	0
Thermal switch	Thermal switch, single pole, single throw Normally open above 10°F Metals and Controls M221L002030522	2	2	Visual examination and X-ray Hermetic seal integrity Opening and closing temperatures Contact resistance	1

^{*}One of these (azimuth potentiometer) was Spectrol.

^{**}See text.

because of the small number present in the camera. Of the six motors, two were tested, one of each type. The remaining motors were not tested, partly to retain them for possible future investigation and partly because such additional tests were not considered likely to provide significant added data, compared to other activities within the total program constraints. Only one connector was tested; the other connectors could not be analyzed meaningfully because they had been uncoupled during the initial removal of the shroud in the Lunar Receiving Laboratory (LRL). The two potentiometers not shown as tested in Table 8-1 had exhibited specific anomalies, and are discussed separately in Section 12. Further breakdown of potentiometer tests is presented later in Table 8-2.

As in the case of electrical components, the test sequence was conducted in three phases. During preliminary examination, a visual inspection was made and basic functional characteristics measured to seek anomalies. One objective of this phase of testing was to confirm or suitably alter previously prepared test procedures. These tests were conducted by component engineers during the subassembly level tests prior to removal of the components from the chassis. These tests were implicitly included in the results described in previous sections.

During the second phase, after removal of the components from the camera, a comprehensive functional test was conducted and critical parameters measured. This phase of the test, which also included detailed visual examination, was nondestructive. Care was taken to ensure that no vital characteristics would be altered by test procedures. Consideration was given, when appropriate, to conducting limited environmental tests of selected parts.

The final phase, destructive in nature, entailed an internal diagnostic examination of selected parts which were disassembled for this purpose. Table 8-1 indicates the number of such parts chosen from the parts removed from the camera.

The mechanical and electromechanical component tests were conducted within the framework of established component test procedures, modified as appropriate. Early in the program, a format was developed to serve as a guide for preparing test plans for each component type, and preliminary test plans for each component were generated. These formats were similar to the one shown in Figure H-l of Appendix H for the tantalum capacitor electrical component. Engineering judgment was used in expanding, reducing, or otherwise modifying standard test procedures, as deemed appropriate. A detailed test procedure was then prepared for each part tested, and was carefully followed. Test procedures and documented results of all tests are available in the program files.

The succeeding subsections summarize the tests and results obtained for each of the components.

8.2 POTENTIOMETER TESTS

Table 8-2 identifies the six potentiometers on the camera and the tests conducted. All six potentiometers are precision wire-wound and servo-mounted, with a nominal end-to-end resistance of 5000 ohms. Five are three-turn types, and the other is a one-turn type. Since the adequacy of potentiometer design for lunar operations had been of concern during the Surveyor program, these tests to determine environmental effects were of special interest. As discussed in Section 2.4.2, the filter wheel potentiometer had indeed failed during lunar operations. The analysis of this potentiometer, as well as that of the azimuth potentiometer which had been noted to have been damaged during the dismantling operations, is treated in Section 12.

Tests of the remaining four potentiometers are summarized here; supplemental discussion of the vacuum test conducted is included in Appendix H. For one of these four, the focal length potentiometer, only the resistance and starting torque measurements are presented here; this potentiometer was selected for wear analysis and other materials tests, as described in Section 10.

Initial tests of the four potentiometers included end-to-end resistance, wiper continuity, visual examination, and X-ray. The end-to-end resistances ranged from 5035 to 5073 ohms. While they were within the 5000 ohm ±3 percent specification requirements, all were on the high side. This is attributed to an increase due to wear, as discussed later in this section. Visual examination uncovered no anomalies.

Tests of the starting torques, noise, and linearity were then conducted. Initial evaluation of these tests was based on the tacit assumption that the potentiometers had been lubricated with niobium diselenide, per specification. While starting torque and noise of lubricated potentiometers are higher in ambient operation, notable improvement occurs under hard vacuum conditions; the opposite is true for unlubricated potentiometers. As the test program progressed, it was determined that apparently none of the potentiometers examined (including the filter wheel potentiometer analyzed for its failure) had been lubricated.

The starting torques of the four potentiometers were measured to range from 0.12 to 0.18 in-oz. While they were all within the specification of 0.18 in-oz, these values were higher than the 0.1 in-oz maximum expected of unlubricated potentiometers under ambient conditions.

Linearity and noise measurements were then conducted on the single-turn elevation potentiometer and on the three-turn focus and iris potentiometers. These tests were not conducted on the focal length potentiometer. The concern of the apparently increased wear led to the decision to subject the focal length potentiometer to special investigation in the Materials Laboratory.

TABLE 8-2. SUMMARY OF POTENTIOMETER TESTS

Potentiometer	Manufacturer	Number of Turns	Functional Tests	Dia gnostic Tests	Failure Analysis
Filter wheel	Duncan	3			X**
Azimuth	Spectrol	3			X**
Focal length	Duncan	3	X	X*	
Iris	Duncan	3	X	x	
Focus	Duncan	3	X		
Elevation	Spectrol	1	x		

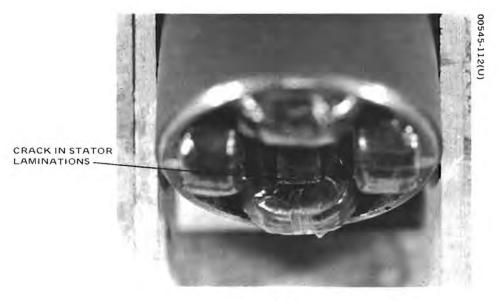
^{*}Conducted as part of Materials Test Program discussed in Section 10.

Linearity measurements were made with a divider head at 10 degree intervals on the single-turn elevation potentiometer and at 25 degree intervals on the focus and iris potentiometers. Results were nominal: The single unit had a maximum deviation of 0.362 percent compared to the specification allowance of 0.375 percent; the three-turn units measured 0.174 and 0.143 percent, respectively, compared to the specification requirement of 0.25 percent.

Noise measurements were then conducted at 4 rpm under ambient conditions. The specification calls for a maximum of 100 ohms of equivalent noise resistance, but typical values under 20 ohms are expected for these unlubricated wire-wound components. The one-turn elevation potentiometer measured 440 ohms, while the three-turn focus and iris potentiometers measured 70 and 900 ohms, respectively. This high noise is also indicative of excessive wear.

Because of the original assumption, later rectified, that the potentiometers were lubricated, a vacuum test was then conducted on the elevation and iris potentiometers in the expectation that reduced noise values would be observed. Results of vacuum testing were inconclusive because it had been determined that insufficient time was allowed for depressurization; while the potentiometers are not completely sealed units, they are partially sealed. These tests are discussed in further detail in Appendix H.

^{**}Failure analysis of these potentiometers is discussed in Section 12.



a) Stator

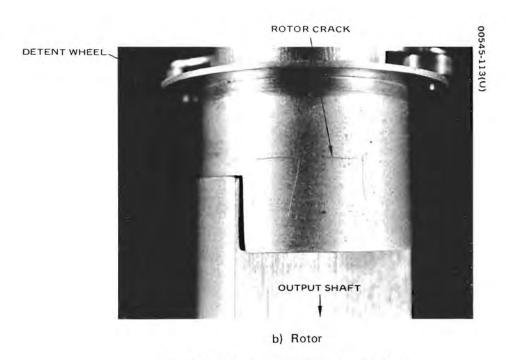


Figure 8-1. Apparent Cracks in Abrams Motor

To verify the suspected absence of lubricants on the potentiometers and obtain a better understanding of the apparent indications of excessive wear, the iris potentiometer was subjected to diagnostic tests. In parallel, tests for presence of lubricants were run on the focal length and filter wheel potentiometers. Presence of niobium diselenide was sought with an electron beam microprobe and by emission spectroscopy; no traces of niobium or silenium were found on any of the three potentiometers. Internal examination of the iris potentiometer clearly indicated that the wear on the wire and wiper was greater than would be expected on a part operating under atmospheric conditions. Similar conclusions were reached after examination of the focal length and filter wheel potentiometers. The amount of wear noted was that which would be expected from at least 100,000 operational cycles at 1 atm. Attempts to uncover evidence of possible cold welding were not successful.

Evidently, the lunar environment significantly aggravated the wear of unlubricated potentiometers. Unfortunately, no conclusions are available regarding the performance of properly lubricated components.

8.3 STEPPER MOTOR TESTS

Two of the six stepper motors were tested for their functional characteristics and subsequently disassembled for internal examination, as indicated in Table 8-1. One of these was the high torque Abrams Instruments size 15 DMA motor, having an output torque of 20 in-oz, and producing 36 degrees rotation per step. The other was a Kearfott size 08 motor, MC40191010, having an output torque of 0.25 in-oz, and producing 90 degrees rotation per step. Visual examination disclosed no apparent anomalies. Some debris was noted in the rear rotor bearing of the Kearfott motor. This material was most likely a residue from the Duroid retainer in the rear rotor bearing. X-rays of the motors were not revealing because of the high opacity of the parts.

Mechanical tests of shaft end and radial play showed compliance with specifications, although the 0.001 inch of end play noted could be indicative of some mechanical wear. Detent measurements were nominal.

The dc resistance, starting torque, running torque, detent torque, stepping rate, insulation resistance, dielectric strength, and angular rotation per step were then measured. Both motors met all specification requirements for these parameters, and no unusual results were noted.

Upon completion of the electrical and mechanical tests, both parts were completely disassembled. Internal examination revealed two cracks in the Abrams motor. A hairline crack was noted on the rotor, and an apparent fracture was observed in the lamination assembly of the stator near its base. These cracks are indicated in Figure 8-1; they are not

believed to be attributable to the lunar environment and apparently had no effect on the operating characteristics of the motor. The rotor fracture could, however, affect life expectancy. The rotor is constructed in two parts, with the output shaft on one part and the detent on the other. Each time the motor is stepped, the area of the crack was stressed. The observed crack could have been present at the time of the original assembly or it could have been caused by the application of the high torque during detent torque measurements, either in earlier testing or during this test program. The stator fracture appears to be the result of the manufacturing process.

The bearings of the Abrams motor were thought to have a rough feel when rotated manually. For this reason further analysis was conducted on three ball bearings: one from the Abrams motor, one from the Kearfott motor, and one from the iris potentiometer. These balls were microsectioned and wear examined at 200X magnification. The surfaces of all three balls were comparable, and no anomalies were noted. The roughness of the Abrams bearing was no worse than that of the other two, and they all appeared to be in excellent condition. It should be noted that the Abrams motor has New Hampshire Micro SR2 standard precision bearings, which are unshielded and have a metallic separator. Conceivably, absence of shielding could have allowed some dust contamination. The other two bearings are the Barden type and use a Duroid retainer. The Abrams bearing was to have been lubricated. Although no coating could be seen on the Abrams bearing, this does not preclude the possibility that a molybdenum disulfide or microseal type of solid lubricant that had been employed had worn off. In view of the absence of any concrete evidence of failure or anomalous behavior, the original concern over the subjective rough feel of the Abrams motor bearings was dispelled.

Internal examination of the Kearfott motor determined that it was in excellent condition. All internal surfaces appeared unchanged relative to their initial condition at manufacture. The bearings, which were self-lubricating crown retainers, were clean and appeared undamaged.

8.4 MAGNETIC COMPONENTS

Three torroidal inductors manufactured by Hughes and the vidicon deflection yoke were tested to determine the effects of the lunar environment on magnetic components. The Hughes-fabricated transformer, located in the ECU, was deleted from the original test plan because of the difficulty of removing this deeply imbedded part without totally dismantling the chassis.

Visual examination revealed no anomalies nor did X-rays of the inductors. The yoke could not be X-rayed because of its metal shield. Dc resistances, inductance at rated conditions, and Q of the coils were then measured. Results obtained for the three inductors and original values of

their resistances and inductances are summarized in Table 8-3. Original data for the deflection yoke were not available. Also included in Table 8-3 are the results of measurements of inductor weight.

Results for the deflection yoke indicated that dc resistances and the inductance of one of its coils, which measured 22.8 mH, were well within specifications; the second coil measured 121 mH in comparison with the specification limit of 110 mH. Since no apparent discrepancies were noted, it was assumed that this was essentially its original reading. The deflection yoke was then subjected to materials tests, as described in Section 10.

The resistances and inductances of the three inductors were all within specifications and compared very well with the original readings, as evident from Table 8-3. The maximum difference in inductance relative to prelaunch data is on the order of 2.5 percent for one of the inductors and much less for the others. This is all within the limits of repeatability of test operations, calibration accuracy, and differences between test equipment used. The values of Q for two inductors are virtually identical with the original data (not shown in Table 8-3); the Q of 116 for the third inductor exceeded the original value by about 15 percent, but this is not considered significant because of the critical dependence on the test equipment, test parameters (e.g., frequency), and operational techniques. The important test result is that no effects of exposure to the lunar environment were observed.

Original weights of the inductors were available for two of the three parts. For these, the measured weights shown in Table 8-3 are approximately 1 percent (0.2 gram) higher. This is attributable to the epoxy bonding material adhering to edges of the parts removed.

Measurements of inductance as a function of magnetization current were then conducted with nominal results. This test was repeated with the magnetization current applied in the reverse direction to determine whether any polarization effects were present; results were nominal.

Diagnostic tests of one of the inductors were then conducted, while another inductor was subjected to materials tests (Section 10). The encapsulant was removed and examined for visual changes, such as shrinking or hardening, and the core was inspected for evidence of internal fracturing. Results were nominal. The inductance of the coil was remeasured after removal of the encapsulation. Results were identical with the values obtained earlier.

8.5 MICRODOT CONNECTOR TESTS

Four circular Microdot series 43 external connectors, mated to the TV camera, were returned with the attached severed cable sections. All of these were of the quick-disconnect, push-pull type. Each connector has

TABLE 8-3. MEASUREMENTS OF TESTS OF TOROIDAL INDUCTORS

	Original Data (Receiving Inspect	1 Data Inspection)	Mea	Measured Parameters	S	
Inductor Serial Number	DC Resistance, ohms	Inductance, mH	DC Resistance, ohms	Inductance*, mH	***	Weight, grams
14	2.50	10.02	2.497	9.93	133	21,80
78	2.61	10.18	2, 638	6.95	116	23.87
44	0.09845	0.377	0.1004	0.386	109	21.87

*S/N 14 and 26 (10 mH) measured at 2 kHz, 0.125 ampere, and 1 volt. S/N 44 (0.38 mH) measured at 10 kHz, 0.4 ampere, and 3 volts.

**S/N 14 and 26 at 6 kHz. S/N 44 at 10 kHz.

0.080 inch contact centers and crimp contacts. Two of the connectors, attached to the TV cable leading from the mirror assembly to the center of the lower shroud, were size A (19 pins); the other two on the lower shroud, attached to the main incoming cables of the camera, were size B (39 pins).

Examination of the connectors was considered significant because of the many design and reliability problems observed in space applications. Connector reliability was of prime concern on the Surveyor program. Of particular importance was the mechanical integrity of contacts, as measured by contact separation forces, contact resistance, presence of contamination, and condition of surfaces.

Since three of the four connectors had been, of necessity, disconnected during the LRL operations in order to remove the lower shroud, meaningful tests on the separation forces and contact resistances could only be conducted on the 19 pin mirror assembly connector, which was carefully left intact for these tests.* To provide comparative readings for the separation forces and contact resistances and ensure that the planned test procedures would not compromise the validity of results, a similar nonflight connector was first tested.

The contact resistances of the individual pins were measured by recording contact voltage drops. Results indicated that the flight connector was in good condition. Its contact voltage drops were generally lower than those measured on the nonflight connector, but these differences were small. The calculated differences in contact resistance between the corresponding pins of the two connectors were in the order of 1 milliohm. The nonflight connector tested had undergone many disconnect operations during its life span, which probably accounts for its generally higher resistance readings.

Contact separation forces were then measured after careful disassembly of the connector for this purpose. This disassembly, which is described in more detail in Appendix H. 8, entailed cutting of the shell and removal of the plastic insert. Again, these operations were conducted first on the nonflight connector and then on the TV camera connector. Results for 17 of the 19 pins indicated that the average contact separation force measured for the flight connector was 2.3 ounces, compared to 2.4 ounces measured on the nonflight connector. The spread was nominal: 1.2 to 3.2 ounces for the flight connector and 1.5 to 3.5 ounces for the nonflight connector. Results again indicated that the camera connector appeared to have been unaffected by the lunar environment.

^{*}Gross connector unmating forces were measured during the LRL operations, as noted in Section 3.2.3. These measurements indicated no significant effects of lunar exposure.

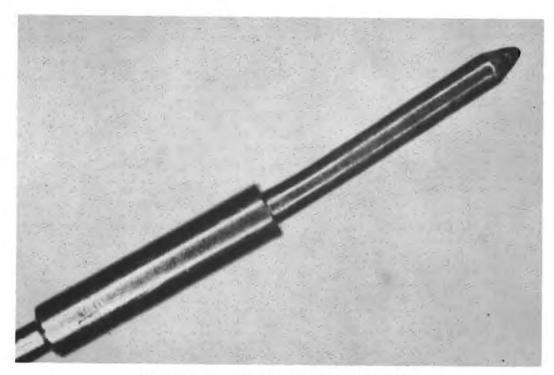


Figure 8-2. Bent Connector Pin (Photo 00545-114)

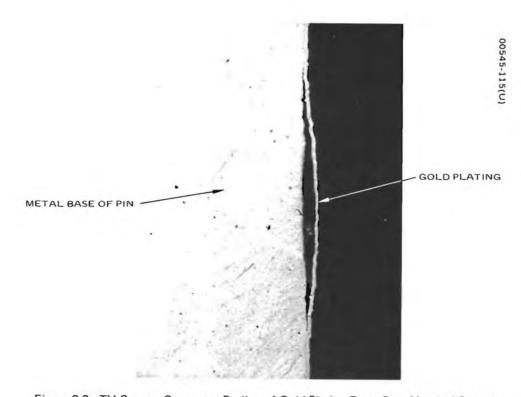


Figure 8-3. TV Camera Connector Peeling of Gold Plating From Base Metal of Contact

In the course of the disassembly of the camera connector, it was noted that two of its pins were bent. Contact separation forces for these two pins were therefore not included in the above test summary. Figure 8-2 shows one of the bent pins. It is reasonably certain that this occurred prior to launch, sometime during the manufacturing or test phases. Apparently, this condition of the pins did not adversely affect the electrical performance.

The TV connector was then subjected to a microscopic and metallographic examination of its contacts. Evidence of significant gold-plate peeling was noted, as indicated in Figure 8-3. Results of analysis indicate that preplating contamination was present, resulting in poor adhesion. The lunar environment did not cause it, but it presumably aggravated an already poor condition. The low pressure environment may have caused vapor pressure gradients to be developed at the plating-base-metal interfaces, and shear stresses may have been developed at the extremely low temperatures.

Insulation resistance was then measured between adjacent contacts at 500 volts dc and between each contact in the connector shell. In all cases, the insulation resistance was greater than 500×10^9 ohms. This indicates that no significant degradation occurred in the insert material.

8.6 THERMAL SWITCH TESTS

The two thermal switches on the camera (S/N 530 and 534) were both Metals and Controls type M221L002030522. They were hermetically sealed, single pole, single throw, designed to normally open above 10°F and to close at 0°F.

The two thermal switches were first tested on the chassis to validate their operation. This was done by cooling them with a Freon gas jet and monitoring their continuity. Results were nominal.

The switches were removed from the camera, visually examined, and X-rayed. No evidence of any damage or of any effects of lunar exposure were noted. The switches were then subjected to a seal test in water at a pressure of 1.3 inches of mercury. No leaks were observed. Contact voltage drops were then measured at 0.1 ampere dc. Past data were available for only one of the two (S/N 530). The 14.2 milliohms measured for switch 530 was consistent with prior data. The 8.8 milliohms measured for switch 534 fell within the 8 to 18.7 milliohms range observed during qualification testing of all the switches, and is well within specifications.

A special test was conducted to assess the values and repeatability of the opening and closing temperatures of the two switches. Each switch was cycled five times. Results of this test are given in Table 8-4. It is noted that both switches were reasonably consistent in their behavior although the average temperature differential was on the order of 10°F, exceeding the specification range of 6°F by about 4°.

TABLE 8-4. RESULTS OF TEMPERATURE CYCLING OF THERMAL SWITCHES

Normally Open Above Approximately 10°F

			Swit	ch 53	0			•	Swi	tch 5	34	
Cycle	Te	mpe	ratur	es, °	F	Average	Ter	nper	atur	es,	°F	Average
Closing of switch	-0.4	0	1.6	1.2	1.6	0.9	0.3	0.3	0	0	0	0.1
Reopening of switch	10.0	8.1	8.1	10.0	9.3	9.1	9•9	8.6	9•9	7.9	9.0	9.1
Temperature differential	10.4	8.1	6.5	8.2	7.7	8.2	9.6	8.3	9•9	7.9	9.0	9.0

To determine whether the cause of this apparent deviation from specifications can be traced to the effects of lunar environment, switch 534 was subjected to further diagnostic tests. The switch was dismantled by grounding off its weld bead and removing the case cover. The assembly was examined microscopically and the internal parts and surfaces compared with another commercial component. No significant anomalies were noted. Some degree of roughness was observed on the contacts and in the concave surface of the snap disk. However, in both instances, the area covered was extremely small. It was concluded that this observation was not related to the increase in temperature differential. No apparent effects of the lunar environment were uncovered.

The cause of the apparent discrepancy in the measured temperature differential between the opening and closing temperatures remains uncertain. The switches were apparently in good condition, capable of many more cycles of satisfactory operation.

During the original qualification tests, all switches were subjected to five temperature cycles ranging from -185° to 250°C. Although past history of similar switches indicates that successive cycling tends to increase the temperature differential somewhat, this alone could not account for the magnitude of the apparent anomaly.

Two hypotheses can be postulated as most likely causes of the apparent out-of-specification characteristics: One is that these particular switches had always, by design, exhibited this somewhat larger temperature

differential, undetected in the original inspection. The second hypothesis is that the extreme thermal cycling on the lunar environment has, indeed, caused this change in characteristics. One such conjectured mechanism of change entails the generation of shearing forces in the bimetallic disk at the interface, which would change the characteristic of this thermostat. Internal examination did not indicate any apparent distortion, but an undetectable permanently set effect could have been induced. No basis is available for a direct comparison with prior structural characteristics of this switch. Microsectioning techniques do not promise to be fruitful because the induced structural distortions would most likely be permanent.

9. OPTICAL COMPONENTS TESTS

9.1 INTRODUCTION

The third and last group of components tested were the optical components, comprising the beryllium TV mirror, the four filters — blue, red, green, and clear — and the elements of the lens contained in the lens barrel subassembly.

Tests of the TV mirror and of the lens barrel subassembly are discussed in this section, with supplementary data on details of visual examination presented in Appendix H. 6. The filters were not tested at Hughes but were immediately transmitted to the Jet Propulsion Laboratory, as directed, for analysis under the parallel science program. Subsequently, selected tests were conducted on the filters at Hughes as part of the surface contamination studies, discussed in Section 11.

Two sets of tests, performed as part of the science investigation on the mirror and filter of the camera at the assembly level, are also briefly reported in Section 9.2 for the sake of completeness. These tests were conducted in the Hughes laboratory under the cognizance of J. Renolson, California Institute of Technology, with the support and participation of Hughes personnel. They were concerned with the assessment of the effect of lunar dust and other possible environmental effects on the optical transmission characteristics of the camera mirror and filter. Specifically, these tests aimed at providing a relative comparison of the magnitude and effect of dust contamination between the condition of the returned camera and the condition of the camera on two prior occasions for which data were available: during the Surveyor mission operations in April 1967 and just before removal of the camera from the spacecraft by the astronauts. The tests included collimated light photographs and evaluation of the contrast attenuation of the mirror assembly.

Optical tests of the lens elements and mechanical tests of the barrel subassembly reported here were conducted by Bell and Howell, the original manufacturers of the lens barrel. This work was done under a Hughes subcontract. The tests were performed on the lens barrel as a unit; the barrel was not further disassembled. In the context of this discussion, the barrel is thus considered to be an optical component.

9.2 SPECIAL PHOTOGRAPHIC AND OPTICAL TESTS BY SCIENCE INVESTIGATORS

9.2.1 Collimated Light Photography

A series of photographs was taken with the camera mirror assembly illuminated with collimated white light at the same angle as that of the sunlight during the lunar photography sequence. A series of exposures was taken at various camera angles, duplicating several of the closeup photographs by the Apollo 12 astronauts on the moon. Comparison between the photographs of the retrieved camera with those taken by the astronauts will provide information for assessing whether any removal or distribution of dust from the mirror had occurred during the retrieval operations and post-return handling.

Initial attempt to take these pictures in the LRL was limited by the low intensity of the available light source, with attendant loss of detail due to small disturbances during the long exposure. The tests were conducted successfully in the Hughes laboratories immediately upon receipt of the Surveyor III camera.

Detailed evaluation has not yet been completed. Preliminary examination of the photographs indicates that no significant changes occurred in the dust layer relative to the pictures taken by the astronauts on the moon. Results of the completed evaluation will be reported separately.

9.2.2 Evaluation of Contrast Attenuation of Mirror Assembly

The second series of tests was conducted to determine the effect of dust and possible other effects on the optical transmission of the mirror and filter optical subsystem of the camera. During Surveyor III operations on the moon, a substantial contrast attenuation was noted. This was attributable to the deposition of dust or pitting of the mirror caused by the abnormal landing of the spacecraft. In addition, there was evidence of considerable veiling glare (scattering light) for pictures taken with the sunlight shining on the moon.*

Measurements were made on the entire mirror assembly as part of the assessment of the condition of the returned optics. These measurements were conducted primarily to provide a comparison of the conditions following the return of the camera with those during the operations of the Surveyor III on the moon.

^{*}Described in Reference 10 and Section 9.4 below.

The returned Surveyor III mirror assembly (including the primary mirror and filters) was installed on a spare Surveyor camera immediately after the removal of the mirror assembly from the Surveyor camera, as discussed in Section 4.1. Contrast attenuation of a known image by the mirror and neutral density filter combination was measured both with and without simulated sunlight (from a xenon lamp) incident on the mirror.

Analysis of results of these tests has not yet been completed. Preliminary evaluation of the scattered light measurements indicates that more dust appears to be present than during the Surveyor III mission operations. This, however, may be a result of the mismatch between the spectral response of the vidicon and the spectral characteristics of the contrast image (tungsten source) and the lamp used for simulating the incident sunlight (xenon source). A detailed analysis of these and other optical test results must be completed before firm conclusions can be reached. Results of these tests will presumably be reported separately.

9.3 TESTS OF TV AZIMUTH MIRROR

9.3.1 Mirror Description

The TV azimuth mirror was manufactured by electrodepositing nickel plating (Kanigen) over a beryllium substrate. The backside of the beryllium substrate was machined to achieve a "waffle" effect. The Kanigen plating was then polished, and a reflecting surface of vapordeposited aluminum was applied over it. A coating of silicon oxide was then applied to the aluminum.

Aluminum foil was bonded to the back surface to prevent lunar dust from collecting in the ribs during landing of the Surveyor. Any dust so collected might later fall into the optical assemblies as the azimuth mirror was tilted during camera operation.

Because of differences in the coefficients of thermal expansion between aluminum and beryllium, a slight warping of the mirror substrate was incurred during bonding of the aluminum foil. This warping was not noted until after the launch of the fourth Surveyor spacecraft. Beginning with Surveyor V, the manufacturing process was corrected by substituting stainless steel for aluminum, and flatness measurements of the mirror were made prior to launch. While it is strongly suspected that the Surveyor III TV mirror had sustained this manufacturing curvature, no original data were available for a direct comparison of flatness measurements.

9.3.2 Test Plan

Tests of the azimuth mirror entailed visual and microscopic examinations, measurements of spectral reflectance, and determination

TABLE 9-1. TV AZIMUTH MIRROR TESTS

	Tests After Removal of Mirror (April 1970)	Final examination	Five regions	Repeated measurement (successful)
Test Conditions	Tests on Mirror Assembly After Removal From Camera (March 1970)		Three regions	Original measurement (unsuccessful)
	Early Tests on TV Camera (February 1970)	Initial examination	One region	
	Tests	Visual and microscopic examination	Spectral reflectance measurement	Flatness determination

of surface flatness. These tests were performed several times, as summarized in Table 9-1. Early examination and testing were conducted to obtain original data before any changes that might result from subsequent handling (such as partial loss of dust coating). Later tests after removal of the mirror were conducted partly because of better access and partly to obtain data on any changes that might have occurred.

Certain constraints were imposed on the conduct of these tests. Because of the desire to retain the optical surfaces reasonably intact for subsequent science investigations, it was directed that no touching, cleaning, or otherwise damaging of the surface of the mirror be permitted, and no disassembly of the mirror was made.

9.3.3 Visual Examination

As indicated in Table 9-1, detailed visual examination was conducted before removal of the mirror assembly and, again, after the removal of the mirror 2 months later. Results of the initial examination were summarized briefly in Section 3.4.5. The appearance of the mirror was shown in Figure 3-27 for two different lighting conditions.*

The azimuth mirror had a uniform layer of material over the surface. The material was grey and had the appearance of fine dust particles. The mirror appeared either very diffuse or specular, depending on the lighting and viewing angle.

As shown in Figure 3-27 and on the frontispiece, a mark was made over the top section of the mirror by one of the astronauts when he wiped its surface with his finger prior to the removal of the camera on the lunar surface. This wiping was done as a contingency test in the event that the camera could not be retrieved. The astronauts took photographs of the mirror before and after wiping in an attempt to obtain some information on the condition of the surface. This wiped area was noted to be cleaner than the rest of the surface; however, it was also covered with small particles of dust.

Several bands were noted on the mirror surface. On close inspection, these appeared to be a result of variation in thickness and composition of the dust coating. The lower band, very faint, appeared to coincide with the outline of the mirror housing; at a particular viewing angle, this band was seen to be aligned with the opening of the lower part of the mirror housing. The upper, broad band showed interference color patterns when viewed under oblique lighting. Further analysis of the mirror optical surface was to be conducted later as part of the parallel science program under JPL coordination.

^{*}Black and white replicas of original color photographs.

The mirror did not appear to be affected physically. Microscopic examination at a magnification of 40X did not reveal evidence of delamination of the vapor-deposited aluminum or of the nickel plating. There was no apparent spallation of the silicon oxide coating.

9.3.4 Specular Reflectance Measurements

Reflectance measurements of the mirror were originally intended to determine if any damage had occurred to the primary reflecting surface or to the silicon oxide overcoating. This original objective had to be modified when it was noted that the mirror was severely coated with dust particles believed to be of lunar origin, with some possibility of the presence of products of outgassing. Since a large amount of scattering was caused by this contamination and since removal of the coating was prohibited, the reflectance measurements were performed primarily to obtain more information on the nature of the contaminant materials. However, by inference, some estimates on the condition of the mirror could also be made.

Reflectance measurements entailed three interdependent tests: those made by Hughes, reported below, those measured in the Hughes Surveyor Laboratory by science investigators under JPL coordination and with Hughes assistance, and those made at various institutions after transfer of the mirror to JPL. It is presumed that the latter two will be reported separately.

The Hughes measurements were conducted at near-normal incidence viewing the specularly reflected portion of the incident collimated beam of light. The other sets of measurements, conducted at several wavelengths, were performed goniometrically over a wide range of incident and reflected angles. These will thus provide spatial and spectral reflectance characteristics for optical performance evaluation, as well as data of potential use for identification and determination of the optical properties and effects of the dust contaminants. In addition to providing basic data on the apparent change in reflection, the Hughes measurements of specular reflection as a function of wavelength could also shed some light on the nature of the contaminants. The structure of the reflected spectrum could be examined for major trends (such as dominance of attenuation in yellow, blue, or other bands) or for the presence of specific absorption peaks, characteristics of certain organic materials.

The specular reflectance measurements, as noted in Table 9-1, were conducted at three different times over the wavelength band from about 0.35 to 1.3 microns. The experimental setup is shown in Figure 9-1*. The xenon source was calibrated at each wavelength, using a

^{*}Science measurements used the same source but a goniometric photometer for the detector.

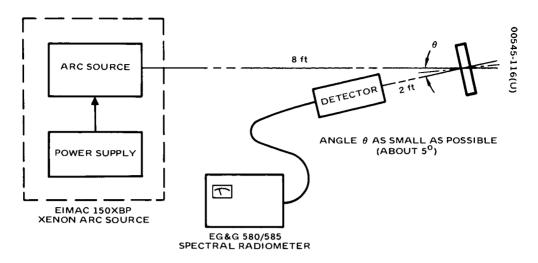


Figure 9-1. Experiment Setup for Specular Reflectance Measurements of TV Mirror

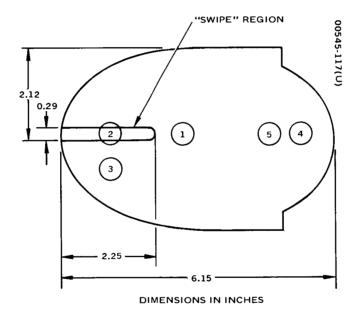


Figure 9-2. TV Mirror Regions Measured for Reflectance

path length equal to the total source-radiometer distance; so the values of reflectance obtained represented the true ratios of energy reflected by the mirror to that produced by the source. The light source illuminated a region approximately 2 inches in diameter on the mirror. The radiometer collected the specular components, as well as the scattered energy within the 6.46×10^{-4} steradian solid angle subtended by its entrance aperture.

Figure 9-2 shows the five regions of the mirror for which reflectance measurements were conducted. Region 2 was in the area that had been wiped by one of the astronauts on the moon before the removal of the camera. Regions 1 and 3 were representative of areas with most of the contamination. Region 4 was representative of an area that was reasonably

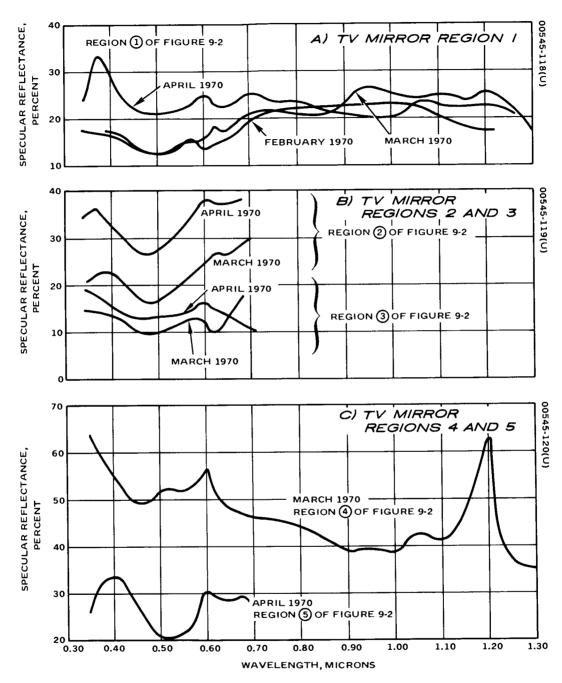


Figure 9-3. Results of Specular Reflectance Measurements

well protected and exhibited much less scattering when viewed at large angles of reflection. Region 5 was in the center of the previously noted discoloration band and represented the transition area between the relatively clean and dusty portions of the mirror.

The results of the specular reflectance measurements are plotted in Figures 9-3a, b, and c for regions 1, 2, and 3, and 4 and 5, respectively. The initial measurement on the TV camera was conducted only on region 1. The second measurements on the mirror assembly were conducted on regions 1, 2, and 3. The final measurements on the disassembled mirror were conducted on all five regions, including regions 4 and 5 in the lower portions of the mirror, previously inaccessible.

It is evident from Figures 9-3a and b that reflectance increased with time. This was particularly true for the most heavily contaminated region 1 and for the disturbed area on the "wipe" in region 2. The increase in reflectance in the visible part of the spectrum between the time that the mirror was on the camera, and the measurement taken after its removal was on the order of 10 percent. This increase is probably the result of loss during storage and in handling of some of the original dust.

Reflectance of all regions was substantially lower than the original value of 88 percent in the visible part of the spectrum, particularly for the measurements made early prior to handling. Reflectance of the more heavily contaminated regions 1 and 3 was then in the 10 to 15 percent range. The relative flatness of these depressed reflectance values over the visible spectrum range suggests that the scattering particles were of much larger size than the wavelengths. The reflectance of the "cleanest" region (4) was in the range of 50 to 60 percent in the visible part of the spectrum, much closer to the original values but still substantially reduced.

Characteristic absorption bands are evident on the figure. The most dominant absorption region at 0.49 micron can be seen on all three curves, and additional absorption maxima at 0.9, 1.0, and 1.3 microns are noticeable in region 4 in Figure 9-3c.

It is not possible without cleaning the mirror to state definitely that the degradation in reflectance is attributable entirely to the deposited contamination. There is a strong suspicion, however, based on the above discussion, that this might be the case.

Detailed evaluation of the mirror is being conducted separately as part of the related science plan and presumably will be reported separately.

9.3.5 Measurement of Mirror Flatness

The flatness of the Surveyor III TV camera was measured to determine whether any distinct significant changes had occurred as a result of exposure to the lunar environment. Although flatness measure-

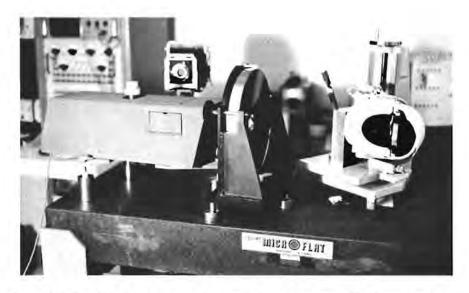


Figure 9-4. Test Setup for Original Measurement of Flatness of TV Mirror on Mirror Assembly (Photo 4R14065)

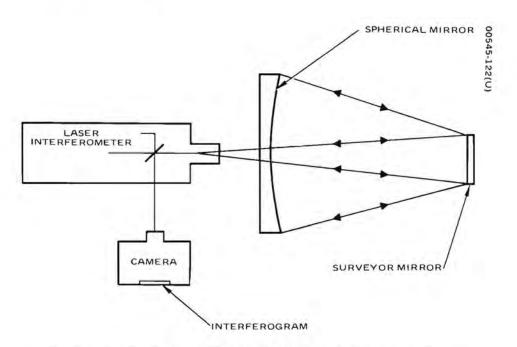


Figure 9-5. Illustration of Double-Pass Interference of Flatness Measurement

ments had not been made on this particular mirror prior to the Surveyor III launch, some inferences could be made based on preflight flatness measurements made on other Surveyor TV camera mirrors.

Initial flatness measurements were attempted on the mirror assembly. This setup, shown in Figure 9-4, utilized a Tinsley unequal path laser interferometer. The TV mirror, interferometer, and auxiliary spherical mirror were placed on a vibration-isolated granite block. The auxiliary spherical mirror, accurate to one-eighth of a wavelength, was required by the optics of the setup illustrated in Figure 9-5 in order to redirect the light reflected from the TV mirror. The double reflection obtained thereby resulted in a much stronger interference pattern which could then be photographed. However, this double-pass interference condition required proper interpretation of the resulting patterns because any error in the mirror flatness was evidenced as double the actual amount. Pictures of the interferogram were taken by a Super Graphic press camera, shown in Figure 9-4, and recorded on 4 x 5 Polaroid film.

The initial measurement on the mirror assembly was only partially successful. Access to portions of the mirror was poor, and the relative orientation of the mirror required a separate low-contrast flat reference mirror, which was not available. Only a dim unstable image of the interference pattern could be seen by eye but could not be photographed. Attempts were made to look at the surface by using only the laser beam. However, the area measured was too small.

After removal of the mirror from the mirror assembly, the flatness measurement was performed using essentially the same setup as shown in Figure 9-4 but with the mirror attached at its pivot supports to a holding mount by means of two rods. The Twyman-Green interferometer was replaced with a Davidson 5 inch Fizeau-type interferometer.

Figure 9-6 shows three of the interference patterns recorded. Figure 9-6a is of the central region of the mirror, and Figures 9-6b and c of the right and left regions, respectively. The right region on Figure 9-6b corresponds to the area of the swipe made by the astronaut. Results were indicative of the saddle-shaped surface. The irregular pattern obtained in Figure 9-6a shows approximately seven to eight fringes of irregularity across the surface. These figures are quite similar to the patterns seen in the earlier examination of the mirror on the mirror assembly, as noted above.

Studies of these patterns indicated that they were attributable to the deformation of the mirror blank in the original manufacture, as mentioned in Section 9.2.1. Absence of original data did not permit a quantitative comparison. However, it was concluded that no evidence could be gleaned from the results obtained that would suggest any changes resulting from lunar exposure.

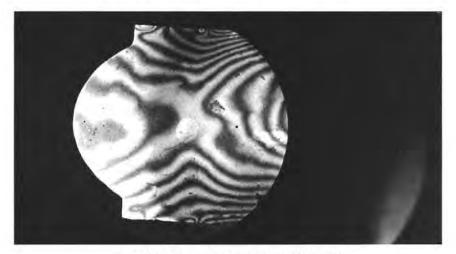
^{*}Modified Twyman-Green interferometer combined with laser source.



a) Center of Mirror (Photo 00545-123)



b) Right Region of Mirror (Photo 4R15371)



c) Left Region of Mirror (Photo 4R15369)
Figure 9-6. Interference Patterns During Flatness Measurements of TV Mirror

9.4 TESTS OF LENS BARREL SUBASSEMBLY

9.4.1 Description

The lens barrel subassembly, shown in Figure 9-7, consists of the basic optical lens barrel, side plates, and circumferential ring gear controlling the focal length, focus, and iris settings. This subassembly was removed from the lens assembly upon completion of the optical subassembly tests, discussed in Section 5, for tests at the component level, reported in this section.

The associated gear trains, motors, and potentiometers normally driving the ring gears had been removed; so tests at the component level were performed without any alteration in settings of the three functions. The principal effect was that setting of the focus cell could only be estimated for resolution measurements.

For the optical tests, the lens barrel subassembly was mounted on the lapped seating surfaces of the side plates. The rigidity of the assembly was improved by temporarily replacing four of the screws attaching the lens side plates to the two separating plates. These four screws were found missing on the returned camera.



Figure 9-7. Lens Barrel Subassembly (Photo 00545-126)

9.4.2 Test Plan and Procedures

Tests of the barrel subassembly were conducted at Bell and Howell under a subcontract from Hughes. The objective of these tests was to determine whether exposure to the lunar environment of this fairly well protected subassembly had produced any significant effects, such as contamination of optical surfaces by outgassing or dust, degradation of optical properties, or other physical or mechanical effects.

Ground rules for these tests stipulated that the lens barrel assembly should not be dismantled and that no films or contaminants were to be removed from the optical surfaces. Consequently, the lens barrel subassembly was returned to Hughes upon completion of tests in the same physical condition in which it was received by Bell and Howell.

The plan included a detailed visual examination, measurement of optical properties, i.e., resolution and transmission, and an assessment of mechanical characteristics. Standard Surveyor test procedures, properly modified and approved by Hughes, were followed in performing the optical and functional measurements.

The detailed visual examination was performed on the external optical surfaces, on the internal optical surfaces, and on the external supporting surfaces. The results are presented with reference to the following orientation of the lens barrel in Figure 9-7: the lens barrel was viewed from the front, with the side plates vertical, the reflex condenser at 9 o'clock, and the focus cell rotated clockwise to the infinity end stop.

The setting of the focus cells for the resolution test was estimated by counting ring gear teeth for the 12 foot focus distance. The focus end stop position had to be used in the lens transmission test, corresponding to infinity in vacuum, instead of the equivalent air focus setting 1-1/2 degrees from the stop, but this difference is not considered significant. Lens centering in the resolution test was accomplished by adjustment of the mounting system rather than by the usual adjustment of screws retaining the focus antibacklash spring (these screws were sealed). A mechanically different, but functionally equivalent, mount was used for the optical transmission test in place of the original test adapter which could not be located.

9.4.3 Visual Examination

Details of the visual examination are presented in Appendix H. 6. This examination included external optical surfaces, internal optical

surfaces, and mechanical support surfaces. The summary of these findings is as follows:

- 1) A fog-like thin film was observed on a portion of the beamsplitter plate. This fog could have resulted in a small veiling
 glare. The source of this contamination is believed to be,
 most likely, the outgassing of the burned-out shutter coil,
 discussed in Section 5.5. Similar deposits were noted on the
 adjacent prime lens cells structure.
- 2) A very thin film, giving a highly specular reflection, was observed on a small portion of the front lens surface. The effect of this film on the total optical transmission of the lens was minor. Similar films had previously been noted after thermal-vacuum tests and were attributable to oil deposits from the diffusion pump. The film was not removed for analysis of contaminants because of the imposed handling restrictions, but it is believed that additional outgassing contributions attributable to the lunar exposure may be present.
- 3) Two small internal fractures were noted on the edge of the glass elements of the zoom (focal length) cell similar to the fractures observed earlier on many lens barrels. The fractures were much too small to significantly affect the lens performance and were attributed to the difference in thermal expansion of the glass and the retaining epoxy. This minor design deficiency was never corrected because the impact on the Surveyor program was not considered justified. It is reasonable to assume that these fractures may have been somewhat aggravated by the thermal cycling on the moon.
- 4) Some "water spots" were noted on the reflex condenser lens, similar to those observed earlier after the preflight thermal-vacuum testing. These had a negligible effect on the performance.
- Minor spots, discolorations, gouges, nicks, and microseal dust and other particle contaminants were noted on the optical surfaces and on some of the adjacent structural surfaces. These are attributable to preflight handling although some of the discoloration of the structural surfaces may have been enhanced by the effect of solar radiation. The effects of the aggregate of these findings on the performance were negligible.

The film on the beamsplitter (item labove) is the only obvious effect of the exposure to the lunar environment although it is probably a result of a secondary failure, as noted in Section 5.5. Lunar low temperature exposure may have contributed to the film on the front lens surface (item 7), and to the small fractures on edges of the focal length cells (item 3). The conclusions of the visual examination therefore indicated that the lens barrel subassembly withstood the lunar exposure exceedingly well.

9.4.4 Functional Measurements

Functional measurements performed included measurement of the resolution of both focal lengths, measurement of the optical transmission of the lens subassembly, and a mechanical check of the length adjustments: focal length ring gears, and iris and focus adjustments and antibacklash springs.

The resolution of both focal lengths compared well with original data. The small changes noted were well within expectations. The average values obtained were 95.0/mm at the effective focal length of 25 mm and 91.5/mm at the effective focal length of 100 mm.

The projected image showed a small increase in the veiling glare, attributable to and consistent with the discovery of the film on the beamsplitter, discussed above. The image contrast was still very good. No image effects traceable to the internal fractures at the extreme edges of the glass element of the zoom cell, discussed above, were noted. The lens was rotated about its mechanical axis at both focal length. Both the lens and the projected image were examined. The irregular fracture areas appeared dark but produced no noticeable amount of reflected light.

Results of lens transmission measurements are shown in Figure 9-8 in relation to the plot of minimum specification requirements. Original test data, measured in March 1965, are also indicated in Figure 9-8 for comparison. The measurements were taken at an effective focal length of 100 mm.

It is seen that a slight decrease in optical transmission occurred although the new values are still close to specification requirements. The loss relative to this March 1965 data was on the order of 5 percent of transmission, that is, on the order of 8 percent of original values. Departure from the specification requirement occurred only in the 0.5 to 0.6 micron region; maximum deviation was about 4 percent.

The observed loss in transmission is likely the result of the dust, film, and contamination, discussed above, particularly the film on the beamsplitter. It should be noted that the greatest decrease in the optical transmission relative to the original data was at the shorter wavelengths.

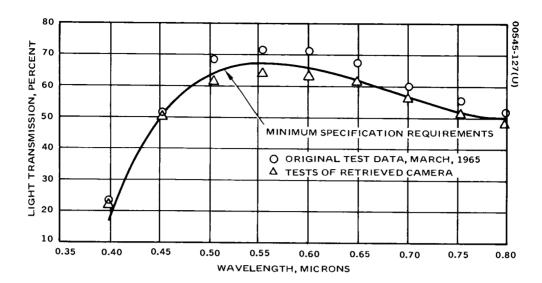


Figure 9-8. Results of Lens Transmission Measurements

This is consistent with the postulate that the effect was caused by deposits of small dust particles. The shielded location of the lens would be expected to preclude significant radiation damage. This would also result in the greatest decrease of optical transmission at shorter wavelengths.

Removal of these contaminants would be expected to lead to a much improved optical transmission plot. The Bell and Howell recommendation to do this could not be implemented because of the restrictions on the removal of contaminants. However, even with this small degradation of optical transmission, the lens would be expected to function well.

Mechanical measurements indicated that all lens adjustments were functioning properly. The three ring gears had a "positive feel" at their end stops, indicating full travel.

Some roughness was noted in the focal length adjustment. Maximum ring gear torque was measured in both the vertical and horizontal lens postures. The vertical torque measured in moving the zoom lens adjustment from the 25 mm position to the 100 mm position was 5-1/2 in-oz. In the reverse direction, similar values were recorded until the vicinity of the 25 mm stop was reached. At this point, peak values of torques were measured to be 16 in-oz vertical and 14 in-oz horizontal. This compares with the original measurement of 4.2 in-oz of horizontal torque. It should be noted that in this orientation, near and toward the 25 mm stop, the cam slot is very steep and the ring gear is essentially lifting vertically the entire weight of the zoom cell. This increase in focal length adjustment torque is undoubtedly due to the effect of the lunar environment. Even with this increase, the torque was still within specification.

The iris and focus adjustments felt smooth. The end tie backlash springs were found to be in good condition and functioning properly. The iris blades were also functioning as well as they did originally.

10. MATERIALS TESTS

10.1 OBJECTIVES AND SCOPE OF TEST PROGRAM

One of the most important objectives of test and evaluation of the returned Surveyor III television camera was to determine the degree of change or degradation of the variety of materials in the camera caused by their prolonged exposure to the lunar environment and to compare these changes with predictions. Therefore, this information may be more widely applicable to future space programs than the specific data presented in the other sections on particular components, circuits, or subassemblies.

Within the limited scope of the program, these studies were conducted to emphasize potential applicability of test results. Materials were selected that would be of most general interest to space system designers, and particular attention was given to the evaluation of parameters most vulnerable to space exposure. Any changes observed were carefully examined to determine their specific relation to the lunar environment.

Sufficient samples were not available, in general, for standard materials tests. Consequently, special nonstandard comparison tests were devised whereby properties and characteristics of retrieved Surveyor III camera materials were compared with those of a similar nonflight camera available from the Surveyor program stores. These tests proved to be very informative. Throughout this section, reference is made to these parallel tests of the spare camera, which had previously undergone type approval tests; this camera is designated as the TAT camera. In some cases, comparison tests were also conducted on Surveyor parts (e.g., chassis) available from program stores. Visual observations and test results were also compared with specifications, prior data, and predictions, as applicable.

Materials selected for the study, and the tests conducted, are grouped for convenience into the following six major categories:

- 1) Electric circuit materials
- 2) Electrical insulation materials

TABLE 10-1. TV CAMERA MATERIALS SELECTED FOR TEST AND EVALUATION

Material	Туре	Location on Camera		
	Electric Circuit Materials			
Epoxy fiberglass circuit circuit boards	Conventional board gold or solder plated etch resist	Internal chassis		
	Board reinforced with foam and aluminum	Internal chassis		
Solder	Resin cored, Sn60	Circuit boards		
Terminals	Bifurcated	Circuit boards		
Wire	Silvered copper strand insulated with teflon FEP and polyimide	Internal harness		
	Silvered copper strand covered with steel coaxial conductor insulated with teflon FEP and TFE			
	Electrical Insulation Materials			
Polyurethane foam	Polyester-toluene-di-isocyanate	Circuit boards		
Conformal coating	Epoxy-polyamide-polyamine-copolymer	Circuit boards		
Potting compound	Diepoxide of bisphenol A	Vidicon yoke		
	Organic (Polymeric) Materials			
Teflon	TFE	Exterior of mirror housing		
Nylon	6 and 6,6	Exterior of mirror housing connector		
Polyimide		Wire insulation, internal and external		
	Adhesive Materials			
Adhesive	Unfilled epoxy polyimide	Chassis		
	Alumina epoxy polimide	Chassis		
	Epiphen 825A	Mirror housing		
	Epibond 104	Mirror housing		
	FM 1000	Chassis		
	Eccobond 57C	Chassis		
	Lubricants: Friction and Wear			
Bearing lubricant	Lubeco 905	TV mirror support		
-	Barden Bartemp	Iris potentiometer and mirror elevation drive		
Gear lubricant	Microseal	Mirror elevation drive; various potentiometers		
Potentiometer carriage	DAP	Various potentiometers		
Potentiometer wire	Karma	Zoom potentiometers		
	Thermal Control Coatings			
Inorganic white paint	China clay (calcium silicate in potassium silicate)	Exterior surfaces of camera		
Organic white paint	3M velvet	Back of mirror		
Organic black paint	3M velvet	Interior of mirror housing		
Polished aluminum	6061-T4	Bottom of TV camera		

- 3) Organic (polymeric) materials
- 4) Adhesives
- 5) Lubricants, friction, and wear
- 6) Thermal control coatings

Materials selected for tests in each of the above categories and their location on the television camera are summarized in Table 10-1.

Additional supporting data are presented in Appendix I. Results obtained and conclusions on the effects observed are included in the discussion in this section of each of the six categories. A summary assessment of the results of materials tests is presented in Section 1.

Additional materials tests were also conducted under the companion NASA contract on the other returned Surveyor III parts. These tests, reported separately in Reference 15, complement some of the findings reported here.

10.2 ELECTRIC CIRCUIT MATERIALS

10.2.1 Introduction

The electric circuit materials tested included circuit boards, interconnections, and internal wire and cable. The circuit boards tested included six chassis (Al, A2, A3, A4, A5, and A6) from the Surveyor III TV camera, as well as five spare chassis available from the Surveyor program, identical to chassis Al through A5. The internal wire and cable included the unshielded hookup wires and a coaxial cable.

The six Surveyor III chassis have been described in some detail in Section 4; Figures 4-12 through 4-14 in Section 4.8.4 illustrated their general appearance, and the cordwood module construction of the camera was discussed in Section 4.3. Several types of construction were represented: conventional and foam-reinforced mother boards, cordwood modules, and terminal boards. The etched circuits used were both gold plated and fused solder plated.

Chassis A1 and A2 entailed a conventional mother board construction with plated-through holes, using either gold or solder plate as the etch resist. The base material was G-10 epoxy fiberglass. These chassis each contained a combination of cordwood modules and terminal-mounted discrete components. A minimum of 0.0015 inch of copper was used in the plated-through holes.

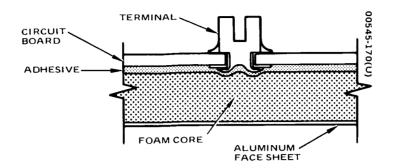


Figure 10-1. Etched Circut Board Sandwich Construction

Chassis A3, A4, A5, and A6 were foam-reinforced mother boards constructed of relatively thin circuit board, reinforced with foam, and faced with aluminum to form a stiff lightweight sandwich construction (Figure 10-1). Gold or solder plate was used as the etch resist.

Cordwood modules were used on the two conventional mother boards chassis A1 and A2, as well as on two of the four foam-reinforced mother boards, chassis A5 and A6. The etched circuit cards used to interconnect the leads were fabricated with redundant circuit patterns on each side of an 8 mil core of G-10 epoxy fiberglass. As with the mother boards, the hole plating was a minimum of 0.0015 inch copper, and the plated resists were either gold or tin-lead.

The solder used to assemble the cordwood modules and to attach the components to the terminals in the mother boards was an Sn60 tin-lead alloy, in accordance with QQ-S-571. Resin-cored solder used was Kester 44, an activated type conforming to type RA or QQ-S-571.

All terminals used in the circuit board assemblies were bifurcated. The terminals were gold plated and after installation were soldered to the circuit traces to ensure good electrical connection.

The boards of the Surveyor III TV camera and of the spare camera are listed and identified in Table 10-2. The number and location of the gold-plated and solder-fused samples tested are also shown in this table.

The hookup wire examined consisted of an unshielded silver-coated AWG-24 stranded copper alloy conductor, insulated with an extruded teflon FEP primary coating and a thin polyimide coating. This wire, referred to as ML-FEP wire, was manufactured to a Hughes material specification by Suprenant Manufacturing Company of Clinton, Massachusetts. In addition, selected tests were conducted on samples of AWG-24 wires, covered by teflon TFE insulation, from the focal length motor and from the filter wheel potentiometer.

The internal coaxial cable tested was a seven-strand 95 ohm impedance cable. The AWG-34 steel inner conductors were copper covered and

TABLE 10-2. CIRCUIT BOARD MATERIALS

		Mother	Board			wood		minal
	Gold F	Plated	Solder	Fused	2000 0 1	lules	F00 - 1	ards
Chassis	Conventional	Foam Reinforced	Conventional	Foam Reinforced	Gold Plated	Solder Fused	Gold Plated	Solde: Fused
			Surveyor III	TV Camera				
A1			ī			5		
AZ	1				4	3		
A3		1	1 1					
A4				1				
A5		1			2 2	3	ĺ	
A6				1	2	6		
			Spare Surveyor	TV Camera				
A1			1		1	5		
AZ			1			7		
A3				1				
A4				1				
A5		-1				5		1
Totals	1	3	3	4	8	34	1	1

silver coated, with teflon FEP insulation. The AWG-38, silver-plated, braided copper wire outer conductor was insulated with teflon FEP. A section of the removed external TV cable was also examined.

10.2.2 Visual Examination of Circuit Boards and Interconnections

A visual microscopic examination was conducted at magnifications to 60X on the six Surveyor III camera chassis and on the five spare chassis listed in Table 10-2. Summarized below are some of the significant anomalies noted that are attributable to exposure from the lunar environment, as well as certain fabrication and workmanship details which might be useful for the selection of materials or processes for future space applications.

Severe cracking of the conformal coating was observed on the chassis, especially in the thicker sections around the discrete components. Heavy buildup in these areas was used to bond and fillet the component bodies to add mechanical integrity to the component assembly. Conformal coatings, subsequently studied in more detail, are discussed in Section 10.3.3 and 12.7. As noted there, some of this cracking had been present prior to launch.

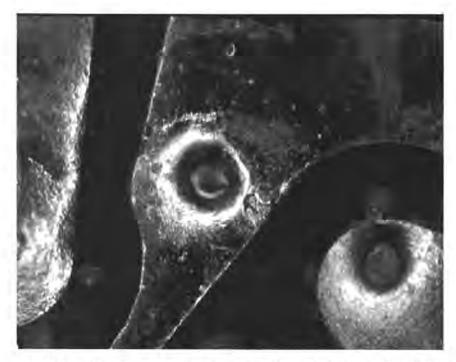


Figure 10-2. Solder Flux on Cordwood Module of Chassis A1 (Photo 00545-171)

Flux residues were observed in and around the solder joints on five of the six Surveyor III chassis but not on the spare TV chassis. The amount of flux on cordwood modules was small for the most part, consisting of small flecks around terminals which were mounted through a metal chassis and foam core on the foam-reinforced mother boards. This type of construction offers limited accessibility for thorough cleaning and flux removal. No evidence of deterioration, such as corrosion, was noted on any of the assemblies. The appearance of the solder flux on a cordwood module of chassis A-l is shown in Figure 10-2.

The solder joints on the cordwood modules were examined carefully to determine whether any cracking or other effects were present.* No anomalies were found. However, many of the solder joints on the mother board of Surveyor III chassis A-1, A-2, A-3, and on the spare chassis A-3 had a wrinkled appearance, as shown in Figure 10-3 for Surveyor III chassis A-1. The wrinkles were formed when wires were soldered to terminals already soldered to the mother board and epoxy coated. The heat of this operation melted the solder under the cured epoxy coating. As it cooled, it reshaped itself and the coating into the new shape. Only those connections with a generous solder fillet displayed this phenomenon.

This had been noted on electrical chassis of the Surveyor landing radar subsystem; it had caused significant problems during the Surveyor test program and concern during the Surveyor missions.

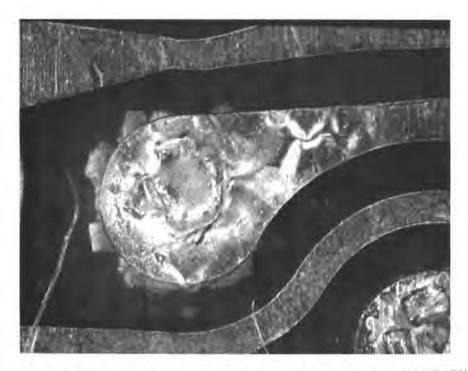


Figure 10-3. Wrinkled Solder Joint on Mother Board of Chassis A1 (Photo 00545-172)

One cordwood module each on Surveyor III chassis A-1, A-5, and A-6 showed some evidence of having been sanded after the soldering operation and before epoxy coating, presumably to meet height restrictions. There was no evidence that this sanding was in any way detrimental to the module. Some degree of "measling" was also observed on at least one cordwood module circuit board on each of the six Surveyor III chassis; however, no anomalies related to this were noted.

10.2.3 Physical Tests of Circuit Boards and Interconnections

The physical tests conducted included the following:

- 1) Solder joint metallurgical examination and pull strength
- 2) Solderability of bifurcated terminals
- 3) Peel strength of conductors
- 4) Specific gravity of circuit board materials
- 5) Circuit board hardness

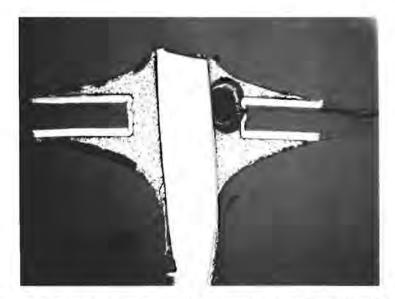


Figure 10-4. Void in Solder Joint of Cordwood Module (Photo 00545-173)

Metallurgical Examination of Solder Joints

Eight different soldered connections, six from cordwood modules and two from carrier boards, were mounted in plastic and cross-sectioned for a thorough metallurgical examination of the joints at various magnifications. The only anomalies noted were voids in soldered joints and some minor manufacturing defects in terminal installation not affecting performance.

Figures 10-4 and 10-5 are typical examples of the extensive photographic analysis that was carried out. Figure 10-4 illustrates a void noted in the solder joint of a cordwood module. Figures 10-5a and b show cross sections of typical solder joints mated to the circuit boards by a resistor and a diode lead, respectively, taken at a magnification of 50X. Figure 10-5c shows a cross section of the solder joint between a stranded wire and the bifurcated terminal at a magnification of 30X and illustrates an incomplete filling of the plated-through hole with solder.

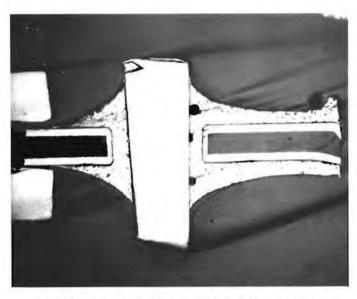
Solder Joint Pull Strength

Five solder joints were removed from component leads of the Surveyor III cordwood modules and from corresponding components of the spare chassis, and a pull test of each was conducted in an Instron tensile testing machine. All lead wires were 0.016 inch in diameter. The Surveyor III leads were gold-plated copper, and the spare samples were tin or silver-plated copper.

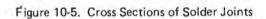
The results of the pull strength test are summarized in Table 10-3 No significant degradation was noted that can be attributed to the lunar environment; the difference in values obtained can be traced to the difference in the wire materials.

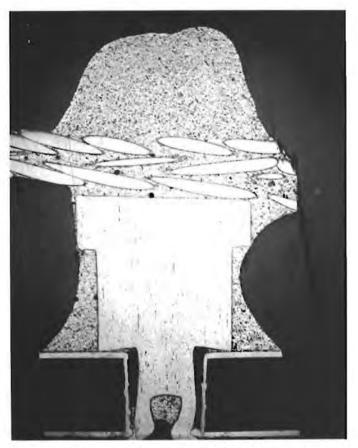


a) Resistor Lead to Circuit Board (50X Magnification) (Photo 00545-174)



b) Diode Lead to Circuit Board (50X Magnification) (Photo 00545-175)





c) Stranded Wire to Bifurcated Terminal (30X Magnification) (Photo 00545-176)

TABLE 10-3. SOLDER JOINT PULL STRENGTH TEST RESULTS

	Solder Joint Yield Load, pounds				
Sample Designation	Surveyor III Camera	Samples From Spare Chassis			
1	7.2	11.3			
2	9.8	10.9			
3	9.7	12.1			
4	9.3	12.3			
5	8. Z	$\frac{11.4}{}$			
Average	8.8	11.6			

It was observed that the solder joints from the Surveyor III module had consistently less solder filleting than those from the nonflight backup unit. It was also observed that a small spot of solder some distance away from the solder joint on one gold-plated lead showed evidence of poor adhesion and had flaked off the lead, leaving bare copper. Adhesion of the solder to the lead in the plated-through hole, however, was much better, as indicated by a visual examination after the pull test.

Solderability of Bifurcated Terminals

Solderability of bifurcated terminals from the lunar sample was checked by soldering wires into terminals from the carrier boards and observing the relative ease with which solder flow and wetting took place. Six terminals were checked on one of the chassis. Two of these had not been used previously, and four were desoldered for this purpose. A mildly activated flux (Alpha 611) was used, along with a soldering iron with a 600°F tip. The terminals soldered with ease, and complete solder wetting occurred on all terminals, demonstrating that the lunar environment had no effect on solderability.

Circuit Peel Strength

Eight relatively straight conductors, four from Surveyor III chassis A-1 and four from a spare chassis A-1, were tested for peel strength. First, the epoxy coating was removed with a hot knife from each test board. The conductors were cut and prepared for peel testing on an Instron testing machine. The test setup is shown in Figure 10-6, and results are summarized in Table 10-4. No significant effects of the lunar environment can be concluded.

TABLE 10-4. CIRCUIT PEEL STRENGTH TEST RESULTS

Samples From	From Peel Force, pounds				
A-1 Chassis	Initial	High	Low	Average	Peel distance, inches
		Surv	eyor III (Samera	
Conductor 1	0.295	0.295	0.215	0.260	1.4
Conductor 2	0.201	0.205	0.119	0.150	1.4
Conductor 3	0.189	0.277	0.105	0.150	1.4
Conductor 4	0.215	0.256	0.122	0.170	1.4
		S	pare Car	nera	
Conductor 1	0.315	0.309	0.195	0.250	1.4
Conductor 2*					
Conductor 3	0.275	0.260	0.125	0.180	1.4
Conductor 4	0.391	0.345	0.235	0.280	1.4

^{*}Inconclusive data; conductor in poor condition.



Figure 10-6. Conductor Peel Strength Test Setup (Photo 00545-177)

Specific Gravity of Circuit Board Material

The specific gravity was measured of three selected pieces of circuit board material from chassis A-1 of the Surveyor III camera and of three pieces selected from chassis A-1 of a spare Surveyor camera. The results indicated that the lunar exposure did not produce any significant degradation.

Circuit Board Hardness

A standard ASTM-D-229 hardness test was conducted on five pieces of circuit board material, one each of the Surveyor III chassis A-1 and A-2 and one each of the spare chassis A-1, A-2, and A-3. Results, summarized in Table 10-5, indicated no major changes occurred from the lunar exposure.

Physical test results indicate that the circuit board materials and interconnections withstood the lunar environment very well. No major detrimental changes were observed that could be attributed to the lunar exposure, and all materials and interconnections were in good condition to continue to perform their required functions.

10.2.4 Internal Wire and Cable Tests

Results of tests conducted on the Surveyor III camera hookup wire and on an internal (harness) cable are summarized in this section, with supporting detailed data presented in Appendix I-1.

Wire tests were conducted on samples of the ML-FEP and teflon TFE-coated wires from the internal harness and on the ML-FEP wires from the filter wheel potentiometer in an area directly exposed to solar radiation. Certain insulation tests of the wire insulation and of the exposed TFE tubing of the filter wheel potentiometer were included in the test program. * Whenever applicable, comparison tests were conducted on similar samples from the spare (TAT) camera.

Tests of the internal cable were also accompanied by comparable tests on a similar cable from the TAT camera and included examination of the attached male/J2 connector.** The external cable and braid with the attached J3 connector, previously removed from the camera during the MSC operations and shown in Figure 3-24 (Section 3), were also examined.

The tests included a detailed visual inspection, microscopic examination, and electrical, metallurgical, and physical measurements.

^{*}Also see Section 10.4.3.

^{**} This connector, J2, was one of the three unfastened during the MSC operations described in Section 3.2.3. Only the male part, attached to the cable, was examined here. Tests of the fourth connector from the mirror assembly were discussed in Section 8.5.

TABLE 10-5. HARDNESS OF CIRCUIT BOARD SAMPLES

Circuit Board	Rockwell E Scale Numbers
Surveyor III Chassis	
Al	25,* 60, 60, 60
A2	60, 55, 50, 65
Spare Chassis	
A1	58, 45, 55
A2	68, 68, 68
A3	65, 62, 65

^{*}Attributable to experimental error.

The general physical appearance of the wire harness was good. The teflon wrap was tight and smooth and appeared unaffected by the lunar exposure; this was also true of the securely tied nylon wraps and other attachments. Closer examination, however, revealed some flaking of the ML coating from the FEP teflon insulation beneath nylon tie wraps, where epoxy adhesive was used for securing the ties, and near bend in the harness. This condition was more pronounced for exposed nylon tie wraps, but also occurred under the teflon wrap. The flaking is illustrated in Figure 10-7. Similar flaking was noted on the TAT camera harness, but comparison indicated that lunar exposure had definitely aggravated this condition on the Surveyor harness.

Further studies indicated that two distinct mechanisms of degradation were involved; surface flaking resulting from the effects of thermal cycling and abrasive action of the tie cords. Improved materials currently employed would, most likely, not be as susceptible to flaking by thermal cycling as the Surveyor III harness; however, the abrasive effects of the tie cords probably would still occur.

Solder joints appeared to be generally unaffected by the lunar exposure. Measurements of voltage drop across the solder junctions of the wire to the socket pins yielded nominal results; measurements of the tensile strength of the solder connector between the contacts and the wire yielded an average value of 25 pounds, compared to 27 pounds for the TAT camera connector. Closer examination of the pins of the J2 connector revealed some physical deterioration of the plastic shell inserts and of the gold finish on the connector contacts, particularly of that portion of the contact that was inserted in the plastic insert. However, these minor changes apparently did not significantly degrade performance.



Figure 10-7. Flaking of ML Coating From Surveyor III Internal Wire Harness (Photo 70-5497)

Minor discoloration was noted on the conductors and on exposed lacing cord tie wraps. The conductors were greenish in appearance near the stripped ends of the wire, but this was also noted on the TAT harness and therefore is not considered significant. The discoloration of the tie wraps was due to the epoxy used to secure the lacing cords of the Surveyor III harness.

The component leads examined included the focal length drive motor leads and the filter wheel potentiometer leads. The former included six color TFE-insulated leads: red, yellow, purple, blue, black, and green. The latter included three ML-FEP-coated wires, and three colored TFE insulated wires, and were partially covered with TFE sleeving. The filter wheel potentiometer leads were partially exposed to solar radiation through the mirror opening. All the component leads, as well as the teflon tubing, appeared totally unaffected by the lunar environment, and all colors were bright and clear.

The internal coaxial cable protected by a wrap of teflon tape appeared to be completely unaffected by the lunar exposure. Upon removal of the teflon, the cable silver braid was found bright and free of cracks and the cable was flexible and appeared intact.

Examination of the external cable confirmed previous results of the visual inspection. The briad had darkened considerably but otherwise seemed unaffected. Visual examination of the ML-FEP wire after the removal of the briad revealed no changes caused by the lunar environment.

Electrical measurements also included connector voltage drops, capacitance, resistance, dielectric strength, and insulation resistance of the wire hearness and of the cable. All capacitance, resistance, and insulation resistance measurements were nominal. Dielectric strength measurements were conducted on twisted pairs of FEP insulated wires. The tests entailed application of 1500 volts at 60 Hz for 1 minute, followed by 3000 volts at 60 Hz applied for 1 minute. All of the Surveyor III camera wires tested, as well as the TAT camera wires tested, passed this test with the leakage current flow below the specified 200 microamperes, with the exception of one Surveyor III twisted pair which had exhibited the flaking. In this one case where the ML coating had flaked off from the FEP surface, breakdown occurred at 1000 volts at 60 Hz.

Physical and metallurgical tests included microhardness tests, wire tensile strength and elongation measurements, and insulation cut-through tests of the wires, in addition to detailed microscopic examination for metallurgical effects. Included in these tests were determination of the tensile strength of connector solder joints, as previously mentioned.

Photomicrographic studies indicated no discernible differences between the Surveyor III specimen and those taken from the TAT camera, as discussed in Appendix I-1 and shown in Figures I-1 through I-6.

Microhardness tests were conducted on AWG 24 alloy wire and on the soft copper shield wire of both the Surveyor III and the TAT camera. No significant effects of the lunar exposure were noted. The hardness of the alloy wire of the Surveyor III camera measured 87.0 on the Rockwell F scale, compared with 91.4 for the TAT camera. This difference is well within the normal variation and not considered significant.

Measurements of the tensile strength and elongation were conducted on the harness wires, insulation, and internal cable of both the Surveyor camera and the TAT camera. The tensile strength of the copper conductor from the Surveyor III camera was found to be 11 percent lower than that of the TAT camera. This is not considered an important reduction; it is within specifications. It should also be noted that tensile strength measurements of the copper conductor of the exterior cable yielded values of 53 percent lower than those obtained for the similar cable of the TAT camera. These measurements were conducted on the companion NASA contract (Reference 1). The reduction in tensile strength of both wires is

attributed to thermal annealing. The exterior wire was at a higher temperature on the lunar surface; thus, the reduction of its tensile strength was much greater. Results of elongation measurements of wires from the interior cable were inconsistent because of the limited length of available samples.

Insulation cut-through measurements were made on samples of the ML-FEP wire and on the TFE wire. Internal harness samples, as well as samples from the mirror filter wheel potentiometer, both under the TFE tubing and exposed outside the tubing, were tested. Results indicated that insulation hardness was reduced for wires exposed to the environment. The hardness of the insulation of the well protected internal harness was the same as that of the TAT camera. The hardness of the insulation of both the TFE and ML-FEP wires under the TFE tubing of the filter potentiometer was lower by about 25 percent. The hardness of the insulation of both the TFE and ML-FEP exposed wires was lower by 50 percent.

Additional studies of effect of lunar exposure on the Surveyor III external cables were conducted as part of the companion contract on the other retrieved Surveyor III parts. Results of these studies, which complement the information summarized above, are presented in Reference 1.

10.3 ELECTRICAL INSULATION MATERIALS

10.3.1 Introduction

The second group of materials tested, electrical insulation materials, is discussed in this subsection. These materials included the polyurethane foam used in the construction of the electrical chassis, conformal coatings used on the camera electronics, and resin potting compounds used as encapsulants for various camera units and components. Tests of wire insulation were discussed in Section 10.2.4.

Visual and microscopic examination was conducted on these materials. In addition, measurements of electrical characteristics, chemical analysis, and tests of physical properties were conducted on selected samples, as deemed appropriate. Comparison tests were also performed on similar samples from the spare (TAT) camera or other spare chassis, as applicable.

The polyurethane foam was polyester-toluene-diescocyanate, blown with carbon dioxide, having a nominal density of 8 lb/ft³. The material was manufactured by the Upjohn Company, CPR Division, and is designated CPR23-8. The foam was used as the spacer between the etched circuit board and the aluminum plate in the sandwich-type chassis. The material was preblown by the manufacturer, then cut to shape and adhesively bonded in the fabrication of the chassis.

The conformal coatings used on the Surveyor electronics were epoxy-polyamide-polyamine copolymers with the filleting material containing an expanded silica. These materials were applied over the components and circuitry to provide electrical insulation and mechanical support for the electronic assemblies.

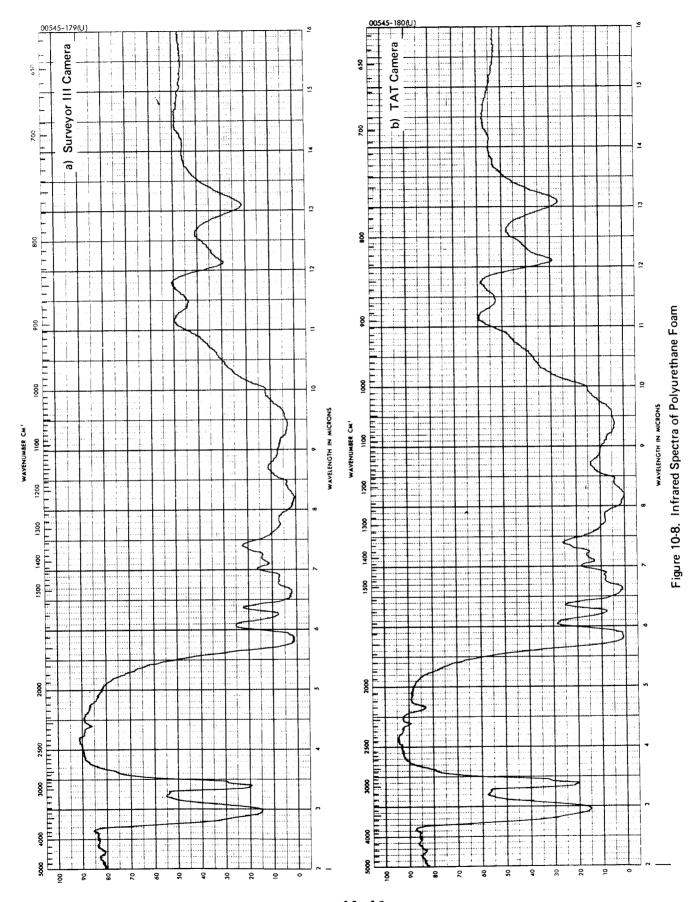
The resin potting compounds tested consisted of a purified diepoxide of bisphenol A cured with two aromatic amine coreactants: aminobenzylthiol and 1,3-benzene diamine. Two types of potting compounds were tested: one with an aluminum oxide filler and the other unfilled. The filled version was used to encapsulate the magnetic reactors. The unfilled potting compound was used to encapsulate windings of the vidicon deflection yoke.

10.3.2 Tests of Polyurethane Foam

The polyurethane foam samples tested were taken from chassis A-4, A-5, and A-6 of the Surveyor III camera and from circuit boards of similar spare chassis available from program stores for comparison. Sections of the aluminum plate were removed using an end mill to provide access to the foam.

The Surveyor III foam was yellowish-white to light tan where it was not coated by the adhesive. The compound appeared coarse and granular and lacked the cell structure of a closed cell foam. The material was quite friable, lacking abrasion resistance and mechanical strength. The samples taken from the spare chassis had an appearance and properties very much like those taken from the Surveyor III camera.

Infrared spectra were made of samples of both the Surveyor III camera and the spare chassis to determine whether any chemical changes had occurred. The samples were dispersed in potassium bromide, pelletized for these tests, with the nominal concentration being 4 percent. The spectograms are shown in Figures 10-8a and b for samples from the Surveyor camera and the spare chassis, respectively. They are identical except in the region between 4.6 and 4.7 microns. The spectral peak in that region corresponds to that of isocyanate, -N=C=O. Apparently, the Surveyor III sample indicates the absence of isocyanate. This is either due to a chemical reaction at an extended elevated temperature or to sublimation. The latter cause is considered less likely because of the relative difficulty of diffusion through the foam and from the protected foam surfaces. The high temperatures during the 32 lunar days are believed to have been the primary source of this occurrence by giving rise to the chemical reactions. This change, however, is not considered to significantly alter the chemical properties of the foam.



10-18

Original plans also include certain physical and electrical tests. These tests were not performed because adequate samples of foam were not obtainable. The absence of new functional groups which could contribute to electrical conductivity and the apparent retention of the chemical composition of the foam (with the exception of the relatively minor change above) would indicate that the electrical and physical properties were probably not significantly altered by lunar exposure.

No further investigation was conducted of possible chemical reactions and of the potential effects of the products of outgassing on other spacecraft components. Such a study of possible application to future designs was considered to be outside the limited scope of this contract.

10.3.3 Tests of Conformal Coatings

Visual Examination

The conformal coatings examined included those on chassis A-1 through A-6 and the ECU of the Surveyor III camera, as well as those on similar spare chassis available from stores. Results of the visual observation conducted are presented in Table 10-6.

The significant finding, universally applicable to almost all of the Surveyor III camera samples examined, was the extensive cracking of the conformal coating. By comparison, the coating of the spare chassis exhibited only slight cracking. The cracking of the Surveyor III conformal coating is illustrated in Figure 10-9. In some cases, primarily the components with glass cases, this cracking of conformal coating resulted in cracking of the case or even in damage to the components. Further discussions of these occurrences of component failures and of Surveyor experience with problems with conformal coatings are presented in Section 12.

It was also noted that, generally, the coatings behaved similarly on similar surfaces of similar components regardless of their location. Radial cracking was found on the coatings around gold-plated terminals, metal case transistors and capacitors, and ceramic case resistors. Axial cracking occurred in the coatings surrounding the ceramic case resistors and the glass case capacitors, with axial cracking in some instances damaging the glass casing of diodes and resistors.

The cracking tendency was apparently influenced by the thickness of the coating. Where the coating thickness exceeded the diameter of a component by 20 to 25 percent or where the coating was thicker than 0.3 inch, cracking was generally observed. Coating thicknesses less than 0.01 inch were essentially crack-free. With the exception of the glass case components, where the coating cracks frequently propagated into the glass, the cracks did not appear to have affected the surface of the components.

TABLE 10-6. RESULTS OF VISUAL INSPECTION OF CONFORMAL COATINGS

	Coating Condition			
Surface and Component Types	Lunar Exposure — Surveyor III Camera	Earth Exposure — Backup Chassis Boards		
General description of coating	Amber transparent film with some cracking (see below) but no chalking. Fillets transparent to translucent with extensive cracking.	Amber transparent film with essentially no cracking or chalking Fillets similar to lunar material but with only slight cracking.		
Epoxy-glass laminate of etched circuit board	No cracking or separation of coating except for small area (less than 1/4 square inch) on chassis A-5 exhibiting some separation near a metal insert.	No cracking or separation of coating.		
Etched circuit lines, gold and tin/lead plated	Occasional slight straining of gold surfaces. No cracking or separation of coating.	No discoloration of surfaces; no cracking or separations.		
Terminals, gold plated	Radial cracking of fillet but apparent adhesive separation or solder joint damage. Thickness 0.01 to 0.05 inch occurrence greater than 50 percent.	Similar to lunar occurrence — approximately 50 percent.		
Glass case diodes	Axial cracking of coating and some cases. Thickness 1/3 to full component diameter. Occurrence 10 to 20 percent for coating, less than 10 percent for case damage.	Axial cracking of coating; case damage inconclusive. Thickness 1/3 to full diameter. Occurrence less than 10 percent.		
Glass case capacitors	Cracking at coating fillet on major axis ground at right angles. Cracks general on one side only. No case damage observed. Thickness 0.03 to 0.1 inch. Occurrence approximately 100 percent.	Similar to lunar conditions.		
Glass case resistors	Axial cracking of fillet with some case damage. Thickness 1/3 to 1/2 diameter. Occurrence less than 20 percent.	Axial cracking of fillet for thick- ness equivalent to diameter. No case damage observed. Occur- rence approximately 20 percent. Thickness less than 1/2 showed no cracking.		
Ceramic case resistors	Axial and radial cracking observed along major axis. Radial cracking over metal end caps. No damage to case. Thickness 1/4 to 1/2 diameter. Occurrence 60 to 80 percent.	No cracking of fillets along major axis or coating over end caps. Thickness less than 1/4 diameter.		
Metal case capacitors	Radial cracking of fillets with no adhesive separation or case damage. Thickness 1/4 to 1/2 diameter. Occurrence approximately 100 percent.	Similar to lunar, but occurrence approximately 50 percent.		
Metal case capacitors having fiberglass insulation	Similar to metal case capacitors; occurrence approximately 100 percent.	Similar to lunar, but occurrence approximately 10 percent.		
Metal case transistors	Radial cracking of fillet with no case damage or adhesive separation. Thickness 0.05 to 0.1 inch. Occurrence approximately 80 percent. Those having no cracks had fillets 0.2 inch or greater.	Similar to lunar samples, but occurrence 30 percent.		
Mold plastic cases	Some radial cracking adjacent to leads. Thickness 1/2 diameter or greater. No case damage. Occurrence approximately 50 percent.	No cracking observed. Thickness 0.01 to 0.05 inch.		



Figure 10-9. Cracking of Conformal Coating on ECU of Surveyor III Camera (Photo 00545-181)

In most cases, the fillets and coatings were still adherent, except for the immediate area of cracking, and were capable of providing the mechanical support.

Two possible explanations were postulated of the cracking of conformal coating: 1) effects of thermal cycling coupled with the differences in thermal coefficients of expansion, and 2) chemical changes in the conformal coating. The chemical analysis and physical tests described below were performed to help explain these anomalies.

Except for the cracking, all of the coatings were similar in color and appearance, both on the Surveyor III chassis and on the spare chassis. The amber color of the coatings did not appear to have changed.

Physical Tests

Hardness measurements were performed, using the "pencil lead" hardness test, on both the Surveyor III and the spare chassis coatings to determine possible effects of the lunar environment on physical properties. Pencil leads of increasing hardness were drawn along the coating surface until an onset of abrasion occurred. The hardness of the coating was then taken to be equal to the hardness number of the lead pencil.

TABLE 10-7. RESULTS OF ELECTRICAL AND PHYSICAL MEASUREMENTS OF CONFORMAL COATINGS

		Solv	Electrical Resistance,			
Source of			Weight After		ohms	
Conformal Coating Sample	Hardness (Equivalent Lead Pencil)	Initial Weight, grams	Solvent Immersion, grams	Percent Increase in Weight	Test at 54 Volts	Test at 180 Volts
Surveyor III camera	6 to 7H	0.150	0.222	48	9.0 x 10 ¹⁰	1.8 x 10 ¹¹
Spare chassis	5 to 6H	0.132	0.193	46	1.5 x 10 ¹³	1.8 x 10 ¹³

Results of this test are indicated in Table 10-7. It is seen that the conformal coatings exposed to the lunar environment were harder than the ones on the spare chassis by about one hardness unit (1H). Such an increase in hardness could result from any of three causes: 1) increased chemical reaction and cross-linkage due to extended high temperature exposure on the moon; 2) variations in coating formulations, and 3) sublimation and reduced pressures of lower molecular weight fragments, which would have a plasticizing effect.

Chemical Analysis

The chemical analysis of both the Surveyor III and spare chassis samples was then conducted to identify changes brought about by the lunar environment, help explain the apparent changes in hardness, and identify the cause of the cracking. This analysis included a solvent swell test and infrared spectroscopy.

The solvent swell test was conducted to determine the differences in cross-linking density between the Surveyor III and spare chassis samples. Samples of the coatings were analyzed in dichloromethane for approximately 250 hours and their change in weight compared. A lower percent of change in weight corresponded to higher cross-linking.*

^{*}In the solvent swell test, higher cross-linking implies greater material degradation and lower absorptance.

Results of this test are indicated in Table 10-7. While the difference between the percent changes in weight of the two samples are small, it is obvious that no significant cross-linking occurred in the lunar environment. In fact, the spare chassis sample would point out a somewhat higher indication of cross-linking than the sample exposed to lunar environment. The solvent swell test thus virtually eliminated this as a potential cause of the observed increase in hardness.

After the immersion cycle, the solvent was analyzed by infrared spectroscopy to determine differences in extractable materials and to help interpret the chemical differences in the coatings. The infrared spectrograms are shown in Figure 10-10 for the Surveyor III and spare chassis samples. These spectra included the solvent blank and the extracts produced during the swell studies.

Comparison of the two figures reveals the presence of peaks at 5.85 and 9.15 microns for the Surveyor III sample, which are not present in the spectra of the spare chassis samples. These peaks represent carbonyl and ether groups and indicate the presence in the extract of polyamide coreactant and low molecular weight fragments of the polymer. A spectogram of the spare chassis sample, Figure 10-10b, on the other hand, shows additional peaks at 2.9 and 6.25 micrograms, attributable to water. This sample was essentially free of polymeric materials.

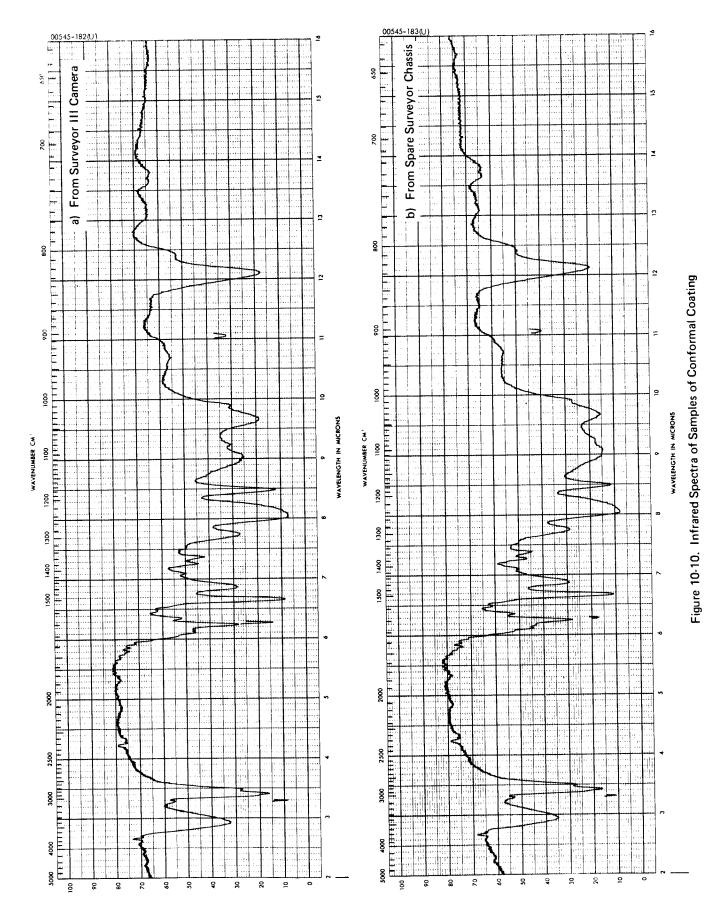
Results of infrared spectroscopy indicated that the low molecular weight fragments were apparently not present in the Surveyor III samples. On the contrary, such materials appeared to be more evident on the sample from the spare chassis. This observation suggested that the observed increase in hardness was not caused by sublimation. This result also tended to eliminate chemical changes as the cause of cracking of the conformal coating.

Results of the above chemical analysis indicated that the increased hardness was most likely attributable to the variation in coating formulations and that the cracking of the coating was caused entirely by thermal cycling in combination with excessive coating thickness.*

Electrical Tests

Measurements of the electrical resistance of the coatings were conducted to determine the effect of lunar exposure on the dielectric properties of the material. The resistance was measured by applying a voltage between two parallel coated conductors and measuring the current flow. Similar chassis with identical circuit connections and circuit geometry were tested: one spare and one from the Surveyor III camera.

^{*}Also see Section 12.7.



10-24

Results of the test, conducted at two different voltage levels, are also given in Table 10-7. Apparently, the samples from the Surveyor III camera had a significantly lower resistance. This result, however, must be qualified since the measurement includes the resistance along the surface of the epoxy-glass circuit board. The values measured therefore depended heavily on the condition of that surface. Presence of flux residues when the coating was applied, for example, would lower the measured resistance value considerably. Similarly, unreacted, or partially reacted amines and amides would result in lower resistance readings. The only positive conclusion that can be drawn from these measurements is that the conformal coating of the Surveyor III camera was more than adequate in its electrical insulation characteristics for all applications except those requiring extremely high impedances.

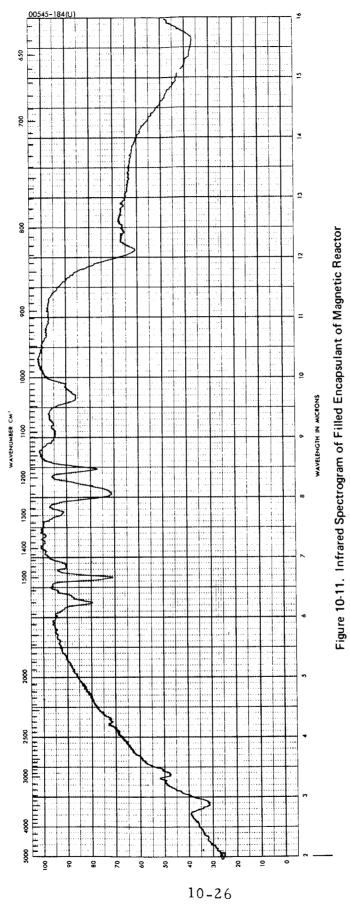
Measurements of the dissipation factor of conformal coating, originally contemplated, were not conducted because of the difficulty in performing meaningful tests.

10.3.4 Potting Compound Tests

Visual Examination

Both the filled resin encapsulant of the magnetic reactors and the unfilled encapsulant of the vidicon deflection yoke were visually examined. The epoxy resin of the filled encapsulant used in the magnetic reactors was a clear light brown and showed no discoloration. No cracking was observed in the resin or around filler particles. However, some adhesive cracking was noted around the steel inserts which extend through the package. Cross-sectioning of a reactor revealed some voids in the interstitial volume of the wire windings. The adhesion to the wire insulation appeared good, and no separation from the diallyl phthalate case was noted. The appearance of the resin in the sectioned area was similar to that which was exposed on top of the reactor package.

A quarter section was removed from the deflection yoke along the major axis to expose the unfilled encapsulant. The color of the resin was light brown, with no sign of discoloration. Some voids and cracks within the resin were observed in densely wound wire bundles. In addition, extensive separations were noted between the electrostatic and electromagnetic shields. This was likely caused during the original assembly of the yoke when problems occurred with the adhesive bonding the yoke to the magnetic shield. No separations of the encapsulant from the wire insulation were seen during the examination. There were, however, some voids present in the dacron matting used as part of the insulating system.



Chemical Analysis

A sample of the filled encapsulant was analyzed, using infrared spectroscopy, to establish the presence of functional groups which would indicate a change in the chemical composition of the polymer. The spectrogram was made by dispersing the encapsulant in potassium bromide and pelletizing the sample.

Figure 10-11 shows the resulting spectrogram for the filled encapsulant. Because of the filler particle size, the region from 2.0 to 6.0 microns is somewhat obscured. However, the hydroxyl (-OH) peak occurring at 2.8 microns is detectable. This peak, combined with the absence of epoxide peaks at 10.95 and 11.6 microns, indicates the complete reaction of the epoxy resin forming the polymer. The spectrum beyond 6.2 microns is not characterized by any absorption peaks that might denote decomposition or significant changes in the chemical composition of the epoxy polymer.

Electrical Tests

The electrical resistance and the partial discharge inception voltage were determined for both the filled and unfilled versions of the encapsulant. The electrical resistance was intended to indicate changes in the electrical loss resulting from the lunar exposure, while the discharge voltage determination was used as a failure indicator to establish the presence of voids or cracks within the materials.

The resistance of the filled encapsulant of the reactor was measured between the steel insert and the inductor element. The resistance of the unfilled encapsulant was measured between the yoke screen and the electrostatic shield. The area/length factors required to convert resistance measurements to the volume resistivities were determined later when the components were cross-sectioned. These area/length factors were 5 and 150 for the reactor and the yoke, respectively. Voltage discharge measurements were made across thin samples of the encapsulant immersed in mineral oil. The thicknesses of the reactor and yoke samples were 0.1 inch and 0.3 inch.

Results of the electrical tests are summarized in Table 10-8. As noted, the volume resistivities obtained are in close agreement with the original value established for these materials. The values of the discharge (breakdown) voltages measured are consistent with the presence of faults, such as voids or cracks, in both encapsulants. These values are what would be expected for an electrical discharge in a gaseous medium, such as might exist in a crack or void. No original breakdown measurements were available for comparison.

TABLE 10-8. ELECTRICAL MEASUREMENTS OF POTTING COMPOUNDS

	Apparent Volu ohm	Partial Discharge Voltage Gradient,	
Potting Compound	Applied Voltage = 90 volts	Applied Voltage = 180 volts	volts/mil
Filled encapsulant, reactor	3 x 10 ¹³	5 x 10 ¹³	30
Unfilled encapsulant, deflection yoke	3 x 10 ¹³	1.5 x 10 ¹³	50

^{*}Original value = 1×10^{13} ohm-cm.

The dielectric constant and dissipation factor measurements originally contemplated were not made because of the difficulty of performing meaningful tests with the samples available and because it was felt that, based on other information, no significant additional information on the effects of lunar exposure would be obtained.

Physical Tests

Hardness measurements were made on both filled and unfilled compounds to establish their general condition. The measurements were of the indentation type, utilizing a durometer, and were conducted in accordance with ASTM D2240-68. Hardness of the magnetic reactor encapsulant was measured on its surface. Hardness of the unfilled yoke encapsulant was conducted on a resinous portion after cross-sectioning of the yoke assembly. Both initial values of hardness and those taken after a 10 second dwell were recorded.

Results of this measurement are presented in Table 10-9. As seen on the table, both the filled and unfilled encapsulants inhibited a hardness which exceeded the specification value and both were within the range usually observed for these compounds.

It was concluded that the lunar exposure produced no significant changes in the properties of either the filled or unfilled potting compounds. With the exception of some separation from the steel inserts of the reactors and limited microcracking in the deflection yoke, the encapsulants demonstrated a high resistance to cracking and separation throughout their exposure to the high temperatures encountered on the moon. Both encapsulants appeared suitable for space applications where extremes of temperature would be encountered, provided that they would not be subjected to voltages higher than 500 volts. For high voltage applications, existing processes require modification to eliminate the voids observed in the Surveyor III encapsulants.

TABLE 10-9. RESULTS OF HARDNESS MEASUREMENTS OF POTTING COMPOUNDS

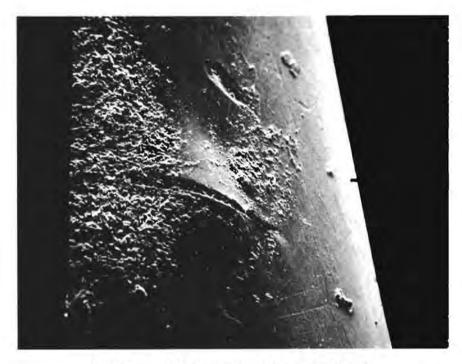
Hardness, Shore D Numb		ss, Shore D Number
Potting Compounds	Initial Value	Value After 10 Seconds
Filled encapsulant, reactor	89 ±1	88 ±1
Unfilled encapsulant, deflection yoke	91 ±2	90 ±2
Minimum specification requirement	85	
Expected range of readings	88 to 92	

10.4 ORGANIC MATERIALS

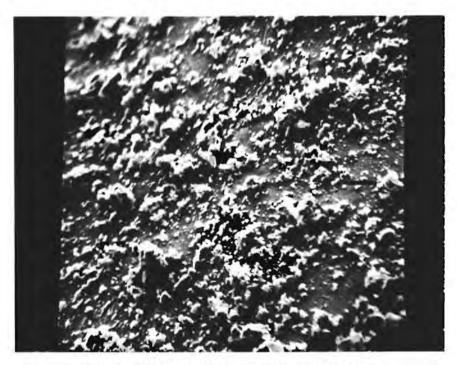
10.4.1 Introduction

The organic (polymeric) materials of the Surveyor III camera, teflon FEP, teflon TFE, nylon, and polyimide, were examined visually and subjected to chemical and physical tests. Where necessary, comparison tests were conducted on samples from a spare (TAT) camera. Results of these tests are presented in this section, with supplementary discussion of chemical analysis tests in Appendix I. 2. Additional data on parallel tests conducted on organic materials from the other retrieved Surveyor III parts are presented in the final report on the parallel NASA contract (Reference 1) and supplement the data presented here. These include nylon ties, polyimide, and TFE wire insulation, and teflon FEP used to wrap the external connectors.

Teflon TFE was examined in several places: one was the horseshoe-shaped seal at the base of the mirror housing, previously shown in Figure 3-25 and also in Figure 3-3a of Section 3. Another was the teflon collar at the base of the mirror housing, shown in Figure 3-26. The teflon in both areas was 2 mils thick and bonded to the substrate with Epiphen 825A adhesive. Both were used as seals to prevent dust from entering the TV camera (the former performed this function with the mirror closed). Tests of the adhesive are discussed in Section 10.5. Other sources of teflon TFE tested included samples of component lead insulation, cable wrap, and tubing used over wire bundles.



a) Surface (122X Magnification) (Photo 00545-185)



b) Debris (1260X Magnification) (Photo 00545-186)

Figure 10-12. SEM Photographs of Polyimide-Coated ML Wire

A separate discussion is presented in Section 12 of the observed curling of the mirror assembly teflon seal.

The nylon braided tie cords tested were the ones used for securing the harness wire bundles, both internally and externally. The polyimide tested was used as the outer coating of the FEP teflon insulated wires, previously referred to as the ML-wires. The FEP teflon insulation of these wires was also tested.

10.4.2 Visual Examination

Examination of the horseshoe area of the teflon hood from the mirror housing after its removal from the housing essentially confirmed results obtained during the initial survey examination, reported in Section 3.4.4. The teflon had turned a dark brown from its original white color and was found turned up along the edges in some areas. However, upon microscopic examination, some minor cracking was noted on the surface. Visual examination of the teflon collar on the mirror assembly similarly confirmed original observations presented in Section 3.4.4.

The nylon cords examined all had a yellowish color which, under microscopic examination, appeared to be only on the top surface of each individual strand. The color changed to a dark brown in the vicinity of the epoxy adhesive used to secure knots in the tie cords, indicating that some of the discoloration may have been the result of the epoxy wicking along the cord and discoloring. The epoxy itself was a dark brown, as expected.

The appearance of the polyimide coating of the ML wires was normal except for a slight frosty appearance on wires which had been exposed to the environment. Figure 10-12a is an SEM photograph of one of these wires. The apparent deformation in the center is attributed to the extrusion process used in manufacture to coat the wire. The area on the right is clear while the area on the left illustrates the frosty appearance. Figure 10-12b is an SEM photograph of this frosty area at high magnification. Study of the appearance of the debris suggested that it is very likely lunar material.

10.4.3 Physical Tests

Measurements of tensile strength and elongation were conducted on samples of organic materials from the Surveyor III camera and, wherever practical, compared with measurements conducted on similar samples from the TAT camera. Because of the limited amount of material available, the sizes, shapes, thicknesses, and lengths of these samples varied to some degree. For various reasons, it was also necessary occasionally to change chart speeds during these tests, which were conducted on the Instron testing apparatus. The data developed during these tests could therefore be used only to indicate general trends and effects. Results could not be interpreted as providing exact values for comparison with standards because of the limited accuracy.

Because of the limited amount of available material, particularly in the case of the teflon TFE, and because of the small size of available samples, measurements of the tensile modulus and tear strength originally contemplated were not conducted.

The samples tested and the results obtained are summarized in Table 10-10. Results are grouped into the categories discussed in the following paragraphs.

TABLE 10-10. MEASUREMENTS OF TENSILE STRENGTH AND ELONGATION OF ORGANIC MATERIALS

	Sample Description		Ultimate Tensile Strength,	Elongation,
Material	Size, inches	Source	psi	percent
Teflon TFE component lead insulation	3 long	Surveyor III camera filter wheel potentiometer	3,600	204
	3 long	Surveyor III camera filter wheel potentiometer	3,760	248
		SM/SS scoop	3,850	180
Teflon TFE	(0.065 x 0.002 x 0.5)	TAT camera circular skirt collar	4,800	160
	(0.090 x 0.002 x 0.5)	Surveyor III camera circular skirt collar	3,700	95
	(0.130 x 0.002 x 0.5)	TAT camera mirror horseshoe seal	7,970	85
	(0.165 x 0.002 x 0.200)	Surveyor III camera mirror horseshoe seal	1,670	62
Teflon TFE cable wrap	(0.002 x 0.9 x 1)	TAT camera internal cable	6,100	310
	(0.002 x 1 x 1)	Surveyor III camera internal cable	2, 175	129
Wire ML	3 long	TAT camera	14,000	56
insulation		Surveyor III camera	10,100	18
FEP	3 long	TAT camera	4,330	351
		Surveyor III camera	4,250	408
TFE tubing (FEP sleeve)		Surveyor III camera filter wheel potentiometer	1,290	

Component Lead Insulation

Results of measurements of the TFE insulation of component leads inside the camera indicated no significant degradation by the lunar environment. Values of tensile strength and elongation were in agreement with expectations. For comparison, Table 10-10 also shows results of tests conducted on teflon TFE from a wire of the soil mechanics/surface sampler (SM/SS), totally exposed to the lunar environment. This test was conducted under the companion NASA contract. While tensile strength of this insulation was unaffected by the lunar exposure, its elongation degraded somewhat.

Teflon TFE From Mirror Housing and Skirt Collar

Some difficulty was encountered in obtaining suitable test samples of the teflon TFE from the horseshoe-shaped mirror housing and from the collar under the mirror assembly due to the epoxy bonding of these dust seals. Samples from both the Surveyor camera and the TAT camera indicated very low elongation values, while the tensile values were as good, or even higher in one instance, than anticipated. This was attributable to the fact that some of the epoxy adhesive was retained by the teflon. Additional error was undoubtedly due to the very small sizes of these samples available for tests (approximately 1/4 by 1/8 inch).

Teflon TFE Cable Wrap

Comparison tests between the Surveyor III and TAT camera cables indicated that the cable wrap degraded appreciably as a result of the lunar exposure. The tensile strength apparently decreased by about 75 percent, while the percent elongation decreased by about 60 percent.

ML-FEP Wire Insulation

Tests of the ML-FEP insulation were difficult to conduct. The two coatings could not be separated for test because of the brittleness of the ML coating. It was therefore necessary to conduct the test on the combined coating samples and to select chart speeds, cross head speeds, and load cell values to distinguish the initial ultimate tensile strength of the ML portion of the specimen from the final reading of the tensile strength corresponding to that of the FEP coating. Of the many runs attempted, four were reasonably successful: one for the TAT camera specimen and three for the Surveyor III camera specimen. The latter gave similar results, and the average of the three readings is shown on Table 10-10.

It appears from the data obtained that the tensile strength of the ML coating was reduced by about 25 percent by the lunar exposure, while its elongation degraded considerably more. On the other hand, the FEP coating suffered only a small degradation in tensile strength. These results can only be interpreted, however, as general trend, rather than as the absolute values, because of the limited accuracy obtainable.

Teflon TFE Tubing

The single piece of TFE tubing tested was that used over the six component lead wires of the filter wheel potentiometer. This tubing was 0.013 inch thick and 0.188 inch in diameter and was exposed to the lunar environment through the camera mirror opening. Because of the difficulty in performing this test, elongation data could not be obtained, and the tensile strength data was only approximate. However, the values measured appeared sufficiently low compared to expectations to suggest a definite degradation by the lunar exposure.

Lacing Tape

Many attempts to obtain tensile and elongation data on samples of the lacing tape were unsuccessful. All samples available were less than l inch long, and they could not be held securely in the testing vise without damage to the individual strands of the tape.

10.4.4 Chemical Analysis

A number of tests were conducted to determine the effect of the lunar environment on the chemical composition and properties of the organic materials. These included infrared spectrochemical analysis, ultraviolet analysis, elemental analysis, relative viscosity measurements for the determination of molecular weight, electron paramagnetic resonance measurements for spin density determination, and differential thermal analysis. No evidence of any significant effects of the lunar environment were uncovered in the course of these tests. Tests conducted and results obtained are discussed in some detail in Appendix I. 2.

10.5 ADHESIVE MATERIALS

10.5.1 Introduction

The different adhesives employed throughout the Surveyor III camera were visually examined and tested to determine whether any changes in their physical and chemical properties were caused by the lunar exposure. The tests conducted included measurements of hardness, shear strength, peel strength, and electrical resistance.

The adhesives examined were from representative locations and usage on the Surveyor III camera: nylon tie knots; component and bracket bonding to circuit boards; and teflon pads to aluminum surfaces. The specific adhesives tested and their locations are listed in Table 10-11.

10.5.2 Visual Examination

No apparent change in color or appearance was seen on adhesives that were not directly exposed to sunlight. The polyamide (unfilled) which

TABLE 10-11. SUR VEYOR III CAMERA ADHESIVES TESTED

Adhesive	Use and Location
Epoxy polyamide (unfilled)	Component bonding, ECU knot securing J-l cable
Epoxy polyamide (alumina filled)	Component bonding, chassis A6 and ECU
Epiphen 825A (Borden Chemical Company)	Teflon pad to camera hood bonding
Epibond 104 (Furane Plastics Company)	Teflon felt to camera hood bonding
FM-1000 (American Cyanimid Company)	Bracket to circuit board frame bonding, chassis A6
Eccobond 57C (Emerson and Cuming, Inc.)	Thermal resistor to circuit board frame bond, chassis A3

was exposed to the sun, however, had darkened from the original light tan to a coffee-colored appearance. There was no loss in its normal gloss except that a slight amount of dust on its surface was noted.

A significant amount of cracking was observed on the unfilled epoxy polyamide adhesives, especially in the heavy beads along the side of components or at the interfaces of gold-plated circuits. Small cracks were also observed in adhesive leads at the edges of aluminum-to-fiberglass board bonds. A large number of bonds survived with no cracking. These included plastic-to-plastic bonds of unfilled epoxy polyamide adhesive; bonds of the same material to glass body resistors; and all bonds of alumina-filled epoxy polyamide adhesive, FM-1000 bonds, and Eccobond 57C bonds. The cracking appeared especially prevalent on bonds between materials with different coefficients of thermal expansion, such as fiberglass-to-aluminum boards and adhesives to gold-plated circuits. It was expected that large stresses in the adhesives could easily have been induced by the large temperature excursions in the lunar environment.

10.5.3 Hardness Measurements

Hardness measurements were conducted on the unfilled polyamide and the FM-1000 adhesives, using a modified Shore A tester. The tester was fitted with a long pointed probe, which had a radial scribe mark 0.006 inch from the tip, as indicated in Figure 10-13. The probe was pushed into the adhesive specimen until the scribe mark was flush with the

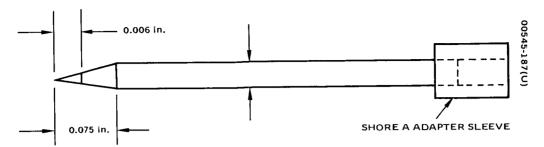


Figure 10-13. Modified Probe for Shore A Tester for Hardness of Adhesives

adhesive surface. The reading of the Shore A tester at this point was taken as the measure of hardness. At least five measurements were taken on each specimen in order to obtain reliable data. Comparison measurements were also conducted on adhesives from similar Surveyor chassis available from storage. It should be noted, however, that this technique yielded only comparative values.

Results of the hardness tests are indicated in Table 10-12. A distinct increase in hardness of the adhesives of the Surveyor III camera, relative to those of the spare chassis, can be noted. Data obtained for the knot ties (Table 10-12) indicated that adhesives which had been exposed to sunlight were apparently harder than those which had been protected. The capacitor and tie knot adhesive beads tested, also shown in Table 10-12, were of different size and shape. Consequently, no significant conclusions can be drawn from their relative hardness values.

10.5.4 Shear Strength Measurements

The shear strength of the unfilled epoxy polyamide and the FM-1000 adhesives was measured on bonded brackets and components of both the Surveyor III chassis and similar unflown chassis from storage. The epoxy polyamide adhesive measurement was conducted by determining the force required to push the bonded components from the chassis. The shear strength of the FM-1000 adhesives was measured by determining the tensile force required to pull the bonded brackets off the chassis. In each case, the direction of the force applied was parallel to the chassis.

Results of the shear strength tests are given in Table 10-13. It is apparent that the lunar exposure resulted in a significant reduction of the shear properties of both adhesives.

The reduction in the adhesive strength of the epoxy polyamide bonds appeared to have two causes. One was hardening and embrittlement of the adhesive by the lunar temperature cycling, which reduced the ability of the adhesive to distribute the loading smoothly throughout the bond area. The second cause was reduction of adhesion to the aluminum. This latter condition was apparently the result of stresses induced during the lunar

TABLE 10-12. MEASUREMENTS OF HARDNESS OF ADHESIVES

			Relative hardness	
Adhesive	Bond Position	Source	Surveyor III Camera	Spare Chassis
Unfilled	Capacitor 1	Chassis A6	70	55
epoxy-polyamide	Capacitor 2	Chassis A6	60.5	47
	Capacitor 3	Chassis A6	69.5	52
Unfilled epoxy-polyamide	Knot tie 1 (exposed)	Cable J2	58	_
	Knot tie 2 (exposed)	Cable J2	61	-
	Knot tie 3 (shielded)	Cable J2	39	-
FM-1000	Bracket to board	Chassis A6	18	12

TABLE 10-13. MEASUREMENT OF SHEAR STRENGTH OF ADHESIVES

			Failing Load	, pounds
Adhesive	Bonded Component	Source	Surveyor III Camera	Spare Chassis
Unfilled epoxy-polyamide	Capacitor 1 Capacitor 2 Capacitor 3	Chassis A6 Chassis A6 Chassis A6	25 32 62	107 127 92
FM-1000	Bracket 1 Bracket 2	Chassis A6	160 183	200 >200*

^{*}Board failed before bracket bond.

temperature excursions by the difference between thermal coefficients of expansion of components and of the aluminum chassis. This phenomenon is also consistent with the cracking noted during the visual examination as discussed above. It was also noted that the Surveyor III board bonds to the aluminum chassis failed adhesively, while those of the spare chassis generally failed cohesively.

The FM-1000 adhesive of the Surveyor III bonds appeared to be markedly embrittled. This was evident from the difference between the manner in which these bonds failed in the course of the shear strength test, as compared with the adhesives from the spare chassis. Under tensile loading, the load offset caused substantial bending of the boards, creating relatively large peeling forces on the edges of the bond. On the Surveyor III boards, the loading first caused a partial cracking of the bond from the heel edge of the bracket. No further peeling was observed as the load was increased to the final cracking of the bond. On the spare chassis, peeling started at the toe edge of the bracket and progressed smoothly until complete failure. In each case, the adhesive embrittled and failed cohesively. It is believed that this embrittlement was caused by the elevated temperatures and resultant outgassing of volatiles.

10.5.5 Peel Strength Measurements

Two adhesive bonds, Epiphen A25A and Epibond 104, were tested for peel strength. The Epiphen A25A was used to bond a 0.025 inch thick teflon pad to the edge of the mirror hood. It was found that it was not possible to pull the teflon from the bond without breaking the teflon. The teflon had become embrittled and weakened from exposure to the lunar environment. Consequently, it was not possible to determine the properties of the adhesive although it was apparent that the adhesive had retained a great deal of its adhesive bond strength.

The test of the Epibond 104 was much more successful. The Epibond 104, a high-temperature adhesive, was used to bond the teflon felt seal around the mirror pivot projecting through the hood. The test indicated that this bond had retained its strength. A force of 3.96 pounds was required to pull the felt off the hood at a 90 degree angle. In doing so, the adhesive pulled the black coating away from the aluminum substrate.

10.5.6 Electrical Resistance Measurements

The last test conducted was to determine the electrical resistance of the Eccobond 57C conductive adhesive, used to bond the thermal resistor to the Surveyor III chassis A-3. This test was also conducted on a spare chassis. The resistance values measured across corresponding bonds on the two chassis indicated 0.20 ohm for the Surveyor III adhesive and 0.44 ohm for the spare chassis adhesive. This change is not significant. It is apparent that no degradation had occurred as a result of lunar exposure although firm conclusions cannot be drawn from the single sample available. The apparent improvement in the conductivity of the adhesive is, however, consistent with data available from other heat-aging tests of similar conductive materials.

10.6 LUBRICANTS: FRICTION AND WEAR EVALUATION

10.6.1 Introduction

This subsection presents the results obtained in testing the lubricants used on the Surveyor III camera and observations of the conditions of wear of various lubricated and unlubricated surfaces of the gears, bearings, and drives. This investigation also included examination for evidence of cold welding. The only suspect cold welding areas found were those on the external surface of one of the connectors, and, possibly, on the windings of the filter wheel potentiometer. Since these two components were treated as "failures", discussion of this possible cold welding evidence is presented in detail in Section 12, Failure Analysis.

The friction and wear analysis is presented here in two parts. Section 10.6.2 discusses the results of the detailed examination of the gears and bearings removed from the TV camera and of the lubricants used. Section 10.6.3 presents the results of the friction tests conducted on the windings of the focal length potentiometer. Expanded description of this test is given in Appendix I.3.

Table 10-14 lists the Surveyor III gears and bearings examined. The focal length potentiometer was previously described in Section 8.2. The helical windings consisted of a single strand of Karma wire. Its Paliney 7 wiper contact was mounted on a DAP carriage.

10.6.2 Analysis of Gears and Bearings for Wear

A preliminary microscopic examination was conducted on all parts listed in Table 10-14. Representative parts were then selected and examined at low (10 to 40X) and high (200 to 1500X) magnifications, as required. Photomicrographs were made of surface conditions. The most significant results of this examination are presented below, together with examples of representative photomicrographs taken. X-ray diffraction measurements originally contemplated for some of the surfaces were not taken because it did not appear productive to do so.

Spur Gear From Mirror Elevation Drive

This gear was lubricated with Microseal lubricant.* Figure 10-14 shows the appearance of the gear teeth. Several teeth had exhibited some plastic deformation — metal rolled over the tooth edges. Two wide, fairly deep scratches extending into the tooth zone can be seen on the gear wheel face. These scratches appeared very fresh; they were probably made during disassembly. The tooth contact was irregular, but there was no evidence of heavy wear.

^{*}A proprietary bonded, solid lubricant.

TABLE 10-14. SURVEYOR III CAMERA GEARS AND BEARINGS EXAMINED FOR WEAR

	Number of Parts Examined	
Source	Gears	Bearings
Filter wheel potentiometer	1	2
Filter wheel	3	7
Mirror elevation drive	2	2
Mirror elevation potentiometer	1	_
Mirror azimuth drive	1	
Mirror azimuth potentiometer	_	1
Iris drive	1	4
Iris potentiometer	2	_
Focal length drive	4	5
Focal length potentiometer	2	_
Focus drive	2	4
Focus potentiometer	1	_
TV mirror support	_	2

TV Mirror Support, Outer Left Ball Bearing

The lubricant used on the bearing was Lubeco 905, a bonded solid lubricant containing molybdenum disulfide, graphite, and lead sulfide. The bearing was observed to rotate freely. The races and bent wire retainers showed good adhesion. The balls appeared to have a multitude of microscopic pits as shown in Figure 10-15. The coating on the balls seemed to be poor, but no evidence of corrosion was noted. Apparently, the lubricant had been wiped off the faces of the bearings prior to oven cure.

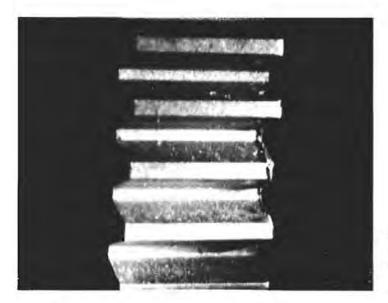


Figure 10-14. Photomicrograph of Spur Gear From Mirror Elevation Drive (13X Magnification) (Photo 00545-188)

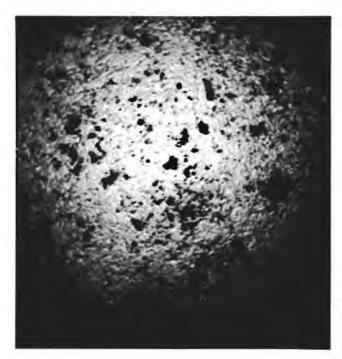


Figure 10-15. Photomicrograph of Ball Surface From TV Mirror Support Bearing (250X Magnification) (Photo 00545-189)

Mirror Elevation Drive Outer Bearing

The mirror elevation drive outer bearing was a Bar-temp bearing, utilizing a Duroid 5813 ball retainer. This material is a fiberglass-reinforced teflon containing 15 percent molybdenum disulfide. As evident from Figure 10-16, only a very slight amount of wear was noted on the retainer.

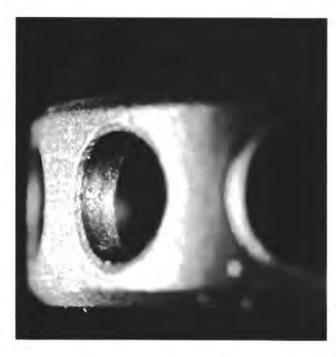


Figure 10-16. Elevation Drive Outer Bearing (20X Magnification) (Photo 00545-190)



Figure 10-17. Film of Transferred Lubricant on Outer Bearing of Elevation Drive (50X Magnification) (Photo 00545-191)



Figure 10-18. Interference Rings on Outer Bearing of Elevation Drive (200X Magnification) (Photo 00545-192)

Figure 10-17 shows that some of the retainer material transferred to the races in rather uniform rows; this material was transferred by the balls. On closer inspection, these rows appeared to be discrete particles mashed so flat that interference fringes can be seen on the edges. This is shown in the closeup photomicrograph of the outer bearing, Figure 10-18, magnified 200X. A minute amount of lubricant was retained by the balls, whose photomicrograph closely resembles that of Figure 10-15. Its surface exhibited microscopic and rather uniform surface roughness, resembling pitting, but showed no evidence of corrosion.

Iris Potentiometer Spur Gear Assembly

This assembly contained the gear and two free-rotating Barden Bar-temp bearings, lubricated with microseal. Examination revealed considerable galling on all the teeth in contact zones. The contact zones were generally on the edges of the teeth, indicating misalignment. The contacts were also usually toward the top of the teeth, indicating a somewhat excessive distance between centers of the gears.

Focal Length Drive Spur Gear

Galling was also noted on all the contact areas of the gear teeth. Edge loading was typical.

Filter Wheel Potentiometer Spur Gear

The teeth of the gears of the filter wheel potentiometer were hard-anodized on all surfaces and lubricated with Microseal. Distinct edge cracking was observed at the tips of the teeth. It is suspected that this cracking was aggravated by the process of applying the Microseal lubricant: the first step in that process is an abrasive blasting with a 425 mesh aluminum oxide. The teeth were not badly worn, but contact surfaces showed galling, typical of sandblasted surfaces in contact.

Focal Length Potentiometer Spur Gear

This gear was also hard-anodized on all surfaces and lubricated with Microseal. Removal of the anodizer by the Microseal, mentioned above, was also noted on this gear. This is clearly evident on the photomicrograph of Figure 10-19. All contact surfaces were irregular and galled.

Potentiometer Carriage Lips

The carriage lips of the filter wheel and focal length potentiometers made of DAP* material were examined to determine whether any wear effects could be noted. This carriage, to which the potentiometer contact is attached, slides against the sides of the helical windings of the potentiometers during operation. The DAP carriage lip of the filter wheel potentiometer

^{*}Diallyl phthalate.



Figure 10-19. Galled Teeth Surfaces on Focal Length Potentiometer Spur Gear (17X Magnification) (Photo 00545-193)



Figure 10-20, DAP Carriage Lip of Focal Length Potentiometer (30X Magnification) (Photo 00545-194)

exhibited a failure; its analysis is presented in Section 12 as part of the discussion of the filter wheel potentiometer anomaly. A photomicrograph of the DAP carriage lip of the focal length potentiometer is shown in Figure 10-20. This potentiometer remained essentially intact except for some wear and chipping on and around the guide track.

Forward and Back Cover Bearings of Focal Length Potentiometer

The focal length potentiometer shaft was supported by two Bar-temp bearings. Transfer lubrication was provided by the bearing retainer, machined from Duroid 5813.



Figure 10-21. Pitting of Bearing Balls of Focal Length Potentiometer (200X Magnification) (Photo 00545-195)

A series of photomicrographs was taken of several bearing balls from the inner races and from the retainer ball pocket. Excessive pitting was noted on many of the balls. One example is shown in Figure 10-21. These pits were so deep and prevalent on the surfaces that it is improbable that they were formed during the mission or even just prior to launch. It is extremely likely that these balls were assembled into the bearings in an already damaged condition. Had the pitting been caused by the lunar environment, considerable corrosion would have been expected. However, no significant corrosion was noted on any of the other balls.

Large inclusions and pits were also observed on the inner race of the back cover bearing. As in the case of the pitted balls, it was concluded that the damage was present at the time of the assembly of the bearings. It was also observed that flattened particles and lubricant debris formed a highly uneven lubricating film on the inner races as well as (although to a much lesser extent) on the balls.

Focal Length Potentiometer Slip Ring

Examination of the slip ring revealed radial wear grooves but no discoloration. This is evident in the photomicrograph shown as Figure 10-22.



Figure 10-22. Wear of Focal Length Potentiometer Slip Rings (45X Magnification) (Photo 00545-196)

Retainer Ball Pocket

Thorough examination of all ball pockets indicated negligible wear of the retainer.

10.6.3 Friction Studies of Focal Length Potentiometer

Objectives and Scope of Studies

The helical winding of the potentiometer, consisting of a single strand of Karma wire wound around a copper conductor and the wiper contact, was subjected to a friction and wear analysis. This analysis included a detailed visual examination and a test conducted on a portion of the wire under vacuum conditions to determine the friction forces present and to confirm the absence of the niobium diselenide lubricant on the contact surfaces. A new wiper contact, similar to that used on the potentiometer, was used for this test as a control. This test, therefore, also served to verify and determine the nature of the observed wear of the wiper contact.

Results of the visual examination and vacuum friction tests are presented here. The test setup and procedure used are described in more detail in Appendix I. 3.

During the Surveyor program — about the time of the final assembly and test of the Surveyor III spacecraft — responsibility for lubricating the TV camera potentiometer was transferred from the vendor to Hughes. It was suspected that some of the parts already installed on several television cameras had not been properly lubricated.* However, in view of the excellent performance of the TV cameras in vacuum tests, it was decided

^{*}It was suspected that the process was at fault since lubricants were later found absent on potentiometers originally lubricated; this process was later revised.

to launch the already assembled and tested cameras on some Surveyors, including Surveyor III, rather than to dismantle and rework the suspect components and retest the system. Therefore, Surveyor III was launched with this documented reservation about a possible partial inoperability of the TV potentiometers since their failure would not be catastrophic. The position of the drives and controls involved could also be determined during the mission from data other than potentiometer position telemetry.

As noted in Section 2.4.2, the filter wheel potentiometer of Surveyor III had, indeed, started to act anomalously half way through the mission operations of the first lunar day. A complete failure analysis of this returned potentiometer was therefore conducted and is presented in Section 12. The studies of the focal length potentiometer (one of the other TV camera's potentiometers) described here were thus conducted to establish under controlled conditions the behavior of the wire and wiper surfaces with typical frictional forces applied.

Visual Examination

A visual examination was conducted of the surfaces of the helical winding and of the wiper contact. The inside diameter of the helical spiral, shown in Figure 10-23, was thoroughly inspected with a long focal length microscope (Technoscope) to observe the appearance of the wear track. The potentiometer wiper contact was examined similarly.

The wear track was clearly visible on the wires of the helical winding at all magnifications. One of these photomicrographs is shown on Figure 10-24.* Although the wear appeared somewhat higher than anticipated, it was obvious that no resistance wires had been broken nor had any gross damage occurred. Photomicrographs of the wiper contact also indicated surface wear, with deep grooves and discolorations noted. Figure 10-25* shows one of these photomicrographs. Excessive galling (displaced and torn metal) is clearly visible.

The above results suggest the absence of lubricant. Further examination for evidence of niobium disclenide failed to uncover any traces of it. The elements of the winding did not show any characteristic residual lubricant debris that invariably remains in small but noticeable quantities between the wire windings. No tapping, vacuuming, or blowing with a dry inert gas could dislodge any traces of niobium disclenide powder that might have been present. On the other hand, the copious debris from the blue DAP carriage lip was clearly visible. The difference in appearance between these two types of debris was unmistakable.

If niobium disclenide had been present on the windings, some of it would have transferred to the wiper contact during operation. No such evidence was uncovered in examining the wiper. Blue sheen in the reflected

^{*}Original in color.



Figure 10-23. Helical Winding of Focal Length Potentiometer (Photo 00545-197)

light observed in viewing the contact was believed to have been caused by the trapped DAP powder or to be the result of a frictional burn rather than of any niobium diselenide film.

Friction Tests

A friction test was conducted next on a sample of the Karma wire-wound section of the copper conductor from the Surveyor III focal length potentiometer. A section of the wire was removed and straightened out to a highly precise taut shape, using the heat treatment method described in Appendix I. 3. Three specimen were cut from this section and placed in the friction and wear test jig. Brand new Paliney 7 wiper contacts were then inserted in the jig, as shown in Appendix I. 3, and positioned to simulate the wiping motion of the Surveyor III wiper contact on the potentiometer wire during the lunar operations.

Two tests were conducted: the first on the area of the wire specimen, previously worn during the lunar operations, and the second on the adjacent unworn areas. Separate sets of new wipers were used for each test. The arrangement of the elements and wipers and the test setup employed to measure the frictional forces and to observe the surfaces are presented in Appendix I. 3.

The procedure followed in the two tests, also discussed in more detail in Appendix I. 3, entailed initial runs at atmospheric pressure, followed by 2500 cycles in vacuum, and culminated in an additional 100 cycles in air. The initial run in air was conducted for each test for about 30 cycles: 10 cycles at each of the three cycling frequencies used of 3.5, 20, and 40 cpm, respectively. This was done to verify the integrity

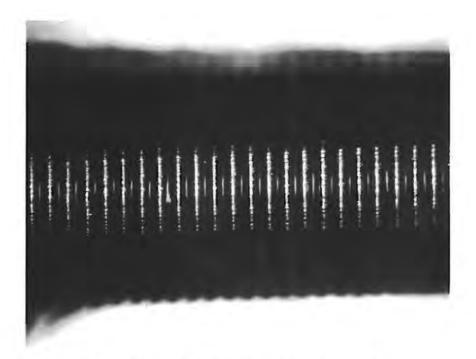


Figure 10-24. Wear Track on Wires of Surveyor III Focal Length Potentiometer Winding (65X Magnification) (Photo 00545-198)



Figure 10-25. Surface Wear of Wiper Contact of Surveyor III Focal Length Potentiometer (100X Magnification) (Photo 00545-199)

of the setup, obtain ambient frictional forces for comparison, and observe the effect, if any, of changing the cycling frequency. The vacuum test and the subsequent cycling in air were conducted at 40 cpm.

The friction tests were conducted with a load of 14 grams applied perpendicular to the rubbing surfaces, corresponding to the potentiometer spring tension in its operation (i.e., about 5 grams of force per contact). The frictional forces measured, recorded on the strip chart recorder, were those generated by all three specimen surfaces in contact with the wipers. The coefficients of friction were calculated by dividing the average value of the kinetic friction force over the interval of wiper motion by the 14 gram load. The higher static friction forces recorded at the ends of each traverse were ignored in taking these averages.

The results of the two sets are summarized in Tables 10-15 and 10-16 for the worn and unworn specimens, respectively. As seen from these tables, the coefficients of friction for both surfaces were significantly higher in vacuum than in the air. This confirmed the absence of the lubricant since the opposite effect would then be expected. The values of the coefficients of friction were also measured to be considerably higher than the values expected from lubricated surfaces. Table 10-17 summarizes the ranges of the measured friction coefficients and compares them with values expected from lubricated surfaces, in support of the above conclusions.

The second important observation was that the onset of cold welding appeared to occur on both specimens after they had been subjected to several hundred cycles: 800 cycles for the worn specimen and 400 cycles for the originally undisturbed surfaces. This occurrence of cold welding was deduced from the observed sudden chatter of the specimen in the course of the test, as noted in Tables 10-15 and 10-16. In the case of the previously unworn surface, the friction coefficient at this point actually increased by about 50 percent; the friction coefficient subsequently decreased as the area of the developed cold weld apparently wore down.

The fact that the onset of cold welding occurred after a somewhat different number of cycles for the two specimen, 800 versus 400, was believed only to reflect the limited accuracy of the test although this difference may be related to the relative surface conditions of the two specimens. What is significant is that this onset of cold welding occurred below 1000 cycles. This further confirms the absence of the lubricant since for lubricated surfaces this effect would not be expected to take place until after some 25,000 cycles.

The areas of contact were also examined during and after the test by a microscope provided in the test setup. Photomicrographs were taken of all the surfaces of the wire specimen and of the wiper contacts involved.

Figure 10-26* shows the appearance after completion of the test of the wiper contact which had rubbed during the test against the unworn surface of the potentiometer wire. The resemblance between this surface

^{*}Original in color.



Figure 10-26. Surface Wear of the Test Wiper Contact After the Friction Test (40X Magnification) (Photo 00545-200)

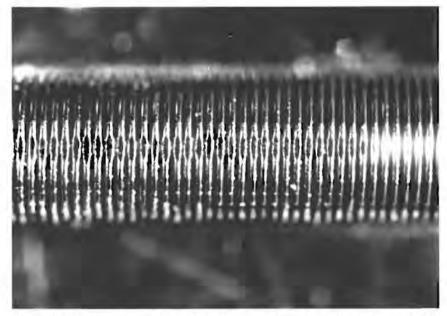


Figure 10-27. Appearance of Surveyor III Focal Length Potentiometer Wire After the Friction Test (40X Magnification) (Photo 00545-201)

and that of the Surveyor III wiper contact, shown in Figure 10-25, is striking. Evidence of cold welding can also be gleaned from both of these photomicrographs.

Figure 10-27 shows the appearance of the surface of the originally worn wire element after the friction test. Comparision with the appearance of this worn surface after lunar operations but before the friction test, shown in Figure 10-24, indicated that a further degradation had taken place. The original wear track was now found damaged to the point of flattening the tops of the 1 mil resistance wire.

It was evident from the test conducted that, in spite of the definite absence of lubrication, the potentiometer was still operative and would have continued to perform reasonably well.

TABLE 10-15. RESULTS OF FRICTION TEST ON WORN AREA OF SURVEYOR III FOCAL LENGTH POTENTIOMETER WIRE

Brand New Paliney 7 Bare Contact 14 Gram Load, Room Temperature

											_				
Remarks	Specimen well aligned	Smooth sliding	Violent chatter												
Measured Coefficient of Friction	0.20	0.26	0.26	0.26	0.46	0.49	0.49	65.0	0.51	0.59	0.51	0.57	0.55	65.0	0.37
Cumulative Number of Cycles	1	10	20	30	50	300	400	200	009	700	800	1000	2000	2500	2600
Cycling Frequency, cpm	3.5	3.5	20	40	40	40	40	40	40	40	40	40	40	40	40
Pressure, Torr	160	760	160	760	Less than 10-8	Less than 10-8	Less than 10-8	Less than 10-8	092						

TABLE 10-16. RESULTS OF FRICTION TEST ON UNWORN AREA OF SURVEYOR III FOCAL LENGTH POTENTIOMETER WIRE

Brand New Paliney 7 Bare Contact 14 Gram Load, Room Temperature

					r														
Remarks	Specimen well aligned	Smooth sliding	Violent chatter of contacts																
Measured Coefficient of Friction	0.22	0.19	0.20	0.23	0.42	0.50	0.55	0.53	0.73	0.50	99.0	0.68	0.75	99.0	0.61	0.61	0.61	0.55	0.39
Cumulative Number of Cycles	1	10	20	30	50	100	200	300	400	200	009	200	800	006	1000	1500	2000	2500	2600
Cycling Frequency, cpm	3.5	3.5	20	40	40	40	40	40	40	40	40	40	40	40	40	40	40	40	40
Pressure, Torr	092	092	160	160	Less than 10-8	Less than 10-8	Less than 10-8	Less than 10-8	Less than 10-8	Less than 10-8	Less than 10^{-8}	Less than 10-8	Less than 10-8	Less than 10-8	260				

TABLE 10-17. RELATIVE VALUES OF FRICTION COEFFICIENTS FOR LUBRICATED AND UNLUBRICATED SURFACES

Karma Wire-Wound Potentiometer Paliney 7 Wiper Contact Niobium Diselenide Lubricant

	Coefficients of Friction				
Wire/Wiper Contact	Vacuum	Air			
Results of friction tests, Surveyor III potentiometer wire and new wiper					
Worn area of wire	0.46 to 0.59	0.20 to 0.37			
Unworn area of wire	0.42 to 0.75	0.19 to 0.40			
Predicted values for lubricated wires	0.07	0.17			

10.7 THERMAL CONTROL COATINGS AND MATERIALS

10.7.1 Introduction

Tests of the paint used as thermal control coatings on the Surveyor III TV camera and of the polished aluminum surfaces are grouped in this subsection as the last category of materials examined.

The tests included visual and microscopic examination, and measurements of optical properties. Only the results of the visual examination are presented here. Optical property measurements are included in Section 11 as an integral part of the more comprehensive evaluation conducted on these and other surfaces.

A number of tests to determine the physical characteristics of samples of the paints were originally contemplated. The proposed physical tests, destructive in nature, included measurements of brittleness, hardness, thickness, flexibility, cohesion, and adhesion properties of the paints. These tests were not conducted by direction of the JPL Technical Coordinator in the spirit of program ground rule 2 stated in Section 2.6.1, limiting the number of destructive tests allowed, although these measurements had been recommended by Hughes. Such tests were considered to be particularly illuminating in providing a better understanding of the apparent extensive "mud-cracking" observed on the painted surfaces, as discussed in Section 10.7.3.

The visual examination conducted here was the second such examination following the original inspection conducted as part of the early survey (discussed in Section 3.4).

10.7.2 Description of Materials

Four types of radiative temperature control coatings were used on the exterior surfaces of the Surveyor III TV camera: inorganic white, organic white, organic black, and polished aluminum.

Inorganic White Paint

The inorganic white paint was used on the exterior surfaces of the lower shroud, upper shroud, and mirror housing, and was the primary temperature control coating on the camera. It consisted of a calcined china clay pigment, primarily an aluminum silicate, in a potassium silicate binder. The coating was applied to a thickness of 6 to 8 mils on a 6061-T4 aluminum alloy substrate. This paint is characterized by low initial solar absorptance and high initial emittance.

Organic White Paint

The organic white paint was used primarily on the back of the mirror as an aluminum foil substrate. It was also used as a touchup paint for areas of the inorganic paint that had to be repaired. The paint was a 3M velvet titanium dioxide pigment in an alkyd resin binder.

Organic Black Paint

The organic black paint was used inside the mirror assembly as an antireflection coating. It is a highly diffuse 3M velvet paint with carbon dispersed in an alkyd binder.

Polished Aluminum

Polished aluminum was used on the bottom of the lower shroud and on the vidicon radiator. The aluminum was a 6061-T4 alloy. The surface was polished with conventional polishing materials to achieve a highly specular surface. Polishing was required to reduce the thermal coupling with the lunar surface.

10.7.3 Visual Examination

A comprehensive microscopic examination was conducted of the painted and polished aluminum surfaces as a sequel to the original survey. While previous results (reported in Section 3.4) were confirmed, little additional information was obtained.

The polished aluminum appeared unaffected by the lunar exposure except for the coating with dust. Lightening of the black organic paint was confirmed and determined to have been caused by bleaching and by the deposition of lunar materials. The white organic paint exhibited some

significant and expected color changes and some cracking, noted earlier. However, the coating appeared to be still satisfactory, with no loss of adhesion.

The major effect of the lunar environment observed was, again, on the white inorganic paint. Its most obvious change was in color. A range of colors noticed included gray, brown, and yellow, compared to the original white. In some areas where the paint surfaces had been protected, such as under brackets and screw heads, the paint was still white. The second major change noted, confirming previous observations, was the somewhat extensive mud-cracking. These effects were previously described (Section 3.4.1) with the aid of Figures 3-19 through 3-22.

The discoloration of the white inorganic paint varied in color, degree, and appearance. Its cause could be attributed to lunar dust imparted during the Surveyor landing and Lunar Module landing, to effects of radiation exposure, deposition of the products of outgassing from nearby Surveyor materials, or to combinations of these. Its varied appearance seemed to depend on the orientation of the surfaces relative to the lunar terrain and to the Lunar Module, on the orientation of the surface relative to the sources of outgassing, and also on the original condition of the surface and the degree of handling before launch, by the astronauts, and after recovery. Considerable difference in shadowing was also observed, depending on the angle of viewing. Surprisingly little evidence of micrometeoroid impact and damage was noted. Further analysis of the discoloration and contamination characteristics of the inorganic white paint was conducted in the course of the surface contamination studies (Section 11).

The mud-cracking noted, clearly shown in Figures 3-20 and 3-21 (Section 3) on the lower shroud, was more extensive than anticipated.* The visible degree of mud-cracking was not uniform. Some areas of the exposed surface, as well as protected areas, such as under screwheads, were apparently free of this effect. A series of tests was proposed to provide better insight on this occurrence. The tests included measurement of physical characteristics of the coating such as adhesion, hardness, flexibility, brittleness, and cohesion, and other binder-influenced properties. It was felt that a study of the Surveyor inorganic coating would be applicable to all other inorganic white thermal coatings; these are and will be used extensively as thermal finishes on space vehicles as the lightest and cheapest method of providing temperature control. All these inorganic white coatings are essentially similar from the standpoint of physical characteristics. They all use potassium silicate as a binder, highly loaded with a transparent metal oxide pigment.

^{*}Mud-cracking was originally classified as a failure. This discussion is included here for continuity, rather than in Section 12, Failure Analysis.

The proposed destructive tests were not conducted by direction of the Technical Monitor because of the desire to minimize the amount of destructive tests and because of the general feeling that results of such tests would be difficult to interpret. Mud-cracking was observed on laboratory samples and on painted surfaces prior to launch. Separation of the effects of lunar environment from other effects and interpretation of the physical tests was considered too difficult. However, it may still be advisable to conduct such tests on the Surveyor III TV camera surface samples at a future date. Two samples 1/2 by 5 inches would suffice. The 5 inch length would be necessary for the critical bending tests, a major technique for determining adhesion and cohesion. All of the other physical tests could be conducted on each end of these bent samples. Pending such additional data, the cause of this enhanced mud-cracking is believed to be the thermal cycling experienced during lunar exposure.

11. SURFACE DISCOLORATION AND CONTAMINATION STUDIES

11.1 INTRODUCTION

Results of surface discoloration and contamination studies, designated as DOR studies,* are presented in this section and supporting data in Appendix J. These studies were conducted as a joint effort** on the two Hughes contracts on the returned Surveyor III parts: the TV camera (JPL contract) and other parts (NASA-MSC contract).

The studies were undertaken as a result of the initial observation that significant discoloration occurred on the external painted and polished surfaces of the television camera and on the polished aluminum tube from the spacecraft structure. The sealed container in which the painted tube section was returned was not opened until later.

Initial observations indicated both the extensive and complex nature of the discoloration and the difficulty in understanding its nature and separating the contributory causes. During the visual examination of the television camera at the LRL in January 1970, it became apparent that the discoloration of the painted surfaces was greater than had been anticipated. Expected patterns of radiation damage were not present. In addition, unique surface shadow patterns were noticed. *** It was obvious that measurement of spectral reflectance of the inorganic white paint would not sufficiently describe what had occurred to these surfaces during their lunar exposure.

^{*}The letters D O R denote the suspected major contributions to surface effects — lunar <u>dust</u>, contamination by <u>organic materials</u>, <u>radiation effects</u> — after effects of micrometeroid impacts were found to be of relatively small significance.

^{**}This section and its corresponding appendix are labeled 11 and J, respectively, in the sequential context of the TV camera contract Final Report. These two parts of the report and a separate references page are incorporated verbatim for ease of publication into the Final Reports on both contracts.

^{***}These patterns were not those that would be expected from radiation darkening of the paint, as determined by the geometry associated with the incident sunlight.

Preliminary analysis indicated that discoloration of the surfaces was caused by some combination of the following three factors:

- 1) Dust from the lunar surface from Surveyor III or lunar module landing, or both
- 2) Organic contamination outgassed from Surveyor III or deposited from prelaunch environments; also contamination from rocket exhaust
- 3) Solar radiation affecting the paints and/or the organic or other contaminants present

A special task was established to study this problem by analysis, supporting tests, and coordination with pertinent efforts conducted as part of the parallel science studies. The study was motivated by the desire to understand the nature and cause of this discoloration in order to assess the effects of lunar exposure for possible applications to future designs.

Contamination of surfaces is important to optical systems. Transport of lunar fines and their associated effects on thermal control surfaces are significant for future lunar operations. Analysis of the discoloration and contamination effects could also help obtain reasonable estimates of the thermal history of the camera, which would be of importance to biology and engineering investigations and other science studies.

An initial plan of attack was developed but had to be abandoned later on. This plan was based on physical removal of successive layers of dust and other contaminants from the surfaces by a variety of postulated techniques. It was thought that this sequence would permit the identification and separate examination of the contributions of the various sources of discoloration. Preliminary tests conducted revealed that the surface structure of the paint and its porosity would preclude such removal techniques.

The plan finally pursued (discussed in Section 11.3) was based on an alternate approach which proved reasonably successful. This plan entailed careful selection of a variety of samples and selective measurements supported by analytical studies of the total properties of these surfaces. The separation of the contributory factors would thus be accomplished by analysis and by interpretation of the test data obtained by the various techniques employed, using to the maximum possible advantage the knowledge of the relative locations of the selected samples at which the contributory effects were present in significantly different amounts.

The test and analysis program included spectral reflectance studies at Hughes, supported by measurements at TRW, Inc. under a Hughes subcontract; analytical studies at JPL; and use of supporting data obtained from parallel science investigations coordinated by JPL. Results of these

contributory inputs were then assessed by Hughes and JPL, leading to the preliminary results reported here. It should be emphasized that the study is by no means complete. While significant progress has been made and an initial general understanding of the nature and causes of discoloration achieved with a reasonable assurance of validity, much additional work may be warranted. In particular, further inputs from the yet incomplete preliminary science investigations may be of specific import.

Results of the study reported here include numerous reflectance measurements of the surfaces conducted by Hughes. Associated with these reflectance measurements were studies of optical and thermal bleachings associated with the radiation damage. A methodical analysis of the reflectance data, conducted by JPL, is also summarized. Results of this study were used in conjunction with the reflectance measurements to separate the relative effects of lunar dust and radiation.

Inputs from the parallel science investigations, approved by NASA and coordinated by JPL, are also included. The ion microprobe studies conducted at the GCA Corporation* were helpful in indicating the amounts of lunar material on the painted and other surfaces, the depth of lunar material penetration, and the presence of other materials. Measurements of the quantity of trapped solar wind gas, conducted at the State University of New York (SUNY),** were also used to advantage in indicating relative amounts of lunar materials on the various surfaces***. Results of these parallel science studies at GCA and SUNY are only briefly discussed here; details of their investigations are expected to be published separately at a later date.

11.2 DATA AVAILABLE FROM PRELAUNCH, LANDING, AND POST-RECOVERY EXAMINATION

A summary assessment of the data available prior to the finalization of the DOR study and test plan is presented in this section. Subsequent discussion of the plan itself and of the test results obtained is to a large extent based on this information. Available data included prelaunch operations and their effects, effects and observations during the lunar recovery operations and during the return of the parts to earth, and results of visual examination of the returned parts.

^{*}By Dr. F.G. Satkiewicz.

^{**}By Professor O. Schaeffer.

^{***} This approach was originally suggested by F. Fanali of JPL.

11.2.1 Prelaunch Effects

The exterior surfaces of the Surveyor III camera were, for the most part, coated with white inorganic paint used as the primary temperature control coating. The inorganic white paint was used on the exterior surfaces of the lower shroud, upper shroud, and mirror housing.

The paint consisted of a calcined china clay pigment, primarily an aluminum silicate, in a potassium silicate binder. The coating was applied to a thickness of 6 to 8 mils on a 6061-T4 aluminum alloy substrate. The paint was characterized by a low initial solar absorptance and a high initial emittance.

Prior to launch, the Surveyor III camera was exposed to many possible sources of contamination, including those incurred in manufacturing and during thermal-vacuum testing. A rework of the thermal control surfaces was conducted on all Surveyors, including Surveyor III, just prior to launch in order to remove all visible contamination. Areas where the paint was missing were touched up with an organic coating. Other areas of discoloration were sanded down. Further details of prelaunch operations on the painted surfaces are presented in Appendix J-I.

Two subsequent observations which have a definite relationship to the above prelaunch operations should be noted. The areas touched up with organic paint were observed on the returned camera to have discolored less than the adjacent areas covered with inorganic white paint. The scope of the study did not permit an exhaustive analysis of this effect, and further work may be warranted. However, it is postulated that the likely explanation of this apparent anomaly is that lunar dust does not adhere to organic paints as well as it does to inorganic paints.

The second observation during the visual examination of the camera also related to the prelaunch touching up operations. Areas of inorganic white paint which had been sanded down appeared to have discolored less than the unsanded areas. Similarly, the scope of the program did not allow a more extensive pursuit of this phenomenon, and further work may be warranted. *

^{*}One of the suggested follow-on tests in the Final Report of the Surveyor III camera tests, Section 1.6.3. One postulated mechanism is that the inorganic white paint was originally contaminated with some organic materials which were removed by the sanding operation; hence, the contribution total discoloration attributable to radiation would be less for the sanded areas. This, however, conflicts with the fact that no significant traces of organics were found on the discolored inorganic white surfaces in the course of the study, as discussed later.

It is believed that no contamination of the external surfaces occurred during the prelaunch and transit phases. The spacecraft was covered with a protective shroud at launch. This shroud was ejected 203 seconds after launch.

11.2.2 Lunar and Recovery Operations

Surveyor III landed in a cloud of dust. The landing was abnormal: the Surveyor bounced three times along the slope of the crater. Details of the orientation of the spacecraft and of the camera are presented in Appendix J. 1. The dust generated during the landing affected the condition of the surfaces of the Surveyor III camera. One evidence of this effect was the considerable veiling glare noted in the television pictures obtained by the spacecraft during its lunar day operations.

No major events are known to have occurred in the adjacent areas during the 2-1/2 years of residence of Surveyor III on the lunar surface until the arrival of the Apollo XII lunar module.*

The lunar module approached the Surveyor III spacecraft from the east, passed to the north of it, and landed 535 feet away. Details of the landing operations and of the landing configuration are presented in Appendix J. 1. Again, the important observation is that a significant amount of dust appears to have been deposited on the Surveyor III spacecraft as a result of this landing.

During the second extravehicular activity period, the astronauts of Apollo XII arrived at the Surveyor III site and removed the various recovered items. A piece of a painted tube and several cable sections cut from the spacecraft were placed in a special container called the sample environmental sealed container (SESC), which was tightly sealed and returned in vacuum and darkness. All of the remaining parts, which were cut free of the spacecraft, including the television camera, a section of polished aluminum tubing, and the soil mechanics/surface sampler (SM/SS) scoop, were placed in separate pockets of the backpack.

In photographing the spacecraft in the course of the above operations, the astronauts reported it had an extensive brown appearance. This report was repeated during the postflight debriefing when the astronauts described the Surveyor III spacecraft as "looking like it had been driven down a dusty road, rained upon, and finally left in the sun to bake".

Upon return to the lunar module, the astronauts stored the backpack under a shelf. All parts were later transferred to the command module and

^{*}See Appendix J. 1. 2. Also effects of landing of nearby meteroids, while purely speculative, cannot be totally discounted.

strapped into position. Thus complete immobilization was not achieved. For example, it is believed that the two dents in the sun visor of the camera seen in the frontispiece* were probably incurred at the time of the hard landing of the command module in the Pacific Ocean.

The parts were exposed to the oxygen environment of the command module during the return to earth at a pressure of about 3 to 4 psi. The backpack containing the parts was transferred to the NASA Houston Lunar Receiving Laboratory (LRL) with the astronauts. Early in the quarantine period, the parts were taken out of the backpack. They were first photographed and then double-bagged in heat-sealed polyethylene until their release from quarantine on 7 January 1970.

11.2.3 Visual Observation

Visual observation of the returned parts was conducted at the LRL in early January by Hughes, JPL, and NASA personnel. More detailed results of the visual observation conducted, insofar as it applies to the surface discoloration studies, are presented in Appendix J. 2. A more comprehensive discussion of the visual examination of the television camera is presented in Section 3.4.** The highlights of this examination are summarized below.

Both extensive and non-uniform discoloration of the camera were noted, including unique shadow patterns mentioned earlier. These surface shadow patterns provided the basic background used to develop the surface discoloration and contamination study test plan.

Discoloration was observed on all surfaces of the television camera, with colors ranging from gray to light tan. It was generally darker than expected. Shadow patterns were discovered on the painted surface on the side of the camera facing the lunar northwest. These areas were associated with surface protrusions, such as screw heads, and overlying parts, such as wires, cables, and struts. The television camera mirror was hazy.

The shadow patterns appeared to be related uniquely to the location of the lunar module relative to the Surveyor III camera. It was assumed as a result of the visual examination that the landing of the lunar module caused a severe shower of lunar dust which "sandblasted" the unshielded Surveyor III surfaces, eroding away previously darkened surfaces.

^{*}Frontispiece of the JPL contract (Television Camera Test Program)
Final Report; not included in the NASA-MSC contract Final Report.

^{**}Not included in the NASA-MSC contract Final Report.

It should be noted that discoloration by solar radiation had been expected for the white painted surfaces. Return of the camera in the air environment was not expected to cause bleaching. It was conjectured that exposure to light would eventually cause bleaching. It was originally recommended by Hughes and JPL that all parts, including the television camera, be returned in light-tight vacuum containers. This, however, was not possible for reasons of weight, space, and schedule.

11.3 EVOLUTION OF TEST PLAN

As noted earlier, the surface discoloration study plan underwent several cycles of changes. The process of arriving at the test plan was guided largely by the understanding of the mechanisms of damage, as it evolved, and by the applicability of the various test techniques considered. As these mechanisms became more evident, appropriate changes in the plan were instituted. The final test plan thus reflects the eventually postulated mechanisms of damage.

This section briefly summarizes the evolution of the final test plan, leading to a summary outline of the test program conducted, described in the succeeding section. It is considered appropriate and useful to the understanding of the final plan to review the factors that were involved in its development.

A preliminary model of surface damage was postulated before the recovery of the Surveyor III parts as part of the original planning operations, discussed in Reference 101.* This earlier model considered meteroid damage as possibly significant and relegated lunar dust to a second-order effect. However, visual examination of the returned camera indicated that meteoroids were not significant; only one primary meteroid impact on the entire camera surface was reported by NASA (Reference 102). The lunar dust was found to be a significant factor, as noted in the previous discussion of visual observations.

Based on the above, the following preliminary damage model was then proposed: Some organic contamination had been deposited on the spacecraft prior to launch. This contamination was not removed during the cleanup operations on the thermal finish. During the landing on the moon, some solid matter from rocket exhaust was deposited on the various surfaces. The gaseous products from the vernier descent engines, which had a high vapor pressure, are not believed to have been deposited. During the landing of Surveyor III, some small amount of dust was deposited on the spacecraft. In the course of the succeeding 2-1/2 years prior to the landing of Apollo XII, ultraviolet radiation and low energy protons (1 kev) degraded

^{*}References for Section 11 and Appendix J are common to both reports and listed apart from other references at the end of the volume.

the optical properties of the surfaces. The extent of this degradation depended on the amount of exposure of each surface to sunlight, as noted in the discussion in Appendix J. 1. 2. In addition, organic materials were deposited on the various painted surfaces of the spacecraft as a result of outgassing from nearby parts of the spacecraft. These, too, were degraded by radiation. The landing of the Apollo XII lunar module was a major event, resulting in the showering of the Surveyor III with dust particles. Resultant shadow patterns are uniquely related to the relative location and orientation of the lunar module on the lunar surface. It was believed that the majority of the dust present on the surfaces of Surveyor III was deposited at the time of the landing of the Apollo XII lunar module.

The initial test plan was based on the preliminary damage model just described. This plan entailed the sequential removal of the various deposited materials (organics and dust) by means of several proposed techniques. It had been hoped that this would separate out each constituent of the damage. With proper selection of surface samples, a reasonably quantitative model could thus be constructed.

The various techniques proposed for the removal of the dust were tapes, collodion casts, and nonaqueous liquid wash. Solvent soak was proposed for the removal of organics and dust. Upon removal of the organics and dust, it was hoped that only the effects of radiation damage to the paint would remain. This procedure was to be supplemented with several analytical techniques used prior to, in the course of, and after the removal of the various deposited contaminants. These techniques included scanning electron microscope (SEM) studies, various elemental probes, mass spectral analysis. The plan was not successful because it was impossible to separate the various contaminant levels. For example, collodion casts removed not only the large particles of lunar debris but the paint as well. Very fine lunar dust particles caught in the cracks and pores of the rough surfaces of the inorganic paint could be removed. As another example, SEM studies of the samples cut from the painted surfaces proved futile. Lunar material could not be separated against dielectric paint background, except in the case of unique spherelike particles.

The final test plan developed and pursued entailed a direct analysis of carefully selected samples, with only localized disturbances of surface conditions. Selective separation of contributory factors was accomplished by use of different techniques selected to emphasize the presence of particular sources of contamination, by selection of different samples exposed to predominantly different sources of contamination, and by supporting analytical techniques which were of assistance in correlating and separating the contributory effects.

In summary, the test and analysis plan, finally embarked upon, included the following parts:

- 1) Careful selection of samples from various surfaces of the television camera:
 - a) Separate lunar module dust effects from Surveyor dust effects
 - b) Separate areas of high incident solar radiation from areas of no solar radiation
 - c) Separate areas of possible high organic contamination from no organic contamination
- 2) Measurements of spectral reflectance of the various surfaces as a primary test technique
- 3) Use of supplementary measurements* to attempt to isolate and define the extent of specific contributory factors:
 - a) Ion microprobe studies for analysis of contaminants
 - b) Measurement of trapped helium to determine the amount of lunar material present
 - c) Measurements to determine the amount of organic materials present
- 4) Analysis:
 - a) Direct analysis of the above experimental data
 - b) Mathematical analysis, furnished by JPL, of the contributory effects of lunar dust to spectral reflectance

The proper selection of samples was of major importance. Since the northern side of the camera apparently received a great deal of dust from the lunar module, while the southern side had received little or no dust, samples from both sides were selected. Since one of the major suspected contributors to deposition of organic materials was the backside of the solar panel coated with an epoxy paint which could readily outgas, a sample of the top of the

^{*}These measurements, conducted by various science investigators as part of the parallel science program, were coordinated by JPL. Selected inputs from these studies were furnished to Hughes for possible inclusion in this assessment.

television camera directly under the solar panel was included. Similarly, samples were selected from areas of both high and low incident solar radiation.

The ion microprobe analysis of selected samples was conducted by the GCA Corporation.* This technique consisted of sputtering surface materials and analyzing the formed ions. Sputtering continued to remove material at the rate of 400 Å/min. Thus, depth profiles of contaminants such as dust, organics, etc., on the surface of the paint could be obtained.

Direct analysis of the amount of the lunar material present on the various surfaces was conducted at SUNY. ** Lunar fines, very rich in helium, have been deposited by the solar wind over the centuries. By measuring the helium content of samples, the volume of lunar material present could be determined for the various surfaces (Reference 11-3).

Organic analysis was conducted at the University of California, Berkeley, *** on samples prepared by Hughes. Experimental results have not yet been reported and were not available for inclusion in this analysis.

Spectral reflectance measurements were conducted prior to submittal of all samples to outside investigators. Extensive spectral reflectance tests were also conducted by Hughes on many of the other samples, as discussed in the following subsection. Some measurements were conducted at a TRW facility under a Hughes subcontract.

In addition, controlled photo bleaching and thermal exposures were conducted by Hughes on samples in an attempt to selectively bleach out the radiation damage. These experiments became necessary when it was observed that the discoloration of the painted surfaces exposed to room light was disappearing with time. This effect is also described in detail in the next section.

11.4 SUMMARY OF TEST RESULTS

This subsection contains a summary of the results of the tests conducted in accordance with the general plan outlined in Section 11.3. The basic data gathered in these studies are presented in Appendix J. 4. The bulk of the material presented here pertains to the measurements of spectral reflectance of samples of returned Surveyor III parts, as well as

^{*}Dr. F.G. Satkiewicz.

^{**}Dr. Oliver Schaeffer.

^{***}Dr. A. L. Burlingame.

of control laboratory samples of surfaces painted with the same type of white inorganic paint. The measurements include results obtained during various attempts to intentionally alter the reflectance of selected control samples by chemical, thermal, and optical techniques in order to obtain supporting data. Also included in this section is a summary of the analysis conducted by JPL of the relation of lunar dust to the degradation of spectral reflectance. A mathematical expression was derived, which, coupled with experimental data, could be used to separate dust effects from radiation effects. Further details of this analysis are presented in Appendix J. 5.

A summary of the results of chemical analysis conducted as part of the science effort by SUNY and GCA Corporation, coordinated by JPL, is also included. The reflectance measurements of the Surveyor III samples submitted to these investigators are discussed in Appendix J. 4. 6.

11.4.1 Spectral Reflectance Measurements

Initial Measurements

The reflectance of the lower shroud of the television camera was measured at seven locations (Figure 11-1). Throughout this subsection, these numbered positions are referred to as "TRW positions". Positions 5, 6, and 7 were on the side of the shroud facing the landing site of the lunar module. Positions 1 and 2 corresponded to the front of the shroud, which faced the lunar northeast.

The reflectance of the lower shroud was measured in April 1970 over the range from 0.3 to 2.6 microns. The technique used was substitutional, with the shroud placed at the wall of an integrating sphere since sample cutting was prohibited at that time. These are the only measurements reported in this document where this technique was used. All other measurements were made by placing the sample at the center of a Gier-Dunkle integrating sphere. The data taken in this series of tests are self-consistent but must be modified when comparing to the later measurements. These first measurements were approximately 5 percent high.

A decrease in reflectance over original values at 1.5 microns was found on most surfaces. This was not seen on TRW position 1 of Figure 11-1. This location was protected from the lunar environment by a bracket, whose photographs are shown in Appendix J (Figures J-19 and J-20). Laboratory studies have shown that neither ultraviolet nor solar wind protons will cause a reflectance decrease at 1.5 microns for this clay-silicate inorganic paint. Thus, the reflectance drop is attributed to lunar dust. Organic contaminants were ruled out as discussed later. The variance in the magnitude of the reflectance at 1.5 microns is a measure of the amount of lunar material present on the surface. Table 11-1 summarizes the significant results obtained. An expression relating dust coverage to the reflectance is presented in Section 11.4.2.

TABLE 11-1. REFLECTANCE MEASUREMENTS OF SAMPLES FROM LOWER SHROUD OF SURVEYOR III CAMERA

Measured in April 1970

(1)	2 Front Facing Lunar East	32	45	51	99	09	63	0.2	73
ee Figure 11-1	3 Side Away From LM	59	92	83	98	88	68	68	89
V Positions (se	4 Side Away From LM	48	63	20	75	22	80	82	84
Percent Reflectance at TRW Positions (see Figure 11-1)	5 Side Toward LM	33	43	47	50	53	58	63	29
Percent Ref	7 Rear Toward LM	18	28	36	40	44	20	99	62
	l Beneath Bracket	85	06	06	06	06	06	06	06
	Wavelength, microns	0.4	0.5	9.0	0.7	0.8	1.0	1.2	1.5

*LM = Apollo XII lunar module.

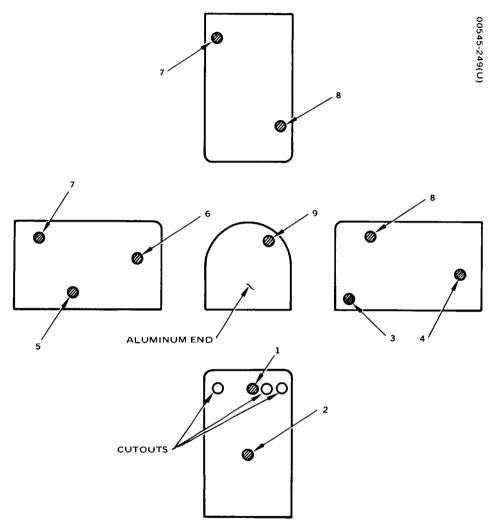


Figure 11-1. Lower Shroud of Surveyor III Camera, Showing TRW Measurement Positions

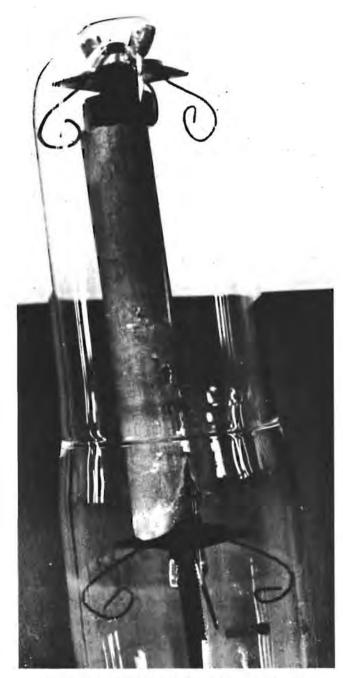


Figure 11-2. White Painted Tube Section Returned From Moon in SESC in Quartz Vacuum Chamber (Photo 00545-292)

Measurement of Tube Section From SESC

An important spectral reflectance test was planned for the white painted tube sample returned in vacuum by the Apollo XII astronauts. This tube was cut from one of the struts of the tripod bracket of the camera support collar and was to be tested in vacuum and then in air. However, a leak was found in the SESC. The proposed test was conducted even though it could no longer be assumed that the part had been returned in vacuum. The white painted tube found in the SESC was cut, and a section was transferred to a quartz vacuum chamber made light-tight with an external shroud. This is shown in Figure 11-2. The transfer was accomplished in an argon atmosphere, and the quartz chamber was then evacuated. The reflectance of the white painted tube was measured in vacuum (1 x 10-7 Torr), in partial vacuum, and then at 1 atm. Several days later, for the first time since return to earth, the tube was exposed for 48 hours to bring light free from ultraviolet. Its reflectance was then remeasured.

No effect was noted on the reflectance as a result of the increase in pressure, first to 12 microns and then to 1 atm. This is consistent with earlier work by Hughes and others, which indicated that this paint did not exhibit atmospheric bleaching. Had the white painted tube been at 1 atm previously as a result of the leak in the SESC, vacuum bleaching would not have been noted in this test.

No white light was allowed to strike the sample during these tests of the white painted tube section. When light was necessary, low level red illumination was used. Any photo-induced bleaching could thus be studied under controlled conditions.

The photo bleaching test was conducted while the tube was at 1 atm. No bleaching occurred at 1.5 microns, but an increase of approximately 8 percent was found at 0.4 micron. The tube, which was dark yellow when returned from the moon, lost its yellow appearance and turned a dirty gray over the half exposed to the white light; the other half reamined a uniform dark yellow. This increase in reflectance (i.e., loss of yellow color) is due to the photo bleaching of the radiation damage within the paint.

No additional work was done with the tube. It was exposed briefly for photography (photofloods) and then returned to its light-tight container.

Tests of Section of Camera Tube Stored in Dark

A parallel experiment was conducted on another tube from the support collar. This collar was removed from the camera at LRL in January 1970 and was immediately stored in the dark. The collar was removed from the dark storage, and a section of the tube was cut off. Visual examination of this tube revealed that it was yellow with two regions parallel to the axis—one dark yellow and the other gray.

The tests conducted on this tube are discussed in detail in Appendix J. 4.4. The tests consisted of measurements of spectral reflectance before and after the following two consecutive operations: a carbon tetrachloride soak and a thermal bleach. Results of these measurements, summarized below, are discussed in Appendix J and plotted in Figure J-25 for the three regions of the tube (gray, light yellow, and dark yellow). It is recognized that some changes in the values of reflectance obtained in successive measurements may be attributed to the loss of lunar material or to the failure to perform the measurements at identical sample positions.

The carbon tetrachloride soak was performed in an attempt to remove organics from the surface. Measurements after the soaking revealed a very small increase in reflectance. Thus, results of this test indicated either an absence of organic materials or, at the very least, the absence of such organic materials that were removed by carbon tetrachloride. Subsequent ion microprobe tests conducted at GCA indicated little organic material on the surface of the camera. Additional mass spectrometer tests now in progress as part of the science investigation may shed further light when results are reported.

A thermal bleach test using this tube section was then conducted. The tube section was raised to about 430°F for 18 hours in air. Remeasurement of the spectral reflectance indicated a significant increase in reflectance in the visible portion of the spectrum. The yellow color disappeared and the tube appeared dirty gray-white, similar to the tube that was photo bleached.

It was also noted that following the thermal bleach, unlike the photo bleach, the reflectance increased at wavelengths longer than about 1 micron. This is not surprising. The same increase was found at wavelengths longer than 1.3 microns in similar laboratory tests of unexposed Surveyor inorganic white paint. The increase can be attributed to the loss of water, loosely bound within the silicate structure.

These bleaching tests were undertaken in an attempt to remove the effect of radiation on the optical properties of the white paint, leaving only the dust discoloration. On the basis of the laboratory ultraviolet exposure of a sample of the same white paint, it does not appear that 18 hours at 450°F is sufficient to completely bleach out all the radiation damage. Tests at higher temperatures were not conducted.

Effects of Thermal and Photo Bleaching

It is apparent from the observed gradual bleaching of the lower shroud of the camera that a complete isolation of the returned materials from light and excessive heat was required. When this apparent lightening of color first became apparent, it was tentatively attributed to a gradual loss of deposited lunar material, or to bleaching of the paint. Optical measurements made as late as November 1970 showed that the reflectance

at 1.5 microns remained nearly constant, indicating that very little lunar dust had been lost. The lightening of the surface must therefore be attributed to photo bleaching of the paint.

The magnitude of this was clearly established in May 1970 when the cable bracket from the lower shroud was examined. This bracket had been kept dark since its removal from the camera in January 1970. Photographs of the bracket and lower shroud showed at that time that both had the same brownish yellow color. However, in May the shroud appeared grayish white, while the bracket retained the brownish color previously noted.

Samples cut from the lower shroud were exposed in November 1970 to the thermal annealing test conducted on the two tube sections. No increase in reflectance was observed. Time-dependent photo bleaching by ambient (room) lighting had already raised the reflectance. This can be seen in Table 11-2, which summarizes the results of these tests. Very little change with time occurred at 1.5 microns. It is surmised that the reflectance at 0.4 micron at the time of return from the moon must have been still lower than 27 percent, the value shown in Table 11-2 for the April 1970 measurement. Based on the measurements of the tube returned in the SESC and the bracket which had been previously exposed to light, the reflectance is estimated to have been about 20 percent at the time of return to earth. It should be noted that this sample was taken from a region facing east, a surface which was exposed to maximum solar radiation.

Four samples were cut from the cable bracket (also facing east) in May 1970, and their spectral reflectance was measured. The samples were then returned to dark storage until August 1970 when the spectral reflectance was remeasured. No increase in reflectance was found. The spectral reflectance was remeasured in November 1970 after additional dark storage. There was still no change in reflectance. It therefore appears that dark storage preserved the optical conditions for many months.

Two samples from the cable bracket were then exposed in November 1970 to the same light as the television camera, i.e., the fluorescent lighting of a laminar flow bench. The intensity of the light at the unprotected sample surface was 200 watts/cm². One sample was protected by 0.002 inch of clear teflon FEP film and the other by the teflon and 0.012 inch of polyethylene. The polyethylene simulated the condition in which the television camera was maintained from the time of return until 6 January 1970. Actual room lighting conditions during the storage were not known. The light intensity reaching the samples was about 170 watts/cm².

The spectral reflectance increased about 1 percent after 72 hours of exposure to the light. After 17 days, significant bleaching occurred, with an increase in reflectance of 13 percent at 0.4 micron for both samples. This experiment may be interpreted to mean that the television camera probably saw very little light during its LRL quarantine period since the camera was quite brown when first viewed in January 1970.

TABLE 11-2. VARIATION OF REFLECTANCE WITH TIME AS A RESULT OF PHOTO BLEACHING Lower Shroud Sample: TRW Position 2 (See Figure 11-1)

Wavelength, April 1970* 0.4 27 0.6 46 1.0 60	July 1970 36 63	Seflectance, Percent Measured at Successive Dates Ann	After Thermal Annealing (Late October 1970) 38 52 66

*April 1970 data adjusted (see text).

A set of experiments was conducted to further assess the effect of thermal soak on reflectance and to determine the role attributable to the presence of oxygen in this process. Results are summarized in Table 11-3, with additional details in Appendix J.4. Laboratory samples previously exposed to ultraviolet radiation and a sample of the returned Surveyor III camera were tested. As seen in Table 11-3, some of the samples were exposed in vacuum and some in air. All thermal soaks were performed for 18 hours at 450°F.

Thermal soak in air of the laboratory samples gave results similar to those obtained for the returned lunar sample. While some restoration of reflectance was produced, exposure in air for 18 hours at 450°F did not completely restore the optical properties.

As seen in Table 11-3, an entirely different result was obtained when the laboratory and the lunar samples were thermally exposed in vacuum. The reflectance of both samples was found to decrease significantly. Measurements of reflectance following the thermal exposure in vacuum were made in air. Subsequent thermal soak in air of the laboratory sample, which had been subjected to heat in vacuum, resulted in restoration of its reflectance to the same values obtained for the sample exposed only to air and heat. This can also be seen in Table 11-3.

Reduction of reflectance as a result of thermal exposure in vacuum is not understood. It was originally thought that the reflectance of these samples would rise as the trapped electrons (color centers) were thermally depleted. For that reason, the presence of oxygen was not considered significant; results of thermal exposure in air and in vacuum had been expected to be identical. Evidently, this was not the case. However, this unexpected result had no direct bearing on the surface discoloration and contamination studies of the returned samples. This result may be unique to the clay-silicate paint. Further tests may be warranted if it is desired to explain the results of thermal bleaching in vacuum.

11.4.2 Analysis

The discoloration model postulated that the loss of reflectance was due to a combination of two effects: solar radiation and surface coating by a layer of lunar dust. The latter reduction of spectral reflectance occurred when the incident light passed through the dust layer and after reflection of the light from the painted surface in transmission through the dust.

An analysis was conducted at JPL to attempt to derive a mathematical expression for the contribution of the lunar dust to the overall decrease of reflectance. Results of this analysis are described in Appendix J.5. As

TABLE 11-3. EFFECT OF THERMAL BLEACHING (VACUUM VERSUS AIR) ON SPECTRAL REFLECTANCE OF IRRADIATED SAMPLES OF INORGANIC WHITE PAINT USED FOR SURVEYORS

	Surveyor III Sample (Log 909 — Test Log Book)	After Thermal Bleaching - Vacuum	18	28	40	95	29
	Surveyor (Log Test Lo	Before Thermal Bleaching	33	47	62	69	73
ercent	xposed	After Thermal Bleaching -	71	78	82	81	80
Reflectance, F	Reflectance, Percent Laboratory Sample Exposed to Ultraviolet	After Thermal Bleaching - Vacuum	43	99	29	78	78
	sample raviolet	Before Thermal Bleaching	50	63	2.2	81	80
		After Thermal Bleaching -	7.1	77	80	81	82
	Laboratory S Exposed to Ult	Before Thermal Bleaching	52	7 66	28	80	92
		Wavelength, microns	0.4	0.5	0.7	1.0	1.5

shown there, the measured reflectance at any one wavelength can be effectively expressed as

$$\rho_{\rm m} = \rho_{\rm o} \, D \, (1 - KA_{\rm d})^2$$

where

 ρ_{m} = measured spectral reflectance of surface

 ρ_0 = original spectral reflectance of painted surface

D = ratio of reflectance of surface degraded by solar radiation and contamination (other than dust) to original reflectance

K = experimentally determined constant (function of wavelength)

A_d = fraction of area covered by dust

Using the above expression, it is possible to separate analytically the effects of dust from those due to radiation and contamination (term D). To do so, the factor KA_d must be determined experimentally in addition to the measurement of the final spectral reflectance and the knowledge of the original spectral reflectance.

An example of the results obtained by this technique is shown in Figure 11-3. Curve A shows the original reflectance of the paint, and curve B shows the measured reflectance of one of the samples of the returned Surveyor III camera. * Curve C shows what the reflectance of the surface of the sample would be if the dust were removed. Thus, curve C indicates the degradation caused by radiation damage only. Similarly, curve D shows what the reflectance of this sample would be in the absence of radiation damage and with degradation by dust only.

It should be noted that the same evidence is apparent from the measurements discussed in Appendix J. 4.1. In particular, results obtained for the two samples, shown in Figures J-10c and J-10f, should be compared with the results shown in Figure 11-3. Figure J-10c applies to the samples whose reflectance degradation is predominantly attributable to radiation,

^{*}Designated as 521 in Program Test Log Book.

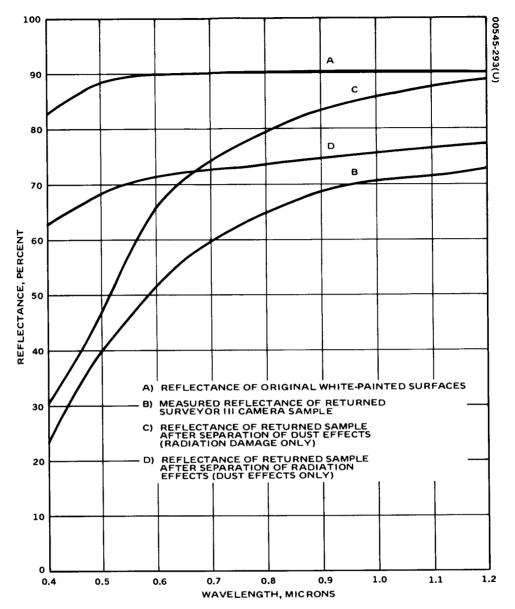


Figure 11-3. Separated Radiation and Dust Effects on Spectral Reflectance. White inorganic painted surfaces of Surveyor III camera

while Figure J-10f applies to a sample primarily degraded by lunar dust. Comparison of Figure J-10c and Figure 11-3c illustrates the photo bleaching effect described in Section 11.4.1.

11.4.3 Results of Related Investigations

As described earlier, the surface discoloration and contamination studies utilized to the maximum extent possible the results of the effort conducted as part of the parallel science investigations under JPL coordination. Results of these investigations will be reported separately.

Some of the results obtained by using inputs available to date from the science investigators are summarized here. Table 11-4 compares results obtained by several techniques for a number of samples from the returned Surveyor III camera. The samples include surfaces covered by inorganic white paint, as well as a polished aluminum surface from the bottom of the lunar shroud. This particular comparison, shown here as an example, relates to the calculation of the fraction of the area covered by lunar dust at several locations. This calculation was made using total reflectance measurements as the basic raw data. For each technique listed in Table 11-4, location A is taken as a reference. The three techniques compared are the analytical technique described in Section 11.3.2, the trapped helium experiments conducted at SUNY, and the ion microprobe work conducted at GCA.

With the exception of the value obtained from reflectance analysis for location D (polished aluminum), the results in Table 11-4 show decreasing amounts of lunar dust on the various surfaces in the order shown. An additional exception from ion microprobe data, not shown in Table 11-4, indicates highest dust coverage on location B for a depth less than 0.4 micron.

The values for location D were computed from Equation 4, Appendix J. 5, using experimentally determined values of K_{λ} for painted surfaces. The polished aluminum is a smooth surface and a specular reflector, while the painted surface is rough and a diffuse reflector. Thus, the assumption of equivalent K_{λ} is in error by an undetermined amount. Determination of K_{λ} for the aluminum surface and resolution of the apparent inconsistency would not alter or improve the understanding of the discoloration. If warranted, additional measurements could be made in the future.

Since K₂ and K₃ of Equation 1 in Appendix J. 5 are proportional to the transmission through the lunar particles, the apparent heavier coating of fines for location B (not shown in Table 11-4) is not inconsistent with reflectance determinations: the smaller particles would absorb less light.

It was possible to determine A_d as equal to approximately 0.14 for the polished surface from scanning electron microsopy.

TABLE 11-4. COMPARISON OF SEVERAL TECHNIQUES FOR ASSESSMENT OF FRACTIONAL AREA COVERED BY LUNAR DUST

III Camera
Surveyor]
Surface of
amples From
Various Sam

1 A)	Ion Microprobe (GCA)	1.0	0.95	0.79	0.29
Lunar Dust Area in Location	Trapped Helium (SUNY)	1.0	0.75	0.42	0.29
Area Covered by Lunar Dust (Fractional Area Relative to Area in Location A)	Reflectance Analysis (Appendix J. 5)	1.0	0.87	0.37	0.40
(Fra	Total Reflectance Measurement at 1 Micron	1.0	0.87	0.67	0.72
	Sample Location	Location A Top of hood (inorganic white paint)	Location B Side facing LM* (inorganic white paint)	Location C Side away from LM (inorganic white paint)	Location D Bottom of lower shroud (polished aluminum)

*Lunar module.

11.5 DAMAGE MODEL

11.5.1 General Assessment

An overall assessment of results to date of the surface discoloration and contamination studies, initiated and conducted with an awareness of the complexity of the problem and with due reservations, can now be attempted. It is believed that a reasonably good damage model has been obtained within the limits of the scope of this program and the time available.

The model proposes that the discoloration of the surfaces of the returned Surveyor III hardware is attributable to a combination of two dominant effects: radiation damage and lunar dust, the latter both from the original Surveyor landing and from the landing of the Apollo lunar module. There is some still inconclusive evidence of organic contamination, but its contribution to the total discoloration is believed to be minor.

The camera painted surfaces showed an overall dirty color in varying degrees, shades, and tones. This variation is the result of the two contributory effects: radiation damage to the paint and lunar dust coverage. While some areas are primarly affected by one or the other source, the majority of areas indicate varying contributions from both sources.

The contribution attributable to radiation damage is proportional to the extent of solar exposure experienced. The dust coverage was significantly greater than originally anticipated. Interaction of the lunar model descent engine with the lunar terrain disturbed the surface material and caused a major interaction with the Surveyor spacecraft even though the landing site was over 500 feet away.

The proposed model has been quantitatively demonstrated to be a reasonably correct one at several selected areas of the affected Surveyor III surfaces. The model has not been fully tested for all of the surfaces in order to synthesize the total complex discoloration pattern. Further investigation may be warranted if the additional degree of detailed knowledge is desired. Science studies currently under way may yield additional information of value to this model.

The dust effects on reflectance and the lunar interaction effects may be of value for future lunar operations. The radiation damage information for the specific thermal coatings used on the Surveyor was not expected to have a significant impact on future space or lunar operations.

A summary discussion of the above contributing factors is presented in the remainder of this section.

11.5.2 Effects of Lunar Dust

With the exception of one small area designated in Figure 11-1 as TRW position 3, described below, all exposed surfaces of the camera had a coating of fine lunar material. The amount of this coating varied from area to area: the "dirtiest" area was estimated to be about four to five times more heavily coated than the "cleanest" area. The various sources of lunar dust are listed in Table 11-5. These variations in the degree of cleanliness may thus be attributed to the quantity of dust imparted from the various sources to the differences in the adhesion of the dust to camera surfaces and to the various mechanisms of removal of the dust: prior to camera retrieval, during return, and during subsequent handling. In addition, there was some variation in surface roughness of the paint; the rougher areas tended to hold more material during deposition and during disturbances in handling.

As discussed in Appendix J. 1. 3, the surfaces on the northwest side of the camera exposed to the lunar module landing site were substantially lighter than the immediately adjacent areas protected by projecting hardware such as struts. This difference in color was largely due to the removal of adhering lunar material from these exposed surfaces probably by the "sandblasting" effect of material disturbed by the lunar module (LM) landing. These lighter areas on the LM side were darker than the overall color of the opposite side of the camera (away from the LM, facing southeast). Analysis indicated that less than half as much lunar material was present on the side away from LM as on the sandblasted areas facing the LM. These differences may be the result of one or more of the following: a much higher initial coverage on the LM side (Table 11-5, sources 1, 2, or 3a), incomplete removal by the LM effect of sandblasting, and deposition of particles disturbed by the LM, arriving later (Table 11-5, source 3a).

The front of the lower shroud showed slightly less dust than the sandblasted parts facing the LM but still approximately twice as much as the side away from the LM. The differences between front and sides, toward and away from the LM, may be due to differences in geometry or adhesion during sources 1 and/or 2 (Table 11-5). The side of the camera's lower shroud away from the LM landing site was in the view of the approaching LM, until the LM was several hundred feet east of its final landing site and at an altitude of 200 to 300 feet. The front was exposed at a small angle with respect to the location at which the "first visible dust" was noted. This is discussed in Appendix J. 1. 3 and can be seen in Figure J-4.

Although it might be argued that all of the contrast was due to dust stirred by the approach of the lunar modules, the absence of localized asymmetry around protrusions on the side away from LM indicates that the contribution from LM approach was minimal on that side. It is not possible to conclude that the LM contribution was minimal on the front.

TABLE 11-5. POSSIBLE SOURCES OF DUST CONTRIBUTION TO DISCOLORATION

Number	Possible Source				
1	Surveyor landing				
2	Lunar transport (i.e., secondary debris from meteoroid impacts)				
3	Lunar module				
	a) Approach				
	b) Final descent ("sandblasting" effect)				
	c) Late arriving fines from final descent				
4	Redistribution during return and handling				

The camera hood showed more dust than the lower shroud, with the highest concentration on the top and the side facing the LM. The paint in this area had a rougher texture, which would tend to trap and hold deposited dust more effectively. However, particles from any of several sources with a high ballistic trajectory, sources 1, 2, 3b, and 3c in Table 11-5, would deposit preferentially on top of the hood.

The mirror was known to have been dusty and/or pitted as a result of the abnormal landing of Surveyor III, as discussed in Appendix J. 1. 2. Comparison of the amount of dust present immediately after the Surveyor landing to that present at the time of the retrieval of the camera is under study as part of the parallel science investigation and will be reported separately. Any increase noted would be the result of sources 2 or 3a in Table 11-5.

A small area on the side away from LM, designated as TRW position 3 in Figure 11-1, appeared to be free of dust. This area was beneath the cable running from the front, along the left side of the camera.* The absence of dust may be due to "shadowing" of the surface from the incident dust or caused by a removal mechanism not fully understood.

Seen in the frontispiece of the JPL contract Final Report; not included in the NASA-MSC Contract Final Report.

Preliminary examination of screws from various parts of the camera showed quantities of lunar material that were in general agreement with the amounts on the painted surfaces, discussed above. These examinations were informative since the dielectric lunar material could be identified on metallic surfaces but not on the dielectric paint. The screw head surfaces, partially exposed to the LM sandblast, showed asymmetry in dust coverage, with less material on the exposed than on the shadowed portions. Screws from the opposite side of the camera showed less material than the sandblasted surfaces. These studies are being pursued as part of the science tests. They have not yet been completed and will be reported separately.

Shadow patterns due to dust coverage are not apparent on the side of the lower shroud away from LM. Sources 3a, b, and c in Table 11-5 would produce asymmetry if they are significant contributors to dust coverage. Asymmetry is not obvious from the examination to date of the screws from this side of the camera. Redistribution of dust (source 4 in Table 11-5) did not appear to be a major factor. The lunar material on the side away from the LM landing site was therefore most probably the result of the initial Surveyor landing although lunar transport cannot be totally disregarded.

11.5.3 Organic Contamination

One of the findings of the study was that the contribution of organic contamination to the discoloration appeared insignificant compared to the radiation and dust effects. Some evidence of minor organic contamination on some surfaces was reported in the parallel science studies, as noted in Reference 104, but this was not believed to have a significant bearing on the overall assessment presented here. Samples are still being analyzed for organic materials by science investigators, and results will be reported separately when available.

It should be recognized that the organic contaminants, even if small enough to be of no significance to the discoloration of the Surveyor III camera, could be important to the design of optical instruments for future spacecraft. Analysis of their presence and identification of their sources may therefore be required.

11.5.4 Radiation Damage

Radiation damage to the white paint was originally anticipated to be a major factor in the discoloration of the surfaces of the Surveyor III television camera. It was expected that the solar absorptance, and hence the amount of discoloration, would bear a direct relationship to the degree of solar exposure determined by the geometry of the Surveyor spacecraft on the moon. However, the patterns expected were not evident during the initial examination.

As reported above, it was reasonably possible to isolate by measurement and analysis the contributions of the lunar dust coverage from the total reflectance from the painted surfaces. This made it possible to separately analyze the patterns of discoloration and damage attributable to solar radiation only. As illustrated in Figure 11-4, it was then verified that the discoloration in the paint attributable to radiation effects is indeed proportional to the degree of solar exposure. The two locations on the lower shroud of the camera, positions 2 and 5 in Figure 11-4, correspond to areas of near-maximum and near-minimum solar exposure, respectively.

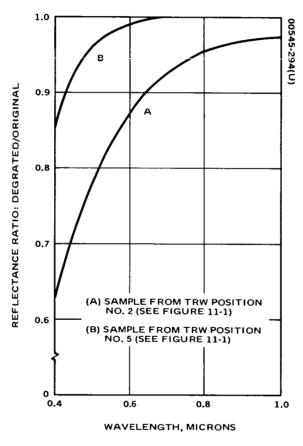


Figure 11-4. Effect of Radiation on Spectral Reflectance of White Inorganic Painted Surfaces of Surveyor III Camera (Contributions of Lunar Dust Removed Analytically)

12. FAILURE ANALYSIS

12.1 INTRODUCTION

As noted in Section 2.6.2, the failure analysis task was established to separately evaluate the significant anomalies identified in the course of the test and evaluation program. The special attention given to these anomalies was prompted partly by the desire to fully understand the contributory factors of lunar exposure and partly by the normal interest concerning any failures uncovered. The emphasis was also warranted by the fact that some of these anomalies, as noted earlier, had also been observed during actual mission operations. In retrospect, it is now evident that the degree of emphasis may not have been justified since the effects of the lunar exposure played a relatively minor role as causes of these anomalies. It should, therefore, be recognized that the most significant results of the program are contained in other sections of this report rather than in the findings presented here.

A summary discussion of the failure analyses conducted on the program is presented in this section; supplementary data on several of the more detailed studies are given in Appendix K. Comprehensive reports on the failure analyses conducted are available in the program files.

A closely monitored trouble and failure report (TFR) system analogous to that originally employed on the Surveyor program was instituted for identification, documentation, and disposition of all these anomalies (see Appendix A. 4). This disposition process entailed sequential decision points in close coordination with the customer.

After identification and preliminary assessment of an anomaly, the first decision was to determine whether a detailed failure analysis was warranted. As a general policy, no additional effort was authorized 1) when the explanation was obvious, 2) when no significant data were expected to be generated by additional tests or analyses, 3) when it was apparent that the lunar environment did not play a significant role in causing the anomaly, 4) when the benefit to future programs from further investigation would be negligible (e.g., when the part that failed was of obsolete design), or 5) when a combination of these reasons applied. In such cases, the anomaly was closed with a documented explanation.

TABLE 12-1. LIST OF ANOMALIES

Identification of Anomaly		Report Section Reference		
1)	Suspected cold weld of connector shell to shroud	12.3 and K.1		
*2)	Anomalous operation of filter wheel potentiometer	12.4 and K.2		
3)	Open shutter drive transistor	12.5 and K.3		
4)	Burned out and shorted solenoid coil	12.5 and K.3		
5)	Evaporated vidicon photoconductor and and torn grid 5 mesh	6.4.4 and 6.5.2		
6)	Mud-cracking of external painted surfaces	10.7.3		
*7)	Discoloration of TV mirror	Science report		
8)	Dust on filter glass	Science report		
9)	Discoloration and curling of teflon skirt	12.6		
10)	Cracked glass cases of 24 diodes and 3 resistors	12.7 and K.4		
11)	Open diode	12.7		
12)	12) Excessive diode leakage current 12.7			
13)	Shorted tantalum capacitor	12.8		
14)	Open alloy transistor	12.8		
15)	Open metal film resistor	12.8		
16)	16) Shift in calibration of vidicon temperature readout circuit 12.8			
17)	Excessive shutter breakaway current	12.9		
*18)	Deformed teeth of azimuth ring gear	12.9		
19)	Broken safety wire on filter wheel	12.9		
20)	Detached back of azimuth potentiometer	12. 9		

^{*}Related to reported Surveyor III mission anomalies.

If additional information on the nature or cause of the anomaly appeared desirable, a formal failure analysis process was instituted. This failure analysis activity was scrutinized as it proceeded in light of its usefulness and applicability. Failure analysis tests and evaluation progressed until such time that either a satisfactory explanation was obtained or a complete assessment of the effect of the lunar environment was fully understood, or further effort appeared futile — whichever occurred first.

The failure analysis effort entailed thorough evaluation of the evidence uncovered, review of pertinent past design and test data, and conduct of appropriate functional and diagnostic tests. In some cases, detailed records available from Surveyor mission operations were also consulted. Supplementary tests on similar parts and a review of literature were also conducted when necessary.

Some 33 TFRs were written in all, in addition to some minor discrepancies uncovered in the course of routine testing discussed in the preceding section (e.g., bent connector pin) for which TFRs did not seem necessary. In retrospect, it appears rather surprising that the total number was so low. Two of these TFRs proved inappropriate — no failures had, in fact, occurred. The remaining 31 TFRs represented 20 anomalies.*

Table 12-1 presents the list of the 20 anomalies examined. Many of these have been referred to in preceding sections of the report, as their existence became apparent in the course of the program. The evaporated vidicon photoconductor and the torn grid 5 mesh have been exhaustively treated in Section 6 rather than here because of their intrinsic relationship to the vidicon test program. Similarly, the mud-cracking of external surfaces was discussed in Section 10 as part of the materials task. Discoloration of the TV mirror, described in Sections 3.4.5 and 9.4.3, and dust on the filter glass were, by customer direction, relegated to subsequent science investigations although they were also considered to a degree in the surface contamination studies, presented in Section 11. The remaining 16 anomalies are treated in this section. Five of these-suspected connector cold weld, anomalous operation of the filter wheel potentiometer, cracked glass envelopes, and damaged solenoid and burned out shutter drive transistor-are discussed in more detailed in Appendix K. The solenoid coil and shutter drive transistor are related failures and hence are treated jointly.

Each of the above anomalies is briefly assessed in the succeeding subsections, with considerable additional detail available in program files. Each anomaly is briefly described, its effect on the camera operation noted, the tests and analysis conducted are summarized, and conclusions are stated as to its cause. The degree to which the lunar environment contributed to the anomaly is emphasized, as well as its possible significance to future applications.

^{*}Fourteen TFRs were written for cracked glass envelopes of 29 components (3 resistors and 26 diodes). Two diodes, one open, and one with a high leakage current, were treated as separate anomalies. The remaining 27 cracked envelopes were then grouped as a single anomaly after it was determined that the same mechanism of failure was involved for all.

TABLE 12-2. FAILURE ANALYSIS SUMMARY MATRIX

		Cause*			Significance**	
	Identification of Anomaly	Primary	Secondary	Contributory	To Surveyor TV Camera	To Future Application
1)	Connector cold weld	0		L	0	+
2)	Filter wheel potentiometer	0	0		+	0
3)	Shutter transistor	0	0	L(?)	++	+
4)	Shutter solenoid	S(3)		0		
5)	Vidicon photoconductor and grid 5 mesh	S(4)		L		
6)	Mud-cracking	0	L		+	+
7)	Discoloration on TV mirror	L	A		+	++
8)	Dust on filter glass	L	A		0	+
9)	Teflon skirt	L	A	0	+	+
10)	Cracked glass cases	L		0	0	+
11)	Open diodes	0	0	L	+	+
12)	Excessive diode leakage current	0	0	L	0	0
13)	Shorted tantalum capacitor	L			++	+
14)	Open alloy transistor	L			++	0
15)	Open metal film resistor	L			++	0
16)	Vidicon temperature calibration	L			+	0
17)	Shutter breakaway current	0		L	0	0
18)	Deformed gear teeth	0		L	+	0
19)	Broken safety wire	0			0	0
20)	Detached back of potentiometer	0			0	0

L = effect of lunar environment

+ = minor

++ = major

A = effect of Apollo lunar module and/or Surveyor landing

O = other causes, such as manufacturing defect, prior stress in test or assembly, operational or procedure error, prior or subsequent handling, etc.

S = result of secondary failure; in this case, the related anomaly in the table is referenced in parenthesis, and the "Significance" column is left blank.

^{0 =} none or negligible

As noted in Table 12-1, three of these anomalies corresponded to the three Surveyor mission anomalies (discussed in Section 2.4.2). Their existence was confirmed and their explanation became apparent in the course of the program.

The discoloration and contamination of the external surfaces of the camera, which might also have been termed an anomaly, were exhaustively treated in Section 11 and therefore excluded from the list of anomalies treated in this section.

12. 2 GENERAL ASSESSMENT OF ANOMALIES

A summary assessment of the 20 anomalies discussed in more detail in succeeding sections is presented in Table 12-2. Causes of the anomalies and their relative significance to the integrity and functioning of the TV camera itself and to potential future applications are presented in accordance with the described code. Both the primary and the secondary causes are indicated, as well as contributory causes, i.e., in some cases factors were present which contributed either to the primary cause or to the secondary cause or both.

For this general assessment,*anomaly causes were grouped into four general categories, as shown in Table 12-2. The lunar environment was, generally, either a primary cause or a contributory factor. Landing of the lunar module, which contributed a blast of lunar particles, was considered a secondary cause for the three surface effects noted. Similar contributions of the original Surveyor landing were arbitrarily included in the lunar environment category. Category O was used to group together all other causes not related to the lunar environment. The two failures which were strictly in the nature of a secondary effect were noted separately. Thus, the solenoid failure was basically caused by the fact that the shutter drive transistor had failed, and failure of the vidicon photoconductor and grid 5 was incurred because the shutter was open for a proloned time. The lunar environment contributed by virtue of solar thermal radiation input to the faceplate.

The significance of these anomalies to the integrity and operability of the TV camera was virtually nil or negligible, with the exception of the four cases indicated in Table 12-2. The failed shutter drive transistor, which resulted in vidicon failure, resulted in total inoperability of the camera. Similarly, any of the three component failures uncovered (items 13, 14, and 15 in the table) would individually have resulted in total loss of video information.

^{*}The assessment of failures presented here reflects the technical judgment of the authors. It is recognized that for any particular future application the relative significance of some of the findings could be assessed differently.

Of perhaps more significance is the potential impact of the observed anomalies on future space applications. Here it is difficult to find an instance of major significance with the possible exception of the implication of the observed discoloration of the TV mirror. Such a degradation of optical surfaces, or contamination by lunar dust, could be important for future applications.

The other effects were considered of minor importance when the causes of the failures were understood. The suspect cold weld spot on the connector was, to a large extent, attributable to installation techniques or errors. Occurrence of cold welding was generally conspicuous by its absence. Mud-cracking or teflon degradation were relatively minor effects which would have had a small impact on performance but should be considered in future designs.

The failure of the filter wheel potentiometer, discussed in Section 12.4, was found to have been caused by a prior defect, coupled with faulty installation and procedure.

The conformal coating problems, discussed in Section 12.7, associated with items 10, 11, and 12 (Table 12-2) can be and are being avoided in present and future designs by the use of improved coatings with a better thermal match to the materials to which they are applied. It is noteworthy that the cracks in the glass envelopes did not per se cause any component failures. The only two component anomalies noted here (items 11 and 12) were basically attributable to other causes, as discussed later; and the cracking of the glass merely aggravated the condition.

The tantalum capacitor failure represented a significant effect of the lunar environment which had, indeed, been anticipated. Surveyor III was launched with these components recognized as suspect. It was, in fact, somewhat surprising that only one of the 76 tantalum capacitors in the camera failed under cryogenic conditions. Improved capacitors are or will undoubtedly be used in the future. The alloy transistor and metal film resistor which failed are of obsolete design. Again, it was somewhat of a surprise that so few had failed.

Failure of the shutter drive transistor (and the associated secondary failures of the solenoid and vidicon) was attributable primarily to a prior condition, coupled with inadvertent operational procedures performed without the knowledge of this failure. Exposure to the lunar night environment may have contributed to this failure although this cannot be proven. The implication for future programs here is primarily one of reliability, entailing care in component selection and prelaunch testing.

^{*}The Surveyor spacecraft, as mentioned earlier, was basically not required to survive the lunar night.

The remaining anomalies were minor and were attributable to factors other than the lunar environment, and thus have no significance for future applications.

As evident from the above discussion and Table 12-2, the effect of the lunar environment was significant only in a few of the 20 anomalies although it was a contributing factor to many others. Of much more importance is that very few of the 20 anomalies can be characterized both as being caused by the lunar environment and being of major significance. In fact, only the discoloration of the TV mirror falls in this category, with, perhaps mudcracking, degradation of the teflon skirt, dust on the filter glass, non-destructive cracking of glass cases by conformal coating, and the failed tantalum capacitor deserving honorable mention. In the light of these findings, the surface contamination studies (discussed in Section 11) appear in retrospect to represent the most significant effect of the lunar environment identified in this program insofar as direct impact of the findings on future space programs is concerned.

12.3 SUSPECTED COLD WELD OF CONNECTOR J2 SHELL TO SHROUD

During the removal at Houston of the connectors from the lower shroud, a great deal of difficulty was encountered with the right (facing the camera) connector J2, as noted in Section 3.2.3. This connector was finally forced out by twisting and applying considerable force by hand, and a loud popping or breaking sound was heard in the process.

Visual inspection of the connector and microscopic examination indicated surface deformation in a small area at the base of the external thread of the connector, which had made contact to the inner edge of the hole in the shroud. A small blob of metal was clearly visible in the connector thread area. Because of the possibility that cold welding had occurred and because of the importance of cold welding to spacecraft design in general, it was decided to conduct a failure analysis of this anomaly.

The J2 connector is shown in Figure 12-1. The region of contact with the shroud can be seen on the external thread. A segment of the shroud, where the contact was made and which was cut out for analysis, is shown in Figure 12-2.

Details of the test conducted and of the results obtained, together with a number of SEM and microprobe photographs, are given in Appendix K.1. The analysis included visual and microscopic (SEM) examination, electron microprobe studies, and an attempt to perform a metallographic cross section of the suspect area.

Two distinct mechanisms of failure were postulated; the analysis was intended to determine which had occurred. One was a mechanical wedging (galling) of the connector into the shroud; the second was cold



Figure 12-1. J2 Connector Showing Area of Suspected Cold Weld (Photo 00545-202)



Figure 12-2. Segment of Shroud in Contact With Connector J2 (3X Magnification) (Photo 00545-203)

welding. It was observed at the time of dismantling that the connector nut was loose, suggesting that a considerable amount of motion with associated abrasion of the protective coating may have occurred during launch and possibly during operation of the camera on the moon; forces were imparted to the total camera and its cabling as the mirror assembly was rotated. This made it possible to postulate cold welding as a mechanism of failure since the thin iridite coating (less than 0.1 mil) originally applied over the connector could easily have worn off or been scuffed off during repeated insertion. The bare aluminum surfaces would be more susceptible to cold welding.

Visual examination indicated the presence of a blob of metal in the external thread area of the connector where contact occurred. Chemical microprobe analysis showed that this blob came from the connector aluminum rather than from the shroud aluminum.* This tended to indicate that cold welding and wedging was involved; wedging of the two surfaces would be expected to result in a substantial transfer of metal from the shroud to the connector.

Subsequent microprobe examination of the surrounding area of the connector surface adjacent to the blob and of the shroud edge in contact showed evidence of some metal transfer. This type of metal transfer would be consistent with the possibility of cold welding at that point.

^{*}The connector shell was made of 2017 aluminum, while the shroud was made of 6061. Difference in the copper, manganese, and chromium contents was used to determine this (as discussed in Appendix K.1).

Microscopic (SEM) pictures of the edge of the shroud which had been in direct contact with that region of the connector shell also showed evidence of cold welding, as described in Appendix K. 1.

However, attempts to perform a metallographic cross section of the suspect area, which might have conclusively shown the evidence of cold welding, were unsuccessful. The area of interest was polished through in the process of preparing the surface before the examination was made.

Based on the above evidence, it was concluded that a strong probability existed that some cold welding had taken place. If so, this would be the only instance of cold welding noted on the returned camera. This occurrence was, however, not a primary effect; it was made possible by a somewhat deficient installation and could therefore be considered as a secondary failure if it had indeed occurred. Looseness of the connector nut allowed for movement and abrasion of the coating. On the other hand, the failure analysis, albeit inconclusive, suggested that the simple wedging or galling postulate was not compatible with the evidence.

12.4 ANALYSIS OF FAILED FILTER WHEEL POTENTIOMETER

Analysis of the filter wheel potentiometer was triggered by the mission anomaly discussed in Section 2.4.2. The potentiometer, which was driven by the filter wheel mechanism to indicate via telemetry the position of the filters, ceased to operate halfway through the Surveyor III lunar day mission operations. Accordingly, the potentiometer was excluded from routine testing and set aside for special investigation which is reported below with supporting data in Appendix K. 2.

12.4.1 Potentiometer Description

The filter wheel potentiometer (Figure 12-3) was one of six similar potentiometers used on the TV camera. It was a three-turn, precision wire-wound device, having an end-to-end resistance of 5000 ohms ±3 percent. It was manufactured by Duncan Electronics and reprocessed at Hughes. Tests of several of the other potentiometers were discussed in Section 8.2; the focal length potentiometer wear analysis was presented in Section 10.6.3 and indicated the absence of the specified niobium disclenide lubricant.

The potentiometer consisted of a helical wire spiral enclosing a wiper block and shaft assembly (Figure 12-4). A guide made of DAP/ plastic* protruding from the assembly fitted inside the turns of the winding. In its operation, the helical winding was stationary and the rotation of the filter wheel turned the shaft of the block assembly, forcing the guide block

^{*}Molded diallyl phthalate glass fiber reinforced.



Figure 12-3. Surveyor III TV Potentiometer (Photo 00545-204)

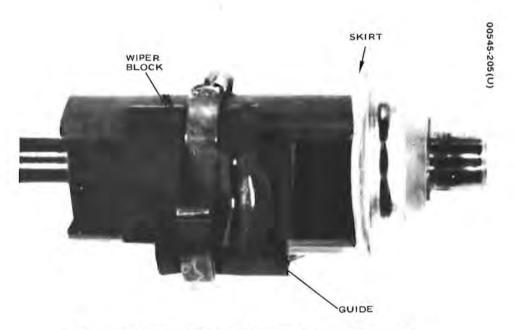


Figure 12-4. Wiper Block and Shaft Assembly of Potentiometer

to slide inside the helical winding. The wiper, which rotated with this assembly, was pulled longitudinally with the block along the slot in the shaft by the resulting longitudinal displacement of the guide as it transversed within the helix; the wiper thus made a continuous contact with the helix and generated an accurate indication of the angular displacement of the filter wheel. A protective nylon skirt can be seen in Figure 12-4.as a white disk at the right edge of a gray block.

12.4.2 Preliminary Examination

The potentiometer was subjected to an initial visual and X-ray examination and to electrical performance evaluation. The mission anomaly was verified in that the potentiometer functioned nominally for one full turn; after one revolution, the reading returned to the original value rather than continuing to increase, thereby confirming the lunar anomaly. In all other respects, the appearance and performance of the potentiometer were normal. There was no evidence of any obstruction of mechanical seizing of wires, or of loose gears. No excessive wear was observed. The visual examination also did not reveal any signs of cold welding.

12.4.3 Examination of Disassembled Potentiometer

The potentiometer was then disassembled by removing the wiper block and shaft assembly. It was noted that the guide had broken off the block assembly and that it had cracked into two pieces. Furthermore, these two pieces had physically separated from the helix. Figure 12-5 shows the appearance of this broken and cracked guide after the two pieces were fitted together for the photograph.

This finding immediately explained the nature of the anomaly: the failed guide no longer provided the positive longitudinal motion required to pull the wiper. The cause of this failure remained to be determined.

Further examination revealed that the edge of the DAP guide which had been in contact with the helical wire showed evidence of significant edge abrasion (Figure 12-5). Significant damage in the nature of abrasion and tearing was also noted on the nylon skirt.



Figure 12-5. Cracked and Broken Off Guide Block of Filter Wheel Potentiometer (30X Magnification) (Photo 00545-206)

12.4.4 Summary of Failure Analysis Tests

It was decided to conduct a more detailed analysis of the failed guide, damaged nylon skirt, and wiper block and shaft assembly to determine the cause of this anomaly partly because of the possibility that exposure to the lunar environment may have significantly contributed to this failure. It was recognized that two distinct processes had to occur to explain this failure: breaking off of the guide from the block and its cracking, as well as physical removal of the guide from the helix.

A good wiper block and shaft assembly was inserted into the winding of the filter wheel potentiometer to determine whether the damage could have been caused by jamming due to contamination in the grooves of the helix or any other obvious causes. It was found that this new assembly worked normally: the travel was smooth and unimpaired.

A diagnostic failure analysis was then conducted, including an SEM evaluation of failed surfaces, electron microprobe analysis for evidence of cold welding, emission spectroscopy for presence of lubricants, and other studies. Parallel tests were also conducted on another "good" potentiometer (the Surveyor III TV camera focal length potentiometer) used as control and on samples of the DAP plastic obtained from the manufacturer. Some of these tests are discussed in more detail in Appendix K. 2; a summary of the findings is given below.

The DAP guide was first forcibly removed from the good focal length potentiometer to determine the force required and obtain the broken surfaces for comparison studies. A similar test was also conducted on a good sample of the DAP material. Results indicated that the force required to break the focal length potentiometer guide was much smaller than that required to break the standard DAP sample, suggesting that the DAP material used on the Surveyor potentiometers was of defective quality. The force required to break the focal length potentiometer guide, however, was still about 50 percent higher than the maximum force calculated to exist in the normal operation of the potentiometer, suggesting that additional factors were involved.

Visual examination of the guides and blocks from the Surveyor III potentiometers revealed that small cracks were present, further suggesting a generally poor design or prior minor cracking resulting from prelaunch operations and handling. In particular, both blocks evidenced fracture regions behind the wiper, presumably caused by the original process of wedging the wiper into the block.

An SEM examination of the surfaces of both blocks in the area under the severed guide indicated that the texture of the filter wheel block appeared faulty compared with the focal length potentiometer block. Additional SEM photographs were taken of the regions of the blocks which had a normal appearance and of samples of the DAP material obtained from the manufacturer. Comparison of these revealed a definite deficiency of the DAP material used for the filter wheel potentiometer. The material was poorly loaded with glass fibers. The fiber lengths and concentrations did not correspond to those expected and seen on the samples of properly manufactured, stronger DAP compounds.

Examination of the abraded edge of the guide and of the nylon skirt reveal definite signs of wear and damage. Damage to the nylon skirt appeared to be associated with prior rubbing and tearing. Abrasion of the guide indicated significant wear and contact with the wires of the helix.

Electron microprobe analysis and emission spectroscopy, which were conducted on the wires and on the wipers, confirmed the absence of the niobium diselenide lubricant. The microprobe analysis also failed to reveal any significant amount of metal transfer, indicating that no significant cold welding had taken place.

12.4.5 Postulated Cause of Failure

Based on the above evidence, it was concluded that the DAP material used in the filter wheel potentiometer, and most likely in the other Surveyor III potentiometers, was defective. Furthermore, the cracks which eventually led to the breaking of the guide in two places probably existed before launch as a result of handling and prior operation of this defective component. By itself, this may not have caused the failure. However, it also appeared that a somewhat faulty installation resulted in a contact of the misaligned assembly with the nylon skirt during operation. Eventual binding into the nylon skirt, coupled with the associated rubbing of the guide against the helical wires, generated a sufficiently high force to break the defective guide off the block and to pull it out of the helix. This process was aided by the failure to properly lubricate the potentiometer. *

The failure of the filter wheel potentiometer was thus determined to have been caused by an original error or defect in manufacture, coupled with a mechanical misalignment in assembly. Absence of lubrication may have accelerated the failure. Effects of lunar exposure did not appear to contribute significantly.

12.5 OPEN SHUTTER ANOMALY AND RELATED FAILURES

12.5.1 Description of Failures and Their Interrelations

This subsection summarizes the comprehensive analysis conducted on the open shutter and three associated failures, listed as items 3, 4, and 5 in Table 12-1: the open shutter drive circuit transistor, the shorted shutter solenoid coil, and the evaporated photoconductor and torn grid 5 of the vidicon.

^{*}This was discussed in Section 10.6.3.

These failures were pursued in great detail partly because they were catastrophic to the television camera but mainly because it was judged necessary to obtain a complete understanding of the underlying causes to ensure that no major effects of the lunar environment were overlooked. The extensive discussion presented below reflects the scope of this investigation although it was later determined that the effects of lunar exposure played a relatively minor role in causing these failures.

It was definitely established that these failures were interrelated. Existence of a conductive path between the emitter and the collector of the shutter drive transistor Q5,* coupled with the application of a voltage to the solenoid drive circuit, caused a current flow through the solenoid coil. This is illustrated in the simplified schematic of the shutter drive circuits (Figure 12-6) and constituted the initial anomaly which triggered the subsequent chain of events.

The shutter contains two solenoids, A and B, each comprised of two bifilar windings. The four coils, designated A1, A2, B1, and B2, are driven from a common voltage source marked as point V in Figure 12-6. Each coil is individually triggered by actuation of a similar series

*This conductive path, as discussed later, was a failure rather than the result of turning the transistor on, either inadvertently or by command.

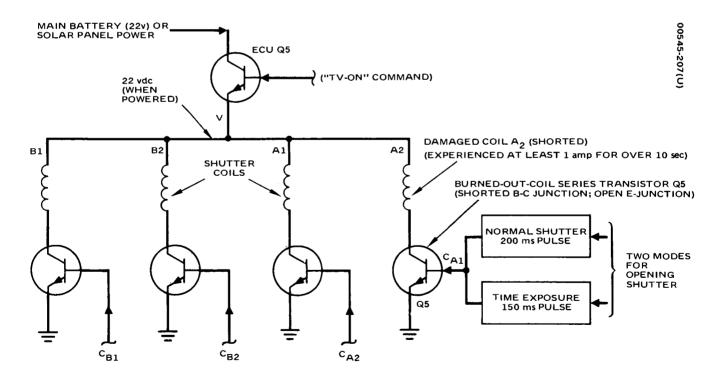


Figure 12-6. Simplified Schematic of Shutter Coils and Drive Circuits

transistor, designated Q5 in the circuit of the failed coil A2. Normally Q5 is activated by sending one of the two commands indicated.

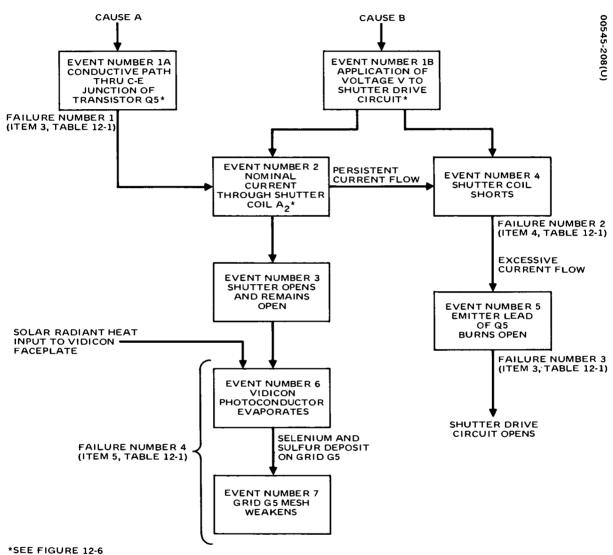
In normal shutter mode, the activating 200 ms pulse turns on the transistor Q5, which closes the ground return for and causes the current to flow through winding A2 of coil A. This causes blade A to move, opening the shutter. Following this pulse, 150 ms later, coil B2 is activated, causing blade B to move to close the shutter. A subsequent automatic sequence activates coils A1 and B1, restoring the shutter blades to their original positions.

In the time exposure mode, a 150 ms pulse is generated which activates coil A2, opening the shutter. The shutter remains open until a TIME EXPOSURE Off command followed by a START FRAME command is sent to initiate the normal shutter sequence of events, resulting in the movement of blade B and subsequent return of both blades to their original positions.

It became immediately obvious from the preliminary analysis that all subsequent failures occurred because the current flow through coil A2 was of unduly long duration either because the activating pulses had persisted too long, maintaining transistor Q5 in the ON state, or because its conductive emitter-to-collector path was permanently maintained as a result of an internal failure. As discussed later, the former possibility was subsequently discounted. As a result of this long-duration current through coil A2, two effects occurred, causing the remaining interrelated failures to occur. This is illustrated in the logic block diagram of Figure 12-7.

The two effects were opening of the shutter (event 3 in Figure 12-7) and eventual burning of the insulation of coil A2 and shorting of its windings (event 4). A necessary condition for these events, as evident from Figure 12-6, was, in addition to the collector-emitter short of transistor Q5, the continuing presence of the applied voltage at point V in Figure 12-6. Damage to coil A2, as discussed in Section 5.5, resulted in reduction of its winding resistance from an original value of 33 ohms to the final measured value of 0.2 ohm. This caused an increase in current through Q5, which, in turn, eventually burned out the emitter lead of the Q5 transistor, leaving it in the open condition found (event 5 in Figure 12-7). Thus, the Q5 transistor initially shorted and later opened (failures 1 and 3 in Figure 12-7).

The open shutter remained in that position from then on in the absence of any corrective signals. It should be noted that this opening of the shutter presumably occurred after the first lunar day of the normal operation of the Surveyor III camera. The vidicon failure, as discussed in Section 6, took place later; it was a secondary consequence of the opened shutter through which solar radiant heat input was transmitted to the vidicon faceplate over a prolonged period. The resulting elevated temperatures of



NOTE: OBJECTIVE OF FAILURE ANALYSIS WAS TO DETERMINE CAUSES A AND B

Figure 12-7. Logic Block Diagram Showing Relationship and Sequence of Failures of Shutter Drive Transistor, Shutter Coil, and Vidicon Photoconductor and Grid

the faceplate caused the photoconductor to evaporate (event 6, Figure 12-7). Subsequent deposition of sulfur and selenium from the photoconductor onto its grid 5 caused a physical/chemical change and a weakening of the copper mesh (event 7, Figure 12-7). The grid eventually shattered — either on the moon or during subsequent handling.

This summary represents a complex sequence of events. Fortunately, sufficient data were available so that with a considerable test and analysis effort and some aid from available past records a reasonably comprehensive picture was reconstructed and a plausible explanation generated of the postulated causes and mechanisms of these failures.

As evident from the above discussion, the key to the explanation of this sequence of events and failures was the nature of the cause of the original conductive path between the emitter and the collector of transistor Q5 and the cause of the presence of line voltage at point V in Figure 12-6. The bulk of the discussion in this section, supplemented by the discussion in Appendix K.3, is devoted to these two events (events 1A and 1B in Figure 12-7). Discussion of the nature of the associated failures — the shorted solenoid coil and the open emitter lead of transistor Q5 is also presented in this section as part of this analysis. The vidicon photoconductor and grid 5 failures are exhaustively discussed in Section 6 and Appendix G, where the mechanisms of these failures are fully described and verified.

12.5.2 Failure Analysis Plan

The failure of the shutter drive transistor would by itself have resulted in a total loss of video information even if the photoconductor had not evaporated from the vidicon faceplate since the shutter could not be operated. However, the main reason for conducting this comprehensive failure analysis was to determine whether any significant effects of the lunar exposure were involved of potential importance to future programs. It became evident at the conclusion of this investigation that no such major effects occurred. The only significant effect of the lunar environment, if any, may have been a contributory one: the Q5 transistor, possibly defective for reasons traceable to its manufacture or prelaunch tests, may have been further degraded by exposure to thermal cycling through the lunar night. It subsequently failed as a result of a voltage breakdown, as discussed below.

The analysis included a complete failure analysis of transistor Q5 and of the shorted solenoid winding, together with a review of past test data and of the signals transmitted to the Surveyor spacecraft at the end of the first lunar day and thereafter. Assessment of the evidence collected and

^{*}Had this been known a priori, some of the extensive work conducted might not have been warranted.

review of design features of the television, power, communication, and command subsystems of the Surveyor III spacecraft, led to the development of a failure logic tree and study of the many possible modes of failure. This analysis stressed the occurrences of the two original events, noted as events 1A and 1B in Figure 12-7, which would explain the subsequent occurrences.

The analysis led to the final postulate of the causes, mechanisms, and sequences of these failures, primarily by a process of elimination and inference.

The failure analysis of transistor Q5 and of the solenoid coil, including a review of past data, is presented next, with supporting discussion in Appendices K. 3. 1 and K. 3. 2. Logical development of the postulated explanations then follows, with supporting data in Appendices K. 3. 3 and K. 3. 4.

12.5.3 Analysis of Failed Shutter Drive Transistor

The failed shutter circuit drive transistor was an NPN silicon power transistor, manufactured by Fairchild, similar to type 2N3891. The transistor was mounted on a TO-5 case.

A comprehensive analysis of the failed transistor was conducted. The tests and findings are presented in Appendix K. 3. 1, and additional details are available in separate analysis reports in the program files. Past records were also examined for supporting evidence of postulated prior stress.

Review of past history of this transistor revealed two significant facts bearing directly on its failure. The original test data for this transistor indicated that its collector-to-base breakdown voltage was somewhat lower than that of the three similar transistors in the drive circuits of three other solenoid coils. This breakdown voltage, while within specification, had been measured as only 116 volts, compared to the 170 to 180 volt range for the three other transistors. No data were available for the collector-to-emitter breakdown voltage more directly involved in this analysis, rated as 80 volts minimum; but the above findings sufficed to establish a degree of susceptibility of the construction of the transistor to partial overstress. The second finding was that this particular transistor had been stressed in prelaunch tests, as was indicated in Section 2.4.1 and discussed below.

During the prelaunch test of a similar Surveyor TV camera, a test equipment problem occurred which caused an overstress of the shutter drive transistor in that camera and damage to the insulation of the winding of its shutter solenoid. This malfunction was traced to an improper termination of a coaxial cable which caused shorting of the vertical blanking pulse and disabling of the video logic circuit. When a START FRAME command

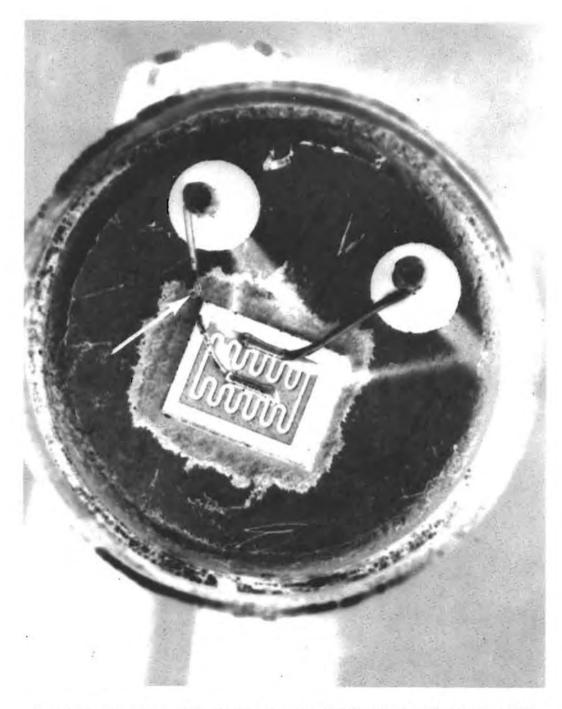


Figure 12-8. Failed Shutter Solenoid Drive Transistor (Q5) Showing Open Emitter Lead (10X Magnification) (Photo 00545-209)

was subsequently sent to operate the shutter, a noise spike was generated to trigger the video logic multivibrator, which, in turn activated the shutter solenoid drive circuits. In the absence of an OFF pulse due to the cable short, the current through this drive circuit, identical to the circuit of the Surveyor III TV camera, existed for an unknown length of time. This was later found to have caused the overstress of the Q5 transistor and the chaffing of the insulation of the coil in a manner virtually identical with that found here.

This problem was not identified until after the Surveyor III camera had been subjected to prelaunch tests at the same test position approximately I month after the original failure. It is, therefore, possible that the Surveyor III transistor had been subjected to an unknown degree of stress. This fact was not unrecognized before the launch of Surveyor III. As mentioned in Section 2.4.1, the camera subsystem and particularly its shutter drive circuit were subjected to special tests to validate proper operation. Launching of the camera with this lien, subsequently validated by its successful operation throughout the entire lunar day, was a calculated risk. This risk was determined to be acceptable, based on proper functioning of the camera in test, and was taken by weighing the undesirable alternatives of major reassembly and retests of the camera and the entire spacecraft against the available evidence.

The failure analysis conducted on the Surveyor III Q5 transistor revealed that the emitter lead was open as a result of excessive collector-emitter current flow. This open emitter lead is clearly seen in Figure 12-8 which shows the overall view of the transistor. More detailed photographs are shown in Appendix K. 2. 1.

Further investigation into the mechanism of failure associated with the excessive current flow to determine the original cause of this occurrence (prior to the final opening of the emitter) revealed that the basic mechanism was a voltage breakdown from the collector to emitter. An overcurrent failure would have resulted in a more uniform melting of the aluminum metallization than was observed. An excessive junction current would also have produced some evidence of rediffusion; none were uncovered. On the other hand, microsectioning of the junction indicated a voltage punchthrough mechanism of failure.

The conclusion of the failure analysis was that a voltage spike of sufficient magnitude had been generated which caused the emitter-to-collector breakdown of this transistor and that, with a nominal voltage applied to the transistor drive circuit, this puncture resulted in an excessive collector-to-emitter current which eventually burned out the emitter lead. Possible prior stress of the transistor, and the fact that it had a somewhat lower original breakdown voltage rating, may have contributed to this occurrence. As a further possibility, not confirmed by laboratory analysis, the thermal cycling through the lunar night of this suspect transistor may have further aggravated its condition if the postulated occurrence of the circuit voltage and of the voltage breakdown spike did, indeed, take place after the first lunar night. This postulate

of the time of occurrence of this failure is compatible with other evidence, as discussed below.

12.5.4 Analysis of Failed Solenoid Coil

The failed shutter solenoid coil was on one of its bifilar solenoids. A brief description of this subassembly was given in Section 5.5. Figure 12-9 shows the appearance of the subassembly with evidence of the burned insulation clearly visible.

The complete failure analysis, entailing visual examination, electrical tests, X-ray analysis, and dissection was conducted; results are presented in Appendix K. 3. 2.

The evidence of failure was that the insulation was burned on one of the windings and both coils of the windings were damaged. One of the coils had a resistance of 24 ohms, compared to the original value of 33 ohms, showing some degradation due to shorted windings. The other coil, corresponding to coil A2 in Figure 12-6, was virtually completely shorted. It measured 0.2 ohm, compared to 33 ohms nominal.

Analysis indicated that the failure was undoubtedly caused by excessive heating resulting from either an excessively high current or from a current of unduly long duration. It should be noted that the coil is rated at only about 2 watts. In its normal operation, the coil dissipates approximately 14 watts for the very short times of the 150 or 200 ms driving pulses.



Figure 12-9. Damaged Shutter Solenoid Coil (Photo 70-4885)

It was apparent that prolonged maintenance of the 22 volt line voltage normally applied during the pulse duration would easily account for the observed mode of failure.

12.5.5 Assessment of Evidence and Initial Causes of Failure

Results of the preliminary assessment of the shutter drive circuit in Figure 12-6 and of the failure analysis of the Q5 transistor and solenoid coil focused attention on the next, more difficult, task of explaining the two primary independent events (events 1A and 1B in Figure 12-7): the original occurrence of the voltage breakdown between the collector and the emitter of the transistor, and the existence of line voltage at point V in Figure 12-6. Both of these had to occur to cause the subsequent problems.

Cause of Short of Transistor Q5

The evidence relating to the cause of the collector-emitter short was somewhat more complex, but the explanation did not admit of as many possibilities as those attributable to the second problem, that of the presence of the line voltage. This evidence can be summarized as follows:

- 1) Transistor Q5 had a lower breakdown rating than the three other shutter coil drive transistors.
- 2) The transistor may have been overstressed in prelaunch tests.
- 3) The transistor operated normally throughout the entire first lunar day.
- 4) Review of mission operations verified proper shutdown of the shutter drive circuits, as well as other circuits, at the end of the first lunar day.
- 5) No commands were transmitted during the first lunar night.
- 6) The transistor may have degraded as a result of thermal cycling through the lunar night (this was not verified by diagnostic analysis).
- 7) The transistor primary failure mode was found to have been a catastrophic voltage breakdown between the collector and the emitter.
- 8) No evidence was found of any commands sent after the first lunar day to turn the shutter circuits on.
- 9) A variety of other commands was sent to the spacecraft on the second lunar day and even later in the attempt to revive it.

Item 1 helps to explain why the other three coil transistors did not fail at the time that a presumed voltage may have caused the breakdown of the Q5 transistor. This evidence also confirms by inference a degree of shortcoming of the Q5 transistor.

Item 2, and possibly item 6 in conjunction with item 3, suggests that perhaps a further degree of degradation existed or occurred which contributed to the eventual failure of this transistor. This, however, can only be inferred.

Item 7 indicates that a voltage excitation occurred which damaged the transistor. The value of the voltage required for this to occur cannot be firmly assessed in view of the uncertain condition of this device, as noted above. While it is doubtful that the nominal circuit voltage of up to 30, or even 40.* volts might have caused this failure, this possibility cannot be totally discounted. In view of item 9 above, and the resulting uncertainty of the Surveyor III configuration after the lunar night, it is equally if not more reasonable to postulate that a voltage spike of sufficiently high magnitude, in excess of 40 volts or even above the nominal breakdown value of 80 volts, occurred to precipitate this breakdown. It is possible that such a voltage may also have been generated by electrostatic means. It should be noted that the duration of such a high voltage spike need not be greater than a fraction of a millisecond to cause this type of failure, as verified by unfortunate experiences during the Surveyor test program.

Although item 8 indicates that in all probability no commanded activation of the Q5 transistor occurred, a faulty triggering of the drive circuits for a prolonged time period could not be discounted a priori in view of item 9. Inadvertent prolonged activation of the drive circuit of transistor Q5 would independently account for the burnout of the solenoid coil even though the transistor could by its rating have withstood the full 0.67 ampere for a very long period of time. This hypothesis, if valid, would suggest an alternate sequence of events whereby the solenoid coil failure would occur first. The resultant application of the full 22 volts (which would have had to be present) might then have contributed to the thus hypothesized subsequent failure of the collector emitter junction, as well as resulted in the burnout of the emitter lead.**

A complete assessment of this alternate mode of failure was conducted; results are summarized in Appendix K. 3. 3. This mode of failure was disproved by the absence of evidence of damage to other components on the retrieved chassis.

^{*}As discussed later, up to 40 volts might have been supplied by the solar panel under optimum conditions through defective or degraded circuits.

^{**}This type of collector-emitter failure mode was already shown to be incompatible with evidence from failure analysis; however, for the sake of completeness, it was not totally discounted.

Cause of Presence of Voltage Across Shutter Coil Circuit

The presence of voltage of appreciable duration across the shutter coil drive circuit (point V in Figure 12-6) after the first lunar night was established to be the second necessary condition for the failure of the solenoid coil and subsequent events. A review of mission records confirmed that no anomalous effects were noted at the end of the first lunar day and that the shutter had been properly closed for the lunar night. The effort to explain the existence of the coil voltage entailed analysis of the available evidence summarized earlier, additional tests of the returned chassis and components, a review of operational commands sent to the spacecraft after the first lunar night, and a study of the electrical subsystems of the spacecraft for possible alternate modes of failure which, in conjunction with the commands transmitted, might provide a plausible explanation.

The eight basic ways by which the voltage could be made to appear at point V (Figure 12-6) are summarized in the logic diagram of Figure 12-10. These eight logic paths entail combinations of faults and commands. All of them were examined to the maximum extent feasible for validity. All but path F and perhaps G were proven invalid or highly unlikely.

Paths A and B postulated a "frozen battery" condition whereby the solar panel could directly activate the circuit. This could occur in one of two ways. Path A would require a permanent defect in the transistor of the retrieved ECU. As seen below in the discussion of path D, this was proved not to have occurred. Path B could occur provided that the solar panel power was sufficiently high to maintain a voltage across the ECU transistor in excess of its breakdown potential of 80 volts. The transistor would then become conductive, but it would subsequently recover so that no evidence of degradation would necessarily be noticeable later. However, analysis of the solar panel subsystem determined that the incident solar energy could only generate a maximum of 0.5 watt of power in the 10 square foot solar panel in its final lunar orientation. Assuming a 10 percent efficiency, the maximum sustained voltage that the solar panel could provide to the circuit could therefore not exceed 40 volts.

The remaining six paths required that a command be sent to turn on the main power system of the spacecraft. This command, known as OTC ON,* supplies +29 volts to the TV camera and to the TV camera auxiliary, which is a separate electronic compartment not retrieved by the Apollo astronauts. Mission records indicate that this command had indeed been sent repeatedly on the second lunar day as the basic spacecraft activation signal.

The OTC ON command in the absence of other signals or failures cannot by itself produce the voltage in question. Normal means for

^{*}Overload trip circuit.

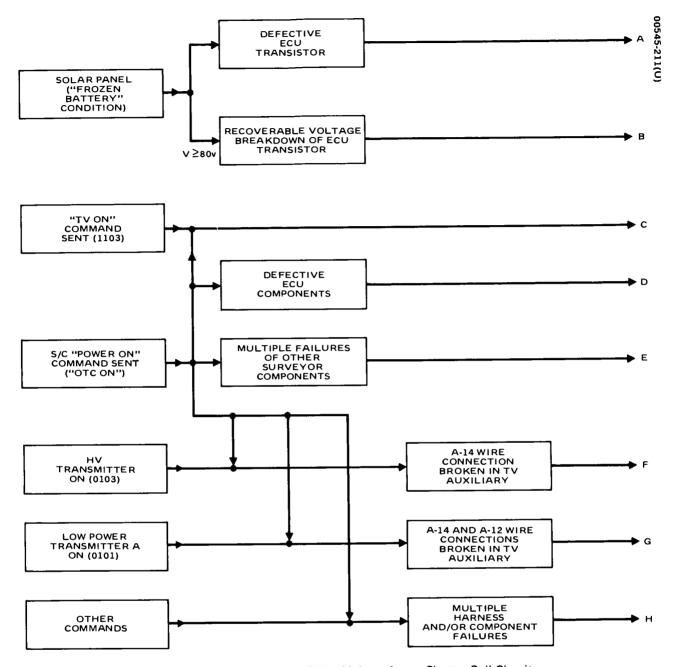


Figure 12-10. Possible Causes of Line Voltage Across Shutter Coil Circuit

accomplishing this entail the transmission of a separate command, whose code was 1103, shown as TV ON command in Figure 12-10. This command, then, in conjunction with the OTC ON command, is designated in Figure 12-10 as a possible path C. Extensive search of mission records revealed no trace of this command.

The remaining five ways of generating the voltage V all entail some sort of failure in addition to the OTC ON command. Paths F, G, and H also require transmission of additional command.

Path D entails the real possibility that defective components of the ECU of the camera, in conjunction with the OTC ON command, somehow permitted the ECU to be turned on, thereby supplying the voltage to the shutter circuit. This path also included the possibility of other modes of ECU failure to produce this voltage through direct faulty transmission of the main spacecraft bus power. For example, one faulty transistor known as the ECU Q5,* could account for this occurrence. This possibility was therefore analyzed in more detail—fortunately, the ECU had been retrieved as part of the Surveyor III camera and could be physically examined and tested. Results of this examination are presented in Appendix K. 3. 4. No traces of component degradation, which would be a necessary consequence of this mode of activation of the shutter circuit, were uncovered.

The alternate path E was considered to be highly hypothetical, purely speculative in nature, entailing numerous failures of other components. This unlikely explanation was not pursued further in view of its futility and the much more plausible explanations entailing many fewer failures, as discussed below.

A search was then conducted for a combination of minimal numbers of hypothetical yet plausible failures, which, coupled with other commands sent to the spacecraft in conjunction with the OTC ON command, would account for the anomaly. The general category of such possibilities is shown for completeness in Figure 12-10 as path H. Of the multiplicity of such failure possibilities, two appeared most likely in light of the commands transmitted and the circuit characteristics considered. These are designated as paths F and G in Figure 12-10.

Path F is considered, by far, to be the most likely source of the anomaly. For this event to take place, it was necessary to verify that command 0103, similar to the TV ON command 1103, had been sent. This signal 0103, which commands transmitter A of the spacecraft to its high voltage mode, was, indeed, uncovered in mission records to have been transmitted on at least three occasions during the second lunar day. Circuit analysis indicated that a single broken connection between the TV auxiliary and the Surveyor camera, designated in Figure 12-10 as wire A14, would immediately transform this 0103 command into the 1103 signal necessary to activate the ECU and apply voltage to the shutter coil circuit. The postulate of such a broken connection appears to be highly plausible. The failure of a single solder joint in the TV auxiliary, not difficult to visualize, would account for it.

The second, somewhat less likely, possibility entails a malfunction of another wire, designated A12 in Figure 12-10, in addition to the open condition of the A14 wire. The reason that this alternate failure (path G) should also be considered is that this occurrence would transform a command 0101 into the TV ON command 1103; mission records indicated that

^{*}ECU Q5 should not be confused with transistor Q5 of the shutter circuit.

the 0101 command, which turns the transmitter A into its low power mode, was transmitted to the spacecraft a great many times during the second lunar day.

12.5.6 Postulated Mechanism of Failure

In summary, the most plausible cause and sequence of events can now be postulated and is summarized below. It should be noted that insofar as camera failures are concerned the lunar environment appeared to have played an extremely minor role, if any. The only possible contribution, for which no positive evidence was uncovered, was a hypothetical additional degradation of the Q5 transistor in the shutter drive circuit prior to its ultimate failure(s).

After normal performance during the first lunar day, a series of commands was sent to the spacecraft on the second lunar day in the attempt to revive it. These commands included nominal commands to turn on the main power system, as well as many other commands.

It appears that one or more soldered connections may have opened during the lunar night although no solder failures were found in the returned television camera.* In particular, the Al4 wire from the TV auxiliary to the TV camera may have become unsoldered or broken. Upon transmission of the command to attempt to turn the spacecraft transmitter A on, an erroneous signal was probably generated by the spacecraft, which inadvertently turned on its ECU, applying voltage to the shutter coil circuit.

One of the shutter coil circuits had as its drive transistor a unit which, while within specification, had a relatively low breakdown voltage characteristic. It is not known to what extent the condition of this transistor was degraded by its prior stress history in testing or by exposure to thermal cycling. It is also not firmly known whether this potential degradation had any direct bearing on the subsequent chain of events. However, the appearance of a voltage pulse in the transistor drive circuit resulted in a voltage breakdown between its emitter and collector.

This voltage could have been caused by a variety of reasons, including a transient spike from the instant application of the line voltage, other transient noise spikes, or even electrostatic charges. It should be noted that, because of the possibility of other Surveyor III component and subsystem failures, the Surveyor spacecraft configuration on the second lunar day may have been different from what it was originally. The presence of reasonably high voltage pulses following the multiplicity of commands sent in the attempt to revive the spacecraft therefore cannot be discounted.

^{*}It was noted during Surveyor thermal-vacuum tests that the various space-craft units experienced different solder joint problems because of the differences in manufacturing techniques.

It is not known what voltage level might have been sufficient to cause this transistor breakdown. The transistor was known to have had a somewhat lower breakdown characteristic relative to its companion transistors in the other shutter drive circuits.* Furthermore, it is not known to what extent possible prior recorded stress in test, or even effect of the lunar night, could have further increased its susceptibility.

Unfortunately, emitter-to-collector breakdown occurred in the most vulnerable part of the shutter subassembly, that which drives the shutter to the OPEN position. This was because the transistors in series with the other three coils happened to have had a higher voltage breakdown rating.

The remaining chain of events leading to the observed anomalies appears to have been inevitable and straightforward. With the emitter shorted to the collector and with the line voltage inadvertently present, nominal shutter solenoid current opened the shutter. In the absence of normal signals to turn the shutter current off and to restore the shutter to its closed position, the shutter remained open and the solenoid current continued to flow. The solenoid, not rated for continuous operation in this mode, soon overheated. Its insulation burned and its coil shorted. This, in turn, raised the circuit current to an extremely high value, beyond the rating of the series transistor. Eventually, the emitter lead of the series transistor burned out, opening the circuit, and interrupting the current flow.

Meanwhile, with the shutter open for the remaining 31 lunar day/ nigh cycles,** sufficient solar radiation energy impinged upon the vidicon faceplate to cause its temperature to rise to a value of about 100°C, substantially above its rating. This resulted in evaporation of the photoconductor from the faceplate. The photoconductor, which contained selenium and sulfur, deposited on the neighboring copper wire mesh of its grid 5, causing a physical and chemical change in its structure. The thickness of the copper mesh shrunk to a structurally deficient value, and the mesh tore and shattered, either on the lunar surface or during subsequent handling of the camera retrieval and return.

12.6 DISCOLORATION AND CURLING OF TEFLON SKIRT

The 2 mil thick teflon TFE skirt (see Figure 3-29, Section 3) was used as a seal in the opening between the rotating mirror assembly and the

^{*}Its collector-to-base breakdown voltage was 116 volts, compared to 170 to 180 volts for the others; but its collector-to-emitter breakdown voltage was not previously measured. The specifications required 80 volts minimum.

^{**}Or, perhaps, 30, if the failure occurred on the third lunar day.

camera body to prevent lunar dust from entering the camera. The skirt was bonded to the base of the mirror assembly over approximately half of its width. The epoxy adhesive used was Epiphen 825A, made by the Borden Chemical Company.

The anomaly observed during the initial Surveyor operations (reported in Section 3.4.4) was that the teflon appeared discolored and had curled up and under the hood. The teflon appeared to be light brown, in contrast to its original milky white appearance. It also appeared brittle. Some of the epoxy was also noted to be present on the inward side of the unsupported teflon.

The curling of the teflon may have allowed a small quantity of lunar dust to enter the camera, particularly as a result of the "sandblasting" effect of the descent of the Apollo Lunar Module. While the effect on the integrity of camera operation would not be expected to have been major, it was decided to conduct a failure analysis of this anomaly primarily to assess the effect of the lunar environment on the properties of this widely used material.

The failure analysis was designed to determine the cause and nature of the observed discoloration and curling, to assess the degree to which these effects could be attributed to changes in the epoxy rather than teflon, and to identify the specific components of the lunar environment to which these effects could have been attributed. Discoloration and curling of teflon TFE samples exposed to simulated lunar radiation environments had been observed in laboratory testing. The curling may be, in part, attributable to the blast produced by the lunar module landing although nondegraded teflon may have withstood this effect better.

Prior tests were conducted on similar samples of the epoxy, as discussed in Section 10.5, and were therefore not repeated as part of this failure analysis. As reported there, a definite increase in hardness of the epoxy had been observed.

Physical measurements of the TFE teflon samples from other parts of the camera were also conducted as part of routine material tests and were reported in Section 10.4.3. Physical tests of samples of the curled portions of this teflon skirt could not be conducted because of the limited amount of material available. Physical changes noted in these other TFE teflon samples would not have accounted for this curling effect; no similar curling of teflon TFE was observed elsewhere. No evidence of significant increase in brittleness of the teflon TFE was noted.

In addition to the visual examination, additional tests conducted as part of this failure analysis include ultraviolet and infrared spectrochemical analysis, elemental analysis, electron paramagnetic resonance, and differential thermal analysis. One of the objectives of these tests was to determine whether any chemical changes had taken place in the teflon.

The only effect observed was an indication of some defluorination, found by the ultraviolet spectrochemical analysis. This test, however,

revealed no structural changes. The observed defluorination would not be sufficient to have caused the observed effects.

Similarly, infrared spectrochemical analysis revealed no structural changes. It verified the presence of the epoxy adhesive on the interior of the unbonded surfaces of the unsupported area of the skirt. Elemental analysis indicated no changes in the chemical composition. No change of free radical concentration was found as a result of the electron paramagnetic resonance test, and no changes in thermal properties were noted as a result of the thermal analysis.

The presence of the epoxy on the unbonded surfaces, coupled with the previously verified increase in the hardness of the epoxy, was believed to have been the major cause of the observed condition of the skirt. The increase in hardness was accompanied by some shrinkage. This shrinkage of the epoxy is believed to have caused the teflon to curl inward.

Results of the failure analysis revealed that no basic effects of concern were induced on the teflon by the lunar environment. The only significant effect was the expected and reasonably well understood increase in hardness of the epoxy adhesive. The presence of epoxy on unbonded areas was unwarranted and can be attributed to improper manufacturing and installation techniques.

12.7 CRACKED GLASS ENVELOPES ON DIODES AND RESISTORS AND RELATED COMPONENT FAILURES

12.7.1 Introduction

This subsection summarizes the results of the failure analysis conducted on 29 components which were found to have cracks in their glass cases (items 10, 11, and 12 in Table 12-1). These included 26 diodes and 3 resistors.

Fourteen TFRs were written for these anomalies. Twelve of these dealt with 27 components: 24 diodes and 3 resistors whose glass cases were cracked but which appeared electrically unaffected. These were then grouped into one generic anomaly since the symptoms, and presumably the causes, appeared virtually identical. The remaining two TFRs were written for the other two diodes with cracked cases which also exhibited electrical anomalies: one TFR for the diode which was found electrically open and one TFR for the diode which exhibited an excessive leakage current.

In all 29 cases, extensive cracking was also observed of the conformal coating applied over the glass envelopes. This cracking of conformal coating was also noted on many other components where no damage to the glass envelopes occurred. No separate TFRs were written for these



Figure 12-11. Cracked Diode Glass Envolope (Photo 00545-212)

cracks partly because they did not per se entail a significant malfunction, partly because their occurrence was expected* for the type of coating used, and partly because this problem was necessarily included in the treatment of the above 29 anomalies.

The general discussion of cracking of the glass envelopes is presented first. The two diodes which exhibited electrical malfunctions are then treated in further depth, with supplementary failure analysis data included in Appendix K.4.

12.7.2 Preliminary Examination of Cracked Glass Envelopes

A failure analysis of the cracked glass cases was conducted since it was felt that the cracking occurred as a result of the lunar thermal cycling. The first phase of this effort included a visual and microscopic examination of the cracked cases, a review of past records, and tests of the two diodes which had failed.

Visual examination revealed that all of the cracked cases were on components which had been bonded and which were covered with a reasonably thick layer of conformal coating. Extensive cracking of the conformal coating was also observed on all of these components. Figure 12-11, taken of a cracked diode case, illustrates these effects.

A summary of the 29 cracked glass envelopes is presented in Table 12-3. The types and chassis locations of these resistors and diodes are shown on the table, and the two diodes which exhibited functional failures are indicated. Also noted on the table are the two diodes and one resistor that were damaged in the process of removal; the two damaged diodes could not be tested, but the resistor was measured on the chassis and appeared to be electrically normal.

While the total number of cracked cases was not negligible, it was a small fraction of the total number of similar components present on the camera, as indicated in Table 12-3. Certainly two failed diodes was a small fraction of the total number of diodes in the camera. As seen from the subsequent discussion, the occurrence of these two failures was of even lesser concern since it was found that these failures were basically traceable to original manufacturing defects or other causes and not lunar exposure.

12.7.3 Review of Past Data

Numerous past records were available on similar occurrences of cracked conformal coatings and glass cases of components during cryogenic

^{*}Similar effects were noted following prelaunch solar-thermal-vacuum tests.

TABLE 12-3. SUMMARY OF COMPONENTS OF SURVEYOR III CAMERA WITH CRACKED GLASS ENVELOPES

Total Number in TV Camera		261	37	17	315	424	240	664	626
Number of Cracked Envelopes on Chassis	Total	17	∞	-	26	1	2	3	67
	ECU	9	7	1(3)	14				14
	A10	1			1				
	A 6		·		0				0
	A5	1	1(2)		2	1(4)		1	3
f Crac	A4				0		2	2	2
mber o	A3	3(1)			3				3
Nu	A2	2			2				2
	A 1	4(3)			4				4
	Type	IN3070	IN3730	IN754A		RCR07	RN55G		
Manufacturer		Fairchild	Raytheon	Continental Devices	. Diodes	Allen-Bradley	Texas Instruments	Totals for Resistors	Totals
988 Part Component Designation		703-1	723-1	732-1	Totals for Diodes	601	610		
		High speed switch diode	Switching diode	Zener voltage regulator diode		Carbon composition resistor	Carbon film resistor		

Blank entry means that no component was found cracked, or that no component of this type was on the chassis. Legend:

1) One of these diodes was found open (see failure analysis discussion).

2) This diode had excessive leakage (see failure analysis discussion).

3) One of these diodes was destroyed during removal from chassis.

This resistor was partially destroyed on removal.

cycling. These data were available from the Surveyor program, on which many TFRs had been written dating back to 1963, and from other programs. The following conclusions were drawn from the review of these records:

- Cryogenic cycling caused frequent cracking of conformal coatings when the components were subjected to temperatures below -100°F and wherever the thickness of the coating exceeded about 10 mils.
- Very few instances of cracking of the conformal coating were uncovered when the coating was uniformly applied and when its thickness was less than 10 mils.
- Occasional occurrence of associated cracking of glass envelopes was noted when the conformal coating was thick and when the components were bonded. Very few occurrences of cracked glass envelopes were noted when the components were not bonded.
- Cryogenic cycling generally succeeded in isolating partial failures. Those components whose glass cases survived initial cycling were rarely affected by subsequent cycling.
- Electrical failures of properly manufactured components were extremely rare even in cases where the glass envelope cracked.

As a result of past tests and analysis, it was concluded that the basic problem was a thermal mismatch between the conformal coating and the materials to which it was applied. The problem was particularly severe when the component was bonded and when the coating was thick. Inherent stresses or weaknesses in the glass envelopes introduced at the time of their original assembly would subsequently lead to cracking. Cryogenic cycling of components was effective in isolating such vulnerable components.

These studies led to the following corrective measures, which, however, could not be applied until the fifth Surveyor:

- Conformal coating was applied by spraying the components, and a thickness less than 10 mils was maintained to the maximum extent feasible.
- Conformal coating in the fillet areas was brushed to reduce buildup.
- Bonded components and other suspect parts were cryogenically cycled to screen out marginal parts.

Subsequently, improved materials were available for use as conformal coatings to ensure a better thermal match to the glass envelopes. These materials were not used on the Surveyor program but are applicable to future designs.

It was considered that the above information was directly applicable to the analysis of the cracked envelopes on the Surveyor III camera. There appeared little doubt that the problem was caused by the extreme and repeated thermal cycling of these bonded components through the lunar nights, particularly in view of the fact that in each of the 29 cases noted the thickness of the conformal coating appears appreciably higher than 10 mils. It should be noted that the Surveyor III camera experienced many more cycles than the number to which the components discussed above had been subjected in test.

It should also be pointed out that the evidence available in testing of the parts of the retrieved Surveyor III camera may have been somewhat distorted; i.e., they had been subjected to handling and effects of the ambient environment in the course of their return from the moon. Thus, the state and performance of the components with cracked envelopes may be different now than it was, or would have been, had they remained in the lunar vacuum environment in their cracked condition. In particular, contamination and moisture which could have entered the components through the cracked cases could have appreciably altered their characteristics.

12.7.4 Results of Failure Analysis of Two Defective Diodes

In light of these findings, it was felt that a detailed failure analysis of all the cracked glass envelopes was not warranted. Such an analysis, perhaps entailing thermal simulation of the cracked glass, would not be expected to generate data not already available from past records. The failure analysis work was therefore confined primarily to investigation of the two diodes which exhibited electrical anomalies.

As noted previously, all of the components with cracked envelopes, with the exception of the two diodes, appeared to have survived electrically intact. One possible exception was the cracking of the carbon composition resistor in the process of its removal from chassis A5. This resistor was broken into several pieces when its lead was unsoldered. Subsequent physical reconstruction of the pieces resulted in a resistance value which was still within 10 percent of its prelaunch reading. Examination of this resistor and of the place on the chassis from which it was removed showed evidence of an excessive stress. The method of mounting and bonding resulted in its leads being formed unduly close to its body. Other radial cracks around the lead were also observed. Subsequent cryogenic cycling undoubtedly caused fracture of the resistor body itself in this particular instance.

Details of the failure analysis conducted on the two diodes are presented in Appendix K.4. Results of this analysis, summarized below, revealed that in both cases a previous manufacturing defect existed.

Examination of the open diode, type IN3070, on chassis A3 revealed an intermittent contact between the spring whisker and the gold ball contact on the die. Manipulation of the diode leads could cause the diode body to move around the crack in the glass and to restore the contact between the whisker and the ball.

It was apparent that the cracking of the envelope was a necessary condition for this anomaly to occur. Since other similar components did not exhibit this anomaly, it could be, in part, attributed to a manufacturing variation such as a residual strain. The construction of this diode entailed a pressure contact vulnerable to this effect. Had an improved construction been utilized, such as a fuzed contact, the cracking of the glass would probably not have resulted in this anomaly.

Evidence indicated that, in spite of the open condition found in testing, the diode was probably still operative in the cracked case condition while on the lunar surface. It could not be positively ascertained to what extent subsequent handling induced the final opening of the lead. Very likely, the ball was shifted when one of the leads was unsoldered in the process of the removal so that the electrical failure was actually triggered by laboratory handling and testing.

In all other respects, the performance of the diode was nominal. Measured parameters were normal when physical contact was restored by jiggling the contacts and probing.

The second electrical component failure was the high reverse leakage current observed on the IN3730 diode on chassis A5 (6.6 micro-amperes compared with 0.1 microampere maximum specified). Failure analysis revealed later that the breakdown voltage was also considerably below specification (50 volts observed versus 200 volts minimum required).

Detailed examination uncovered a fracture in the die consisting of a small crack from one edge of the chip to the metallization. There was evidence that this fracture was produced in original manufacture, probably during the chip mounting process. The die was well mounted to the stud and fully supported by it.

The thermal stress associated with the break in the glass envelope may have caused the original fracture to propagate through the junction. The effect of such a crack in the junction would be a lowering in the breakdown voltage resulting from the vertical displacement of one-half the chip and the associated effective decrease of the depletion region. Some increase in leakage current could accompany this, but the relatively high value of 6 microamperes need not have necessarily existed on the lunar surface. In any event, the diode was probably fully functional during the operation of the camera on the moon.

It appeared likely that subsequent handling and return to the ambient environment enhanced the reverse leakage current. The high leakage could be the result of contamination of the exposed junction along the fracture. Moisture or other contaminants might have entered through the cracked glass.

While the lunar environment definitely caused the cracking of the glass of this diode and aggravated its electrical characteristics, the basic cause of this anomaly must be an original manufacturing discrepancy.

12.7.5 Concluding Comments

Results of the physical examination and preliminary investigation of the cracked glass cases and of the failure analysis of the two defective diodes, coupled with the review of past data, provided a plausible explanation of the anomalies noted.

Thermal cycling through the lunar nights caused excessive stresses to be developed in the conformal coating and in the glass envelopes as a result of the thermal mismatch between them. These stresses were aggravated in some cases by the excessive thickness of the coating and by the nature of the component bonding technique employed. Numerous cracks in the coatings resulted, as anticipated; in 29 cases out of some 980 components involved, these stresses resulted in the cracking of the glass envelopes. The occurrence of these cracks was not unexpected and was compatible with past test experience.

Some concern over these occurrences led to effective corrective measures, incorporated in subsequent spacecraft after Surveyor III.

With few exceptions, the cracks in the envelopes did not cause any electrical malfunction of the components. The two notable exceptions were one open diode and one diode with excessive reverse leakage current. Failure analysis of these components revealed that in one case an original manufacturing deficiency or defect was present. In both cases, cracking of the glass precipitated or contributed to the final malfunction. In both cases, the degree of malfunction was significantly aggravated by subsequent handling. Additionally, it appeared that in both cases the components still were or would have been electrically operative in their original lunar environment.

In the absence of any unusual findings, and because of the now available remedial measures, it was concluded that the observed cracks in the glass envelopes, while they did represent an effect of the lunar environment, would be of negligible concern for future programs.

12.8 OTHER ELECTRICAL ANOMALIES

12.8.1 Summary Assessment of Four Anomalies

This subsection summarizes the failure analyses conducted on the four electric circuit and component anomalies listed as items 12 through 16 in Table 12-1. Exposure to the lunar environment was believed to be a prime factor in each of these occurrences. As noted in Table 12-2, these were the only lunar environment-induced electrical failures except, perhaps, for the cracked glass cases discussed in the preceding subsection. It is significant that of the some 1500 electrical components of the TV camera, listed in Table 7-1 in Section 7, so few seemed to be seriously affected by their prolonged lunar exposure and subsequent return to the ambient environment.

These four components and a brief description of the nature and significance of the problems associated with them are presented in Table 12-4. The first three components - the tantalum capacitor, the alloy transistor, and the metal film resistor - were classified as failures and would have had a catastrophic effect on the operability of the Surveyor III camera. However, only the capacitor failure is of some significance to future applications. Accordingly, failure analysis of the tantalum capacitor is discussed in further detail in Section 12.8.2. The fourth anomaly, that of the erroneous reading of the vidicon temperature circuit, was initially attributed to a change brought about by the lunar environment in the characteristics of the matched transistor pair, as noted in Table 12-4. This anomaly was further investigated in some detail, as discussed in Section 12.8.3, to determine the extent of this possible degradation. Only minor changes in transistor characteristics were found, and the anomaly was determined to be attributable to the sensitivity of the circuit used. Thus, this was proved to be of negligible importance to future applications.

No failure analysis was performed on the damaged alloy transistor or metal film resistor. Both were of obsolete design no longer used in space programs. The alloy transistor chip was post-mounted. The susceptibility of its design was well understood: chip bond failure and termination failure are unique to this construction. Similarly, the failed metal film resistor was known to be susceptible to a failure mechanism wherein a fracture develops in the solder bond connecting the metal clip to the pad on the substrate. This type of failure mechanism is typical of solder-supported junctions. Both of these components failed open. The Surveyor spacecraft was launched in recognition that these components may not survive the lunar night. It was somewhat of a surprise that only 1 of the 49 transistors and only 1 of the 33 resistors of these respective types present in the camera were found to have failed.

12.8.2 Results of Failure Analysis of Tantalum Capacitor

The failed capacitor was a 4.7 microfarad (±10 percent) solid electrolyte tantalum capacitor, hermetically sealed, manufactured by Sprague, similar to type CSR13. Similar components manufactured by the Kemet Division of Union Carbide were also used interchangeably on Surveyors. These capacitors have been used extensively in the design of spacecraft. Modified versions developed later were capable of better survival at cryogenic temperatures.

The capacitor was used in the TV camera across the feedback path between the base of the emitter follower and the voltage amplifier of the video preamplifier (on camera chassis A5). The circuit functioned normally during the first lunar day. During chassis tests (described in Section 4.5), the capacitor was found resistively shorted: the ohmmeter reading indicated 4000 ohms. This short disabled the feedback path to the base circuit of the emitter follower, which, in turn, rendered the amplifier inoperative and would have resulted in a total loss of video information.

To determine the degree of the contribution of lunar exposure to this failure and because of the wide applicability of these types of components,

TABLE 12-4. ELECTRICAL COMPONENT ANOMALIES INDUCED BY LUNAR ENVIRONMENT

Importance to Future Applications		Moderate concern (improved capacitor design used extensively)	None (part obsolete)	None (part obsolete)	Negligible (anomaly reflects sensitivity of circuit used—insignificant change of transistor characteristics)	
	Effect on TV Camera	Catastrophic (loss of video)	Catastrophic (loss of video) Catastrophic (loss of video)		Minor (inaccurate data on vidicon temperature)	
Description of	Anomaly	Internal short (video preamplifier on chassis A-5)	Open (vertical blanking amplifier on chassis A-4)	Open (horizontal sweep generator on chassis A-4)	Change in calibration of vidicon temperature readout circuit on chassis A-6	
Total Number of Similar	in Camera	76	49	33	52	
scription	Manufacturer	Sprague CSR-13	Sprague 2N859	Allen-Bradley CAH	Fairchild 2N871	
Component Description	Type	Solid electrolyte tantalum capacitor	PNP alloy transistor	Metal film resistor	NPN high voltage amplifier transistors (matched pair)	

it was decided to conduct a comprehensive failure analysis of this anomaly. As noted in Section 12.2, effects of lunar exposure on this component had been of concern throughout the Surveyor program. Extensive past data were therefore available, including a great many diagnostic tests, design studies, and investigations of similar failures experienced during the Surveyor test program. Based on this experience, it was somewhat of a surprise that only 1 of the 76 similar components used in the camera had failed.

As discussed in Section 7.3.1, routine examination of a large number of these 76 similar components was conducted as part of the electrical components test program. Thirty-six components were checked on the chassis, and seven were functionally examined off the chassis; diagnostic tests were conducted on two of the seven. Definite degradation by lunar exposure was noted even on these nonfailed parts. This degradation was exhibited in the form of increased leakage current and increased slope of leakage current versus temperature characteristics. As discussed below, past experience indicated the observed failure of the tantalum capacitor was a more extreme manifestation of the same basic mechanism which caused the smaller changes on the other similar components.

The failure analysis conducted entailed a careful review of past records and systematic tests of the failed component. The latter included visual and X-ray examination, electrical tests, internal microscopic examination following a careful disassembly, and a number of additional tests especially designed to identify the mode of failure.

The internal structure of the tantalum capacitor is indicated in Figure 12-12, which shows the porous sintered tantalum anode used. The dry semiconductor electrolyte provides for relative freedom from corrosion or electrolyte leakage. The metal case is the negative terminal, and the positive dielectric lead is welded within the case. This allows for sharp lead bends without damage to the internal weld. The porous anode slug is manufactured by sintering a pressed mass of tantalum powder at high temperatures and reduced pressures. Surface area of this slug is anodically coated with a dielectric layer of tantalum pentoxide, which is then covered with a thin layer of electrically conductive manganese dioxide. Improved electrical contact is made to the coating of the manganese dioxide by the use of graphite, followed by a conducting silver paste. The unit is soldered into its metal enclosure, and the final sealing is made with a compression glass end seal. A feedthrough eyelet is provided for the anode wire.

Review of past records revealed a number of cryogenic failures generally entailing an excessive leakage current or a short through the tantalum pentoxide dielectric. A large number of these failures occurred

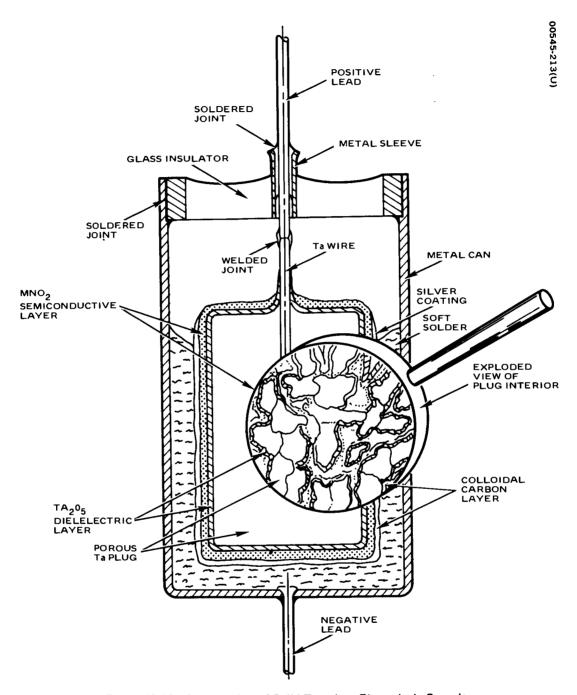


Figure 12-12. Construction of Solid Tantalum Electrolytic Capacitor

on capacitors in the early Surveyor television camera. A variety of causes were postulated or were determined to have existed. These included:

- Impurities in sintered anodes
- Uneven thickness of tantalum pentoxide dielectric
- Various other manufacturing process deficiencies
- Electrical and/or mechanical overstress at user's facility
- Stresses resulting from cycling beyond thermal specification limits of capacitor
- Stresses resulting from excessive number of thermal cycles

A special effort was instituted early in 1967 to identify the causes of these failures and to propose corrective actions. Results of this effort were not available for Surveyor III, but were applicable to later spacecraft. This effort entailed a comprehensive review of test data and past failure analysis, consultation with manufacturers, additional controlled tests, and consultation with other aerospace companies with experience in the use of these components. No specific causes of failure could be identified, nor could any fool-proof corrective measures be proposed, compatible with functional and environmental recommendations for these parts. However, a number of highly suspect design deficiencies were uncovered, and promising design improvement measures and worthwhile screening procedures were recommended.

One of the prime reasons for the cryogenic failures was believed to be mismatch in the thermal expansion coefficients of the elements of the capacitor. The expansion coefficients of the solid tantalum wire is six times greater than that of the tantalum pentoxide. This condition caused cracks or fissures to develop in the dielectric, or shifts in defect sites, which could reduce the breakdown voltage. These were believed to be subsequently aggravated by differences in the coefficients of expansion of other capacitor materials.

Another area of concern was the use of an epoxy cap in the region where the tantalum wire enters the anode. Thermal stresses developed during cryogenic exposure were believed to contribute to dielectric fractures in this area.

Subsequent design improvements entailed, among others, a better matching of expansion coefficients and elimination of the epoxy cap. Also, cryogenic screening was instituted, which seemed to decrease the occurrence of cryogenic failures. These improvements, available for future designs, were not instituted on the Surveyor program until Surveyor V. The failed

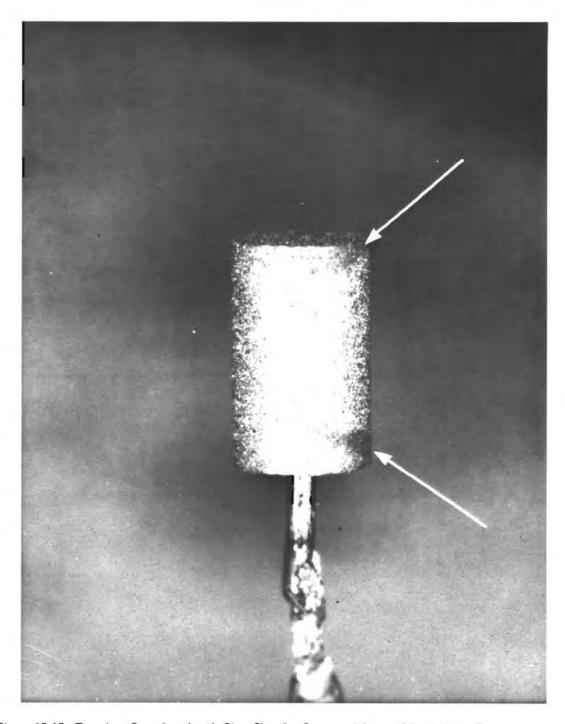


Figure 12-13. Tantalum Capacitor Anode Slug, Showing Suspected Areas of Breakdown (Photo 00545-214)

Surveyor III capacitor, for example, still had the epoxy cap in its internal construction. Surveyor III was launched with the realization that lunar night survival of its tantalum capacitors could not be assured.

Consideration was given to the replacement of these types of components with other components better qualified to meet the cryogenic exposures. In particular, a fixed nonsolid electrolyte tantalum capacitor was considered. Unfortunately, these other components have a poorer ripple voltage characteristic, higher dissipation factor, and larger capacitances versus temperature coefficient. However, these replacements may be adequate for other space applications.

The failure analysis of the Surveyor III tantalum capacitor was conducted in full cognizance of the above background information. Preliminary examination revealed no manufacturing deficiencies and no evidence of mishandling.

Electrolyte tests confirmed the 4 kilohm resistive short and indicated an excessive symmetrical leakage at voltages considerably below the 10 volts rated value. Both the forward and the reverse leakage currents were on the order of 0.5 ma, many orders of magnitude higher than normal.

The various coatings were chemically removed from the anode slug. Subsequent examination of the slug revealed the presence of the suspected defective areas shown in Figure 12-13. Since the surface of the anode was free of gray oxide points of scintillation, the breakdown area must have been internal to the anode. Reformation indicated oxide anomalies at approximately 5 volts.

It appeared that the lunar environment caused microcracks to develop in the dielectric at points of high stresses. The extent of oxide crystallization would be limited by the 1 megohm series resistance in the external circuit. However, this degradation after one or more thermal cycles would be sufficient, as evidenced by past history, to cause the observed failure upon the application of voltages much lower than rated, perhaps as low as 1 or 2 volts. It appears that the capacitor failed either upon the application of the rated or less than rated voltage during the attempts to revive the spacecraft after the first lunar night (e.g., the voltage which caused the solenoid drive circuit failures, discussed in Section 12.5) or upon the application of a nominal voltage during the chassis tests of the returned camera (discussed in Section 4.6).

12.8.3 Vidicon Temperature Readout Anomaly

As noted in Section 4.7, tests of electric chassis A-6 revealed an anomalous reading of the vidicon temperature readout circuit. The output voltage of 0.66 volt corresponded to a temperature of 8°F according to prior calibration data. The actual temperature of 85°F should have produced a reading of 3.002 volts.

The vidicon readout circuit was one of two similar temperature sensing and indicating circuits on the camera. The second circuit measured the output of the temperature sensor on the ECU chassis. Both circuits employed a common voltage regulator which used a 9 volt zener diode to

provide excitation to the bridge circuits. Each of the two temperature readout circuits, in addition to the voltage regulator, consisted of a balanced bridge circuit and a highly stable differential amplifier. Each bridge circuit employed a microdiode temperature sensor in its respective sensing locations.

The temperature readout circuit of the ECU performed nominally. This eliminated its components, including the 9 volt zener diode common to both circuits, as the source of the problem. Examination of the vidicon bridge circuit indicated that its components, including the microdiode sensor, were nominal. This was verified in two ways. The vidicon diode was first replaced by the microdiode of the ECU; the vidicon temperature readouts were then still anomalous. The vidicon diode was then replaced with a potentiometer whose setting was adjusted to correspond to the nominal room temperature readout. Anomalous readings of the readout circuits were again obtained, and the adjusted potentiometer resistance was measured to be identical with the forward resistance of the vidicon diode. By varying the resistance of the potentiometer, the output could then be adjusted between the nominal limits of 0 to 5 volts dc. The other components of the bridge circuit were also measured and found nominal.

The above tests pinpointed the source of the problem as being attributable to the differential amplifier of the vidicon readout circuit. In particular, it appeared that one or both of the matched* transistors had changed characteristics relative to prelaunch readings, thereby altering the circuit calibration. The suspect transistors were Fairchild NPN 2N2871 high voltage amplifier transistors. Tests of similar transistors in the returned TV camera (reported in Section 7.5.3) uncovered no significant effects of the lunar environment on these components.

Functional tests of the suspect transistor package could not be readily performed on the chassis because of the difficulty of access to the cordwood modules in which they were buried. The transistor package was therefore removed and tested in the Hughes Components Laboratory. The package was found to be in excellent condition. Tests revealed no discrepancies relative to specification requirements. However, comparison with original receiving inspection data indicate that the collector-base and emitter-base currents of both transistors appeared to have changed.

It is recognized that, because of instrumentation differences and the inherent nature of original inspection measurements, the accuracy of this comparison cannot be assured. Furthermore, it should be noted that determination of static characteristics may be a poor measure of the match of the dynamic characteristics of these two components.

This apparent change of the collector and emitter currents must be viewed with the above reservations as resulting from the lunar exposure (presumably thermal cycling) and as providing the explanation for the shifting of the circuit calibration. The values of these two parameters actually appeared to have improved. This calibration anomaly was concluded to be the result of these small changes and reflects the critical sensitivity of the circuit employed.

^{*}This matched pair was contained in a single TO-5 can.

This anomaly was therefore concluded not to be of major significance. It is certainly of negligible importance to future applications as long as it is recognized in circuit design that the lunar environment, or any similar exposure to temperature extremes, may result in minor parameter changes for these types of components.

12.9 OTHER MECHANICAL AND ELECTROMECHANICAL ANALYSES

Results of the analysis of the four remaining anomalies, items 17 through 20 in Table 12-1, are presented in this section. These anomalies were found to be relatively insignificant, both with respect to the operation of the Surveyor camera and as to application to future programs. They were all attributable to primary causes other than the lunar environment: prelaunch defects, handling, and normal wear effects. In two of these, however, lunar exposure may have had a contributory effect.

12. 9. 1 Excessive Shutter Breakaway Current

As discussed in Section 5.5, tests of the electromechanical characteristics of the undamaged solenoid B of the shutter assembly indicated an excessive value of its breakaway current.* The observed range from 250 to 325 ma was about 30 percent higher than its specified range of from 190 to 235 ma.

The solenoid contained a permanent magnet rotor whose movement activated the shutter blades. The actuating force was generated by the current through stator windings. The current required to actuate the rotor depended on the airgap between the rotor and the stator.

The rotor shaft was supported by teflon bushings. The rotor was made of soft iron plated with copper. The external surface of the rotor was originally coated with molybdenum disulfide lubricant 1 to 2 mils thick.

In operation, the rotor rotated in steps. The average effective value of the airgap, which depended on the characteristics of the teflon bushings, clearances, and other design variables, changed somewhat depending on the angular orientation. This accounts for the relatively wide range of the breakaway current values, both specified and measured. It also illustrates the somewhat critical dependence of the force and therefore of the required stator solenoid current on the airgap.

An increase in the airgap would result in an increase in the break-away current. This could be caused by the wear of the teflon bushings or by the wear of the rotor. Examination revealed that the rotor, indeed, showed signs of wear. The molybdenum disulfide lubricant had worn off in the rotor pole face areas, exposing the copper plating.

^{*}Solenoid A was damaged, and its failure analysis is presented in Section 12.5.

This observed wear was not surprising and reflects many cycles of operation. Exposure to the lunar environment may have contributed to some unknown extent. Even in its present condition the shutter blade was fully operable since the current requirements were entirely within the normal capability of the camera power subsystem. This effect is of negligible importance to future applications since normal effects of wear are expected to be included in all design considerations.

12.9.2 Deformed and Worn Azimuth Drive Gear Teeth

As noted in Section 2. 4. 2, one of the Surveyor III mission anomalies reported was faulty operation of the azimuth drive. The mission TFR stated that the mirror azimuth drive failed to step 432 times out of a total of 10,045 right commands but failed to step only twice out of an approximately similar number of left commands. This failure generally occurred at two positions of the azimuth drive: +3 and -27 degrees. It was also most noticeable during rapid temperature changes, such as during lunar sunrise, solar eclipse, and lunar sunset.

Prior to return of the camera, the suspected cause was believed to be one of the following: 1) binding of the azimuth bearing at the particular locations noted, resulting from localized stresses aggravated by temperature gradients; 2) degradation associated with motor wear, caused by its total accumulated steps; or 3) increased friction of the ring gear, caused by lunar dust, and possibly localized in the suspected areas.

The impact of this anomaly on the operation of the TV camera was minimal. It was still possible to orient the mirror assembly to any desired position. However, it was decided to conduct a failure analysis of the retrieved azimuth ring gear because of the possible implications of a potential effect of the lunar environment.

Examination of the azimuth ring gear revealed bent teeth and evidence of associated wear in two locations. This is shown in the photograph of the retrieved azimuth drive gear (Figure 12-14). The two locations were 36 degrees apart. In one location, three teeth were worn; in the second location, one and one-half teeth were worn.

It is noted that the difference between the two angular positions of the mirror assembly, +3 and -27 degrees, at which problems occurred during the Surveyor III mission operations was 30 degrees, very close to the observed 36 degree angular separation of damaged teeth, considering all factors involved. Furthermore, the pinion of the motor driving the mirror assembly in the azimuth gear ring and the gear of the azimuth readout potentiometer, both permanently affixed to the movable mirror assembly, were also displaced from each other by 36 degrees. The pinion and the gear can be seen in Figure 3-26 of Section 3.

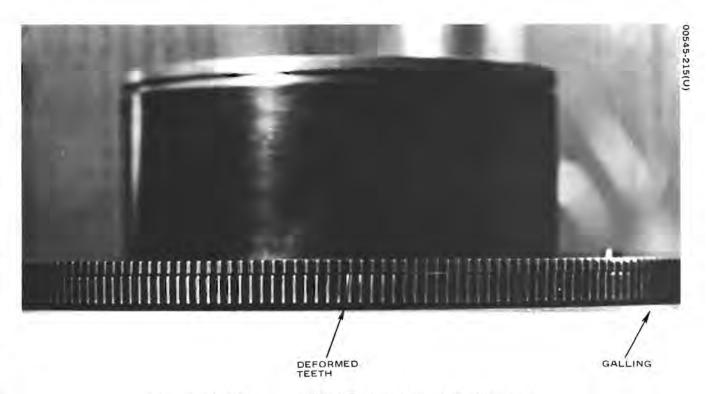


Figure 12-14. Deformed and Galled Teeth of Azimuth Drive Gear Train

Reconstruction of the orientation of the mirror assembly within the azimuth drive gear ring in the position of the reported anomaly revealed that one of the worn areas of the azimuth ring gear* closely corresponded to the position of the motor drive pinion when the mirror was in the reported +3 degree azimuth orientation. Hence, it appeared that this anomaly was associated with the contact between the motor drive pinion and the observed worn and bent ring gear teeth. At that time, the potentiometer gear was probably in direct contact with the second observed worn area on the gear teeth, 36 degrees away. Similarly, the second reported anomalous angular position of the mirror assembly probably corresponded to the potentiometer gear directly in contact with the first of the two above worn areas.

It was also noted that the two regions of the worn and bent teeth of the ring gear, permanently affixed to the camera body, were in an uphill position during lunar operations of the camera, which was mounted on the Surveyor in a tilted position about 23 degrees from the vertical. When the motor pinion or the potentiometer gear was in contact with these worn and bent teeth, the anomalous behavior of azimuth stepping operations was aggravated by the lateral forces resulting from the mirror assembly weight, acting through its center of gravity. The clearance between the motor

^{*}The area where three teeth were worn.

pinion and the azimuth gear or between the potentiometer gear and the azimuth gear, would thus be reduced. This uphill position of maximum interference, coupled with the defective azimuth teeth, could readily explain the observed anomaly, even though in prelaunch tests with the azimuth ring gear horizontal such an occasional failure to respond to azimuth commands had not been noticed.

The above findings appeared to localize the nature of the anomalous readings as being associated with the observed bent and worn teeth of the azimuth ring gear. Efforts to determine the origin of this defect were then initiated.

Examination of the returned motor pinion and potentiometer gear revealed no anomalies, suggesting that the defects in the azimuth ring gear were of an earlier origin. A systematic review of records and test history was then conducted.

It was discovered that two TFRs had been written in 1966 on the azimuth operation of this mirror assembly, indicating anomalous operations. One TFR had resulted in the replacement of the potentiometer, whereupon it was found that the potentiometer shaft was bent. The damage was assumed to have been caused by misalignment during the assembly. The second resulted in the replacement of the motor assembly, and poor operation was attributed to worn parts inside the motor. Following the replacement of these two parts, the mirror assembly functioned in accordance with specifications in all subsequent tests. These anomalies were reported after the camera had already been installed on the spacecraft, so the above procedures and corrective actions were taken after the examination of the mirror assembly removed from this camera, Since the components of the mirror assembly were suspected, no detailed diagnostic examination or tests were conducted on the azimuth ring gear itself, which had remained affixed to the body of the camera on the spacecraft. Only system level functional verification tests of the camera were conducted later.

At this point of the failure analysis, it was suspected that the ring gear was already in its present damaged condition when the above mentioned replacements were made on the spacecraft in 1966. A further examination of the records indicated a number of likely, albeit speculative, occurrences which might explain the origin of this deformation of the azimuth gear teeth. The camera log book indicated at least four vibration tests before January 1967 and two additional vibration tests during 1967. The bending of the shaft, which occurred following one of these vibration tests, might suggest that a severe jolt was received. It should be noted that in all of these vibration tests the position of the mirror assembly was nearly the same as that corresponding to the +3 degree position of the mission anomalies. It appears likely that the defect in the azimuth teeth occurred during one of these tests and remained undetected as a result of the procedures described above. The fact that the relatively weaker potentiometer shaft was bent, while the motor pinion shaft was apparently undamaged, further

substantiates this hypothesis since relatively greater degradation was found on the azimuth ring gear teeth opposite the location of the motor pinion: the yielding of the weaker potentiometer shaft would tend to lessen the damage to the ring gear at that point.

In view of these findings, it was concluded that the anomaly was attributable to an undetected prelaunch condition of the azimuth ring gear. Lunar operations may have aggravated this condition somewhat, particularly in view of the effect of the forces of gravity in the tilted camera position, noted above, and partially because of a possible increase in the wear of the surfaces in contact. Such additional contributions of the effect of the lunar environment would be secondary, however. It is not considered that this anomaly has any particular significance for future applications.

12.9.3 Broken Safety Wire of Filter Wheel

Examination of the filter wheel subassembly, discussed in Section 5.3, revealed a symmetrical scratch pattern on one of the filter wheel gears (Figure 12-15). It was also observed that a nearby safety wire was broken. The wear pattern indicated that the scratches were caused by this broken safety wire as it retraced many times over the surface of the filter wheel during the lunar operations.

From examination of the safety wire, it was concluded that this anomaly was attributable to an original installation of handling defect. Excessive twisting or bending either caused this break prior to flight or weakened the wire to the point where it failed during subsequent operations: during vibration tests prior to launch, during the launch phase, during the landing, or during the lunar operations.

It is not believed that the lunar environment played any role whatsoever in this anomaly. Scratches on the filter wheel indicated that the camera operated after the break occurred. This anomaly was therefore considered to be of no consequence either to the camera or to future applications.

12. 9. 4 Detached Back of Azimuth Potentiometer

When the azimuth potentiometer was removed from the retrieved camera, it was observed during the initial electrical and visual examination that the potentiometer was partially disassembled. The three screws which retained the back cover and bearing assembly had apparently been forced out. The back cover and bearing assembly were now free, and the shaft assembly was unrestrained.

Further examination revealed that the potentiometer was apparently damaged during the disassembly; it had been necessary to drill out a pin holding the gear onto the shaft. This occurred inadvertently in the process of the disassembly of the retrieved camera. A wobble in the drill during the removal of the pin caused a substantial force to be exerted on the back



Figure 12-15. Scratch Marks on Filter Wheel Gear Caused by Broken Safety Wire (Photo 4R15019)

plate, tearing the three screws from their plastic retainer. At that time, or subsequently, the pickup wire was bent because the personnel handling the potentiometer were not aware of the fact that the back was loose. As a result, the shaft assembly was free to shift backward, thereby deforming the pickup wire. An open circuit thus developed between the wiper and either end of the potentiometer winding.

Since this anomaly was determined to be strictly attributable to faulty disassembly operations, it was considered of no significance either to the camera or to future applications.

REFERENCES

- 1. Surveyor III Parts and Materials: Evaluation of Lunar Effects, Hughes Aircraft Company Report P70-504, December 1970.
- 2. Plan for Postflight Test and Analysis of Parts and Materials of Surveyor III Retrieved From Lunar Surface by Apollo 12, Volume I, Technical Plan, Hughes Aircraft Company Report SSD 90397, November 1969.
- 3. Memorandum 2292/163 from L. E. Blanchard to R. K. Cheng, 11 January 1967, "Surveyor Spacecraft Components of Scientific and Engineering Value Worthy of Recovery During Apollo Missions."
- 4. Memorandum from E. I. Hawthorne to R. E. Sears, 1 August 1969, "Surveyor III Recovery Operations Plan."
- 5. Letter from E. I. Hawthorne to James Peacock, NASA-MSC, 8 August 1969.
- 6. Hughes Aircraft Company letter 69(22)6679/C0116, 22 August 1969, "Apollo 12 Recovery Operations of Parts of Surveyor III."
- 7. Apollo 12 Preliminary Science Report, NASA SP-235, Section 13, "Preliminary Results from Surveyor III Analysis."
- 8. D. R. Montgomery and F. J. Wolf, "The Surveyor Lunar Landing Television System," <u>IEEE Spectrum</u>, Volume 3, August 1966, pp. 54-61.
- 9. Surveyor Final Engineering Report, Hughes Aircraft Company, June 1968.
- 10. Surveyor III Mission Report, JPL Technical Report 32-1177, 1967.
- 11. NASA Headquarters letter to Surveyor Parts Steering Group, 18 June 1970, "Approval of Expanded Surveyor III Parts Analysis Plan."

- 12. Memorandum from Stephen Jacobs, ES8, NASA-MSC, with eight enclosures, 2 February 1970, "Summary of Activity From Release of Surveyor III Returned Materials to Shipment to Hughes January 7, 1970."
- 13. Memorandum from Richard E. Benson, NASA-MSC, 22 January 1970, "Gamma Spectrometric Analysis of the Surveyor III Television Camera."
- 14. S. Dushman, Scientific Foundation of Vacuum Technique, John Wiley and Sons, first edition, 1949.
- 15. A. Fafarman and D. K. Matherly, "Gas Ratio Measurement by Ion Growth," <u>IEEE Transactions</u>, Ed-17, February 1970.
- 16. S. C. Brown, <u>Basic Data of Plasma Physics</u>, John Wiley and Sons, 1959.
- 17. J. T. Tate and P. T. Smith, Physical Review, 1932.
- 18. A. Fafarman and R. S. Burritz, "Beam Transmission in Electron Guns Having a Single-Apertured Control Grid," IEEE Transactions, Ed-15. October 1968.
- 19. W. A. Hagemeyer, "Surveyor Camera Vidicon Face Plate Temperatures," JPL interoffice memorandum, 1 June 1970.
- 20. C. T. Leondes and R. W. Vance, editors, <u>Lunar Missions and</u> Explorations, John Wiley and Sons, Inc., 1964.
- 21. Surveyor V: A Preliminary Report, NASA SP-163, 1967.
- 22. Surveyor Program Results, NASA SP-184, 1969.
- 23. J. W. Haffner, Radiation and Shielding in Space, Academic Press, 1967.
- W. R. Webber, An Evaluation of Solar Cosmic-Ray Events
 During Solar Minimum, Boeing Company Report DZ-84274,
 June 1966.
- W. R. Webber, "An Evaluation of the Radiation Hazard Due to Solar Particle Events," Boeing Company Report DZ-90469, 1963.
- W. R. Webber, An Evaluation of the Radiation Hazard Due to Solar-Particle Events, Boeing Company Report DZ-90469, December 1963.

- 27. R. Boring, "Lunar Surface Solar Array Characteristics," Intersociety Energy Conversion Engineering Converence, 1968.
- 28. R. E. Smith et al., Space Environment Criteria Guidelines for Use in Space Vehicle Development, NASA TM-X-53521, 1967.
- 29. M. Knoll and B. Kazan, <u>Storage Tubes and Their Basic Principles</u>, John Wiley and Sons, New York, 1952.
- 30. P.K. Weimer, S.V. Forgue, and R. Goodrich, Electronics, Volume 23, May 1950.
- 31. H.B. Law, Review of Scientific Instruments, Volume 19, 1948.

REFERENCES FOR SURFACE DISCOLORATION AND CONTAMINATION STUDIES*

- 101. Surveyor III Parts and Materials: Evaluation of Lunar Effects, Hughes Aircraft Company Report P70-504, December 1970.
- 102. B. Cour-Palais (NASA MSC), private communication.
- 103. O. Schaeffer (SUNY), private communication.
- 104. F. G. Satkiewicz (GCA), private communication.
- 105. Surveyor III Mission Report, JPL TR 32-1177.
- 106. L.D. Jaffee (JPL), private communication.
- 107. Apollo 12 Mission Report, MSC 01855, NASA MSC, Houston, Texas, March 1970.
- 108. R. F. Scott et al., Apollo 12 Preliminary Science Report, NASA SP-235.
- 109. P. M. Blair and G. R. Blair, "Summary Report on White Paint Development for Surveyor Spacecraft," Hughes Aircraft Company, TM 800, Culver City, California, December 1964.
- P. M. Blair et al., <u>Development of a Low Solar Absorptance</u>
 Thermal Control Coating, Hughes Aircraft Company, P69-147,
 Culver City, California, April 1969.
- 111. G. A. Zerlaut and J. E. Gilligan, "Study of In-situ Degradation of Thermal Control Surfaces," IITRI-U6061, 17 March 1969.
- 112. Mark Adams (JPL), private communication.
- 113. J. B. Adams et al., "Spectral Reflectivity of Lunar Samples," Science, Volume 167, No. 3918, January 1970.
- 114. D. Nash (JPL), private communication.

^{*}Included in both Hughes reports on returned Surveyor III parts (SSD 00545R and P70-504).